

VU Research Portal

Exploring the Chemokine Receptor CXCR2

de Kruijf, P.

2011

document version

Publisher's PDF, also known as Version of record

[Link to publication in VU Research Portal](#)

citation for published version (APA)

de Kruijf, P. (2011). *Exploring the Chemokine Receptor CXCR2: Ligand Recognition and Response*. [PhD-Thesis - Research and graduation internal, Vrije Universiteit Amsterdam].

General rights

Copyright and moral rights for the publications made accessible in the public portal are retained by the authors and/or other copyright owners and it is a condition of accessing publications that users recognise and abide by the legal requirements associated with these rights.

- Users may download and print one copy of any publication from the public portal for the purpose of private study or research.
- You may not further distribute the material or use it for any profit-making activity or commercial gain
- You may freely distribute the URL identifying the publication in the public portal

Take down policy

If you believe that this document breaches copyright please contact us providing details, and we will remove access to the work immediately and investigate your claim.

E-mail address:

vuresearchportal.ub@vu.nl

General introduction and objective of this thesis

Chapter 1

Chemokine receptors as members of the family of G-protein coupled receptors

Chemokine receptors belong to the family of G-protein coupled receptors (GPCRs). Currently, around 30% of drugs on the market target GPCRs. Pharmaceutical companies show therefore a great interest in this type of receptors [1]. GPCRs form a large family of transmembrane (TM) proteins that transduce extracellular signals into intracellular responses. All GPCRs consist of an extracellular N-terminus, seven transmembrane helices connected by three extracellular- and three intracellular loops, and an intracellular C-terminus (see Figure 1.1). The GPCR superfamily consists of five main classes: glutamate, rhodopsin, adhesion, frizzled/taste and secretin [2]. Earlier classification systems grouped the GPCR superfamily in classes A-F [3, 4]. The chemokine receptors belong to the γ -group of rhodopsin receptors or family A, respectively [2-4]. This family is characterized by containing the conserved residues N^{1.50} in TM 1, D^{2.50} in TM2, R^{3.50} in TM3, W^{4.50} in TM4, P^{5.50} in TM5, P^{6.50} in TM6 and P^{7.50} in TM7 on which the Ballesteros Weinstein numbering is based [5]. Furthermore, this family has a conserved D(E)RY motif at the border between TM3 and intracellular loop 2, a LAxxD motif in TM2 and a NSxxNPxxY motif in TM7 [2, 6].

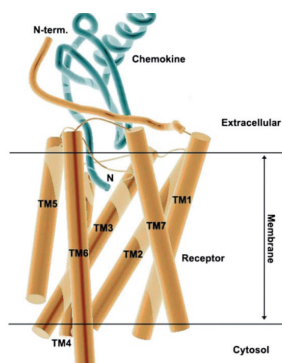


Figure 1.1: Model of the interaction of a chemokine with the chemokine receptor (GPCRs). Adapted from [14].

Once an agonist binds (at the extracellular side) to the GPCR, the receptor is considered to undergo a conformational change to an activated receptor state. Subsequently, the $G\alpha$ -subunit of the G-protein will exchange bound guanine diphosphate (GDP) for guanine triphosphate (GTP), leading to the dissociation of the G protein complex into a $G\alpha$ -subunit and $G\beta/\gamma$ subunit. Both subunits can stimulate or inhibit a broad variety of signal transduction pathways [7]. Contradicting this model, Bünemann *et al* [8] reported that heterotrimeric G proteins of the G_i family undergo a conformational rearrangement upon receptor activation, rather than subunit dissociation. Activated GPCRs are phosphorylated on the C-terminus by G-protein coupled receptors kinases (GRKs), leading to the recruitment of β -arrestins. β -arrestins in turn, promote GPCR internalization, which can be either followed by receptor degradation or recycling back to the cell surface [9]. Furthermore, as recently shown, β -arrestins can also serve as scaffolding proteins that initiate (in)activation of distinct signaling pathways [10, 11].

Chemokines and chemokine receptors

Chemokines and their receptors play an essential role in coordinating the movement of leukocytes to sites of inflammation. To date, approximately 50 chemokines and 20 chemokine receptors are identified (see Figure 1.2) [12]. Furthermore, herpesviruses were shown to encode chemokines and chemokine receptors as well [13]. Some receptors only bind one chemokine, whereas others bind multiple chemokines. Furthermore, a chemokine can either bind a single chemokine receptor or bind to multiple receptors (see Figure 1.2). Chemokines are categorized into C, CC, CXC and CX3C chemokines based on the number and spacing between conserved cysteine residues in their N-terminus. The CXC chemokine are further divided into ELR⁺ and ELR⁻ chemokines, depending on the presence of the glutamate-leucine-arginine motif in their N-terminus.

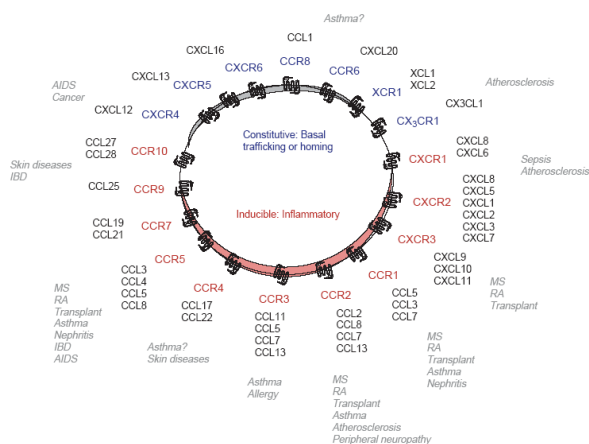


Figure 1.2: Interaction of chemokines with their chemokine receptors. Picture adapted from [76].

The chemokine/chemokine receptor interaction has been considered as a 2-step process [14]. First, the N-loop of the chemokine binds, mostly via ionic interactions, with the N-terminus and extracellular loops of the receptor. Second, the flexible N-terminus of the chemokine is positioned in such a way that it interacts with another site of the receptor, namely extracellular loops and the transmembrane domains [15]. This 2-step binding model is supported by studies with N-terminus truncated chemokines that still show binding to the receptor but loss of agonist activity [16, 17].

Chemokine receptors as disease targets

Change in expression profile of various chemokines and chemokine receptors have been correlated with the development of clinical symptoms of diseases. Prolonged expression of chemokines can lead to excessive infiltration of certain leukocytes to sites of inflammation, resulting in e.g. chronic inflammation and autoimmune diseases (see **Chapter 2**, [18, 19]). Also, upregulation of chemokine and chemokine receptors are correlated with several hall marks of cancer, including metastasis and angiogenesis [13, 20-22]. Furthermore, CCR5 and

CXCR4 serve as the most important co-receptors for HIV entry into CD4⁺ cells [23-25]. Hence, the chemokine receptors gained increasing attention as potential drug targets. Several chemokine receptor antagonists have been developed, although not very successfully since a lot of them failed in clinical trials. However, with the approval of Maraviroc (a CCR5 antagonist, anti-HIV treatment) in 2007 by the FDA and AMD3100 (a CXCR4 antagonist, hematopoietic stem cell mobilization), together with ongoing clinical trials with several small molecules targeting various chemokine receptors, the field has strong faith that the chemokine system can be a valuable drug target [26].

Crystal structures of GPCRs

To find potential drug candidates, high-throughput screening is one of the strategies used by pharmaceutical companies. Another approach is to design ligands based on structural knowledge of GPCRs. In 2000 the first crystal structure of a GPCR, bovine rhodopsin, was solved [27]. Between 2000 and 2007 several related crystal structures of the (inactive, dark) 11-*cis*-retinal bound receptor were published [28-31]. The bovine rhodopsin structures served a long time as the only templates for *in silico* modeling of GPCRs, as it appeared to be challenging to crystallize other GPCRs. Using either a T4-lysosome fusion strategy or the use of a modified antibody (Fab), there was a major break-through in 2007: two crystal structures of the β_2 -adrenergic receptor were solved [32-34]. In 2008 another β_2 -adrenergic receptor crystal structure followed [35], as well as the crystal structures of turkey β_1 -adrenergic receptor [36] and the human A_{2A} adenosine receptor [37]. Furthermore, in 2008 crystal structures of an active state of a GPCR, opsin, were solved for the first time [38, 39]. In 2010 the crystal structures of the human chemokine receptor CXCR4 [40] and the human dopamine D₃ receptor [41] were published. Both receptors were crystallized in their inactive conformation. Active conformations of GPCRs are less stable and therefore more difficult to obtain in crystal form. A series of breakthroughs followed this year. Rasmussen *et al* [42] crystallized the β_2 -adrenergic receptor in an active conformation using besides the T4 lysozyme fusion also a nanobody that acts as a surrogate Gs protein. Furthermore, the same lab obtained crystal structures of the β_2 -adrenergic receptor irreversible bound to the agonist FAUC50 [43]. Xu *et al* [44] crystallized the adenosine A_{2A} receptor in its active conformation with the agonist UK432097 in its binding site. Similarly, Lebon *et al* [45] crystallized the same receptor in an intermediate conformation (between active/inactive) by receptor thermostabilization resulting in two crystal structures with A_{2A} receptor bound to the agonists adenosine and NECA. Also for the turkey β_1 -adrenergic receptor new crystal structures were obtained, although those structures only show bound antagonists [46]. Finally, Shimamura *et al* [47] were able to construct a crystal structure for the histamine H₁ receptor. All the above mentioned crystal structures (Table 1.1) provide insight to create better *in silico* models of GPCRs of interest. This in turn will allow a better understanding of receptor ligand interactions and guide e.g. receptor mutagenesis and/or medicinal chemistry projects.

Table 1.1: Overview of recently solved crystal structures of GPCRs.

year	receptor	modification	conformation	co-crystallized with	ref
2000	bovine rhodopsin	-	inactive	11-cis-retinal	27
2007	human β_2 -adrenergic	fusion to T4-lysozyme (IL3)	inactive	carazolol (inverse agonist)	32
2007	human β_2 -adrenergic	complex with antibody Fab fragment (IL3)	inactive	carazolol (inverse agonist)	33
2008	human β_2 -adrenergic	fysio to T4-lysozyme (IL3) + E3.41W (thermically stabilized)	inactive	timolol (inverse agonist) +cholesterol	35
2008	turkey β_1 -adrenergic	mutations to a thermically stabilized receptor (B1AR-M23)	inactive	cyanopindolol (antagonist)	36
2008	human A_{2A} -adenosine	fusion to T4-lysozyme (IL3) and deletion of C-terminal domain	inactive	ZM241385 (antagonist)	37
2008	bovine opsin	-	active	(ligand free)	38
2008	bovine opsin	Ga-CT synthetic compound	G-protein bound	opsin/rhodopsin	39
2010	human CXCR4	fusion to T4-lysozyme (IL3) + L3.41W (thermically stabilized)	inactive	IT1t or CVX15 (antagonist)	40
2010	human dopamine D ₃	fusion to T4-lysozyme (IL3) + L3.41W (thermically stabilized)	inactive	eticlopride (antagonist)	41
2011	human β_2 -adrenergic	fusion to T4-lysozyme (IL3) + complex with nanobody Nb80	active	BI-167107 (agonist)	42
2011	human β_2 -adrenergic	fusion to T4-lysozyme (IL3) + H2.64C (for interaction FAUC50)	inactive	FAUC50 (inverse agonist)	43
2011	bovine rhodopsin	E3.28Q (opsin: CAM) + thermically stabilized (N2C/D282C)	active	all-trans-retinal (agonist)	31
2011	turkey β_1 -adrenergic	mutations to a thermically stabilized receptor + deletion (β 36-m23)	inactive	cyanopindolor or iodocyanopindolor	46
2011	human A_{2A} -adenosine	fusio to T4-lysozyme (IL3) + deletion of C-terminal domain	active	UK-432097 (agonist)	44
2011	human A_{2A} -adenosine	1-316; L48A + A54L + T65A + Q89A + N154A (thermically stabilized)	intermediate	adenosine or NECA (both agonists)	45
2011	histamine H ₁	fusion to T4-lysozyme (IL3) and truncation amino acids 1-19	inactive	doxepin (antagonist)	47
2011	human β_2 -adrenergic	fusion to T4-lysozyme (IL3) and with nanobody Nb35	active	BI-167107 and complex G α_s	77

Chemokine receptor CXCR2

In the major part of this thesis we focus on the chemokine receptor CXCR2. As shown in Figure 1.2, CXCR2 interacts with seven endogenous chemokines. All these chemokines contain a CXC and an ELR motif in their N-terminus. Both motifs have shown to play a crucial role in binding and activation of CXCR2 [48-52]. Furthermore, the N-loop of approximately ten residues (followed after the second conserved cysteine) is responsible for receptor binding and controls receptor specificity [53-55].

As will be discussed in **Chapter 2**, CXCR2 and its chemokines play a role in different inflammatory diseases. Studies with patient material showed that CXCR2 expression is e.g. increased in bronchial biopsies of COPD patients and in psoriatic epidermis [56, 57]. Furthermore, the number of neutrophils is increased in bronchoalveolar lavage fluid of COPD patients due to increased production of CXCL1, CXCL5 and CXCL8 [58-63]. Also in atherosclerotic lesions, psoriatic epidermis, inflammatory bowel disease mucosa and inflamed rheumatoid arthritis joints, different CXCR2 interacting chemokines have been detected [56, 64-70]. This can lead to increased infiltration of CXCR2 expressing leukocytes, subsequently leading to worsening of the clinical symptoms. As such, blocking the CXCR2 receptor has therapeutic potential. Pharmaceutical industries have developed distinct small molecular weight CXCR2 antagonists. Amongst them, SCH527123 is currently in phase II clinical trial for COPD (ThomsonPharma database; <http://partnering.thomson-pharma.com>), indicating that CXCR2 is indeed a druggable target.

Chemokines are large molecules (8-14 kDa), while small molecular weight antagonists can vary approximately between 300-700 Da. Already from the size differences, it seems likely that small molecular weight antagonist will not act via simple steric hinderance or competition, but rather via allosteric mechanisms. This means that antagonists will most likely bind to sites that are topographically distinct from the orthosteric endogenous (chemokine) ligand binding site [71, 72]. Indeed, several chemokine receptor antagonists have been shown to bind in the transmembrane domain of the receptor, whereas for CCR4 and CXCR2 some antagonists were shown to bind to intracellular sites (see extensively review [71]).

Aim and outline of this thesis

The aim of this thesis was to get more insights on the binding pocket(s) and mechanism of action of low molecular weight CXCR2 antagonists. We found that compounds belonging to the diarylurea, thiazolopyrimidine and imidazolylpyrimidine chemical classes, antagonize CXCL8 most likely via a noncompetitive allosteric mechanism (**Chapter 3**). Using the diarylurea [³H]-SB265610 compound, we have identified that compounds of different chemical classes bind to distinct binding sites at CXCR2 (**Chapter 3**). Furthermore, we elucidated the binding mode of an imidazolylpyrimidine compound using different CXCR2 orthologs, chimeric proteins, site-directed mutagenesis and *in silico* modeling (**Chapter 4**).

At the start of this research project, a recent article [73] reported that besides chemokines, also the small collagen-breakdown product N-acetyl-Proline-Glycine-Proline (N- α -PGP) is able to induce chemotaxis of neutrophils mediated via CXCR1 and CXCR2. As such, N- α -PGP can also increase the clinical symptoms of inflammatory diseases. Our original aim was to characterize the binding mode of N- α -PGP at CXCR2 and to find antagonists that are able to block the N- α -PGP induced signals. Yet, we show that in our experimental settings N- α -PGP has no direct interaction with human CXCR2, when expressed in HEK293T or L1.2 cells (**Chapter 5**).

Besides the endogenous chemokines, also the cytomegalovirus (CMV)-encoded vCXCL1 showed to be an agonist for CXCR2 [74, 75]. The CMV probably produces vCXCL1 in endothelial cells after transfection to attract neutrophils via CXCR1/2, subsequently using neutrophils as carriers of the virus to easily infect other endothelial cells [75]. As such, blocking CXCR2 can have also a positive outcome in this situation. We have characterized vCXCL1s isolated from different clinical CMV strains. Subsequently, we have determined the binding affinity and potency of the vCXCL1s at human CXCR2 (**Chapter 6**).

An additional objective in this thesis involved the identification of novel chemotactic receptor targets in inflammatory bowel disease (IBD). For this, we used a RT-qPCR approach. We established a RT-qPCR primer set of different chemotactic receptors, including chemokine receptors and have profiled some cell lines and IBD patient material (**Chapter 7**).

References

1. Heilker, R., et al., G-protein-coupled receptor-focused drug discovery using a target class platform approach. *Drug Discov Today*, 2009. 14(5-6): p. 231-40.
2. Fredriksson, R., et al., The G-protein-coupled receptors in the human genome form five main families. Phylogenetic analysis, paralogon groups, and fingerprints. *Mol Pharmacol*, 2003. 63(6): p. 1256-72.
3. Attwood, T.K. and J.B. Findlay, Fingerprinting G-protein-coupled receptors. *Protein Eng*, 1994. 7(2): p. 195-203.
4. Kolakowski, L.F., Jr., GCRDb: a G-protein-coupled receptor database. *Receptors Channels*, 1994. 2(1): p. 1-7.
5. Ballesteros, J.A. and H. Weinstein, Integrated methods for the construction of three-dimensional models and computational probing of structure-function relations in G protein-coupled receptors. *Methods Neuroscience*, 1995. 25: 366-428.
6. Bissantz, C., A. Logean, and D. Rognan, High-throughput modeling of human G-protein coupled receptors: amino acid sequence alignment, three-dimensional model building, and receptor library screening. *J Chem Inf Comput Sci*, 2004. 44(3): p. 1162-76.
7. Hamm, H.E., The many faces of G protein signaling. *J Biol Chem*, 1998. 273(2): p. 669-72.
8. Bunemann, M., M. Frank, and M.J. Lohse, Gi protein activation in intact cells involves subunit rearrangement rather than dissociation. *Proc Natl Acad Sci U S A*, 2003. 100(26): p. 16077-82.
9. Zhang, J., et al., Molecular mechanisms of G protein-coupled receptor signaling: role of G protein-coupled receptor kinases and arrestins in receptor desensitization and resensitization. *Receptors Channels*, 1997. 5(3-4): p. 193-9.
10. Kovacs, J.J., et al., Arrestin development: emerging roles for beta-arrestins in developmental signaling pathways. *Dev Cell*, 2009. 17(4): p. 443-58.
11. Violin, J.D. and R.J. Lefkowitz, Beta-arrestin-biased ligands at seven-transmembrane receptors. *Trends Pharmacol Sci*, 2007. 28(8): p. 416-22.
12. Viola, A. and A.D. Luster, Chemokines and Their Receptors: Drug Targets in Immunity and Inflammation. *Annu Rev Pharmacol Toxicol*, 2008. 48: p. 171-197.
13. Balkwill, F., Cancer and the chemokine network. *Nat Rev Cancer*, 2004. 4(7): p. 540-50.
14. Allen, S.J., S.E. Crown, and T.M. Handel, Chemokine: receptor structure, interactions, and antagonism. *Annu Rev Immunol*, 2007. 25: p. 787-820.
15. Rajagopalan, L. and K. Rajarathnam, Structural basis of chemokine receptor function--a model for binding affinity and ligand selectivity. *Biosci Rep*, 2006. 26(5): p. 325-39.
16. Clark-Lewis, I., et al., Structure-function relationship between the human chemokine receptor CXCR3 and its ligands. *J Biol Chem*, 2003. 278(1): p. 289-95.
17. Gong, J.H. and I. Clark-Lewis, Antagonists of monocyte chemoattractant protein 1 identified by modification of functionally critical NH2-terminal residues. *J Exp Med*, 1995. 181(2): p. 631-40.
18. Kraneveld, A.D., et al., Chemokine receptors in inflammatory diseases, in *Chemokine Receptors as Drug Targets* M.J. Smit, Lira, S.A., Leurs, R, Editor. 2011, Wiley-VCH Verlag GmbH&Co. KGaA, Weinheim. p. 105-150.
19. Koelink, P.J., et al., Targeting chemokine receptors in chronic inflammatory diseases: An extensive review. *Pharmacol Ther*, 2011. in press
20. Zlotnik, A., A.M. Burkhardt, and B. Homey, Homeostatic chemokine receptors and organ-specific metastasis. *Nat Rev Immunol*, 2011. 11(9): p. 597-606.
21. Vandercappellen, J., J. Van Damme, and S. Struyf, The role of the CXC chemokines platelet factor-4 (CXCL4/PF-4) and its variant (CXCL4L1/PF-4var) in inflammation, angiogenesis and cancer. *Cytokine Growth Factor Rev*, 2011. 22(1): p. 1-18.
22. Lazenec, G. and A. Richmond, Chemokines and chemokine receptors: new insights into cancer-related inflammation. *Trends Mol Med*, 2010. 16(3): p. 133-44.
23. Feng, Y., et al., HIV-1 entry cofactor: functional cDNA cloning of a seven-transmembrane, G protein-coupled receptor. *Science*, 1996. 272(5263): p. 872-7.
24. Dragic, T., et al., HIV-1 entry into CD4+ cells is mediated by the chemokine receptor CC-CKR-5. *Nature*, 1996. 381(6584): p. 667-73.
25. Deng, H., et al., Identification of a major co-receptor for primary isolates of HIV-1. *Nature*, 1996. 381(6584): p. 661-6.
26. Proudfoot, A.E., C.A. Power, and M.K. Schwarz, Anti-chemokine small molecule drugs: a promising future? *Expert Opin Investig Drugs*, 2010. 19(3): p. 345-55.
27. Palczewski, K., et al., Crystal structure of rhodopsin: A G protein-coupled receptor. *Science*, 2000. 289(5480): p. 739-45.
28. Li, J., et al., Structure of bovine rhodopsin in a trigonal crystal form. *J Mol Biol*, 2004. 343(5): p. 1409-38.
29. Okada, T., et al., The retinal conformation and its environment in rhodopsin in light of a new 2.2 Å crystal structure. *J Mol Biol*, 2004. 342(2): p. 571-83.
30. Salom, D., et al., Crystal structure of a photoactivated deprotonated intermediate of rhodopsin. *Proc Natl Acad Sci U S A*, 2006. 103(44): p. 16123-8.
31. Standfuss, J., et al., Crystal structure of a thermally stable rhodopsin mutant. *J Mol Biol*, 2007. 372(5): p. 1179-88.
32. Cherezov, V., et al., High-resolution crystal structure of an engineered human beta2-adrenergic G protein-coupled receptor. *Science*, 2007. 318(5854): p. 1258-65.
33. Rasmussen, S.G., et al., Crystal structure of the human beta2 adrenergic G-protein-coupled receptor. *Nature*, 2007. 450(7168): p. 383-7.

34. Rosenbaum, D.M., et al., GPCR engineering yields high-resolution structural insights into beta2-adrenergic receptor function. *Science*, 2007. 318(5854): p. 1266-73.
35. Hanson, M.A., et al., A specific cholesterol binding site is established by the 2.8 Å structure of the human beta2-adrenergic receptor. *Structure*, 2008. 16(6): p. 897-905.
36. Warne, T., et al., Structure of a beta1-adrenergic G-protein-coupled receptor. *Nature*, 2008. 454(7203): p. 486-91.
37. Jaakola, V.P., et al., The 2.6 angstrom crystal structure of a human A2A adenosine receptor bound to an antagonist. *Science*, 2008. 322(5905): p. 1211-7.
38. Park, J.H., et al., Crystal structure of the ligand-free G-protein-coupled receptor opsin. *Nature*, 2008. 454(7201): p. 183-7.
39. Scheerer, P., et al., Crystal structure of opsin in its G-protein-interacting conformation. *Nature*, 2008. 455(7212): p. 497-502.
40. Wu, B., et al., Structures of the CXCR4 chemokine GPCR with small-molecule and cyclic peptide antagonists. *Science*, 2010. 330(6007): p. 1066-71.
41. Chien, E.Y., et al., Structure of the human dopamine D3 receptor in complex with a D2/D3 selective antagonist. *Science*, 2010. 330(6007): p. 1091-5.
42. Rasmussen, S.G., et al., Structure of a nanobody-stabilized active state of the beta(2) adrenoceptor. *Nature*, 2011. 469(7329): p. 175-80.
43. Rosenbaum, D.M., et al., Structure and function of an irreversible agonist-beta(2) adrenoceptor complex. *Nature*, 2011. 469(7329): p. 236-40.
44. Xu, F., et al., Structure of an agonist-bound human A2A adenosine receptor. *Science*, 2011. 332(6027): p. 322-7.
45. Lebon, G., et al., Agonist-bound adenosine A(2A) receptor structures reveal common features of GPCR activation. *Nature*, 2011. 474: 521-525.
46. Moukhametzianov, R., et al., Two distinct conformations of helix 6 observed in antagonist-bound structures of a {beta}1-adrenergic receptor. *Proc Natl Acad Sci U S A*, 2011. 108(20): p. 8228-32.
47. Shimamura, T., et al., Structure of the human histamine H1 receptor complex with doxepin. *Nature*, 2011. 475: 65-70.
48. Joseph, P.R., et al., Probing the role of CXC motif in chemokine CXCL8 for high affinity binding and activation of CXCR1 and CXCR2 receptors. *J Biol Chem*, 2010. 285(38): p. 29262-9.
49. Hebert, C.A., R.V. Vitangcol, and J.B. Baker, Scanning mutagenesis of interleukin-8 identifies a cluster of residues required for receptor binding. *J Biol Chem*, 1991. 266(28): p. 18989-94.
50. Clark-Lewis, I., et al., Platelet factor 4 binds to interleukin 8 receptors and activates neutrophils when its N terminus is modified with Glu-Leu-Arg. *Proc Natl Acad Sci U S A*, 1993. 90(8): p. 3574-7.
51. Schraufstatter, I.U., et al., Multiple sites on IL-8 responsible for binding to alpha and beta IL-8 receptors. *J Immunol*, 1993. 151(11): p. 6418-28.
52. Clark-Lewis, I., et al., Structure-activity relationships of interleukin-8 determined using chemically synthesized analogs. Critical role of NH2-terminal residues and evidence for uncoupling of neutrophil chemotaxis, exocytosis, and receptor binding activities. *J Biol Chem*, 1991. 266(34): p. 23128-34.
53. Clark-Lewis, I., et al., Structural requirements for interleukin-8 function identified by design of analogs and CXC chemokine hybrids. *J Biol Chem*, 1994. 269(23): p. 16075-81.
54. Fernandez, E.J. and E. Lolis, Structure, function, and inhibition of chemokines. *Annu Rev Pharmacol Toxicol*, 2002. 42: p. 469-99.
55. Lowman, H.B., et al., Exchanging interleukin-8 and melanoma growth-stimulating activity receptor binding specificities. *J Biol Chem*, 1996. 271(24): p. 14344-52.
56. Kulke, R., et al., The CXC receptor 2 is overexpressed in psoriatic epidermis. *J Invest Dermatol*, 1998. 110(1): p. 90-4.
57. Qiu, Y., et al., Biopsy neutrophilia, neutrophil chemokine and receptor gene expression in severe exacerbations of chronic obstructive pulmonary disease. *Am J Respir Crit Care Med*, 2003. 168(8): p. 968-75.
58. Barnes, P.J., Mediators of chronic obstructive pulmonary disease. *Pharmacol Rev*, 2004. 56(4): p. 515-48.
59. Barnes, P.J., Immunology of asthma and chronic obstructive pulmonary disease. *Nat Rev Immunol*, 2008. 8(3): p. 183-92.
60. Donnelly, L.E. and P.J. Barnes, Chemokine receptors as therapeutic targets in chronic obstructive pulmonary disease. *Trends Pharmacol Sci*, 2006. 27(10): p. 546-53.
61. Keatings, V.M., et al., Differences in interleukin-8 and tumor necrosis factor-alpha in induced sputum from patients with chronic obstructive pulmonary disease or asthma. *Am J Respir Crit Care Med*, 1996. 153(2): p. 530-4.
62. Morrison, D., et al., Neutrophil chemokines in bronchoalveolar lavage fluid and leukocyte-conditioned medium from nonsmokers and smokers. *Eur Respir J*, 1998. 12(5): p. 1067-72.
63. Yamamoto, C., et al., Airway inflammation in COPD assessed by sputum levels of interleukin-8. *Chest*, 1997. 112(2): p. 505-10.
64. Ajuebor, M.N., M.G. Swain, and M. Perretti, Chemokines as novel therapeutic targets in inflammatory diseases. *Biochem Pharmacol*, 2002. 63(7): p. 1191-6.
65. Apostolopoulos, J., P. Davenport, and P.G. Tipping, Interleukin-8 production by macrophages from atherosclerotic plaques. *Arterioscler Thromb Vasc Biol*, 1996. 16(8): p. 1007-12.
66. Banks, C., et al., Chemokine expression in IBD. Mucosal chemokine expression is unselectively increased in both ulcerative colitis and Crohn's disease. *J Pathol*, 2003. 199(1): p. 28-35.
67. Deleuran, B., et al., Localisation of interleukin 8 in the synovial membrane, cartilage-pannus junction and chondrocytes in rheumatoid arthritis. *Scand J Rheumatol*, 1994. 23(1): p. 2-7.

68. Endo, H., et al., Elevation of interleukin-8 (IL-8) levels in joint fluids of patients with rheumatoid arthritis and the induction by IL-8 of leukocyte infiltration and synovitis in rabbit joints. *Lymphokine Cytokine Res*, 1991. 10(4): p. 245-52.
69. Kraan, M.C., et al., The development of clinical signs of rheumatoid synovial inflammation is associated with increased synthesis of the chemokine CXCL8 (interleukin-8). *Arthritis Res*, 2001. 3(1): p. 65-71.
70. Wang, N., et al., Interleukin 8 is induced by cholesterol loading of macrophages and expressed by macrophage foam cells in human atheroma. *J Biol Chem*, 1996. 271(15): p. 8837-42.
71. Scholten, D.J., et al., Pharmacological Modulation of Chemokine Receptor Function. *British Journal of Pharmacology*, 2011. in press
72. Christopoulos, A. and T. Kenakin, G protein-coupled receptor allostereism and complexing. *Pharmacol Rev*, 2002. 54(2): p. 323-74.
73. Weathington, N.M., et al., A novel peptide CXCR ligand derived from extracellular matrix degradation during airway inflammation. *Nat Med*, 2006. 12(3): p. 317-23.
74. Penfold, M.E., et al., Cytomegalovirus encodes a potent alpha chemokine. *Proc Natl Acad Sci U S A*, 1999. 96(17): p. 9839-44.
75. Lutichau, H.R., The cytomegalovirus UL146 gene product vCXCL1 targets both CXCR1 and CXCR2 as an agonist. *J Biol Chem*, 2010. 285(12): p. 9137-46.
76. Johnson, Z., et al., Multi-faceted strategies to combat disease by interference with the chemokine system. *Trends Immunol*, 2005. 26(5): p. 268-74.
77. Rasmussen, S.G. et al., Crystal structure of the $\beta(2)$ adrenergic receptor-Gs protein complex. *Nature* 2011. In press.

Chemokine receptors in Inflammatory Diseases

Chapter 2

Petra de Kruijf ^{A,1}, Pim Koelink ^{B,1}, Saskia Braber ^{B,1}, Saskia Overbeek ^{B,1},
Aletta D. Kraneveld ^B, Gert Folkerts ^B and Martine J. Smit ^A

^A Leiden/Amsterdam Center for Drug Research, Division of Medicinal Chemistry,
Vrije Universiteit Amsterdam, The Netherlands

^B Division of Pharmacology and Pathophysiology, Utrecht Institute for Pharmaceutical Sciences,
Faculty of Science, Utrecht University, Utrecht, The Netherlands

¹ Contributed equally

Published as:

Chapter 6 in *Chemokine Receptors as Drug Targets* M.J. Smit, Lira, S.A., Leurs, R,
Editor. 2011, Wiley-VCH verlag GmbH&Co. KGaA, Weinheim.

and: *Pharmacol Ther.* 2011, *in press*

Abstract

Trafficking of different types of immune cells is an important aspect in the immune response. Chemokines are soluble peptides that are able to attract cells by interaction with chemokine receptors on their target cells. Several different chemokines and receptors exist enabling the specific trafficking of different immune cells. In chronic inflammatory disorders there is abundance of immune cells present at the inflammatory site. This chapter focuses on the role of chemokine receptors in chronic inflammatory disorders, like Chronic Obstructive Pulmonary Disease (COPD), asthma, Inflammatory Bowel Disease (IBD), Rheumatoid Arthritis (RA), atherosclerosis, Multiple Sclerosis (MS) and psoriasis.

Acknowledgements

This chapter was written within the framework of the Dutch Top Institute Pharma project T101-3.

Introduction

Inflammation and the immune system are closely related. An immune reaction is a complex reaction to tissue injury and infection, characterized by the classic response of rubor (redness), calor (heat), tumor (swelling), dolor (pain) and *functio laesa* (loss of function). The immune system consists of cells and soluble factors that mediate the reaction in order to eliminate the immune stimulus and initiate the process of immunological memory. Diseases of immunity can occur due to inappropriate inflammation or when the normal immune response progresses to chronic inflammation, either because of a long-term inappropriate response to stimuli (e.g., allergies) or because the offending agent is not removed (e.g., autoimmunity).

The major events in chronic inflammatory responses are continuous activating tissue resident immune cells and ongoing infiltration of circulating immune cells after which mechanisms of innate and adaptive immunity serve to neutralize and remove the inflammatory stimulus. Chemokines are a subset of cytokines that promote immune cell trafficking and localization to sites of inflammation.

Several pharmacological strategies are used to target the pathophysiology of inflammatory, c.q. immune, diseases. One involves modification of the signaling mediators of the inflammatory process. A second approach is to induce suppression of components of the immune system. Both approaches are the rational for drugs that affect the production of inflammatory mediators and cells from the immune system. The molecular events in the relevant pathways leading to immune diseases are still not fully unraveled but more understanding promises to yield a number of new drugs in the foreseeable future.

This chapter discusses the role of chemokines and their receptors in inflammatory diseases of the airways (asthma and COPD), the intestinal tract (inflammatory bowel diseases), the joints (arthritis), the blood vessels (arteriosclerosis), the central nervous system (multiple sclerosis) and the skin (psoriasis). Investigations of receptor-mediated and intracellular signal pathways in chemokine-receptor interactions might help to develop more effective therapeutic approaches for chronic inflammatory diseases.

Chemokine receptors on inflammatory/immune cells

There are many different cell types in the immune system and these cells interact in a complex reaction of signaling and communication to create the overall response. The cells of the immune system derive from two types of cells in the bone marrow; myeloid stem cells and lymphoid stem cells. Myeloid cells give rise to precursor cells of the innate immune system, whereas lymphoid cells generate precursors of cells of the adaptive immune system. Chemokine receptors are found on almost all immune cells.

The major cell types of the innate immune system include monocytes (blood precursor cells of antigen-presenting cells), antigen-presenting cells (macrophages and dendritic cells), granulocytes (neutrophil, eosinophils and basophils), mast cells and natural killer cells. All these cells express a specific subset of chemokine receptors (see Table 2.1-2.3) that direct migration through interaction with their respective chemokines. Besides they are also an important source for chemokines. Upon stimulation, monocytes and macrophages can e.g. release CCL1-10, CCL12, CCL15-18, CCL20, CCL22-24, CXCL1-3, CXCL6, CXCL8-11, CXCL13, CXCL14 and CXCL16. Neutrophils release CCL2-4, CCL19, CCL20, CXCL1-3 and CXCL8-11, eosinophils release CCL3, CCL4 and CCL11 and basophils can be a source for the chemokines CCL4 and CXCL8. Furthermore, after cross-linking with the IgE receptor, human mast cells can release CCL1-5, CCL7, CCL11, CCL19, CXCL1, CXCL2, CXCL5, CXCL8 and XCL1. In addition, natural killer cells can produce CCL1, CCL3-5, CCL15, CCL22, CXCL8 and XCL1-2 [1-4].

Table 2.1: CXCR chemokine receptor family and inflammatory cells [2, 4, 117, 181, 203-209].

Receptor	Ligands	Expression
CXCR1	CXCL6, CXCL7, CXCL8	neutro, baso, mono/mΦ, immature mDC, NK cell, MC
CXCR2	CXCL1, CXCL2, CXCL3, CXCL5, CXCL6, CXCL7, CXCL8	neutro, eosino, mono/mΦ, immature mDC, microvascular endothelial cell, T cell, NK cell, MC
CXCR3A	CXCL9, CXCL10, CXCL11	neutro, eosino, pDC, Th1 cell, B cell, NK cell, MC
CXCR3B	CXCL4, CXCL9, CXCL10, CXCL11	microvascular endothelial cell, neoplastic cell
CXCR4	CXCL12	neutro, eosino, baso, mono/mΦ, immature mDC, mature mDC, pDC, naïve T cell, memory T cell, Th1 cell, Th2 cell, Th17 cell, Treg cell, B cell, NK cell, platelets
CXCR5	CXCL13	B cell, T cell
CXCR6	CXCL16	memory T cell, Th1 cell, NK cell
CXCR7	CXCL11, CXCL12	tumor cell

Neuto: neutrophils; eosino: eosinophils; baso: basophils; mono: monocytes; mΦ: macrophages; DS: dendritic cells; pDC: plasmoid dendritic cells; mDC: myeloid dendritic cells; Th cell: Thelper cells; Treg cells: regulatory T cells; fibro: fibroblasten; NK cells: natural killer cells; MC: mast cells.

While innate immune mechanisms contribute to the first line of defense, at the same time, pathogens are taken up and presented by antigen-presenting cells to adaptive immune cells to allow the induction of an antigen-specific immune response directed against distinctive molecular targets. This process will lead either to a humoral immune response, where antigen-specific immunoglobulins produced by B lymphocytes play a central role, or to a cellular immune response, where antigen-specific CD4⁺ T lymphocytes (Thelper1, Thelper2 and Thelper 17 cells) or CD8⁺ T cells (cytotoxic T cells) are the central players. Chemokines are crucially involved in the migration and homing of B cells and T cells.

Table 2.2: CC chemokine receptor family and inflammatory cells [2, 4, 117, 203, 205-209].

Receptor	Ligands	Expression
CCR1	CCL2, CCL3, CCL3, CCL4, CCL5, CCL7, CCL8, CCL13, CCL14, CCL15, CCL16, CCL23	neutro, eosino, baso, mono/ mΦ, immature DC, memory T cell, B cell, NK cell, MC
CCR2	CCL2, CCL7, CCL8, CCL13, CCL16	neutro, eosino, baso, mono/ mΦ, immature DC, pDC, B cell, memory T cell, Treg cell, NK cell
CCR3	CCL5, CCL7, CCL8, CCL11, CCL13, CCL15, CCL16, CCL24, CCL26, CCL28	neutro, eosino, baso, T cell, Th2 cell, MC, platelets, endothelial cell
CCR4	CCL17, CCL22	eosino, baso, mono/mΦ, immature DC, mature DC, Th2 cell, Treg cell, NK cell, thymocyte, platelets
CCR5	CCL3, CCL4, CCL5, CCL7, CCL8, CCL11, CCL13, CCL14, CCL16	mono/mΦ, pDC, immature mDC, mature mDC, Th1 cell, Treg cell, B cell, NK cell, thymocyte
CCR6	CCL20	immature mDC, memory T cell, Th17 cell, Treg cell, B cell
CCR7	CCL19, CCL21	mature mDC, pDC, naïve T cell, Th1 cell, Th2 cell, Treg cell, B cell, NK cell
CCR8	CCL1	neutro, mono/mΦ, DC, Th2 cell, Treg cell, B cell, thymocyte
CCR9	CCL25	memory T cell, thymocyte, epithelial cell, IgA+ plasma cell
CCR10	CCL27, CCL28	memory T cell, B cell, fibro, epithelial cell

Neutro: neutrophils; eosino: eosinophils; baso: basophils; mono: monocytes; mΦ: macrophages; DC: dendritic cells; pDC: plasmoid dendritic cells; mDC: myeloid dendritic cells; Th cell: Thelper cells; Treg cells: regulatory T cells; fibro: fibroblasten; NK cells: natural killer cells; MC: mast cells.

Table 2.3: XC and CX3C chemokine receptor and inflammatory cells [2, 4, 117, 203, 205, 207-210].

Receptor	Ligands	Expression
XCR1	XCL1, XCL2	T cell, NK cell, MC
CX ₃ CR1	CX3CL1	neutro, mono/mΦ, DC, Th1 cell, NK cell, endothelial cell

Neutro: neutrophils; mono: monocytes; mΦ: macrophages; DC: dendritic cells; Th cell: Thelper cells; NK cells: natural killer cells; MC: mast cells.

Both B-cells and the six different types of T cells (helper T-cells (Th), cytotoxic T-cells (Tc), memory T-cells, regulatory T-cells (Treg), natural killer T-cells (NKT) and $\gamma\delta$ T-cells) express different chemokine receptors (Table 2.1-2.3). Like the cells of the innate immune system, they are a source of chemokines. B-cells can release CCL15, CCL22, CXCL14 and CXCL16, whereas T-cells produce CCL1, CCL5, CCL15, CCL20, CCL22, CCL24, CXCL8, CX3CL1, XCL1 and XCL2 [2, 4].

In general, CXC chemokines are attractants for neutrophils and T lymphocytes; ELR-CXC chemokines for B and T lymphocytes (Table 2.1); CC chemokines induced chemotaxis of multiple subsets of white blood cells, such as monocytes, basophils, dendritic cells, macrophages, NK cells and T cells (Table 2.2). C chemokines are important for travelling of T cells to the thymus and the CX3C chemokine, fractalkine, also acting as an adhesion molecule, seems to be important for the infiltration of T cells, NK cells and monocytes (Table 2.3).

Chemokine receptors and inflammatory lung diseases

The two most prevalent chronic inflammatory lung diseases are asthma and chronic obstructive pulmonary disease (COPD). These diseases are a major and increasing global health problem. Both asthma and COPD share some clinical features such as, increased airway obstruction, mucous hypersecretion, acute exacerbations and respiratory symptoms. Asthma and COPD are identified by the presence of chronic inflammation of the airways, which is controlled by the increased expression of inflammatory proteins, including cytokines, chemokines, receptors, enzymes and adhesion molecules [5, 6]. Although there is a considerable overlap in the pathogenesis between COPD and asthma, there are marked differences in the characteristics of this inflammatory process. Asthma and COPD may be distinguished by the site of inflammation, types of inflammatory cells, different mediators, different inflammatory effects, and different response to treatment [5-7].

COPD

COPD, a term referring to two lung diseases: chronic bronchitis and emphysema, is characterized by airflow limitation that is not fully reversible, is usually progressive, and is associated with an abnormal inflammatory response of the lungs to noxious particles or gases [8]. COPD is primarily associated with cigarette smoke where recurrent lung inflammation lead to a progressive decline in lung function. Most of the pathologic changes caused by inflammation are found in the small airways and in lung parenchyma [7]. COPD is a complex inflammatory disease that involves different inflammatory cell types, like macrophages, neutrophils, and CD8⁺ T lymphocytes [5, 9, 10].

Chemokines and their receptors in COPD

In COPD the inflammatory cascade starts with exposure to cigarette smoke or other irritants, which activate the epithelial cells and the macrophages in the respiratory tract. When these cells are activated they have the capacity to release several chemotactic factors. Chemotactic factors use specific chemokine receptors to induce inflammatory cell migration to the airways (See Fig. 2.1 [5]).

First, the chemotactic factor CCL2 (MCP-1) is a CC-chemokine that mediates its effects via the CCR2 chemokine receptor. This specific receptor for CCL2 is expressed by monocytes, macrophages, T lymphocytes and epithelial cells. It is known from literature that the chemoattractant CCL2 and the receptor CCR2 are involved in the recruitment of monocytes into the airway epithelium in COPD. Under migration into tissues, monocytes differentiate into macrophages. Macrophages are important in the pathogenesis of COPD, reflecting in an increased number of macrophages in the lungs of COPD patients [11-13]. Nevertheless, the CCR2 receptor might play a crucial role in COPD, since CCL2 levels are increased in the sputum, BALF and lungs of patients suffering from COPD [13].

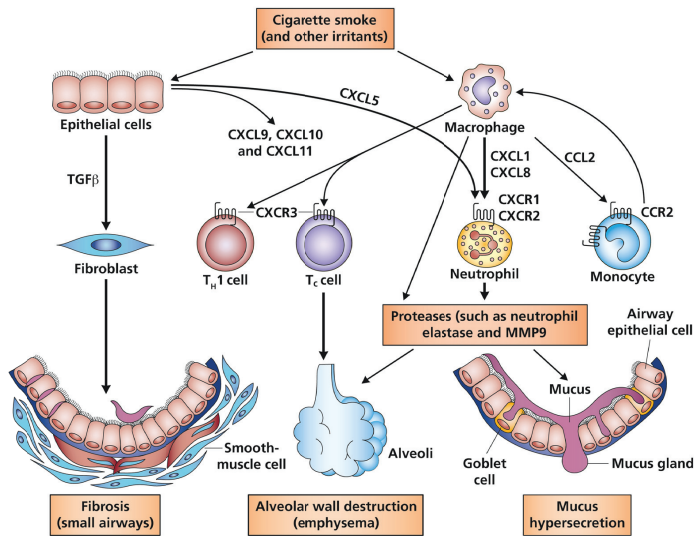


Figure 2.1: Involvement of chemokines and chemokine receptors and different cell types in the inflammation of COPD. Chemokines released from epithelial cells and macrophages in the lung recruit inflammatory cells from the circulation leading to the development of COPD. Adapted from [201].

One of the most important chemokines associated in the recruitment of inflammatory cells in COPD is the CXC-chemokine CXCL8 [9]. CXCL8 binds to both CXCR1 and CXCR2 chemokine receptors, which are expressed on a broad range of leukocytes, predominantly neutrophils. Recent studies demonstrated a significantly increased expression of CXCR1 on circulating neutrophils in COPD patients compared to healthy controls [14]. Furthermore, it is established that the expression of CXCR2 in bronchial biopsies of COPD patients is increased [15]. These two receptors have the capacity to regulate the migration of neutrophils into the pulmonary tissue during the neutrophilic inflammation in COPD. Also activated neutrophils are undoubtedly crucial players in the pathogenesis of COPD. CXCL8, is secreted by several cell types, like macrophages, neutrophils and airway epithelial cells and is

a powerful chemotactic mediator for neutrophils. Among CXCL8, the CXCR2 receptor is also selectively activated by CXCL1 (GRO- α). CXCL1 is secreted by alveolar macrophages and airway epithelial cells and is a potent chemoattractant of neutrophils and monocytes. The concentration neutrophils is increased in the sputum and bronchoalveolar lavage fluid (BALF) of COPD patients and this is related to the increased production of CXCL1 and CXCL8 [5, 9, 12, 16, 17]. It has been considered in neutrophil chemotaxis that the CXCR2 receptor responds not only to CXCL8 and CXCL1, but also to other chemokines including, CXCL2, CXCL3, CXCL5, CXCL6 and CXCL7. CXCL5 is predominantly derived from epithelial cells and BALF cells from smokers release more CXCL5 than cells from non-smokers [18]. CXCL7 is chemotactic for neutrophils as well as for monocytes and shows an enhanced chemotactic activity for monocytes from COPD patients which is similar to the chemotactic activity of CXCL1 [19].

In addition to macrophages and neutrophils, the T cell is also a potentially important factor in the initial inflammatory process leading to COPD. This is supported by the finding of an increased number of T-cells in the airways and in lung parenchyma COPD patients, to a greater extent in CD8⁺ T cells compared to CD4⁺ cells [20, 21]. Lymphocytes, particularly type-1 T lymphocytes (Th1/Tc1 cells), express the chemokine receptor CXCR3. In the airways of COPD patients an increase in the number of CXCR3⁺ T cells and an increased expression of CXCR3 was observed. T cells may be attracted to the lungs by IFN γ and IFN γ -induced CXCR3 receptor ligands: CXCL9 (MIG), CXCL10 (IP-10) and CXCL11 (I-TAC). All three chemokines activate CXCR3 and are present at high levels in COPD airways [22, 23]. Kelsen and coworkers demonstrated that human airway epithelial cells also express the CXCR3 chemokine receptor and activation of CXCR3 by CXCL9, CXCL10 and CXCL11 may contribute to airway inflammation/remodelling in the development of COPD [24]. Furthermore, CXCR3 knockout mice showed less lung inflammation induced by cigarette smoke exposure compared with the wildtype mice [25]. Even as the CXCR3 receptor, the CCR5 receptor is also expressed on Th1 and Tc1 cells and might have a cooperative role with CXCR3 in the recruitment of these cells into the lungs [26]. The CCR5 ligand CCL5 is elevated in sputum from COPD patients, this increase is also observed in the airways and sputum of COPD patients during exacerbations [22, 27].

Due to the activity of these inflammatory cells as well as the epithelial cells by receptor-ligand interactions, the inflammatory response in COPD is further augmented leading to the induction and release of different proteases, including, matrix metalloproteinases (MMPs, e.g. MMP-9) and neutrophil elastase. This proteolytic cascade leads to the remodelling of the lung tissue by collagen and elastin degradation (emphysema) and mucus hypersecretion (chronic bronchitis). The protease-antiprotease imbalance hypothesis is thought to play a key role in the development of COPD [5, 28, 29].

Finally, epithelial cells and macrophages in the small airways also regulate the proliferation of fibroblasts by releasing transforming growth factor- β (TGF β), resulting in fibrosis, a clinical

feature of COPD [30]. (See Fig. 2.1 [5]). In Table 2.4 the different chemokine receptors and their ligands demonstrated to be involved in COPD are summarized.

Table 2.4: Chemokine receptors and their ligands demonstrated to be involved in COPD [5, 12, 22, 27, 54, 211-216].

Receptor	Ligands	Target cells in COPD
CXCR1	CXCL6, CXCL7, CXCL8	neutro, mono/mΦ
CXCR2	CXCL1, CXCL2, CXCL3, CXCL5, CXCL6, CXCL7, CXCL8	neutro, mono/mΦ
CXCR3	CXCL9, CXCL10, CXCL11	T cell
CCR2	CCL2	mono/mΦ, T cell
CCR5	CCL5	T cell

neutro: neutrophils; mono: monocytes; mΦ: macrophages.

Asthma

Asthma is defined by three characteristic features: airway inflammation, intermittent reversible airway obstruction and airway hyperresponsiveness [31]. This results in the clinical expression of a lower airway obstruction that usually is reversible. Asthma involves inflammation in the lower airways but without involvement of the lung parenchyma [7]. This inflammatory disease is characterized by activated T helper type 2 (Th2) lymphocytes, eosinophils and activated mast cells [32]. Several distinct asthma phenotypes exist, in particular atopic and non-atopic asthma. Atopic asthma is correlated with an elevation of total and allergen-specific IgE in the serum in contrast with the non-atopic asthmatics. In these patients there is no evidence of allergen-specific serum IgE and even total serum IgE levels are within the normal range [33].

Chemokines and their receptors in asthma

In asthma the allergic cascade, which is crucial in the development of airway inflammation, starts with exposure to inhaled allergens and other exogenous stimuli (Fig. 2.2). These allergens bind to allergen-specific immunoglobulin E (IgE) on mast cells, crosslinking the IgE molecules and aggregating the underlying FcεRI receptors. Activation of mast cells leads to the release of several mediators, like histamine, leukotrienes and prostaglandins, which cause bronchoconstriction of the airway smooth muscle cells [5, 34]. In addition, mast cells also release T helper 2 (Th2) - derived cytokines, like IL-4, IL-5 and IL-13, which trigger eosinophilia, mucus hypersecretion and IgE production by B cells [35]. Besides the FcεRI receptor, the human lung mast cells also express different chemokine receptors, particularly CCR1, CCR3, CXCR1, CXCR3 and CXCR4. Lung mast cell migration to the airway smooth muscle is induced through activation of these receptors by the respective ligands CCL5, CCL11, CXCL8, CXCL10 and CXCL12. This infiltration of mast cells into the airway

smooth muscle has been related to airway hyperresponsiveness, found in asthma. The most abundant chemokine receptor on lung mast cells in the airway smooth muscle in asthma is the CXCR3 receptor. This is correlated with the increased expression of the CXCR3 ligand CXCL10 in bronchial biopsies of asthma patients compared to healthy controls [36-39].

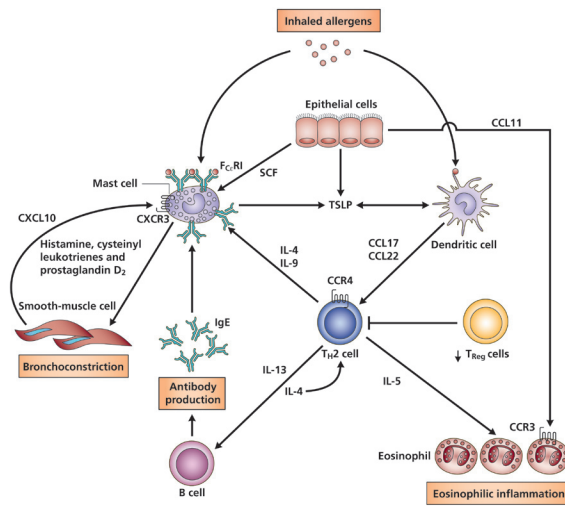


Figure 2.2: Involvement of chemokines, chemokine receptors and different cell types in the development asthma. Adapted from [201].

Asthma is a disease in which Th2 cells play a critical role, but the mechanisms of Th2 recruitment within the lungs remain poorly defined. Th2 cells express the chemokine receptors CCR8 and CCR4 [40, 41]. After a challenge with an allergen, the CCR4 receptor and, to a lesser extent, CCR8 mark the majority of T cells infiltrating the lung of asthmatics [42]. These receptors play an important role in the recruitment of Th2 cells to the sites of inflammation in (late) asthmatic responses. It has been described that DCs can produce two ligands, which can activate the CCR4 receptor: CCL17 and CCL22. Furthermore, it is demonstrated that CCR4^{-/-} and CCR8^{-/-} mice develop less airway hyperresponsiveness and show a reduction of eosinophils infiltration in the airways [43, 44]. Moreover, the CXCR3 and the CCR5 receptor are also expressed on human lung T-cells [45] and this expression is increased after ovalbumin challenge in mice. Recent studies indicated that targeting these two receptors can prevent the development of asthma in a mouse model [46]. The CCR2 chemokine receptor on Th2 cells and the ligand CCL2 have also been proposed to play a role in pulmonary T cell recruitment in asthma. *In vivo* studies demonstrated that CCR2^{-/-} mice are resistant to bronchial hyperreactivity after allergen challenge compared to control mice [47]. Additionally, it has been suggested that the CXCR4 chemokine receptor expressed on Th2 cells is a potential therapeutic target in asthma. This because it has previously been shown that CXCL12, the CXCR4 ligand, has chemotactic properties for a variety of cells

[48, 49]. Finally, there is growing evidence that besides Th2 cells, T regulatory (Treg) cells are involved in the development asthma [50, 51].

Last but not least, the eosinophil is another important participant in the pathogenesis of asthmatic inflammation and about 80% of the asthma patients show an increased number of eosinophils. Airway epithelial cells are an important source of chemokines and contribute to recruitment of eosinophils to and within the lung. Predominantly, the CCR3 ligand CCL11 (eotaxin) attracts and activates eosinophils by acting via the most prominent chemokine receptor on eosinophils: the CCR3. Ying and coworkers demonstrated an enhanced level of eotaxin and CCR3 in asthmatic patients compared to healthy controls [52]. Other potent eosinophil chemoattractants who induce eosinophil recruitment into the airways via the CCR3 receptor are CCL5 (RANTES), CCL7 (MCP-3) and CCL13 (MCP-4) [53]. Although eosinophils are the major granulocytes in the development of COPD, a neutrophil influx is detected during acute exacerbations, in severe asthma patients and in non-eosinophilic asthma. This influx is mediated by CXCL8, which act on the two CXCL8 chemokine receptors on neutrophils: CXCR1 and CXCR2, whereas CXCR1 is important in neutrophil activation [54, 55]. In Table 2.5 the different chemokine receptors and their ligands demonstrated to be involved in asthma are summarized.

Table 2.5: Chemokine receptors and their ligands demonstrated to be involved in asthma [1, 2, 4, 37, 41, 42, 46, 49, 55, 216, 217].

Receptor	Ligands	Target cells in asthma
CCR1	CCL5	MC, T cell, eosino
CCR2	CCL2	T cell
CCR3	CCL5, CCL7, CCL11, CCL13	eosino, T cell (Th2), MC
CCR4	CCL17, CCL22	T cell (Th2)
CCR5	CCL5	T cell
CCR8	CCL1	T cell (Th2)
CXCR1/2	CXCL8	MC, neutro
CXCR3	CXCL10	MC
CXCR4	CXCL12	T cell (Th2), MC

MC: mast cells; eosino: eosinophils

Inflammatory bowel disease

The term inflammatory bowel disease is used to describe chronic inflammatory conditions of the gastro-intestinal tract. Inflammatory bowel disease is an idiopathic disease characterized by swings between intestinal inflammation and remission. Patients suffer from abdominal pain and cramps, weight loss, diarrhea, cachexia, disrupted digestion, rectal bleeding and a substantial personal burden. Inflammatory bowel disease can be subdivided into two

major representatives, Crohn's Disease and ulcerative colitis. Although the clinical pathological phenotype of these two disorders is similar, they can be separated by different localization of the inflammation in the gastro-intestinal tract and immunological and histological pattern. Roughly it can be stated that Crohn's disease is characterized by a transmural inflammation which can be found throughout the whole gastro-intestinal tract but mainly in the terminal ileum, ulcerative colitis is a mucosal inflammation restricted to the colon. Moreover, Crohn's disease is postulated to be a T-helper1 and T-helper17-mediated disease [56] whereas ulcerative colitis is mainly a T-helper2-mediated disorder [57].

The exact etiology of inflammatory bowel disease remains unknown but is thought to be a complex interaction of genetic, environmental (i.e. enteric microflora) and immunological factors [58, 59]. Current investigations and observations suggest that the initial event in inflammatory bowel disease is a result of a dysregulated inflammatory response rather than an aggressive inflammatory response by a defective intestinal immune system [60]. Although it is suggested that inflammatory bowel disease might be an autoimmune disease, potential enteric antigens for the exacerbation of inflammatory bowel disease are luminal bacteria, parasitic nematodes or food allergens [59, 61]. Therapy for inflammatory bowel disease is merely symptom relieving and relies highly on the use of aminosalicylates, corticosteroids and immunosuppressive drugs [62]. However, new developments in treating inflammatory bowel disease can be found in biological treatments with antibodies directed against tumor necrosis factor- α [63] and with pro- and prebiotics as well [64].

Chemokines and their receptors in inflammatory bowel disease

The contribution of chemokines to the pathogenesis of inflammatory bowel disease stems from a series of clinical and animal model studies (Table 2.6) [65, 66]. Several chemokines have been described in both ulcerative colitis and Crohn's disease and their expression is consistently increased during the active phase of disease. Especially, CXCL1 (Gro- α), CXCL2 (Gro- β), CXCL5 (ENA-78), CXCL6 (GCP-2) and CXCL8 (IL-8) and their receptor CXCR1 and 2 are upregulated in inflammatory bowel disease as are CXCR3 and 4 receptor ligands, such as interferon inducible protein 10 (CXCL10) and stromal cell derived factor 1 (CXCL12), respectively [65, 67-69]. In addition, CCR1, CCR2, CCR3 and CCR5 receptor ligands are reported to be increased in inflammatory bowel disease: CCL2 (MCP-1), CCL3 (MIP-1 α), CCL4 (MIP-1 β), CCL7 (MCP-3) and CCL8 (MCP-2) and regulated on activation, normal T cells express and secrete CCL5 (RANTES) [65-67, 70]. A number of recent studies has demonstrated that antagonists targeted against chemokine or their receptors are effective in inhibiting acute and chronic inflammation in animal models for inflammatory bowel disease. In trinitrobenzene sulfonic acid-induced colitis, the increased colonic expression of KC/mCXCL1 and CXCR2 receptor expression was associated with leukocyte recruitment, whereas increased CCL3 expression was associated with both leukocyte infiltration and the onset of ulcerative lesions [65]. In addition, CCR2 and CCR5 receptor deficient mice exhibited a reduction in colonic inflammation [71]. Notably, CCL5 (RANTES) has been shown to be crucial in the transition from acute to chronic disease in experimental model of colitis [72].

Table 2.6: Chemokines and chemokine receptors and target cells demonstrated to be involved in inflammatory bowel disease [65-69].

Receptor	Ligands	Target cells in IBD
	CCL2	Th cell, mono, baso
	CCL3	Tc cell
	CCL4	Th cell
	CCL7	mono, baso
	CCL8	neutro, baso, mono
CCR4	?	Treg cell
CCR5	CCL5	Th cell, mono, baso
CCR6	CCL25	Th 17 cell
CCR7	?	Treg cell
CCR9	CCL25	Th 17 cell
CXCR1/2	CXCL1, CXCL2, CXCL5, CXCL6, CXCL8	neutro, baso
CXCR3	CXCL10	T cell, mono
	CXCL12	T cell, B cell
CX ₃ CR1	CX3CL1	mono, DC

Tc cell: cytotoxic T cell; Th cell: T helper cell; Treg cell: regulatory T cell; neutro: neutrophils; baso: basophils; mono: monocytes; DC: dendritic cells.

Targeting Th1 cells via CXCR3, using antibodies directed against CXCL10 or blocking the CXCR3 receptor, in different animal models demonstrated prevention of onset and cure of pre-existing colitis [69]. Th17 cells are getting more and more attention in relation to inflammatory bowel disease, especially Crohn's Disease. CCR6 and its ligand CCL20 have been identified on Th17 cells in inflammatory lesions of Crohn's patients [73]. Moreover, it has also been reported that colonic epithelial cells from IBD patients show an increased expression of CCL20 [74, 75]. In addition, neutralizing CCL20 significantly ameliorated murine colitis, which was associated with a decreased influx of CCR6⁺ T cells, probably of Th17 subtype, in the lamina propria [76].

CCR9, the receptor for CCL25, is abundantly expressed on intraepithelial and lamina propria T cells. Infiltration of CCR9⁺ T cells into the intestinal mucosa has been shown to play a role in IBD. These mucosal CCR9⁺ T cells might be Th17 cells, since it has been demonstrated that Th17 cells express CCR9 and CCR9⁺ T cells can produce IL17. Its targetability in IBD has recently been reviewed by Koenecke and coworkers [77]. At the Digestive Disease Week 2009, the results of a phase II/III clinical trial using CCR9 antagonist in moderate to severe Crohn's Disease patients were presented. Oral treatment with the CCR9 receptor antagonist resulted in reduced disease severity, associated with colonoscopic evidence of improvement [78]. Although clinical trials are being conducted, preclinical data in animal models of IBD are lacking. Only one study reported that antibody blockade of CCR9 and CCL25 using attenuated early development of ileitis in mice but showed no therapeutic efficacy during the

later stages [79]. CCR9 could be a very promising target for Crohn's Disease, however more preclinical and clinical research is needed.

Regulatory T cells (Treg cells) are a critical subpopulation T cells essential for the maintenance of self-tolerance. It has been hypothesized that reduced regulatory T cell function is related to exacerbations of inflammatory bowel disease. Two reports describe the critical role of CCR4 and CCR7 in homing of Treg cells to the intestine. An inefficient accumulation of CCR4 deficient Treg cells correlated with the development of colitis [80]. And CCR7 is required for the in vivo function of Treg cells, since CCR7 deficient Treg cells have less capacity to provide protection in murine colitis [81].

Rheumatoid arthritis

Rheumatoid arthritis (RA) is a chronic inflammatory disease affecting symmetrically synovial tissue in polyarticular joints of the hands and feet. The inflammatory process is characterized by infiltration of inflammatory cells into the joints leading to swelling, proliferation of synoviocytes and painful joints. The inflammatory process may result in destruction of cartilage and bone, causing disability [82]. In RA synovial tissue, the infiltrating cells such as macrophages, T cells, B cells and dendritic cells play important role in the pathogenesis of RA. Migration of leukocytes into the synovium is a regulated multi-step process, involving interactions between leukocytes and endothelial cells, cellular adhesion molecules, as well as chemokines and chemokine receptors [83].

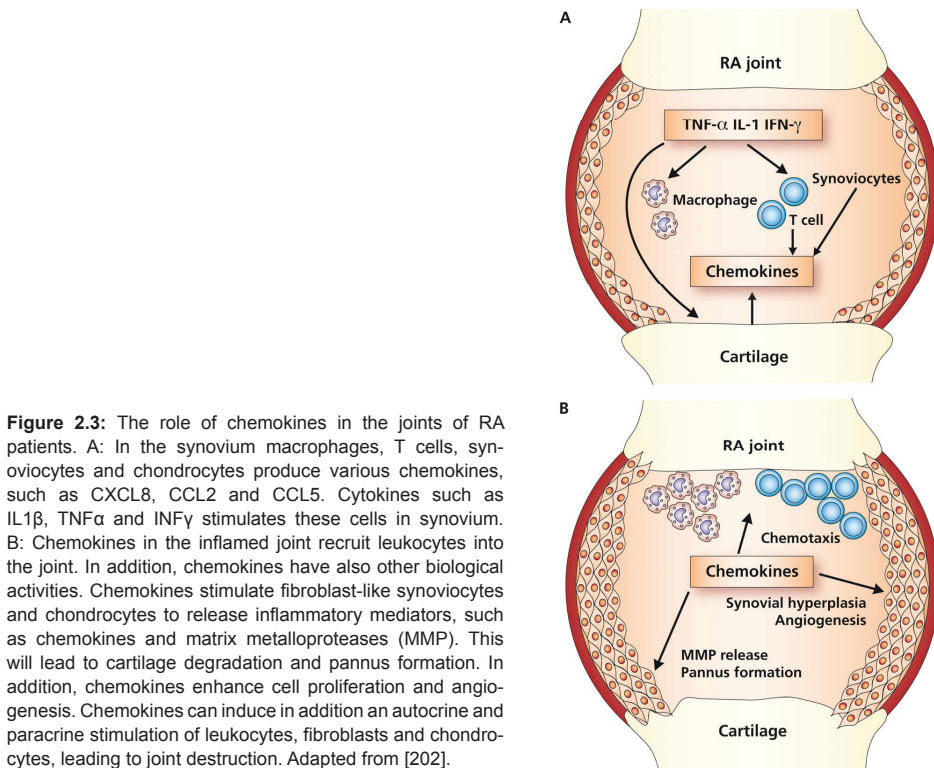
Chemokines and their receptors in rheumatoid arthritis

Chemokine expression in the inflamed synovium from human and experimental arthritis models is found to be markedly increased compared to normal tissue. For general overview see Figure 2.3. The neutrophil chemoattractant, CXCL8 (IL8), is abundantly present in both synovial tissue and fluid in clinically inflamed RA joints and correlates with the disease activity [84-87]. In the LPS/IL1-induced murine model of RA, blockade of CXCL8 using an antibody, prevented neutrophil infiltration reduced tissue inflammation [88]. First clinical trials using anti-CXCL8 antibodies did not result in clinical improvement in RA patients. It is premature to conclude that CXCL8 is not an appropriate therapeutic target in RA, because treatment with anti-CXCL8 resulted in increased levels of CXCL8 (probably antibody-antigen complexes) and poor clearance of the complexes [89].

CCL2 (MCP-1), the ligand for CCR2, is also highly expressed in RA synovial tissue [90]. This leads to the recruitment of CCR2 expressing T cells, DC, basophils and NK cells. CCR2⁺ monocytes/macrophages are found in inflamed joints [91]. Treatment with a CCL2 antibody in a rat model of collagen-induced arthritis resulted in a reduced paw swelling associated with lower numbers of macrophages in the joints [92]. This finding was confirmed in a murine model of RA using the antagonist MCP-1 (9-76) [93]. However, in the clinic, monoclonal antibodies directed against CCL2 as well as CCR2 antagonist MK0812 did

not show any beneficial effects in RA patients [94, 95]. Recently, the role of CCR2 in RA became ambiguous, since it was demonstrated that the absence of CCR2 worsens experimental arthritis in mice mimicking severe human RA [96]. Taking together, CCR2 is not likely to be a promising target for RA.

CCL5 (RANTES), the ligand for CCR1, CCR3 and CCR5, is an important chemoattractant for T cells and monocytes. Increased expression of CCL5, CCR1 and CCR5 is found of fibroblast-like synoviocytes, monocytes and T cells in the synovium of RA patients [91, 97]. In addition, in epidemiological studies, loss of function mutation of CCR5 has been associated with protection from RA [98, 99]. Blocking CCL5 or administration of Met-RANTES (a CCR1/CCR5 antagonist) and non-peptide CCR5 antagonist in rodent and monkey arthritis models resulted in a markedly reduced inflammatory response [100, 101]. Short term treatment of patients with active RA with de CCR1 antagonist, CP-481,715 showed a trend towards clinical improvement when compared to control patients [94]. This was associated with a marked decrease in the number of synovial macrophages. A phase II clinical study with CP-481715 did not demonstrate clinical efficacy after 6 wks treatment [102]. More and longer clinical trials need to be carried out to validate CCR1 as a potential therapeutic target.



Atherosclerosis

Atherosclerosis is an inflammatory disease that is characterized by lesions in the large arteries containing lipids, immune infiltrates (particularly monocytes/macrophages and T-cells), connective tissue elements and debris [103-106]. This can lead to myocardial infarction in the heart and/or to ischemic stroke in the arteries. The atherosclerotic process is initiated when plasma levels of the cholesterol-rich very low-density lipoproteins (VLDL) and low-density lipoproteins (LDL) rise. Risk factors are high-saturated fat diet, smoking, diabetes, hypertension and obesity. Once LDL concentrations rise, LDL diffuses from the blood into the innermost layer of the artery where it undergoes oxidative modification (see Fig. 2.4). Oxidized LDL in turn, leads to release of bioactive phospholipids that activate endothelial cells to express for example vascular cell adhesion molecule 1 (VCAM1). Both monocytes and T-cells can adhere to VCAM1 expressing endothelial cells. Upon a chemokine gradient these immune cells will migrate into the arterial intima (innermost layer, see Fig. 2.4). In the intima, monocytes differentiate into macrophages in response to the local over-expressed macrophage-colony-stimulating factor (M-CSF). During this process, innate immune receptors are up-regulated, including scavenger receptors (ScRs). ScRs mediate the uptake of oxidated LDL by macrophages and causes LDL cholesterol accumulation and consequently the transformation of macrophages into foam cells (characterization of the early-stage atherosclerosis). Furthermore, foam cells and activated macrophages drive lesion progression by secreting growth factors for smooth muscle cells and secreting pro-inflammatory mediators like reactive oxygen species, pro-inflammatory cytokines and of proteases. Infiltrated T-cells are activated by encountering antigens, such as oxidized LDL and heat-shock proteins, bound to major histocompatibility complex (MHC) molecules on the surface of antigen-presenting cells. In the lesion, T-cell activation leads most prevalently to a T helper-1 response. Consequently, interferon- γ (IFN- γ) and tumor-necrosis factor (TNF) are produced that activate macrophages. Thus, crosstalk between T-cells and monocytes/macrophages will induce an amplification loop of the inflammatory response, resulting in promotion of lesion formation. As the lesion becomes more bulky, the arterial lumen narrows which can lead to ischemic symptoms. Furthermore, depending of the stability of the lesion, the plaque may rupture and causes thrombosis, leading to acute cardiovascular events that result in myocardial infarction and stroke [103-109].

Chemokines and their receptors in atherosclerosis

Extensive research has been performed in mice to determine the factors involved in the pathogenesis of atherosclerosis (see Table 2.7). Two knock-out mouse strains were used: apolipoprotein E (ApoE^{-/-}) mice that develop spontaneous atherosclerosis that progresses to myocardial infarction and stroke and LDL receptor (Ldlr^{-/-}) mice that develop hypercholesterolemia and lesion development upon fat feeding [110]. Cross-breeding of this mice with mice that carry deletions in genes of the immune system indicate an essential role of chemokines and their receptors in the early phase of atherosclerosis (for excellent reviews, see: [111, 112]).

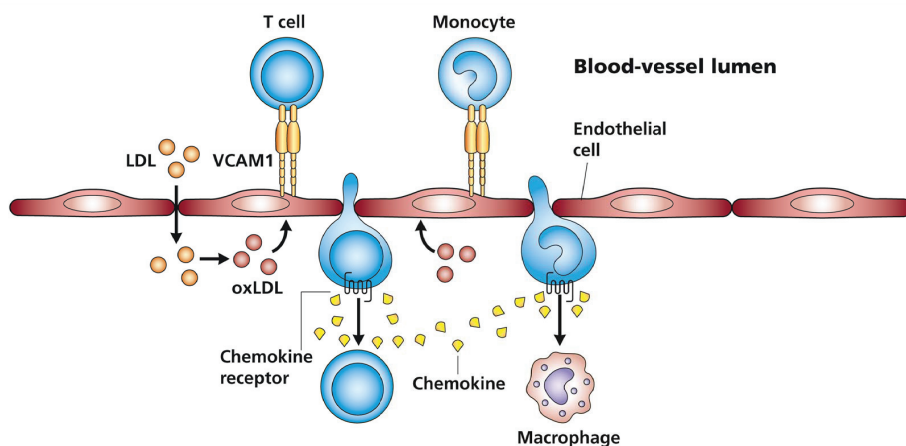


Figure 2.4: The role of chemokines in the recruitment of immune cells in atherosclerotic plaques. Low-density lipoprotein (LDL) diffuses from the blood into the innermost layer of the artery, where LDL particles can associate with proteoglycans of the extracellular matrix. The LDL of the extracellular pool is modified by enzymes and oxygen radicals to form molecules such as oxidized LDL (oxLDL). Biologically active lipids are released and induce endothelial cells to express leukocyte adhesion molecules, such as vascular cell-adhesion molecule 1 (VCAM1). Monocytes and T cells bind to VCAM-1 expressing endothelial cells through very late antigen4 (VLA4) and respond to locally produced chemokines by migrating into the arterial tissue. Adapted from [104].

CCL2 (monocyte chemoattractant protein-1) and its receptor (CCR2) play an important role in developing atherosclerosis as shown in both knock-out mice [113, 114] and human material [115, 116]. CCR2 is expressed on monocytes and T-cells. Deletion of either CCL2 or CCR2 decreases the infiltration of monocytes and T-cells into the intima and subsequently the initiation of atherosclerosis. In addition to CCR2, monocytes and T-cells also express CCR1 and CCR5. [117]. CCL5, the chemokine that binds both CCR1 and CCR5, is highly expressed in atherosclerotic lesions [118]. CCR5 deficiency in *Ldlr*^{-/-} mice showed a decrease in inflammation and improved plaque stability. Contradictory, in the same mouse model CCR1 deficiency enhanced inflammation and atherosclerotic lesion development [119, 120]. Thus, in view of developing therapeutics, a selective blocker of CCR5 is required rather than a CCR1 antagonist. Indeed, the nonpeptidergic CCR5 (and CXCR3) antagonist TAK-779, attenuates atherosclerotic lesion formation by blocking T-cells migration into lesions as shown in both DBA/1 and *Ldlr*^{-/-} mice [101, 121]. Not only the chemokine receptors are implicated as drug targets, also efforts are made to target the chemokine CCL5. Administration of the CCL5 antagonist Met-RANTES in *Ldlr*^{-/-} mice reduces the progression of atherosclerosis [122]. Furthermore, a study showed that the ability of CCL5 to recruit monocytes is enhanced when a chemokine heterodimer is formed with CXCL4 [123]. Attenuation of heterodimerization of CCL5 with CXCL4 by the peptide antagonist CKEY2 or its mouse ortholog MKEY causes reduction of monocyte chemotaxis *in vitro* and atherosclerotic lesion reduction *in vivo*, respectively [124].

In human atherosclerotic lesions also expression of the chemokine CX3CL1 (fractalkine) is elevated [125, 126]. CX3CL1 causes recruitment of monocytes and T-cells via its interaction with CX₃CR1. In accordance, CX₃CR1 deficient ApoE^{-/-} mice are less prone to atherosclerosis [127, 128]. CX3CL1 is a unique chemokine (like CXCL16), because it is expressed in both a soluble and transmembrane form. Expressed on the plasma membrane of endothelial cells, CX3CL1 acts as an adhesion molecule. In its soluble form, it acts like other chemokines, as a chemoattractant [111, 112]. Thus, by these means CX3CL1 can contribute to the development of atherosclerosis.

CXCR3 is expressed on T-cells and is activated by the chemokines CXCL9, CXCL10 and CXCL11. These chemokines are highly expressed in human atherosclerotic lesions [129], leading to recruitment of T-cells into the intima. In CXCR3 deficient ApoE^{-/-} mice the lesion formation was reduced, which was associated with an up-regulation of anti-inflammatory molecules IL-10, IL-18BP and increased numbers of regulatory T-lymphocytes that suppress activation of the immune system [130]. Furthermore, the CXCR3 specific antagonist NBI-74330 [131] showed attenuation of formation of atherosclerotic lesion in Ldlr^{-/-} mice [132].

Oxidized LDL is known to induce the production of CXCL8 by monocytes [133]. Various studies have shown that macrophages and foam cells in atherosclerotic lesions produce CXCL8 [134, 135]. This chemokine binds to CXCR1 and CXCR2 [117]. CXCR2 was detected in the macrophage rich areas of human carotid endarterectomy atherosclerotic lesions [136]. In CXCR2 deficient Ldlr^{-/-} mice the progression of advanced atherosclerosis was reduced, associated with reduced recruitment of macrophages [136]. Thus, CXCL8 plays a direct role in directing of macrophages in atherosclerotic lesions. Studies with deficient KC/mCXCL1 Ldlr^{-/-} mice, a chemokine that also binds CXCR2, showed a less pronounced attenuation compared to CXCR2 deficient mice. This suggests that other CXCR2 ligands may compensate for the loss of KC/mCXCL1. Furthermore, the same study showed that KC/mCXCL1 and CXCR2 do not play an essential role in onset of early atherosclerotic lesion formation, but rather in advanced stages associated with macrophage accumulation [137].

Although neutrophils are not the key mediators in atherosclerosis, they appear to participate in atherosclerotic lesion development and are detected at sites of plaque disruption [138]. Neutrophils express among others the chemokine receptor CXCR4 [117]. The function of CXCR4 and its ligand CXCL12 in atherosclerosis was recently described by Zerneck *et al.* [139]. Under healthy conditions, CXCL12 is constitutively expressed in the bone marrow, causing homing of neutrophils into the bone marrow and subsequent clearance. Blockade of CXCR4 by the small-molecule antagonist AMD3465 in both ApoE^{-/-} and Ldlr^{-/-} mice resulted in expansion of bone marrow neutrophils and their egress into the blood leading and attenuating of the homing of neutrophils back to the bone marrow. Thus, the number of neutrophils is increased in the blood stream. Neutrophils express also CXCR2 and upon expression of CXCL1 and CXCL8 in the atherosclerotic plaque, neutrophils are recruited into the plaque. In the plaque they cause secretion of inflammatory mediators,

thereby promoting growth of the plaque and inducing plaque instability. Thus, interference of the CXCL12/CXCR4 axis promotes lesion formation by disruption of neutrophil homeostasis [138, 139].

Table 2.7: Chemokine receptors and their ligands involved in atherosclerosis [113-116, 118-120, 122, 124, 126-130, 132-134, 137-139].

Receptor	Ligands	Relevance
CCR2	CCL2	presence CCL2 in human atherosclerotic lesions ApoE ^{-/-} CCR2 ^{-/-} mice (less development disease) Ldlr ^{-/-} CCL2 ^{-/-} mice (less development disease)
CCR1 CCR5	CCL5	presence of CCL5 in atherosclerotic lesions ApoE ^{-/-} CCR5 ^{-/-} mice (no difference compared to ApoE ^{-/-}) Ldlr ^{-/-} CCR5 ^{-/-} mice (more stable plaque) Ldlr ^{-/-} CCR1 ^{-/-} mice (increased inflammation) Met-RANTES in Ldlr ^{-/-} (reduced progression) CKEY2 attenuates CCL5-CXCL4 formation and mono recruitment
CXCR2	CXCL8	presence of CXCR2 in human atherosclerotic lesions (mΦ rich) CXCR2 overexpression: abundant in atherosclerotic lesions Ldlr ^{-/-} CXCR2 ^{-/-} mice (reduced progression advanced disease) CXCL8 produced by mono/mΦ/foam cells role for CXCR2 in advanced disease
CXCR3	CXCL9 CXCL10 CXCL11	presence of CXCR3 in human disease CXCR3 antagonist (attenuation of lesion formation) ApoE ^{-/-} CXCR3 ^{-/-} mice (less development of disease)
CXCR4	CXCL12	AMD3465 in ApoE ^{-/-} Ldlr ^{-/-} mice (increased neutro in blood) increased plaque instability
CX ₃ CR1	CX3CL1	presence of CX3CL1 in human disease ApoE ^{-/-} Cx ₃ cr1 ^{-/-} mice (less development of disease)

mono: monocytes; mΦ: macrophages; neutro: neutrophils.

Multiple sclerosis

Multiple sclerosis (MS) is a chronic inflammatory disease of the central nervous system. The infiltration of mainly T-lymphocytes and macrophages in the brain causes destruction of myelin sheaths of neurons and apoptosis of oligodendrocytes (myelin forming cells). Subsequently, axonal injury occurs, resulting in impairment of conduction of signals of the affected neurons, leading to both physical and cognitive disability [140-143]. Lesions in multiple sclerosis are mainly found in optic nerves, brain stem and in the white matter of both periventricular regions and the spinal cord [140, 144]. The cause of multiple sclerosis is still unknown; genetic risk factors, environmental factors and auto-immune inflammatory mechanisms are under investigation for their role in the pathogenesis of this disease [140, 142, 144, 145].

Under basal physiological conditions, the central nervous system (CNS) limits inflammation and autoimmunity by its unique structural and functional features, including the presence

of the blood-brain barrier [144, 146]. It is proposed that the crucial step in the development of multiple sclerosis is the activation (for example by infection, superantigen stimulation, reactive metabolites or metabolic stress [147]) of circulating autoreactive T-lymphocytes (both CD4⁺ and CD8⁺). These activated lymphocytes interact with endothelial surface integrins, subsequently leading to breakdown of the blood-brain barrier and influx into the CNS. In addition, also matrix metalloproteinases (particular MMP-9) can disrupt the blood-brain barrier [140-142, 145, 147]. Contradictory, other studies report that the extensive apoptosis of oligodendrocytes, induced by viruses (for example human endogenous retrovirus type W (HERV-W)) or increased levels of glutamate, are the essential step in developing multiple sclerosis. The formed myelin debris trigger the inflammatory system, leading to recruitment of T cells and macrophages into the CNS and subsequently (also) disruption of the blood-brain barrier [143]. Degradation of the blood-brain barrier allows an increased infiltration of inflammatory cells (like macrophages) in the CNS upon a chemokine gradient. Active lesions consist of monocytes/macrophages (containing myelin debris), T-cells and less frequently B-cells [144]. In the CNS, T-lymphocytes recognize myelin as foreign. Consequently, T-cells produce IL-2, IFN- γ and TNF- α to activate macrophages and local microglia cells (intrinsic CNS macrophages [146]) leading to demyelination [140, 141, 146]. Remyelination by oligodendrocytes occurs in the early phase of multiple sclerosis, but once the disease progresses, demyelination cannot be repaired. Consequently, the axons and neurons are irreversibly damaged [141, 147] causing the clinical symptoms of multiple sclerosis.

Chemokines and their receptors in multiple sclerosis

Both patient material and *in vivo* studies using the rodent Experimental Autoimmune Encephalomyelitis (EAE) animal model have shown that chemokines and chemokine receptors are involved in the pathogenesis of multiple sclerosis, see Table 2.8 [145, 148]. Amongst others, CCL2 is detected in human multiple sclerosis lesions [149, 150]. Production of this chemokine by astrocytes, microglia, endothelial cells and macrophages [151, 152] causes the recruitment of monocytes and T-cells via its binding to CCR2, that is expressed on these cells. CCL2-deficient mice [153] and CCR2 knockout mice [154] were resistant to induce EAE and developing of clinical symptoms of the disease, respectively. In addition, mice treated with either INCB3344 (small non-peptidergic CCR2 antagonist) or P8A-MCP-1 (point mutant of CCL2) show significant decrease in the clinical score, indicating a role for CCR2 in MS [155, 156].

At different stages of lesion development the chemokines CCL3, CCL4 and CCL5 are detected in human brain [151, 157-159]. These chemokines bind to both CCR1 and CCR5 [117], thereby causing the infiltration of monocytes and T-cells into the CNS. CCR1 knockout mice show an attenuated form of EAE [160] and administration of the CCR1 antagonist BX471 in rat reduces EAE [161]. In addition, administration of anti-CCL3 antibodies in mice prevented the onset of EAE and infiltration of mononuclear cells into the CNS [162]. Contradictory, the CCR1 and CCR5 antagonist Met-RANTES was not able to block the leukocyte trafficking in chronic-relapsing EAE [163], whereas the RANTES variant 44AANA47-RANTES is indeed able to inhibit EAE development *in vivo* [148].

Astrocytes in active demyelinating lesion express CXCL9 and CXCL10 [145, 164]. Binding of these chemokines to CXCR3 causes the influx of T-cells into the CNS. Multiple sclerosis patients show an upregulation of CXCR3 on CD4⁺ lymphocytes associated with all relapses [165]. Mice treated with anti-CXCL10 antibodies show a decreased incidence of EAE due to less accumulation of CD4⁺ T cells [166]. Contradictory, rat treated with anti-CXCL10 antibodies did not affect the induction of EAE [167]. In addition, both CXCR3 knock-out and CXCL10-deficient mice were more susceptible to EAE [168, 169]. More studies are required to define the role of CXCL10 and CXCR3 in MS.

In addition to the above mentioned receptors, T-cells also express CXCR6. CXCL16, the ligand for CXCR6, has therefore chemoattractant activity for activated T-cells [117, 170]. Administration of anti-CXCL16 in mice causes decreased incidence of acute EAE, associated with reduced infiltration of mononuclear cells into the CNS [170]. Furthermore, T-cells express CCR7 and therefore also the chemokines CCL19 and CCL21 play a role in recruiting T-cells into the CNS in multiple sclerosis or EAE [171].

Table 2.8: Chemokine receptors and their ligands involved in multiple sclerosis [148, 149, 151, 153-156, 159-171].

Receptor	Ligands	Relevance
CCR2	CCL2	presence CCL2 in human MS lesions CCR2 ^{-/-} mice: no EAE symptoms CCL2 ^{-/-} mice: resistant to induce EAE P8A-MCP-1 inhibited clinical symptoms in EAE mice INCB3344 inhibited clinical symptoms in EAE mice
CCR1 CCR5	CCL3 CCL4 CCL5	presence CCL3, CCL4 and CCL5 in human MS lesions CCR1 ^{-/-} mice had attenuated form of EAE CCR1 antagonist BX471 reduced EAE in rat anti-CCL3 antibody prevented onset EAE ⁴⁴ AANA ⁴⁷ -RANTES had inhibitory effect on EAE antagonist Met-RANTES had no effect on EAE
CXCR3	CXCL9 CXCL10	presence of CXCL9 and CXCL10 in human MS lesions upregulation of CXCR3 at CD4 ⁺ cells from MS patients CXCR3 ^{-/-} mice were more susceptible to EAE CXCL10 ^{-/-} mice were more susceptible to EAE anti-CXCL10 antibody induced exacerbation of EAE in rat anti-CXCL10 antibody decreased incidence of EAE in mice
CXCR6	CXCL16	expression of CXCL16 in EAE mice anti-CXCL16 antibody: no induction of EAE in mice
CCR7	CCL19 CCL21	CCL19 and CCL21 involvement in T-cell migration into CNS

Psoriasis

Psoriasis is an inflammatory skin disease characterized by red, scaly, raised plaques. Usually, the psoriasis lesions are several centimeters in diameter and separated by normal-appearing skin [172, 173]. Psoriasis involves a chronic cutaneous pathologic process, driven by interactions between infiltrating leukocytes (T-cells, dendritic cells, macrophages and neutrophils), cytokines, chemokines and keratinocytes, the cells from the epidermis. The disease is initiated or exacerbated by infections, physical and/or emotional stress, antigenic stimuli and various medications (for example lithium and β -blockers [174-176]). Psoriatic plaques can revert back to symptomless skin spontaneously or after treatment with selective immune-targeted agents [172, 173, 175-177].

Upon a stimulus (e.g. an extrinsic pathogen associated signal or an intrinsic signal), the normal skin is converted to an acute psoriatic lesion [176]. This lesion is associated with thickening of the skin primarily due to accumulation of scales caused by aberrant terminal proliferation of keratinocytes, elongation of epidermal rete (network of blood vessels) and enlargement of blood vessels in the dermis. In addition, the amount of lymphocytes, dendritic cells (DCs) and macrophages in the dermis markedly increases and neutrophils are found in the stratum corneum, the outer layer of the epidermis [172, 176, 178]. Lymphocytes in the lesion are mainly memory populations of skin-homing (cutaneous lymphocyte-associated antigen: CLA⁺) CD4⁺ and CD8⁺ T cells. CD4⁺ T lymphocytes are mostly present in the dermis, whereas CD8⁺ T lymphocytes are both present in the dermis and in the epidermis [172, 175]. Both classes of T lymphocytes become activated via the interaction with antigen presenting cells (APCs), like immature myeloid dendritic cells (Langerhans cells), plasmacytoid dendritic cells and mature myeloid dendritic cells. A so-called immunologic synapse is formed between T-cells and dendritic cells [175, 178]. Subsequently, cytokines (like TNF- α and IFN- γ), chemokines (like CCL3, CCL4, CCL5, CCL17, CCL19, CCL20, CCL27, CXCL1, CXCL8, CXCL9, and CXCL10) and growth factors (like TGF- α and VEGF) are released by these T-cells and dendritic APCs. This finally leads to a vicious cycle in which keratinocytes, endothelial cells, neutrophils, T-cells and APCs become activated. Consequently, a chronic psoriatic plaque is formed characterized by the presence of CD8⁺ cells and neutrophils in the epidermis, thickening of the epidermis by increased keratinocyte proliferation and an angiogenic tissue response [176].

Chemokines and their receptors in psoriasis

Chemokines play a key role in recruiting cells into the psoriatic plaque, like T cells that initiate and maintain psoriasis (see Table 2.9) [177]. Upon stimulation of IFN- γ (produced by T-cells) keratinocytes in plaques synthesize CXCL9 and CXCL10. These chemokines bind to CXCR3 (expressed on T-cells), thus causing migration of T-cells into the plaque [178, 179]. As described by Wijtmans and colleagues [180], small CXCR3 antagonists have been considered as therapeutics in skin inflammation, including psoriasis. However, AMG487 failed in clinical II studies in psoriasis patients [181]. Expression of CCL17, CCL22 and CCL27 causes also increased infiltration of skin-homing CLA⁺ memory T-cells via, respec-

tively, their interaction with the highly expressed CCR4 and CCR10 on these cells [179, 182]. Furthermore, CCR6 and its ligand CCL20 are up-regulated in psoriatic skin lesion [183]. CCR6 is expressed on both T-cells and dendritic cells, thus expression of CCL20 results in recruitment of both cell types into the psoriatic plaque [184-186]. Also the expression of CX3CL1 (fractalkine) is increased in psoriatic tissue, leading to migration of CX₃CR1 positive T-cells into the psoriatic lesion [187].

Tabel 2.9: Chemokine receptors and their ligands involved in psoriasis [177, 179, 188, 195-197].

Receptor	Ligands	Relevance
CCR2	CCL2	CCL2 produced by psoriatic keratinocytes
CCR4	CCL17 CCL22	up-regulation of CCL17 and CCL22 in psoriatic lesion
CCR5	CCL3 CCL4 CCL5	high expression of CCL3 in psoriatic tissue high expression of CCL4 in psoriatic tissue high expression of CCL5 in psoriatic tissue
CCR6	CCL20	up-regulation of CCL20 and CCR6 in psoriatic lesion
CCR10	CCL27	up-regulation of CCL27 in psoratic lesion neutralization of CCL27-CCR10 in mice: impaired T-cell recruitment
CXCR2	CXCL1 CXCL8	high levels CXCL1 and CXCL8 found in psoriatic epidermis expression of CXCR2 on psoriatic keratinocytes
CXCR3	CXCL9 CXCL10	up-regulation CXCL9 and CXCL10 in psoriatic lesion
CX ₃ CR1	CX3CL1	up-regulation of CX3CL1 in psoratic lesion

The chemokines CXCL1 and CXCL8 are detected in psoriatic epidermis. Via their interaction with CXCR2, expressed on neutrophils and psoriatic keratinocytes, they recruit neutrophils into the epidermis and stimulate the growth and differentiation of keratinocytes, respectively [188]. Neutrophils in turn, release reactive oxygen intermediates and proteolytic enzymes that cause destruction of the human epidermis [189]. Thus, activation of CXCR2 on both neutrophils and psoriatic keratinocytes, causes epidermal changes observed in psoriasis [177, 188, 190]. For the treatment of psoriasis and other inflammatory diseases, Abgenix has developed a human antibody against CXCL8 [191]. Unfortunately, this antibody was inactive in clinical trials of psoriasis [192]. Although the antibody against CXCL8 gave no improvement, CXCR2 can still be a potential drug target in this disease, for example via treatment with nonpeptidergic CXCR2 antagonists [193].

Keratinocytes of psoriasis patients not only produce CXCL8, CXCL9, CXCL10, but also CCL2, CCL3, CCL4 and CCL5 [177, 194-197]. CCL2 causes recruitment of macrophages into the psoriatic plaque via the interaction with CCR2 [190, 198], whereas CCL3, CCL4 and CCL5 recruit T-cells via the interaction with CCR1 and/or CCR5 [194]. *In vivo* experiments showed that elimination of macrophages causes a reduction of both T cells and dendritic cells in the skin [199]. Clinical studies in psoriasis patients with the small molecule CCR5

antagonist SCH331125 showed no clinical effect and no difference of CCR5 expression in lesion tissue, thereby concluding that CCR5 does not play a crucial role in psoriasis [194]. In addition, targeting CCR1 with the small non-peptidergic CCR1 antagonist BX471 also failed in clinical trials for among other psoriasis [181].

Psoriasis appears to be a unique human disease, as in several animal models single-gene mutations or deletions failed to generate skin lesion with relevant psoriatic characteristics [173, 175, 176]. Nevertheless, immunodeficient mice transplanted with human psoriatic plaques (SCID mice) show the implication of T cells [200]. Furthermore, human symptomless skin engrafted onto AGR129 mice spontaneously develop plaques, which are used to test drug-like compounds to prevent the development of psoriasis [175, 176].

Concluding remarks

Taken together, the above clearly indicates that chemokines and their respective chemokine receptors play an important role in inflammatory diseases. Chemokine receptors can therefore be considered as promising drug targets.

References

1. Lukacs, N.W., Role of chemokines in the pathogenesis of asthma. *Nat Rev Immunol*, 2001. 1(2): p. 108-16.
2. Palmqvist, C., A.J. Wardlaw, and P. Bradding, Chemokines and their receptors as potential targets for the treatment of asthma. *Br J Pharmacol*, 2007. 151(6): p. 725-36.
3. Robertson, M.J., Role of chemokines in the biology of natural killer cells. *J Leukoc Biol*, 2002. 71(2): p. 173-83.
4. Smit, J.J. and N.W. Lukacs, A closer look at chemokines and their role in asthmatic responses. *Eur J Pharmacol*, 2006. 533(1-3): p. 277-88.
5. Barnes, P.J., Immunology of asthma and chronic obstructive pulmonary disease. *Nat Rev Immunol*, 2008. 8(3): p. 183-92.
6. Guerra, S., Overlap of asthma and chronic obstructive pulmonary disease. *Curr Opin Pulm Med*, 2005. 11(1): p. 7-13.
7. Barnes, P.J., Mechanisms in COPD: differences from asthma. *Chest*, 2000. 117(2 Suppl): p. 10S-4S.
8. Rabe, K.F., et al., Global strategy for the diagnosis, management, and prevention of chronic obstructive pulmonary disease: GOLD executive summary. *Am J Respir Crit Care Med*, 2007. 176(6): p. 532-55.
9. Barnes, P.J., Mediators of chronic obstructive pulmonary disease. *Pharmacol Rev*, 2004. 56(4): p. 515-48.
10. Barnes, P.J., S.D. Shapiro, and R.A. Pauwels, Chronic obstructive pulmonary disease: molecular and cellular mechanisms. *Eur Respir J*, 2003. 22(4): p. 672-88.
11. de Boer, W.I., et al., Monocyte chemoattractant protein 1, interleukin 8, and chronic airways inflammation in COPD. *J Pathol*, 2000. 190(5): p. 619-26.
12. Donnelly, L.E. and P.J. Barnes, Chemokine receptors as therapeutic targets in chronic obstructive pulmonary disease. *Trends Pharmacol Sci*, 2006. 27(10): p. 546-53.
13. Traves, S.L., et al., Increased levels of the chemokines GROalpha and MCP-1 in sputum samples from patients with COPD. *Thorax*, 2002. 57(7): p. 590-5.
14. Yamagata, T., et al., Overexpression of CD-11b and CXCR1 on circulating neutrophils: its possible role in COPD. *Chest*, 2007. 132(3): p. 890-9.
15. Qiu, Y., et al., Biopsy neutrophilia, neutrophil chemokine and receptor gene expression in severe exacerbations of chronic obstructive pulmonary disease. *Am J Respir Crit Care Med*, 2003. 168(8): p. 968-75.
16. Yamamoto, C., et al., Airway inflammation in COPD assessed by sputum levels of interleukin-8. *Chest*, 1997. 112(2): p. 505-10.
17. Keatings, V.M., et al., Differences in interleukin-8 and tumor necrosis factor-alpha in induced sputum from patients with chronic obstructive pulmonary disease or asthma. *Am J Respir Crit Care Med*, 1996. 153(2): p. 530-4.
18. Morrison, D., et al., Neutrophil chemokines in bronchoalveolar lavage fluid and leukocyte-conditioned medium from nonsmokers and smokers. *Eur Respir J*, 1998. 12(5): p. 1067-72.

19. Traves, S.L., et al., Specific CXC but not CC chemokines cause elevated monocyte migration in COPD: a role for CXCR2. *J Leukoc Biol*, 2004. 76(2): p. 441-50.
20. Saetta, M., et al., CD8+ve cells in the lungs of smokers with chronic obstructive pulmonary disease. *Am J Respir Crit Care Med*, 1999. 160(2): p. 711-7.
21. Saetta, M., et al., CD8+ T-lymphocytes in peripheral airways of smokers with chronic obstructive pulmonary disease. *Am J Respir Crit Care Med*, 1998. 157(3 Pt 1): p. 822-6.
22. Costa, C., et al., CXCR3 and CCR5 chemokines in induced sputum from patients with COPD. *Chest*, 2008. 133(1): p. 26-33.
23. Saetta, M., et al., Increased expression of the chemokine receptor CXCR3 and its ligand CXCL10 in peripheral airways of smokers with chronic obstructive pulmonary disease. *Am J Respir Crit Care Med*, 2002. 165(10): p. 1404-9.
24. Kelsen, S.G., et al., The chemokine receptor CXCR3 and its splice variant are expressed in human airway epithelial cells. *Am J Physiol Lung Cell Mol Physiol*, 2004. 287(3): p. L584-91.
25. Nie, L., et al., Attenuation of acute lung inflammation induced by cigarette smoke in CXCR3 knockout mice. *Respir Res*, 2008. 9: p. 82.
26. Luther, S.A. and J.G. Cyster, Chemokines as regulators of T cell differentiation. *Nat Immunol*, 2001. 2(2): p. 102-7.
27. Fujimoto, K., et al., Airway inflammation during stable and acutely exacerbated chronic obstructive pulmonary disease. *Eur Respir J*, 2005. 25(4): p. 640-6.
28. Barnes, P.J., Chronic obstructive pulmonary disease. *N Engl J Med*, 2000. 343(4): p. 269-80.
29. Foronjy, R. and J. D'Armiento, The role of collagenase in emphysema. *Respir Res*, 2001. 2(6): p. 348-52.
30. Takizawa, H., et al., Increased expression of transforming growth factor-beta1 in small airway epithelium from tobacco smokers and patients with chronic obstructive pulmonary disease (COPD). *Am J Respir Crit Care Med*, 2001. 163(6): p. 1476-83.
31. Bousquet, J., et al., Asthma. From bronchoconstriction to airways inflammation and remodeling. *Am J Respir Crit Care Med*, 2000. 161(5): p. 1720-45.
32. Ying, S., et al., How much do we know about atopic asthma: where are we now? *Cell Mol Immunol*, 2006. 3(5): p. 321-32.
33. Humbert, M., et al., The immunopathology of extrinsic (atopic) and intrinsic (non-atopic) asthma: more similarities than differences. *Immunol Today*, 1999. 20(11): p. 528-33.
34. Kay, A.B., Allergy and allergic diseases. First of two parts. *N Engl J Med*, 2001. 344(1): p. 30-7.
35. Galli, S.J., et al., Mast cells as "tunable" effector and immunoregulatory cells: recent advances. *Annu Rev Immunol*, 2005. 23: p. 749-86.
36. Bradding, P., A.F. Walls, and S.T. Holgate, The role of the mast cell in the pathophysiology of asthma. *J Allergy Clin Immunol*, 2006. 117(6): p. 1277-84.
37. Brightling, C.E., et al., The CXCL10/CXCR3 axis mediates human lung mast cell migration to asthmatic airway smooth muscle. *Am J Respir Crit Care Med*, 2005. 171(10): p. 1103-8.
38. Brightling, C.E., et al., Differential expression of CCR3 and CXCR3 by human lung and bone marrow-derived mast cells: implications for tissue mast cell migration. *J Leukoc Biol*, 2005. 77(5): p. 759-66.
39. Juremalm, M., et al., The chemokine receptor CXCR4 is expressed within the mast cell lineage and its ligand stromal cell-derived factor-1alpha acts as a mast cell chemotaxin. *Eur J Immunol*, 2000. 30(12): p. 3614-22.
40. Kim, C.H., et al., Rules of chemokine receptor association with T cell polarization in vivo. *J Clin Invest*, 2001. 108(9): p. 1331-9.
41. Lloyd, C.M. and S.M. Rankin, Chemokines in allergic airway disease. *Curr Opin Pharmacol*, 2003. 3(4): p. 443-8.
42. Panina-Bordignon, P., et al., The C-C chemokine receptors CCR4 and CCR8 identify airway T cells of allergen-challenged atopic asthmatics. *J Clin Invest*, 2001. 107(11): p. 1357-64.
43. Chensue, S.W., et al., Aberrant in vivo T helper type 2 cell response and impaired eosinophil recruitment in CC chemokine receptor 8 knockout mice. *J Exp Med*, 2001. 193(5): p. 573-84.
44. Schuh, J.M., et al., Airway hyperresponsiveness, but not airway remodeling, is attenuated during chronic pulmonary allergic responses to *Aspergillus* in CCR4-/- mice. *FASEB J*, 2002. 16(10): p. 1313-5.
45. Campbell, J.J., et al., Expression of chemokine receptors by lung T cells from normal and asthmatic subjects. *J Immunol*, 2001. 166(4): p. 2842-8.
46. Suzuki, Y., et al., A small-molecule compound targeting CCR5 and CXCR3 prevents airway hyperresponsiveness and inflammation. *Eur Respir J*, 2008. 31(4): p. 783-9.
47. Campbell, E.M., et al., Monocyte chemoattractant protein-1 mediates cockroach allergen-induced bronchial hyperactivity in normal but not CCR2-/- mice: the role of mast cells. *J Immunol*, 1999. 163(4): p. 2160-7.
48. Hogaboam, C.M., et al., The therapeutic potential in targeting CCR5 and CXCR4 receptors in infectious and allergic pulmonary disease. *Pharmacol Ther*, 2005. 107(3): p. 314-28.
49. Lukacs, N.W., et al., AMD3100, a CXCR4 antagonist, attenuates allergic lung inflammation and airway hyperactivity. *Am J Pathol*, 2002. 160(4): p. 1353-60.
50. Seroogy, C.M. and J.E. Gern, The role of T regulatory cells in asthma. *J Allergy Clin Immunol*, 2005. 116(5): p. 996-9.
51. Umetsu, D.T., Understanding the immunological basis of asthma; immunotherapy and regulatory T cells. *Arb Paul Ehrlich Inst Bundesamt Sera Impfstoffe Frankfurt A M*, 2006(95): p. 211-4; discussion 215-6.
52. Ying, S., et al., Enhanced expression of eotaxin and CCR3 mRNA and protein in atopic asthma. Association with airway hyperresponsiveness and predominant co-localization of eotaxin mRNA to bronchial epithelial and endothelial cells. *Eur J Immunol*, 1997. 27(12): p. 3507-16.
53. Ying, S., et al., Eosinophil chemotactic chemokines (eotaxin, eotaxin-2, RANTES, monocyte chemoattractant protein-3 (MCP-3), and MCP-4), and C-C chemokine receptor 3 expression in bronchial biopsies from atopic and nonatopic (Intrinsic) asthmatics. *J Immunol*, 1999. 163(11): p. 6321-9.

54. Folkerts, G., A.D. Kraneveld, and F.P. Nijkamp, New endogenous CXC chemokine ligands as potential targets in lung emphysema. *Trends Pharmacol Sci*, 2008. 29(4): p181-5.
55. Ordóñez, C.L., et al., Increased neutrophil numbers and IL-8 levels in airway secretions in acute severe asthma: Clinical and biologic significance. *Am J Respir Crit Care Med*, 2000. 161(4 Pt 1): p. 1185-90.
56. Bamias, G., et al., The Th1 immune pathway as a therapeutic target in Crohn's disease. *Curr Opin Investig Drugs*, 2003. 4(11): p. 1279-86.
57. Targan, S.R. and L.C. Karp, Defects in mucosal immunity leading to ulcerative colitis. *Immunol Rev*, 2005. 206: p. 296-305.
58. Bouma, G. and W. Strober, The immunological and genetic basis of inflammatory bowel disease. *Nat Rev Immunol*, 2003. 3(7): p. 521-33.
59. Lakatos, L., Immunology of inflammatory bowel diseases. *Acta Physiol Hung*, 2000. 87(4): p. 355-72.
60. Bamias, G., et al., New concepts in the pathophysiology of inflammatory bowel disease. *Ann Intern Med*, 2005. 143(12): p. 895-904.
61. Kagnoff, M.F., Immunology of the intestinal tract. *Gastroenterology*, 1993. 105(5): p. 1275-80.
62. Caprilli, R., et al., Efficacy of conventional immunosuppressive drugs in IBD. *Dig Liver Dis*, 2004. 36(11): p. 766-80.
63. Sandborn, W.J., Strategies for targeting tumour necrosis factor in IBD. *Best Pract Res Clin Gastroenterol*, 2003. 17(1): p. 105-17.
64. Geier, M.S., R.N. Butler, and G.S. Howarth, Inflammatory bowel disease: current insights into pathogenesis and new therapeutic options; probiotics, prebiotics and synbiotics. *Int J Food Microbiol*, 2007. 115(1): p. 1-11.
65. Ajuebor, M.N., M.G. Swain, and M. Perretti, Chemokines as novel therapeutic targets in inflammatory diseases. *Biochem Pharmacol*, 2002. 63(7): p. 1191-6.
66. Danese, S. and A. Gasbarrini, Chemokines in inflammatory bowel disease. *J Clin Pathol*, 2005. 58(10): p. 1025-7.
67. Banks, C., et al., Chemokine expression in IBD. Mucosal chemokine expression is unselectively increased in both ulcerative colitis and Crohn's disease. *J Pathol*, 2003. 199(1): p. 28-35.
68. Bizzarri, C., et al., ELR+ CXC chemokines and their receptors (CXC chemokine receptor 1 and CXC chemokine receptor 2) as new therapeutic targets. *Pharmacol Ther*, 2006. 112(1): p. 139-49.
69. Singh, U.P., et al., CXCR3 axis: role in inflammatory bowel disease and its therapeutic implication. *Endocr Metab Immune Disord Drug Targets*, 2007. 7(2): p. 111-23.
70. Singh, S., A. Sadanandam, and R.K. Singh, Chemokines in tumor angiogenesis and metastasis. *Cancer Metastasis Rev*, 2007. 26(3-4): p. 453-67.
71. Andres, P.G., et al., Mice with a selective deletion of the CC chemokine receptors 5 or 2 are protected from dextran sodium sulfate-mediated colitis: lack of CC chemokine receptor 5 expression results in a NK1.1+ lymphocyte-associated Th2-type immune response in the intestine. *J Immunol*, 2000. 164(12): p. 6303-12.
72. Oki, M., et al., Accumulation of CCR5+ T cells around RANTES+ granulomas in Crohn's disease: a pivotal site of Th1-shifted immune response? *Lab Invest*, 2005. 85(1): p. 137-45.
73. Ouyang, W., J.K. Kolls, and Y. Zheng, The biological functions of T helper 17 cell effector cytokines in inflammation. *Immunity*, 2008. 28(4): p. 454-67.
74. Kaser, A., et al., Increased expression of CCL20 in human inflammatory bowel disease. *J Clin Immunol*, 2004. 24(1): p. 74-85.
75. Kwon, J.H., et al., Colonic epithelial cells are a major site of macrophage inflammatory protein 3alpha (MIP-3alpha) production in normal colon and inflammatory bowel disease. *Gut*, 2002. 51(6): p. 818-26.
76. Katchar, K., et al., MIP-3alpha neutralizing monoclonal antibody protects against TNBS-induced colonic injury and inflammation in mice. *Am J Physiol Gastrointest Liver Physiol*, 2007. 292(5): p. G1263-71.
77. Koenecke, C. and R. Forster, CCR9 and inflammatory bowel disease. *Expert Opin Ther Targets*, 2009. 13(3): p. 297-306.
78. Keshav, S., et al., PROTECT-1 study demonstrated efficacy of the intestine-specific chemokine receptor antagonist CCX282-B (Traficet-EN) in treatment of patients with moderate to severe crohn's disease. *Gastroenterology*, 2009. 136(A65).
79. Rivera-Nieves, J., et al., Antibody blockade of CCL25/CCR9 ameliorates early but not late chronic murine ileitis. *Gastroenterology*, 2006. 131(5): p. 1518-29.
80. Yuan, Q., et al., CCR4-dependent regulatory T cell function in inflammatory bowel disease. *J Exp Med*, 2007. 204(6): p. 1327-34.
81. Schneider, M.A., et al., CCR7 is required for the in vivo function of CD4+ CD25+ regulatory T cells. *J Exp Med*, 2007. 204(4): p. 735-45.
82. Tak, P.P. and B. Bresnihan, The pathogenesis and prevention of joint damage in rheumatoid arthritis: advances from synovial biopsy and tissue analysis. *Arthritis Rheum*, 2000. 43(12): p. 2619-33.
83. Buckley, C.D., Michael Mason prize essay 2003. Why do leucocytes accumulate within chronically inflamed joints? *Rheumatology (Oxford)*, 2003. 42(12): p. 1433-44.
84. Deleuran, B., et al., Localisation of interleukin 8 in the synovial membrane, cartilage-pannus junction and chondrocytes in rheumatoid arthritis. *Scand J Rheumatol*, 1994. 23(1): p. 2-7.
85. Endo, H., et al., Elevation of interleukin-8 (IL-8) levels in joint fluids of patients with rheumatoid arthritis and the induction by IL-8 of leukocyte infiltration and synovitis in rabbit joints. *Lymphokine Cytokine Res*, 1991. 10(4): p. 245-52.
86. Getting, S.J., et al., POMC gene-derived peptides activate melanocortin type 3 receptor on murine macrophages, suppress cytokine release, and inhibit neutrophil migration in acute experimental inflammation. *J Immunol*, 1999. 162(12): p. 7446-53.
87. Kraan, M.C., et al., The development of clinical signs of rheumatoid synovial inflammation is associated with increased synthesis of the chemokine CXCL8 (interleukin-8). *Arthritis Res*, 2001. 3(1): p. 65-71.

88. Harada, A., et al., Essential involvement of interleukin-8 (IL-8) in acute inflammation. *J Leukoc Biol*, 1994. 56(5): p. 559-64.
89. Tak, P.P., Chemokine inhibition in inflammatory arthritis. *Best Practice& Research. Clinical Rheumatology*, 2005. 20: p. 929-939.
90. Koch, A.E., et al., Enhanced production of monocyte chemoattractant protein-1 in rheumatoid arthritis. *J Clin Invest*, 1992. 90(3): p. 772-9.
91. Luster, A.D., Chemokines--chemotactic cytokines that mediate inflammation. *N Engl J Med*, 1998. 338(7): p. 436-45.
92. Ogata, H., et al., The role of monocyte chemoattractant protein-1 (MCP-1) in the pathogenesis of collagen-induced arthritis in rats. *J Pathol*, 1997. 182(1): p. 106-14.
93. Gong, J.H., et al., An antagonist of monocyte chemoattractant protein 1 (MCP-1) inhibits arthritis in the MRL-lpr mouse model. *J Exp Med*, 1997. 186(1): p. 131-7.
94. Haringman, J.J., et al., A randomized controlled trial with an anti-CCL2 (anti-monocyte chemotactic protein 1) monoclonal antibody in patients with rheumatoid arthritis. *Arthritis Rheum*, 2006. 54(8): p. 2387-92.
95. Vergunst, C.E., et al., Modulation of CCR2 in rheumatoid arthritis: a double-blind, randomized, placebo-controlled clinical trial. *Arthritis Rheum*, 2008. 58(7): p. 1931-9.
96. Quinones, M.P., et al., Experimental arthritis in CC chemokine receptor 2-null mice closely mimics severe human rheumatoid arthritis. *J Clin Invest*, 2004. 113(6): p. 856-66.
97. Haringman, J.J., et al., Chemokine and chemokine receptor expression in paired peripheral blood mononuclear cells and synovial tissue of patients with rheumatoid arthritis, osteoarthritis, and reactive arthritis. *Ann Rheum Dis*, 2006. 65(3): p. 294-300.
98. Prahalad, S., et al., Association of two functional polymorphisms in the CCR5 gene with juvenile rheumatoid arthritis. *Genes Immun*, 2006. 7(6): p. 468-75.
99. Zapico, I., et al., CCR5 (chemokine receptor-5) DNA-polymorphism influences the severity of rheumatoid arthritis. *Genes Immun*, 2000. 1(4): p. 288-9.
100. Vierboom, M.P., et al., Inhibition of the development of collagen-induced arthritis in rhesus monkeys by a small molecular weight antagonist of CCR5. *Arthritis Rheum*, 2005. 52(2): p. 627-36.
101. Yang, Y.F., et al., A non-peptide CCR5 antagonist inhibits collagen-induced arthritis by modulating T cell migration without affecting anti-collagen T cell responses. *Eur J Immunol*, 2002. 32(8): p. 2124-32.
102. Gladue, R.P., et al., CCR1 antagonists for the treatment of autoimmune diseases. *Curr Opin Investig Drugs*, 2004. 5(5): p. 499-504.
103. Glass, C.K. and J.L. Witztum, Atherosclerosis. the road ahead. *Cell*, 2001. 104(4): p. 503-16.
104. Hansson, G.K. and P. Libby, The immune response in atherosclerosis: a double-edged sword. *Nat Rev Immunol*, 2006. 6(7): p. 508-19.
105. Hansson, G.K., A.K. Robertson, and C. Soderberg-Naucler, Inflammation and atherosclerosis. *Annu Rev Pathol*, 2006. 1: p. 297-329.
106. Libby, P., Inflammation in atherosclerosis. *Nature*, 2002. 420(6917): p. 868-74.
107. Libby, P., Inflammation and cardiovascular disease mechanisms. *Am J Clin Nutr*, 2006. 83(2): p. 456S-460S.
108. Packard, R.R. and P. Libby, Inflammation in atherosclerosis: from vascular biology to biomarker discovery and risk prediction. *Clin Chem*, 2008. 54(1): p. 24-38.
109. Weber, C., A. Zernecke, and P. Libby, The multifaceted contributions of leukocyte subsets to atherosclerosis: lessons from mouse models. *Nat Rev Immunol*, 2008. 8(10): p. 802-15.
110. Breslow, J.L., Mouse models of atherosclerosis. *Science*, 1996. 272(5262): p. 685-8.
111. Brauersreuther, V., F. Mach, and S. Steffens, The specific role of chemokines in atherosclerosis. *Thromb Haemost*, 2007. 97(5): p. 714-21.
112. Zernecke, A., E. Shagdarsuren, and C. Weber, Chemokines in atherosclerosis: an update. *Arterioscler Thromb Vasc Biol*, 2008. 28(11): p. 1897-908.
113. Boring, L., et al., Decreased lesion formation in CCR2-/- mice reveals a role for chemokines in the initiation of atherosclerosis. *Nature*, 1998. 394(6696): p. 894-7.
114. Gu, L., et al., Absence of monocyte chemoattractant protein-1 reduces atherosclerosis in low density lipoprotein receptor-deficient mice. *Mol Cell*, 1998. 2(2): p. 275-81.
115. Nelken, N.A., et al., Monocyte chemoattractant protein-1 in human atheromatous plaques. *J Clin Invest*, 1991. 88(4): p. 1121-7.
116. Yla-Herttuala, S., et al., Expression of monocyte chemoattractant protein 1 in macrophage-rich areas of human and rabbit atherosclerotic lesions. *Proc Natl Acad Sci U S A*, 1991. 88(12): p. 5252-6.
117. Viola, A. and A.D. Luster, Chemokines and Their Receptors: Drug Targets in Immunity and Inflammation. *Annu Rev Pharmacol Toxicol*, 2008. 48: p. 171-197.
118. von Hundelshausen, P., et al., RANTES deposition by platelets triggers monocyte arrest on inflamed and atherosclerotic endothelium. *Circulation*, 2001. 103(13): p. 1772-7.
119. Brauersreuther, V., et al., Ccr5 but not Ccr1 deficiency reduces development of diet-induced atherosclerosis in mice. *Arterioscler Thromb Vasc Biol*, 2007. 27(2): p. 373-9.
120. Potteaux, S., et al., Role of bone marrow-derived CC-chemokine receptor 5 in the development of atherosclerosis of low-density lipoprotein receptor knockout mice. *Arterioscler Thromb Vasc Biol*, 2006. 26(8): p. 1858-63.
121. van Wanrooij, E.J., et al., HIV entry inhibitor TAK-779 attenuates atherogenesis in low-density lipoprotein receptor-deficient mice. *Arterioscler Thromb Vasc Biol*, 2005. 25(12): p. 2642-7.
122. Veillard, N.R., et al., Antagonism of RANTES receptors reduces atherosclerotic plaque formation in mice. *Circ Res*, 2004. 94(2): p. 253-61.
123. von Hundelshausen, P., et al., Heterophilic interactions of platelet factor 4 and RANTES promote monocyte arrest on endothelium. *Blood*, 2005. 105(3): p. 924-30.
124. Koenen, R.R., et al., Disrupting functional interactions between platelet chemokines inhibits atherosclerosis in hyperlipidemic mice. *Nat Med*, 2009. 15(1): p. 97-103.

125. Greaves, D.R., et al., Linked chromosome 16q13 chemokines, macrophage-derived chemokine, fractalkine, and thymus- and activation-regulated chemokine, are expressed in human atherosclerotic lesions. *Arterioscler Thromb Vasc Biol*, 2001. 21(6): p. 923-9.
126. Wong, B.W., D. Wong, and B.M. McManus, Characterization of fractalkine (CX3CL1) and CX3CR1 in human coronary arteries with native atherosclerosis, diabetes mellitus, and transplant vascular disease. *Cardiovasc Pathol*, 2002. 11(6): p. 332-8.
127. Combadiere, C., et al., Decreased atherosclerotic lesion formation in CX3CR1/apolipoprotein E double knockout mice. *Circulation*, 2003. 107(7): p. 1009-16.
128. Lesnik, P., C.A. Haskell, and I.F. Charo, Decreased atherosclerosis in CX3CR1-/- mice reveals a role for fractalkine in atherogenesis. *J Clin Invest*, 2003. 111(3): p. 333-40.
129. Mach, F., et al., Differential expression of three T lymphocyte-activating CXC chemokines by human atheroma-associated cells. *J Clin Invest*, 1999. 104(8): p. 1041-50.
130. Veillard, N.R., et al., Differential influence of chemokine receptors CCR2 and CXCR3 in development of atherosclerosis in vivo. *Circulation*, 2005. 112(6): p. 870-8.
131. Verzijl, D., et al., Noncompetitive antagonism and inverse agonism as mechanism of action of nonpeptidergic antagonists at primate and rodent CXCR3 chemokine receptors. *J Pharmacol Exp Ther*, 2008. 325(2): p. 544-55.
132. van Wanrooij, E.J., et al., CXCR3 antagonist NBI-74330 attenuates atherosclerotic plaque formation in LDL receptor-deficient mice. *Arterioscler Thromb Vasc Biol*, 2008. 28(2): p. 251-7.
133. Terkeltaub, R., et al., Oxidized LDL induces monocytic cell expression of interleukin-8, a chemokine with T-lymphocyte chemotactic activity. *Arterioscler Thromb*, 1994. 14(1): p. 47-53.
134. Apostolopoulos, J., P. Davenport, and P.G. Tipping, Interleukin-8 production by macrophages from atheromatous plaques. *Arterioscler Thromb Vasc Biol*, 1996. 16(8): p. 1007-12.
135. Wang, N., et al., Interleukin 8 is induced by cholesterol loading of macrophages and expressed by macrophage foam cells in human atheroma. *J Biol Chem*, 1996. 271(15): p. 8837-42.
136. Boisvert, W.A., et al., A leukocyte homologue of the IL-8 receptor CXCR-2 mediates the accumulation of macrophages in atherosclerotic lesions of LDL receptor-deficient mice. *J Clin Invest*, 1998. 101(2): p. 353-63.
137. Boisvert, W.A., et al., Up-regulated expression of the CXCR2 ligand KC/GRO-alpha in atherosclerotic lesions plays a central role in macrophage accumulation and lesion progression. *Am J Pathol*, 2006. 168(4): p. 1385-95.
138. Sainz, J. and M. Sata, Open sesame! CXCR4 blockade recruits neutrophils into the plaque. *Circ Res*, 2008. 102(2): p. 154-6.
139. Zernecke, A., et al., Protective role of CXC receptor 4/CXC ligand 12 unveils the importance of neutrophils in atherosclerosis. *Circ Res*, 2008. 102(2): p. 209-17.
140. Bielecki, B., et al., Treatment of multiple sclerosis with methylprednisolone and mitoxantrone modulates the expression of CXC chemokine receptors in PBMC. *J Clin Immunol*, 2008. 28(2): p. 122-30.
141. Lassmann, H., Mechanisms of demyelination and tissue destruction in multiple sclerosis. *Clin Neurol Neurosurg*, 2002. 104(3): p. 168-71.
142. Lopez-Diego, R.S. and H.L. Weiner, Novel therapeutic strategies for multiple sclerosis--a multifaceted adversary. *Nat Rev Drug Discov*, 2008. 7(11): p. 909-25.
143. Matute, C. and F. Perez-Cerda, Multiple sclerosis: novel perspectives on newly forming lesions. *Trends Neurosci*, 2005. 28(4): p. 173-5.
144. Costantino, C.M., C. Baecher-Allan, and D.A. Hafler, Multiple sclerosis and regulatory T cells. *J Clin Immunol*, 2008. 28(6): p. 697-706.
145. Szcucinski, A. and J. Losy, Chemokines and chemokine receptors in multiple sclerosis. Potential targets for new therapies. *Acta Neurol Scand*, 2007. 115(3): p. 137-46.
146. Ambrosini, E. and F. Aloisi, Chemokines and glial cells: a complex network in the central nervous system. *Neurochem Res*, 2004. 29(5): p. 1017-38.
147. Wingerchuk, D.M. and C.F. Lucchinetti, Comparative immunopathogenesis of acute disseminated encephalomyelitis, neuromyelitis optica, and multiple sclerosis. *Curr Opin Neurol*, 2007. 20(3): p. 343-50.
148. Proudfoot, A.E., A.L. de Souza, and V. Muzio, The use of chemokine antagonists in EAE models. *J Neuroimmunol*, 2008. 198(1-2): p. 27-30.
149. McManus, C., et al., MCP-1, MCP-2 and MCP-3 expression in multiple sclerosis lesions: an immunohistochemical and in situ hybridization study. *J Neuroimmunol*, 1998. 86(1): p. 20-9.
150. Ubogu, E.E., M.B. Cossoy, and R.M. Ransohoff, The expression and function of chemokines involved in CNS inflammation. *Trends Pharmacol Sci*, 2006. 27(1): p. 48-55.
151. Simpson, J.E., et al., Expression of monocyte chemoattractant protein-1 and other beta-chemokines by resident glia and inflammatory cells in multiple sclerosis lesions. *J Neuroimmunol*, 1998. 84(2): p. 238-49.
152. Van Der Voorn, P., et al., Expression of MCP-1 by reactive astrocytes in demyelinating multiple sclerosis lesions. *Am J Pathol*, 1999. 154(1): p. 45-51.
153. Huang, D.R., et al., Absence of monocyte chemoattractant protein 1 in mice leads to decreased local macrophage recruitment and antigen-specific T helper cell type 1 immune response in experimental autoimmune encephalomyelitis. *J Exp Med*, 2001. 193(6): p. 713-26.
154. Izikson, L., et al., Resistance to experimental autoimmune encephalomyelitis in mice lacking the CC chemokine receptor (CCR)2. *J Exp Med*, 2000. 192(7): p. 1075-80.
155. Handel, T.M., et al., An engineered monomer of CCL2 has anti-inflammatory properties emphasizing the importance of oligomerization for chemokine activity in vivo. *J Leukoc Biol*, 2008. 84(4): p. 1101-8.
156. Brodmerkel, C.M., et al., Discovery and pharmacological characterization of a novel rodent-active CCR2 antagonist, INCB3344. *J Immunol*, 2005. 175(8): p. 5370-8.

157. Balashov, K.E., et al., CCR5(+) and CXCR3(+) T cells are increased in multiple sclerosis and their ligands MIP-1alpha and IP-10 are expressed in demyelinating brain lesions. *Proc Natl Acad Sci U S A*, 1999. 96(12): p. 6873-8.
158. Bartosik-Psujek, H. and Z. Stelmasiak, The levels of chemokines CXCL8, CCL2 and CCL5 in multiple sclerosis patients are linked to the activity of the disease. *Eur J Neurol*, 2005. 12(1): p. 49-54.
159. Boven, L.A., et al., Macrophage inflammatory protein-1alpha (MIP-1alpha), MIP-1beta, and RANTES mRNA semiquantification and protein expression in active demyelinating multiple sclerosis (MS) lesions. *Clin Exp Immunol*, 2000. 122(2): p. 257-63.
160. Rottman, J.B., et al., Leukocyte recruitment during onset of experimental allergic encephalomyelitis is CCR1 dependent. *Eur J Immunol*, 2000. 30(8): p. 2372-7.
161. Liang, M., et al., Identification and characterization of a potent, selective, and orally active antagonist of the CC chemokine receptor-1. *J Biol Chem*, 2000. 275(25): p. 19000-8.
162. Karpus, W.J., et al., An important role for the chemokine macrophage inflammatory protein-1 alpha in the pathogenesis of the T cell-mediated autoimmune disease, experimental autoimmune encephalomyelitis. *J Immunol*, 1995. 155(10): p. 5003-10.
163. Matsui, M., et al., Treatment of experimental autoimmune encephalomyelitis with the chemokine receptor antagonist Met-RANTES. *J Neuroimmunol*, 2002. 128(1-2): p. 16-22.
164. Sorensen, T.L., et al., Expression of specific chemokines and chemokine receptors in the central nervous system of multiple sclerosis patients. *J Clin Invest*, 1999. 103(6): p. 807-15.
165. Mahad, D.J., et al., Longitudinal study of chemokine receptor expression on peripheral lymphocytes in multiple sclerosis: CXCR3 upregulation is associated with relapse. *Mult Scler*, 2003. 9(2): p. 189-98.
166. Fife, B.T., et al., CXCL10 (IFN-gamma-inducible protein-10) control of encephalitogenic CD4+ T cell accumulation in the central nervous system during experimental autoimmune encephalomyelitis. *J Immunol*, 2001. 166(12): p. 7617-24.
167. Narumi, S., et al., Neutralization of IFN-inducible protein 10/CXCL10 exacerbates experimental autoimmune encephalomyelitis. *Eur J Immunol*, 2002. 32(6): p. 1784-91.
168. Klein, R.S., et al., IFN-inducible protein 10/CXC chemokine ligand 10-independent induction of experimental autoimmune encephalomyelitis. *J Immunol*, 2004. 172(1): p. 550-9.
169. Liu, L., et al., Severe disease, unaltered leukocyte migration, and reduced IFN-gamma production in CXCR3-/- mice with experimental autoimmune encephalomyelitis. *J Immunol*, 2006. 176(7): p. 4399-409.
170. Fukumoto, N., et al., Critical roles of CXC chemokine ligand 16/scavenger receptor that binds phosphatidylserine and oxidized lipoprotein in the pathogenesis of both acute and adoptive transfer experimental autoimmune encephalomyelitis. *J Immunol*, 2004. 173(3): p. 1620-7.
171. Alt, C., M. Laschinger, and B. Engelhardt, Functional expression of the lymphoid chemokines CCL19 (ELC) and CCL 21 (SLC) at the blood-brain barrier suggests their involvement in G-protein-dependent lymphocyte recruitment into the central nervous system during experimental autoimmune encephalomyelitis. *Eur J Immunol*, 2002. 32(8): p. 2133-44.
172. Lew, W., A.M. Bowcock, and J.G. Krueger, Psoriasis vulgaris: cutaneous lymphoid tissue supports T-cell activation and "Type 1" inflammatory gene expression. *Trends Immunol*, 2004. 25(6): p. 295-305.
173. Lowes, M.A., A.M. Bowcock, and J.G. Krueger, Pathogenesis and therapy of psoriasis. *Nature*, 2007. 445(7130): p. 866-73.
174. Nickoloff, B.J., et al., The cytokine and chemokine network in psoriasis. *Clin Dermatol*, 2007. 25(6): p. 568-73.
175. Gaspari, A.A., Innate and adaptive immunity and the pathophysiology of psoriasis. *J Am Acad Dermatol*, 2006. 54(3 Suppl 2): p. S67-80.
176. Nickoloff, B.J. and F.O. Nestle, Recent insights into the immunopathogenesis of psoriasis provide new therapeutic opportunities. *J Clin Invest*, 2004. 113(12): p. 1664-75.
177. Homey, B. and S. Meller, Chemokines and other mediators as therapeutic targets in psoriasis vulgaris. *Clin Dermatol*, 2008. 26(5): p. 539-45.
178. Chamian, F. and J.G. Krueger, Psoriasis vulgaris: an interplay of T lymphocytes, dendritic cells, and inflammatory cytokines in pathogenesis. *Curr Opin Rheumatol*, 2004. 16(4): p. 331-7.
179. Rottman, J.B., et al., Potential role of the chemokine receptors CXCR3, CCR4, and the integrin alphaEbeta7 in the pathogenesis of psoriasis vulgaris. *Lab Invest*, 2001. 81(3): p. 335-47.
180. Wijnmans, M., I.J. De Esch, and R. Leurs, Therapeutic targeting of the CXCR3 Receptor, in *Chemokine Receptors as Drug Targets* M.J. Smit, Lira, S.A., Leurs, R, Editor. 2011, Wiley-VCH Verlag GmbH & Co. KGaA, Weinheim. p. 301-322.
181. Horuk, R., Chemokine receptor antagonists: overcoming developmental hurdles. *Nat Rev Drug Discov*, 2009. 8(1): p. 23-33.
182. Homey, B., et al., CCL27-CCR10 interactions regulate T cell-mediated skin inflammation. *Nat Med*, 2002. 8(2): p. 157-65.
183. Homey, B., et al., Up-regulation of macrophage inflammatory protein-3 alpha/CCL20 and CC chemokine receptor 6 in psoriasis. *J Immunol*, 2000. 164(12): p. 6621-32.
184. Dieu, M.C., et al., Selective recruitment of immature and mature dendritic cells by distinct chemokines expressed in different anatomic sites. *J Exp Med*, 1998. 188(2): p. 373-86.
185. Dieu-Nosjean, M.C., et al., Macrophage inflammatory protein 3alpha is expressed at inflamed epithelial surfaces and is the most potent chemokine known in attracting Langerhans cell precursors. *J Exp Med*, 2000. 192(5): p. 705-18.
186. Liao, F., et al., CC-chemokine receptor 6 is expressed on diverse memory subsets of T cells and determines responsiveness to macrophage inflammatory protein 3 alpha. *J Immunol*, 1999. 162(1): p. 186-94.
187. Raychaudhuri, S.P., W.Y. Jiang, and E.M. Farber, Cellular localization of fractalkine at sites of inflammation: antigen-presenting cells in psoriasis express high levels of fractalkine. *Br J Dermatol*, 2001. 144(6): p. 1105-13.

-
188. Kulke, R., et al., The CXCR2 receptor is overexpressed in psoriatic epidermis. *J Invest Dermatol*, 1998. 110(1): p. 90-4.
189. Ludolph-Hauser, D., C. Schubert, and O. Wiedow, Structural changes of human epidermis induced by human leukocyte-derived proteases. *Exp Dermatol*, 1999. 8(1): p. 46-52.
190. Li, Y.Y., T.M. Zollner, and M.P. Schon, Targeting leukocyte recruitment in the treatment of psoriasis. *Clin Dermatol*, 2008. 26(5): p. 527-38.
191. Yang, X.D., et al., Fully human anti-interleukin-8 monoclonal antibodies: potential therapeutics for the treatment of inflammatory disease states. *J Leukoc Biol*, 1999. 66(3): p. 401-10.
192. Wells, T.N., et al., Chemokine blockers--therapeutics in the making? *Trends Pharmacol Sci*, 2006. 27(1): p. 41-7.
193. de Kruijf, P., et al., Non-peptidergic allosteric antagonists differentially bind to the CXCR2 chemokine receptor. *J Pharmacol Exp Ther*, 2009. 329(2):783-90.
194. de Groot, M., et al., Expression of the chemokine receptor CCR5 in psoriasis and results of a randomized placebo controlled trial with a CCR5 inhibitor. *Arch Dermatol Res*, 2007. 299(7): p. 305-13.
195. Giustizieri, M.L., et al., Keratinocytes from patients with atopic dermatitis and psoriasis show a distinct chemokine production profile in response to T cell-derived cytokines. *J Allergy Clin Immunol*, 2001. 107(5): p. 871-7.
196. Nomura, I., et al., Distinct patterns of gene expression in the skin lesions of atopic dermatitis and psoriasis: a gene microarray analysis. *J Allergy Clin Immunol*, 2003. 112(6): p. 1195-202.
197. Raychaudhuri, S.P., et al., Upregulation of RANTES in psoriatic keratinocytes: a possible pathogenic mechanism for psoriasis. *Acta Derm Venereol*, 1999. 79(1): p. 9-11.
198. Boehncke, W.H., et al., A subset of macrophages located along the basement membrane ("lining cells") is a characteristic histopathological feature of psoriasis. *Am J Dermatopathol*, 1995. 17(2): p. 139-44.
199. Thepen, T., et al., Resolution of cutaneous inflammation after local elimination of macrophages. *Nat Biotechnol*, 2000. 18(1): p. 48-51.
200. Wrone-Smith, T. and B.J. Nickoloff, Dermal injection of immunocytes induces psoriasis. *J Clin Invest*, 1996. 98(8): p. 1878-87.
201. Gordon, S. and P.R. Taylor, Monocyte and macrophage heterogeneity. *Nat Rev Immunol*, 2005. 5(12): p. 953-64.
202. Iwamoto, T., et al., Molecular aspects of rheumatoid arthritis: chemokines in the joints of patients. *FEBS J*, 2008. 275(18): p. 4448-55.
203. Allen, S.J., S.E. Crown, and T.M. Handel, Chemokine: receptor structure, interactions, and antagonism. *Annu Rev Immunol*, 2007. 25: p. 787-820.
204. Burns, J.M., et al., A novel chemokine receptor for SDF-1 and I-TAC involved in cell survival, cell adhesion, and tumor development. *J Exp Med*, 2006. 203(9): p. 2201-13.
205. Charo, I.F. and R.M. Ransohoff, The many roles of chemokines and chemokine receptors in inflammation. *N Engl J Med*, 2006. 354(6): p. 610-21.
206. Horuk, R., Chemokine receptors. *Cytokine Growth Factor Rev*, 2001. 12(4): p. 313-35.
207. Koch, A.E., Chemokines and their receptors in rheumatoid arthritis: future targets? *Arthritis Rheum*, 2005. 52(3): p. 710-21.
208. Murphy, P.M., et al., International union of pharmacology. XXII. Nomenclature for chemokine receptors. *Pharmacol Rev*, 2000. 52(1): p. 145-76.
209. Savarin-Vuillat, C. and R.M. Ransohoff, Chemokines and chemokine receptors in neurological disease: raise, retain, or reduce? *Neurotherapeutics*, 2007. 4(4): p. 590-601.
210. Hartl, D., et al., Infiltrated neutrophils acquire novel chemokine receptor expression and chemokine responsiveness in chronic inflammatory lung diseases. *J Immunol*, 2008. 181(11): p. 8053-67.
211. Bracke, K.R., et al., CC-chemokine receptors in chronic obstructive pulmonary disease. *Inflamm Allergy Drug Targets*, 2007. 6(2): p. 75-9.
212. Chapman, R.W., et al., CXCR2 antagonists for the treatment of pulmonary disease. *Pharmacol Ther*, 2009. 121(1): p. 55-68.
213. D'Ambrosio, D., P. Panina-Bordignon, and F. Sinigaglia, Chemokine receptors in inflammation: an overview. *J Immunol Methods*, 2003. 273(1-2): p. 3-13.
214. de Boer, W.I., Perspectives for cytokine antagonist therapy in COPD. *Drug Discov Today*, 2005. 10(2): p. 93-106.
215. Owen, C., Chemokine receptors in airway disease: which receptors to target? *Pulm Pharmacol Ther*, 2001. 14(3): p. 193-202.
216. Panina-Bordignon, P. and D. D'Ambrosio, Chemokines and their receptors in asthma and chronic obstructive pulmonary disease. *Curr Opin Pulm Med*, 2003. 9(2): p. 104-10.
217. Lukacs, N.W. and K.K. Tekkanat, Role of chemokines in asthmatic airway inflammation. *Immunol Rev*, 2000. 177: p. 21-30.
-

*Non-peptidergic allosteric antagonists differentially
bind to the CXCR2 chemokine receptor*

Chapter 3

Petra de Kruijf ^{A,1}, Jane van Heteren ^{A,1}, Herman D. Lim ^A, Paolo G.M. Conti ^B,
Miranda M.C. van der Lee ^B, Leontien Bosch ^A, Koc-Kan Ho ^C, Douglas
Auld ^C, Michael Ohlmeyer ^C, Martin J. Smit ^B, Jac C.H.M. Wijkmans ^B,
Guido J.R. Zaman ^B, Martine J. Smit ^A and Rob Leurs ^A

^A Leiden/Amsterdam Center for Drug Research, Division of Medicinal Chemistry,
Vrije Universiteit Amsterdam, The Netherlands

^B Merck Research Laboratories, Oss, The Netherlands

^C Pharmacopeia Drug Discovery, Princeton, NJ 08543-5350, USA

¹ Contributed equally

Published as:

De Kruijf *et al*, J Pharmacol Exp Ther. 2009 May;329(2):783-90

Abstract

The chemokine receptor CXCR2 is involved in different inflammatory diseases, like chronic obstructive pulmonary disease, psoriasis, rheumatoid arthritis and ulcerative colitis and therefore considered an attractive drug target. Different classes of small CXCR2 antagonists have been developed. In this study we selected seven CXCR2 antagonists from the diarylurea, imidazolylpyrimidine and thiazolopyrimidine class and studied their mechanisms of action at human CXCR2. All compounds are able to displace [¹²⁵I]-CXCL8 and inhibit CXCL8-induced β -arrestin2 recruitment. Detailed studies with representatives of each class showed that these compounds displace and antagonize CXCL8 most likely via a non-competitive, allosteric mechanism. In addition, we radiolabeled the high affinity CXCR2 antagonist SB265610 and subjected [³H]-SB265610 to a detailed analysis. The binding of this radioligand was saturable and reversible. Using [³H]-SB265610 we found that compounds of the different chemical classes bind to distinct binding sites. Hence, the use of radiolabeled low molecular weight CXCR2 antagonist, serves as a tool to investigate the different binding sites of CXCR2 antagonists in more detail.

Acknowledgements

This study was performed within the framework of the Dutch Top Institute Pharma project T101-3 (to P.d.K., H.L., M.J.S., R.L. and G.J.R.Z) and was supported in part by grant of The Netherlands Organization for Scientific Research (NWO) (to M.J.S.).

Introduction

Chemokine receptors, belonging to the rhodopsin-like family of G protein coupled receptors (GPCRs), play a major role in the control and regulation of the immune system [1]. These GPCRs are expressed on the cell membrane of leukocytes, driving the trafficking of leukocytes to sites of inflammation, upon sensing chemoattractant cytokines. To date, approximately 50 chemokines and 20 chemokine receptors have been identified [2]. Dysregulation of chemokine expression and/or their GPCR targets is implicated in various human diseases, including chronic inflammatory diseases, autoimmune diseases as well as cancer [3, 4]. Consequently, chemokine receptor antagonists are currently seen as a promising approach for new therapeutic options in a wide variety of disorders [5].

The CXCR2 receptor is one of the chemokine receptors that currently attracts a lot attention in drug discovery. It is a promiscuous receptor that binds with high affinity to CXCL1, CXCL2, CXCL3 (growth-related protein α , β or γ respectively), CXCL5 (epithelial cell-derived neutrophil attractant-78), CXCL6 (granulocyte chemotactic peptide-2), CXCL7 (neutrophil activating peptide-2) and CXCL8 (interleukin-8 (IL-8)). CXCR2 is expressed on e.g. endothelial cells, eosinophils, neutrophils, macrophages and monocytes [1, 6], but also on various tumor cells. An important role for CXCR2 and its ligands has been shown in cancer and different inflammatory diseases, like chronic obstructive pulmonary disease [5], psoriasis [7], rheumatoid arthritis [8] and ulcerative colitis [9]. It has been reported that neutralizing CXCR2 antibodies inhibit the early influx of neutrophils in the colon in a rat colitis model [10] and CXCL8 mediated angiogenesis in rat [11]. In addition, in CXCR2 knock-out mice both angiogenesis and primary tumor growth was reduced compared with wild type mice [11, 12]. Moreover, CXCR2 knock-out mice showed also a decrease in PMN infiltration into the mucosa and limited signs of mucosal damage compared to wild type mice in a colitis model [9]. Furthermore, *in vivo* studies with mice, rat and primates, exposed to cigarette smoke or lipopolysaccharide (LPS), demonstrated that the small CXCR2 antagonist Sch527123 reduces neutrophil infiltration into the bronchoalveolar lavage (BAL) fluid, thereby reducing the associated lung tissue damage [13, 14]. Thus, in CXCR2 knock-out mice or wild type mice treated with a CXCR2 antagonist or neutralizing antibody, lung tissue damage and ulcerative colitis are reduced, suggesting that CXCR2 is an important drug target [9]. In view of this therapeutic potential, different classes of small CXCR2 antagonist have been developed, including diarylureas [15], thiazolo- and imidazolylpyrimidines [16, 17], quinoxalines [18], nicotinamide n-oxides [19], indole carboxylic acids [20] and arylpropionic acids [21]. So far, most literature describes *in vitro* data of the different CXCR2 antagonist classes. However, both diarylurea and arylpropionic compounds have shown promising *in vivo* data and clinical trials are ongoing with some of these compounds [6].

Despite the clinical interest in CXCR2 antagonists, little is known about their molecular mechanism of action. The large peptidergic chemokines bind to the N-terminus and extracellular loops of their receptors, but small molecule antagonists are considered generally to bind to the 7TM domains [2, 22, 23], suggesting allosteric interactions between chemokines

and small molecule antagonists. Interestingly, recently the CXCR2 antagonist SB332235 was suggested to bind to the intracellular domain of CXCR2 [24]. In this study, seven different CXCR2 antagonists of three classes have been selected and subjected to a detailed pharmacological characterization. Three compounds of the diarylurea class have been chosen (SB225002, SB332235 and SB265610 [6]), three imidazolylpyrimidine compounds [17, 25, 26] and one thiazolopyrimidine compound from patent literature, named herein VUF10948 [27].

The studies presented in this article show that all compounds are both able to displace [125 I]-CXCL8 from human CXCR2 and to inhibit CXCR2 induced β -arrestin2 recruitment. By investigating one representative of each class in more detail, we suggest that the compounds are allosteric modulators at CXCR2. By radiolabeling the potent CXCR2 antagonist SB265610, we found that compounds of the different chemical classes bind to distinct binding sites.

Material and Methods

Dulbecco's modified Eagle's medium (DMEM), RPMI-1640, penicillin and streptomycin were all obtained from PAA Laboratories (Pasching, Austria). Fetal bovine serum was purchased from Integro B.V. (Dieren, The Netherlands). DMEM containing 25 mM HEPES and L-glutamine, OPTI-MEM, Hygromycin-B and Geneticin were obtained from Gibco (Paisley, United Kingdom) and fetal calf serum was purchased from Cambrex Bio Sciences (Verviers, Belgium). Chloroquine diphosphate and DEAE-dextran were obtained from Sigma-Aldrich (St. Louis, MO, USA). Bovine Serum Albumin Fraction V (BSA) was purchased from Roche (Mannheim, Germany). [125 I]-CXCL8 (2200 Ci/mmol) or [125 I] was obtained from PerkinElmer Life Sciences (Boston, MA, USA), whereas the unlabelled chemokines were purchased from PeproTech (Rock Hill, NJ, USA) or from R&D systems (Minneapolis, USA). All CXCR2 antagonists and [3 H]-SB265610 (26.07 Ci/mmol) were synthesized at the Schering-Plough Research Institute (Oss, The Netherlands).

Cell culture and transfection of hCXCR2

COS-7 cells were grown at 5% CO₂ and 37°C in Dulbecco's modified Eagle's medium supplemented with 5% (v/v) fetal bovine serum, 50 IU/ml penicillin and 50 µg/ml streptomycin. COS-7 cells were transiently transfected using the DEAE-dextran method [28]. Briefly, cells were trypsinized, washed once in RPMI-1640, supplemented with 2% fetal bovine serum, 50 IU/ml penicillin and 50 µg/ml streptomycin and resuspended in the same solution containing 100 µM chloroquine, 0.8 mg/ml DEAE-dextran and 2 µg pcDEF3-hCXCR2 [29] or pcDNA3-hCXCR1 cDNA per 10⁶ cells. Cells were incubated at 5% CO₂ and 37°C for one hour and then plated out in growth medium. After 48 hours, the cells were washed once in PBS, scraped and pelleted for preparation of membranes.

PathHunter™ HEK293-CXCR2 cells (DiscoverX, Fremont, USA), were grown at 5% CO₂ and 37°C in DMEM with 25 mM HEPES and L-glutamine supplemented with 10% (v/v) heat-inactivated FCS, 50 IU/ml penicillin, 50 µg/ml streptomycin, 800 µg/ml Geneticin and 200 µg/ml Hygromycin-B.

Radioligand Binding Assays

Pellets of COS-7 membranes expressing hCXCR1 or hCXCR2 were resuspended in ice cold binding buffer (50 mM Na_2HPO_4 and 50 mM KH_2PO_4 , pH 7.4) and homogenized 15 times with a Dounce homogenizer. Protein concentration in membrane preparations was determined using the BioRad Protein Determination assay 18 from BioRad Laboratories (München, Germany).

Competition binding, saturation binding and binding kinetics analyses of [^{125}I]-CXCL8 and [^3H]-SB265610 were all performed at COS-7 membranes expressing human CXCR1 or CXCR2 in binding buffer (50 mM Na_2HPO_4 and 50 mM KH_2PO_4 , pH 7.4) at room temperature in a final volume of 100–200 μl . After the indicated incubation times, membranes were harvested with a Brandel harvester or with rapid filtration through Unifilter GF/C 96-well filterplates (PerkinElmer, USA) pretreated with 0.3% polyethyleneimine and washed three times with ice-cold wash buffer (50 mM Na_2HPO_4 and 50 mM KH_2PO_4 , pH 7.4). Bound radioactivity was determined using the Tri-Carb 1900 Hewlett Packard counter (PerkinElmer, USA) or a MicroBeta (PerkinElmer, USA), respectively.

For [^{125}I]-CXCL8 competition binding assays, membranes (approximately 10 μg per data point) were incubated with indicated concentrations of antagonists and approximately 300 pM [^{125}I]-CXCL8 for 1 hour. To determine saturation binding of [^{125}I]-CXCL8, membranes (approximately 20 μg per data point) were incubated with indicated concentrations of [^{125}I]-CXCL8 in the absence or presence of 20 nM SB265610, 50 nM compound 1 or 200 nM VUF10948. Non-specific binding was determined with 30 nM CXCL1.

Single point [^3H]-SB265610 competition binding was performed with 8 μg membranes, in absence or presence of 10 μM VUF10948 and 3.8 nM [^3H]-SB265610 for 1 h at room. For experiments to determine the association rate of [^3H]-SB265610, membranes (approximately 2 μg per data point) were incubated for the indicated times with 7 nM [^3H]-SB265610 in the absence or presence of 10 μM VUF10948. To measure the dissociation rate of [^3H]-SB265610, membranes (approximately 2 μg per data point) were incubated for 1 hour with 7 nM [^3H]-SB265610 before the addition of 10 μM VUF10948. Samples were taken at the indicated times, bound and free radioactivity were separated and determined by liquid scintillation.

For saturation binding with [^3H]-SB265610, membranes (approximately 6 μg per data point) were incubated with indicated concentrations of [^3H]-SB265610 for 1 hour in the absence or presence of 10 μM VUF10948 to determine total and non-specific binding.

In competition binding experiments with various concentrations of cold ligands, membranes (approximately 4 μg per data point) were incubated with indicated concentrations of antagonist or chemokines and approximately 10 nM [^3H]-SB265610 for 1 hour at room temperature. Binding data were evaluated by a non-linear curve fitting procedure using GraphPad Prism 4.0 (GraphPad Software, inc., San Diego, CA). Ligand affinities (pK_i) from competition binding experiments were calculated from binding IC_{50} using the Cheng-Prusoff equation [30].

β -arrestin recruitment assay

PathHunter™ HEK293-CXCR2 cells were plated out overnight at 10.000 cells/well (384-wells format) in 20 μl OPTI-MEM. A pre-incubation with CXCR2 antagonists or vehicle (PBS + 0.1 % BSA) of 30 min at 37°C and 5% CO_2 , was followed by 60 min CXCL8 stimulation at 37°C and 5% CO_2 . Next, the plate was placed at room temperature for 30 min, whereafter 12 μl PathHunter Detection Reagents (DiscoverX, Fremont, USA) was added. After an incubation of 60 min at room temperature, β -galactosidase-induced luminescence upon β -arrestin-CXCR2 interaction was measured for 0.3 sec in an Envision 2102 Multilabel Reader (PerkinElmer). Functional data were valuated by a non-linear curve fitting procedure using GraphPad Prism 4.0 (GraphPad Software, inc., San Diego, CA).

Results

Competition binding analysis with [¹²⁵I]-CXCL8 at hCXCR2.

Various non-peptidergic ligands with distinct structural features (Fig. 3.1) have recently been reported to effectively inhibit CXCR2 function [8, 17, 31]. In this study, we examined a selection of recently developed diarylurea and pyrimidine based CXCR2 antagonists in more detail. Membranes of COS-7 cells transiently transfected with human CXCR2 were incubated with [¹²⁵I]-CXCL8 and indicated concentrations of CXCL8, SB265610, compound 1 or VUF10948 (Fig. 3.2A). Analysis of homologous displacement with CXCL8 revealed binding of [¹²⁵I]-CXCL8 with a K_D of $0.49 \text{ nM} \pm 0.07 \text{ nM}$ and a B_{max} of $27.5 \pm 5.8 \text{ fmol/mg protein}$ ($n=3$). All tested CXCR2 antagonists dose-dependently displaced [¹²⁵I]-CXCL8 binding to human CXCR2. The pK_i values of the diarylurea compounds (SB225002, SB332235 and SB265610) are approximately 7.7, whereas the pK_i values of the tested pyrimidine derivatives (VUF10948, compound 1, compound 2 and compound 3) are in the range of 6.4 - 7.3 (Table 3.1).

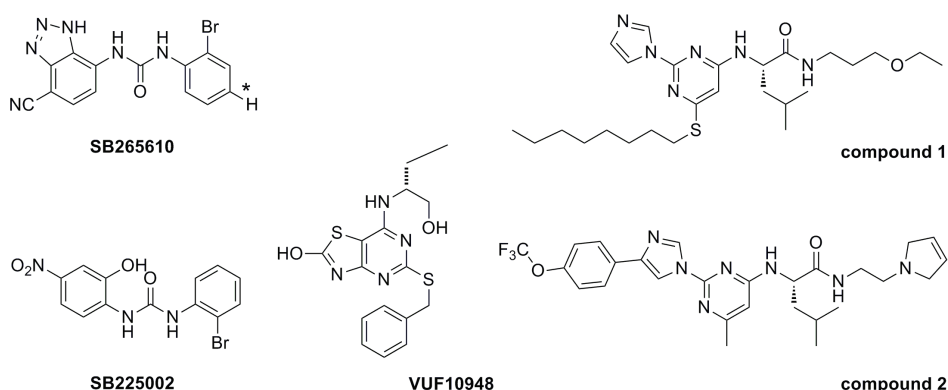


Figure 3.1: The structures of non-peptidergic CXCR2 antagonists are shown. SB265610 (1-(2-bromophenyl)-3-(4-cyano-1H-benzo[d][1,2,3]triazol-7-yl)urea), SB225002 (1-(2-bromophenyl)-3-(4-cyano-1H-benzo[d][1,2,3]triazol-7-yl)urea), and SB332235 (6-chloro-3-(3-(2,3-dichlorophenyl)ureido)-2-hydroxybenzenesulfonamide belong to the diarylurea class. VUF10948 ((R)-5-(benzylthio)-7-(1-hydroxybutan-2-ylamino)thiazolo[4,5-d]pyrimidin-2-ol) belongs to the thiazolopyrimidine class and compound 1 ((S)-2-(2-(1H-imidazol-1-yl)-6-(octylthio)pyrimidin-4-ylamino)-N-(3-ethoxypropyl)-4-methylpentanamide), compound 2 ((S)-N-(2-(2,5-dihydro-1H-pyrrol-1-yl)ethyl)-4-methyl-2-(6-methyl-2-(4-(4-(trifluoromethoxy)phenyl)-1H-imidazol-1-yl)pyrimidin-4-ylamino)pentanamide) and compound 3 ((S)-2-(6-butyl-2-(4-(4-chloro-3-(trifluoromethyl)phenyl)-1H-imidazol-1-yl)pyrimidin-4-ylamino)-4-methyl-N-(4,4,4-trifluorobutyl)pentanamide) belong to the imidazolopyrimidine class.

SB265610 has been labeled with a tritium atom, indicated in the figure with a * on a H-atom.

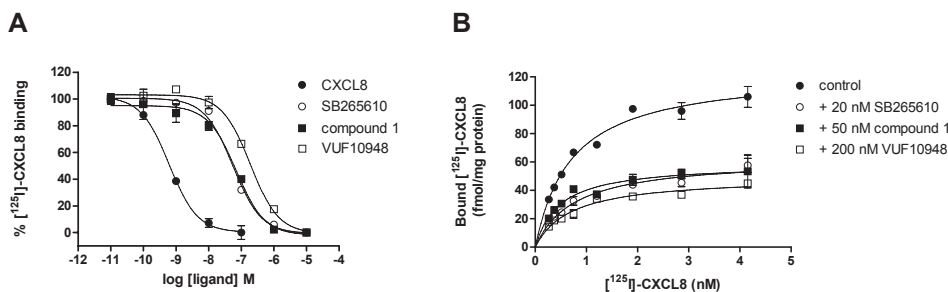


Figure 3.2: Displacement of $[^{125}\text{I}]\text{-CXCL8}$ binding to COS-7 cell membranes with CXCL8, SB265610, compound 1 and VUF10948 (A). Membranes were incubated with the indicated concentrations of CXCL8 (●), SB265610 (○), compound 1 (■) or VUF10948 (□) and approximately 300 pM $[^{125}\text{I}]\text{-CXCL8}$. Data of triplicate determinations from a representative experiment ($n=3-6$) are expressed as the percentage of $[^{125}\text{I}]\text{-CXCL8}$ binding \pm S.E.M. Saturation binding analysis with $[^{125}\text{I}]\text{-CXCL8}$ at COS-7 membranes expressing hCXCR2 (B). Membranes were incubated with the indicated concentrations of $[^{125}\text{I}]\text{-CXCL8}$ in the absence (●) or presence of SB265610 (○), compound 1 (■) or VUF10948 (□). Data show the mean specific binding \pm S.E.M. of triplicate determinations from a representative experiment ($n=2-4$).

Saturation binding of $[^{125}\text{I}]\text{-CXCL8}$ at hCXCR2

Saturation binding analysis of $[^{125}\text{I}]\text{-CXCL8}$ binding to COS-7 cell membranes expressing human CXCR2 (Fig. 3.2B) resulted in a K_D value of 0.66 ± 0.1 nM and a B_{max} value of 131.11 ± 4.1 fmol/mg protein ($n=4$). In the presence of 20 nM SB265610 the K_D value of CXCL8 is not affected (0.56 ± 0.2 nM), whereas the B_{max} decreased to 56.3 ± 6.5 fmol/mg. This indicates that SB265610 is a non-competitive antagonist. Likewise, compound 1, a representative of the imidazolylpyrimidine based CXCR2 antagonists, did not affect the K_D value of CXCL8 (0.36 ± 0.1 nM) but decreased the B_{max} value (52.0 ± 7.1 fmol/mg protein). Furthermore, also the representative of the thiazolopyrimidine class (VUF10948) did not affect the K_D value of CXCL8 (0.76 ± 0.1 nM) whereas the B_{max} value decreased to 65.8 ± 16.1 fmol/mg protein.

Antagonism of CXCL8-stimulated β -arrestin2 recruitment

Activation of CXCR2 by CXCL8 has been shown to lead to recruitment of β -arrestin [32]. To monitor direct interaction of CXCR2 with β -arrestin2, we used a β -arrestin2 recruitment assay for CXCR2 based on enzyme complementation of β -galactosidase [33], as established by DiscoveRx (PathHunter™ HEK293-hCXCR2). Stimulation of the PathHunter™ HEK293-hCXCR2 cells with CXCL8 induces β -arrestin2 recruitment as indicated by a 18.8 ± 1.3 fold increase in β -galactosidase activity ($\text{pEC}_{50} = 8.49 \pm 0.04$, $n=16$) (Fig. 3.3C-E). All CXCR2-antagonists were able to dose-dependently inhibit the CXCL8-induced (at EC_{80} concentration of 7.6 nM) β -arrestin2 recruitment (Fig. 3.3A). Data obtained with this functional assay correlate with the pK_i values of the CXCR2 ligands obtained in the $[^{125}\text{I}]\text{-CXCL8}$ binding studies ($r = 0.73$ (Fig. 3.3B)). The pK_b values of the diarylurea compounds are in the range of 7.9 - 8.9, whereas the pK_b values of the pyrimidine derivatives are in the range of 6.3 - 7.7 (Table 3.1). Interestingly, VUF10948 was the only tested CXCR2 antagonist that was not able to fully inhibit the CXCL8-induced signal, suggesting that this compound behaves as a non-competitive antagonist or as a partial agonist.

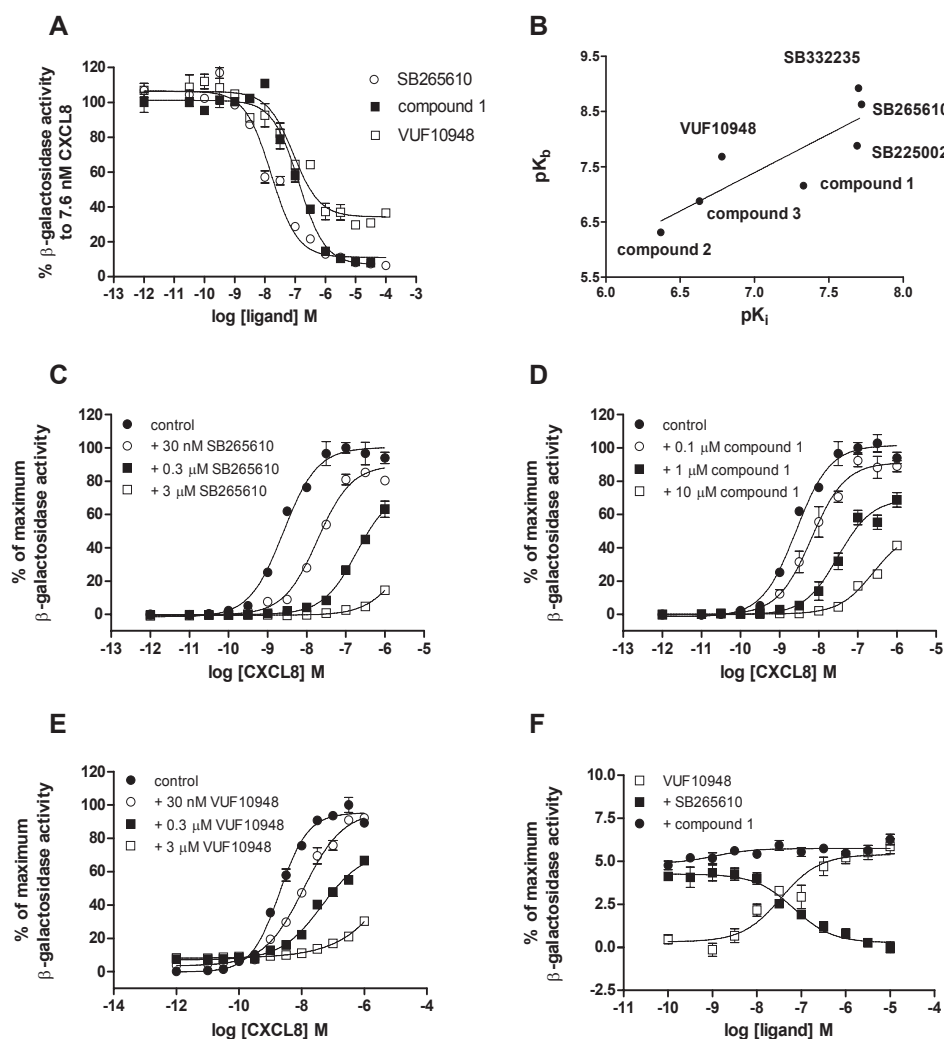


Figure 3.3: Effect of non-peptidergic CXCR2 antagonists on CXCL8-stimulated β -arrestin2 recruitment in PathHunter™ HEK293-hCXCR2 cells. CXCL8 induced β -arrestin2 recruitment is dose-dependent ($pEC_{50} = 8.49 \pm 0.04$, $n=16$). Data are expressed as percentage of maximum β -galactosidase activity \pm S.E.M. of a representative experiment performed in triplicate ($n=16$) (C-E). PathHunter™ HEK293-hCXCR2 cells were pretreated for 30 min with indicated concentrations of SB265610 (○), compound 1 (■) or VUF10948 (□) followed by stimulation with 7.6 nM CXCL8 (EC_{80}). Data of triplicate determinations from a representative experiment ($n=3-6$) are expressed as the percentage of β -galactosidase activity in response to 7.6 nM CXCL8 \pm S.E.M. (A). Relation between the pK_i values as determined in [125 I]-CXCL8 binding assay and the antagonistic potency as determined in the β -arrestin2 recruitment assay is shown ($r^2 = 0.73$) (B). Furthermore, PathHunter™ HEK293-hCXCR2 cells were pretreated with the indicated concentrations of SB265610 (C), compound 1 (D) or VUF10948 (E), followed by dose-dependent stimulation of CXCL8 stimulation. Data of triplicate determinations from a representative experiment ($n=2-4$) are expressed as percentage of maximum β -galactosidase activity \pm S.E.M. VUF10948 dose-dependently ($pEC_{50} = 7.39 \pm 0.14$) partially activates β -arrestin recruitment (□, $n=5$) (F). Pretreatment for 30 min with indicated concentrations of SB265610 (■) or compound 1 (●) was followed by stimulation with 0.3 μ M VUF10948 (EC_{90}). Data of triplicate determinations from a representative experiment ($n=3$) are expressed as the percentage of β -galactosidase activity in response to 100 nM CXCL8 \pm S.E.M.

From the seven compounds tested, a diarylurea (SB265610), an imidazolylpyrimidine (compound 1) as well as a thiazolopyrimidine (VUF10948) were chosen as representatives of their class to evaluate their mode of action in more detail. Cells were stimulated with increasing concentrations of CXCL8 in the absence or presence of SB265610 (Fig. 3.3C), compound 1 (Fig. 3.3D) or VUF10948 (Fig. 3.3E). Pre-incubation with either SB265610, compound 1 or VUF10948 results in a rightward shift of the CXCL8 dose response curve, but also reduces the maximal response of CXCL8 induced β -arrestin2 recruitment, indicating again, that these compounds behave as non-competitive antagonists. Interestingly, VUF10948 showed to be a weak partial CXCR2 agonist (Fig. 3.3F), whereas the other tested compounds showed no partial agonistic effects (data not shown). Stimulation of cells with 10 μ M VUF10948 resulted in 6.18 ± 1.0 % ($n=5$) β -galactosidase activity upon β -arrestin2 recruitment ($pEC_{50} = 7.39 \pm 0.14$). At 0.3 mM (EC_{90} concentration) this signal was dose-dependently inhibited by SB265610 ($pK_b = 8.11 \pm 0.02$). Interestingly, compound 1 was not able to inhibit the partial agonistic effect of VUF10948 (Fig. 3.3F).

Table 3.1: Properties of small non-peptidergic antagonists at human CXCR2.

Competition binding with non-peptidergic CXCR2 antagonists at COS-7 membranes expressing hCXCR2 and inhibition of CXCL8-stimulated β -arrestin2 recruitment of these antagonists in PathHunter™ HEK293-hCXCR2 cells. COS-7-hCXCR2 membranes were incubated with non-peptidergic CXCR2 antagonists (100 nM to 10 μ M) and approximately 300 pM [125 I]-CXCL8 or approximately 10 nM [3 H]-SB265610, respectively. Data shown are mean values of triplicate determinations ($n=2-3$) \pm S.E.M. PathHunter™ HEK293-hCXCR2 cells were pre-incubated for 30 min with non-peptidergic CXCR2 antagonists (1 pM to 100 μ M), followed by stimulation with 7.6 nM CXCL8. Data shown are mean values of triplicate determinations ($n=3-6$) \pm S.E.M.

Antagonist	[125 I]-CXCL8 displacement $pK_i \pm$ S.E.M.	Inhibition of CXCL8-induced β -arrestin2 recruitment $pK_b \pm$ S.E.M.	[3 H]-SB265610 displacement $pK_i \pm$ S.E.M.
SB256510	7.72 ± 0.08	8.63 ± 0.14	8.46 ± 0.06
SB332235	7.70 ± 0.15	8.92 ± 0.13	9.12 ± 0.18
SB225002	7.69 ± 0.21	7.88 ± 0.18	8.26 ± 0.25
VUF10948	6.78 ± 0.10	7.68 ± 0.09	7.71 ± 0.24
compound 1	7.33 ± 0.09	7.16 ± 0.09	n.d.
compound 2	6.37 ± 0.17	6.31 ± 0.20	n.d.
compound 3	6.63 ± 0.11	6.88 ± 0.00	n.d.

n.d. = no displacement of the radiolabeled SB265610 compound by cold ligand.

[3 H]-SB265610 as radioligand for CXCR2

Since the diarylurea class of CXCR2 antagonists has distinct structural features compared to the pyrimidine derivatives (Fig. 3.1), we set out to determine whether they bind to the same site at the human CXCR2. To this end, we radiolabeled the high affinity CXCR2 antagonist SB265610 with tritium and subjected [3 H]-SB265610 to a detailed analysis. Binding of [3 H]-SB265610 is proportional to the amount of membrane protein present (data not

shown). Moreover, [3 H]-SB265610 binds specific to human CXCR2 and does not bind to mock or CXCR1 expressing COS-7 cell membranes (Fig. 3.4A).

In association studies, [3 H]-SB265610 rapidly binds to membranes of COS-7 cells expressing human CXCR2. Half maximal specific binding was reached within 5.2 ± 0.6 minutes and equilibrium at 30 min, remaining stable thereafter (Fig. 3.4B). [3 H]-SB265610 binding was rapidly reversed ($t_{1/2} = 7.5 \pm 2.7$ min) by the addition of 10 μ M VUF10948 (Fig. 3.4C). The association and dissociation constants of [3 H]-SB265610 calculated from the kinetic data given in Figure 3.4 are $8.3 \times 10^6 \text{ min}^{-1}\text{M}^{-1}$ (derived from observed K_{on} $0.19 \pm 0.02 \text{ min}^{-1}$) and $0.13 \pm 0.06 \text{ min}^{-1}$, respectively, yielding a K_D of 16 nM.

Incubation of membranes of cells expressing human CXCR2 with increasing concentrations of [3 H]-SB265610 in the absence or presence of 10 μ M VUF10948 showed that the specific binding of [3 H]-SB265610 was saturable (Fig. 3.4D). The K_D - and B_{max} values obtained from saturation binding experiments were $2.51 \pm 1.5 \text{ nM}$ and around 50 pmol/mg, respectively.

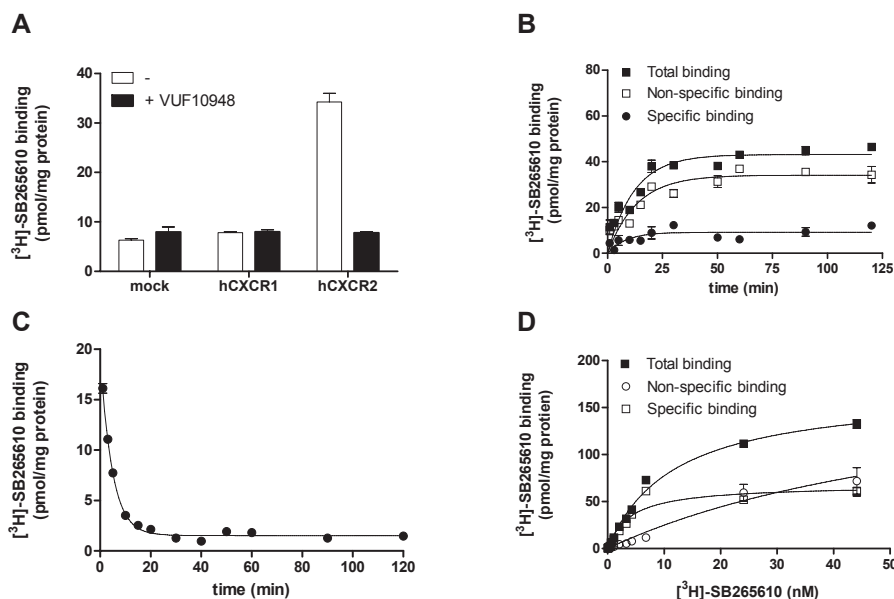


Figure 3.4: Binding of [3 H]-SB265610 to COS-7 membranes expressing hCXCR1 or hCXCR2 (A) in the absence (open bars) or presence of 10 μ M VUF10948 (filled bars). Membranes were incubated at room temperature for 1 hour with 3.8 nM [3 H]-SB265610 ($n=2$). To measure the association rate of [3 H]-SB265610 (B), membranes were incubated at room temperature for the indicated times with 7 nM [3 H]-SB265610 in the absence (\blacksquare , total binding) or presence of 10 μ M VUF10948 (\square , non-specific binding) resulting in specific binding (\bullet). Data show the mean \pm S.E.M of triplicate determinations measured at the indicated times from a representative experiment ($n=6$). To measure the dissociation rate of [3 H]-SB265610 (D), membranes from COS-7-hCXCR2 were incubated with 7 nM [3 H]-SB265610 for 1 hour at room temperature before the addition of 10 μ M VUF10948. Data show the mean \pm S.E.M of triplicate determinations measured at the indicated times from a representative experiment ($n=4$). Saturation binding analysis of [3 H]-SB265610 binding to COS-7 membranes expressing hCXCR2 (D). Membranes were incubated with the indicated concentrations of [3 H]-SB265610 for 1 hour at room temperature. Non-specific binding was determined in the presence of 10 μ M VUF10948. Data show the mean binding \pm S.E.M of triplicate, total binding (\blacksquare), non-specific binding (\square) or specific binding (\bullet) from a representative experiment ($n=2$).

Effect of GTP γ S on [125 I]-CXCL8 and [3 H]-SB265610 binding

To determine whether G-protein coupling affects [125 I]-CXCL8 and [3 H]-SB265610 binding to CXCR2, binding experiments were performed in the absence and presence of GTP γ S. [125 I]-CXCL8 binding analysis in the presence of indicated concentrations of GTP γ S to COS-7 cell membranes expressing human CXCR2 shows a dose-dependently inhibition of [125 I]-CXCL8 binding (Fig. 3.5). Of note, GTP γ S can not fully inhibit the [125 I]-CXCL8 binding. In contrast, the binding of [3 H]-SB265610 is not affected by GTP γ S at 10 μ M (insert Fig 3.5). These results indicate that [125 I]-CXCL8 mainly binds to human CXCR2 coupled to G-proteins, whereas [3 H]-SB265610 can bind to both G-protein coupled and uncoupled human CXCR2 conformations.

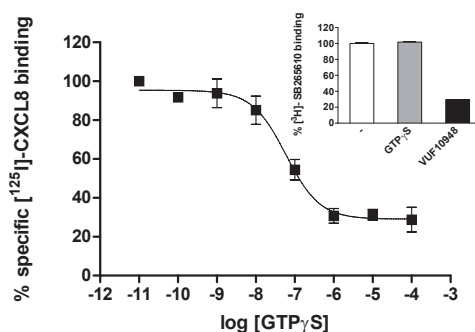


Figure 3.5: Competition binding of [125 I]-CXCL8] or [3 H]-SB265610 and GTP γ S at COS-7 membranes expressing hCXCR2. Membranes were incubated with the indicated concentrations of GTP γ S and approximately 300 pM [125 I]-CXCL8] or 10 μ M GTP γ S and 5 nM [3 H]-SB265610 (insert). Non-specific binding was determined in the presence of 10 μ M VUF10948. Data of triplicate determinations from a representative experiment (n=2) are expressed as the percentage of [125 I]-CXCL8 binding or [3 H]-SB265610 binding \pm SEM, respectively.

Competition binding analysis with [3 H]-SB256510 at hCXCR2

Membranes of COS-7 cells transiently transfected with human CXCR2 were incubated for 1 hour at room temperature with [3 H]-SB265610 and the indicated concentrations of CXCL1, CXCL8, SB265610 (Fig. 3.6A), VUF10948 or compound 1 (Fig. 3.6B). The K_D - and B_{max} values for SB265610 obtained from homologous displacement were $3.48 \text{ nM} \pm 0.63 \text{ nM}$ and $25.7 \pm 8.1 \text{ pmol/mg protein}$, respectively. These values are in good agreement with the data obtained in the saturation binding analysis. As expected, the diarylurea compounds (SB225002, SB332235 and SB265610) all displaced [3 H]-SB265610 with pK_i values in the range of 7.7 – 9.1 (Table 3.1). Yet, the chemokines CXCL8, CXCL1 and the imidazolylpyrimidine compounds (compound 1, compound 2 and compound 3) do not displace [3 H]-SB265610 up to 0.1 μ M and 10 μ M, respectively (Fig.3.6, Table 3.1).

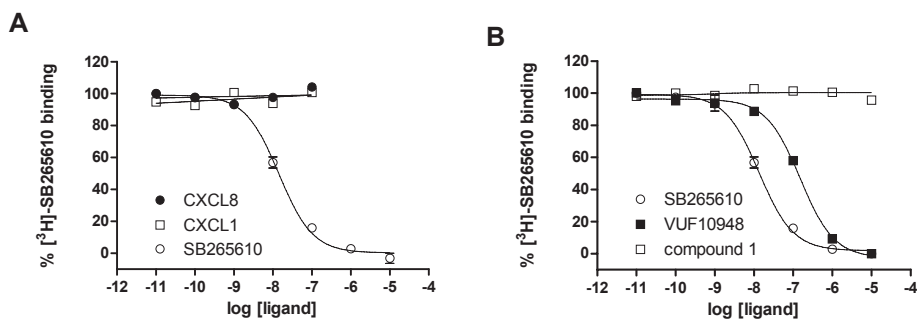


Figure 3.6: Competition binding of [^3H]-SB265610 and CXCL8, CXCL1, SB265610, VUF10948 and compound 1 at COS-7 membranes expressing hCXCR2. Membranes were incubated with the indicated concentrations of CXCL8 (●), CXCL1 (□), SB265610 (○) (A), VUF10948 (■) or compound 1 (□) (B) and approximately 10 nM [^3H]-SB265610 for 1 hour at room temperature. Data of triplicate determinations from a representative experiment ($n=2$) are expressed as the percentage of [^3H]-SB265610 binding \pm S.E.M.

Discussion

CXCR2 has attracted considerable attention as a potential drug target due to its involvement in different inflammatory diseases, like chronic obstructive pulmonary disease, psoriasis, rheumatoid arthritis and ulcerative colitis [5, 7-9]. Consequently, different classes of small CXCR2 antagonists have been developed, including diarylureas, thiazolo- and imidazolopyrimidines, quinoxalines, nicotinamide *n*-oxides, indole carboxylic acids and arylpropionic acids [15-21]. In this study, we selected seven different CXCR2 antagonists from the diarylurea, imidazolopyrimidine and thiazolopyrimidine class and studied their mechanisms of action at human CXCR2. In addition, the potent CXCR2 antagonist SB265610 was radiolabeled and used to identify distinct binding sites at the human CXCR2 for the studied CXCR2 antagonists.

The data presented in this study, show [^{125}I]-CXCL8 displacement by all non-peptidergic CXCR2 antagonists (Fig 3.2). The obtained pK_i values of both the diarylurea and pyrimidine compounds are in good agreement with earlier published data [8, 17, 31, 34, 35]. All tested compounds were able to inhibit CXCL8 induced β -arrestin2 recruitment in human CXCR2 transfected cells, with a rank order SB332235 \sim SB265610 $>$ SB225002 \sim VUF10948 $>$ compound 1 $>$ compound 3 $>$ compound 2 (Fig 3.3). This rank order correlates well with the binding affinity of these compounds to human CXCR2. Furthermore, these data are consistent with previous reported values for SB225002 inhibiting CXCL8 induced β -arrestin2 recruitment [36].

The compounds SB265610, compound 1 and VUF10948 were chosen as representatives of the different chemical CXCR2 antagonist classes and subjected to a detailed study to determine their antagonistic behavior. Schild plot analysis using the β -arrestin2 recruitment assay showed that the dose response curves of CXCL8 in the presence of SB265610, compound 1 or VUF10948 did not reach the maximal response (Fig. 3.3). This indicates

that all studied non-peptidergic antagonists behave as non-competitive antagonists at human CXCR2. Of the different CXCR2 antagonists tested, only VUF10948 was not able to fully inhibit CXCL8-induced β -arrestin2 recruitment. This can be ascribed to the partial agonistic properties of this compound at high concentrations. [125 I]-CXCL8 saturation binding studies in the presence of SB265610, compound 1 or VUF10948 showed a decrease of the maximal number of [125 I]-CXCL8 binding sites but no alteration in the binding affinity of [125 I]-CXCL8 (Fig. 3.2). Hence, the CXCR2 antagonists of the different chemical classes tested in this study, all displace and antagonize CXCL8 most likely via a non-competitive, allosteric mechanism. This mechanism of action is common for other small antagonists targeting chemokine receptors [35, 37]. The allosteric inhibition by the tested CXCR2 antagonists is expected, as in general chemokines, like CXCL8, are thought to bind to the extracellular part of the GPCR protein [2, 22, 23], notably the N-terminus and the extracellular loops. In contrast, small antagonists are considered to bind to the 7TM domains of GPCRs, as shown for AMD3100 at CXCR4, TAK-779 at CCR5 and BX471 at CCR1 [22], or possibly to the intracellular site of the receptor, as recently suggested for a thiazolopyrimidine compound and SB332235 at CXCR2 [24]. It should however be noted that an earlier study on a derivative on SB332235, SB225002, implicated the involvement of the N-terminus and amino acids in the extracellular loops and transmembrane domains in the binding of the CXCR2 antagonist [34].

Subsequently, we tritium labeled SB265610 and used [3 H]-SB265610 as a new tool to investigate the nature of the binding sites of CXCR2 antagonists at the human CXCR2. The binding of this radioligand is reversible and selective for human CXCR2 (Fig 3.4). Compared with the recently radiolabeled CXCR2 antagonist Sch527123 [35], [3 H]-SB265610 has a faster K_{off} and therefore an increased K_D . Of note, the B_{max} value obtained using [3 H]-SB265610 is higher compared to that when using [125 I]-CXCL8. [3 H]-Sch527123 also revealed a higher B_{max} value for CXCR2 compared to the value obtained using [125 I]-CXCL8 [35]. This difference is most likely caused by the fact that [125 I]-CXCL8 mainly binds to the G-protein coupled state of the receptor, as shown by loss of CXCL8 binding in the presence of GTP γ S, whereas [3 H]-SB265610 can bind to both G-protein coupled and uncoupled receptors (Fig. 3.5). This explanation for differences of B_{max} values was reported earlier in studies using different radiolabeled chemokines acting at human CXCR3 [38] or viral-encoded chemokine receptor ORF74 [39].

CXCL8 is not able to displace [3 H]-SB265610, providing evidence that CXCL8 binds to another binding site compared to the small CXCR2 antagonists. Most interestingly, we observed that the imidazolylopyrimidine compounds were not able to displace [3 H]-SB265610, whereas the diarylurea and thiazolopyrimidine compounds inhibited the binding of this radioligand (Fig. 3.6). Furthermore, the partial agonistic effect of the thiazolopyrimidine VUF10948 was inhibited by the diarylurea SB265610, whereas the imidazolylopyrimidine compound 1 was not able to inhibit this effect (Fig. 3.3). Thus, we conclude that there are not only distinct binding sites for chemokines and small non-peptidergic antagonists at human CXCR2, but also for the different CXCR2 antagonists. Although some data

is available on the binding site of CXCR2 antagonists of the diarylurea and thiazolopyrimidine class [24, 34], more research is required to further explore and define the direct interaction sites of the antagonists with CXCR2. Combining CXCR2 modeling studies, based on the recently reported crystal structure of the human beta-adrenergic receptor [40], with mutagenesis studies and use of radiolabeled low molecular weight CXCR2 antagonists, provide opportunities to investigate the different binding sites of CXCR2 antagonists in more detail.

References

1. Murphy, P.M., et al., International union of pharmacology. XXII. Nomenclature for chemokine receptors. *Pharmacol Rev*, 2000. 52(1): p. 145-76.
2. Viola, A. and A.D. Luster, Chemokines and Their Receptors: Drug Targets in Immunity and Inflammation. *Annu Rev Pharmacol Toxicol*, 2008. 48: p. 171-197.
3. Rotondi, M., et al., Role of chemokines in endocrine autoimmune diseases. *Endocr Rev*, 2007. 28(5): p. 492-520.
4. Singh, S., A. Sadanandam, and R.K. Singh, Chemokines in tumor angiogenesis and metastasis. *Cancer Metastasis Rev*, 2007. 26(3-4): p. 453-67.
5. Donnelly, L.E. and P.J. Barnes, Chemokine receptors as therapeutic targets in chronic obstructive pulmonary disease. *Trends Pharmacol Sci*, 2006. 27(10): p. 546-53.
6. Bizzarri, C., et al., ELR+ CXC chemokines and their receptors (CXC chemokine receptor 1 and CXC chemokine receptor 2) as new therapeutic targets. *Pharmacol Ther*, 2006. 112(1): p. 139-49.
7. Kulke, R., et al., The CXC receptor 2 is overexpressed in psoriatic epidermis. *J Invest Dermatol*, 1998. 110(1): p. 90-4.
8. Podolin, P.L., et al., A potent and selective nonpeptide antagonist of CXCR2 inhibits acute and chronic models of arthritis in the rabbit. *J Immunol*, 2002. 169(11): p. 6435-44.
9. Buanne, P., et al., Crucial pathophysiological role of CXCR2 in experimental ulcerative colitis in mice. *J Leukoc Biol*, 2007. 82(5): p. 1239-46.
10. Ajuebor, M.N., et al., Contrasting roles for CXCR2 during experimental colitis. *Exp Mol Pathol*, 2004. 76(1): p. 1-8.
11. Addison, C.L., et al., The CXC chemokine receptor 2, CXCR2, is the putative receptor for ELR+ CXC chemokine-induced angiogenic activity. *J Immunol*, 2000. 165(9): p. 5269-77.
12. Keane, M.P., et al., Depletion of CXCR2 inhibits tumor growth and angiogenesis in a murine model of lung cancer. *J Immunol*, 2004. 172(5): p. 2853-60.
13. Chapman, R.W., et al., A novel, orally active CXCR1/2 receptor antagonist, Sch527123, inhibits neutrophil recruitment, mucus production, and goblet cell hyperplasia in animal models of pulmonary inflammation. *J Pharmacol Exp Ther*, 2007. 322(2): p. 486-93.
14. Thatcher, T.H., et al., Role of CXCR2 in cigarette smoke-induced lung inflammation. *Am J Physiol Lung Cell Mol Physiol*, 2005. 289(2): p. L322-8.
15. Widdowson, K.L., et al., Evaluation of potent and selective small-molecule antagonists for the CXCR2 chemokine receptor. *J Med Chem*, 2004. 47(6): p. 1319-21.
16. Baxter, A., et al., Hit-to-Lead studies: the discovery of potent, orally bioavailable thiazolopyrimidine CXCR2 receptor antagonists. *Bioorg Med Chem Lett*, 2006. 16(4): p. 960-3.
17. Ho, K.K., et al., Imidazolylpyrimidine based CXCR2 chemokine receptor antagonists. *Bioorg Med Chem Lett*, 2006. 16(10): p. 2724-8.
18. Li, J.J., et al., Synthesis and structure-activity relationship of 2-amino-3-heteroaryl-quinoxalines as non-peptide, small-molecule antagonists for interleukin-8 receptor. *Bioorg Med Chem*, 2003. 11(17): p. 3777-90.
19. Cutshall, N.S., et al., Nicotinamide N-oxides as CXCR2 antagonists. *Bioorg Med Chem Lett*, 2001. 11(14): p. 1951-4.
20. Barth, M., P. Dodey, and J.-L. Paquet, Novel 5-cyano-1H-indole derivatives as antagonists of interleukin-8 receptors and their intermediates, pharmaceutical compositions, and use. World patent WO2002092567, 2002.
21. Allegretti, M., et al., Amidines and derivatives thereof and pharmaceutical preparations containing them. World patent WO2005028425, 2005.
22. Allen, S.J., S.E. Crown, and T.M. Handel, Chemokine: receptor structure, interactions, and antagonism. *Annu Rev Immunol*, 2007. 25: p. 787-820.
23. Rajagopalan, L. and K. Rajarathnam, Structural basis of chemokine receptor function--a model for binding affinity and ligand selectivity. *Biosci Rep*, 2006. 26(5): p. 325-39.
24. Nicholls, D.J., et al., Identification of a Putative Intracellular Allosteric Antagonist Binding-Site in the CXC Chemokine Receptors 1 and 2. *Mol Pharmacol*, 2008.
25. Conti, P., et al., Preparation of (2S)-2-[(pyrimidin-4-yl)amino]-4-methylpentanoic acid aminoethylamide derivatives as interleukin 8 receptor modulators for the treatment of atherosclerosis and rheumatoid arthritis. World patent WO2004069829, 2004.

-
26. Erickson, S., et al., Preparation of pyrimidine amino acid derivatives as interleukin-8 (IL-8) receptor antagonists. World patent WO2001025242, 2001.
 27. Willis, P.A., et al., Preparation of novel thiazolo[4,5-d]pyrimidines as modulators of chemokine receptors. World patent WO2004069829, 2004.
 28. Brakenhoff, R.H., E.M. Knippels, and G.A. van Dongen, Optimization and simplification of expression cloning in eukaryotic vector/host systems. *Anal Biochem*, 1994. 218(2): p. 460-3.
 29. Goldman, L.A., et al., Modifications of vectors pEF-BOS, pcDNA1 and pcDNA3 result in improved convenience and expression. *Biotechniques*, 1996. 21(6): p. 1013-5.
 30. Cheng, Y. and W.H. Prusoff, Relationship between the inhibition constant (K_i) and the concentration of inhibitor which causes 50 per cent inhibition (I₅₀) of an enzymatic reaction. *Biochem Pharmacol*, 1973. 22(23): p. 3099-108.
 31. White, J.R., et al., Identification of a potent, selective non-peptide CXCR2 antagonist that inhibits interleukin-8-induced neutrophil migration. *J Biol Chem*, 1998. 273(17): p. 10095-8.
 32. Richardson, R.M., et al., Role of the cytoplasmic tails of CXCR1 and CXCR2 in mediating leukocyte migration, activation, and regulation. *J Immunol*, 2003. 170(6): p. 2904-11.
 33. Olson, K.R. and R.M. Eglen, Beta galactosidase complementation: a cell-based luminescent assay platform for drug discovery. *Assay Drug Dev Technol*, 2007. 5(1): p. 137-44.
 34. Carusse, J., et al., Characterization of the molecular interactions of interleukin-8 (CXCL8), growth related oncogen alpha (CXCL1) and a non-peptide antagonist (SB 225002) with the human CXCR2. *Biochem Pharmacol*, 2003. 65(5): p. 813-21.
 35. Gonsiorek, W., et al., Pharmacological characterization of Sch527123, a potent allosteric CXCR1/CXCR2 antagonist. *J Pharmacol Exp Ther*, 2007. 322(2): p. 477-85.
 36. Yan, Y.X., et al., Cell-based high-throughput screening assay system for monitoring G protein-coupled receptor activation using beta-galactosidase enzyme complementation technology. *J Biomol Screen*, 2002. 7(5): p. 451-9.
 37. Verzijl, D., et al., Noncompetitive antagonism and inverse agonism as mechanism of action of nonpeptidergic antagonists at primate and rodent CXCR3 chemokine receptors. *J Pharmacol Exp Ther*, 2008. 325(2): p. 544-55.
 38. Cox, M.A., et al., Human interferon-inducible 10-kDa protein and human interferon-inducible T cell alpha chemoattractant are allotypic ligands for human CXCR3: differential binding to receptor states. *Mol Pharmacol*, 2001. 59(4): p. 707-15.
 39. Verzijl, D., et al., Helix 8 of the viral chemokine receptor ORF74 directs chemokine binding. *J Biol Chem*, 2006. 281(46): p. 35327-35.
 40. Cherezov, V., et al., High-resolution crystal structure of an engineered human beta2-adrenergic G protein-coupled receptor. *Science*, 2007. 318(5854): p. 1258-65.
-

*Identification of a novel allosteric binding site
in the CXCR2 chemokine receptor*

Chapter 4

Petra de Kruijf^{A,1}, Herman D. Lim^{A,1}, Luc Roumen^{A,1}, Véronique A. Renjaän^A,
Jiuqiao Zhao^C, Maria L. Webb^C, Douglas S. Auld^C, Jac. C.H.M. Wijkmans^B,
Guido J.R. Zaman^B, Martine J. Smit^A, Chris de Graaf^A and Rob Leurs^A

^A Leiden/Amsterdam Center for Drug Research, Division of Medicinal Chemistry,
Vrije Universiteit Amsterdam, The Netherlands

^B Merck Research Laboratories, Oss, The Netherlands

^C Pharmacopeia Drug Discovery, Princeton, NJ 08543-5350, USA

¹ Contributed equally

Accepted as:

De Kruijf *et al.* Mol Pharmacol, 2011

Abstract

We have previously shown that different chemical classes of small molecule antagonists of the human chemokine CXCR2 receptor interact with distinct binding sites of the receptor [1]. While an intracellular binding site for diarylurea CXCR2 antagonists, like SB265610, and thiazolopyrimidine compounds was recently mapped by mutagenesis studies [2, 3], we now report on an imidazolylpyrimidine antagonist binding pocket in the transmembrane domain of CXCR2. Using different CXCR2 orthologs, chimeric proteins, site-directed mutagenesis and *in silico* modeling, we have elucidated the binding mode of this antagonist. Our *in silico* guided mutagenesis studies indicate that the ligand binding cavity for imidazolylpyrimidine compounds in CXCR2 is located between transmembrane (TM) helices 3 (F130^{3.36}), 5 (S217^{5.44}, F220^{5.47}), and 6 (N268^{6.52}, L271^{6.55}) and suggest that these antagonists enter CXCR2 via the TM5-TM6 interface. Interestingly, the same interface is postulated as the ligand entry channel in the opsin receptor [4] and is occupied by lipid molecules in the recently solved crystal structure of the CXCR4 chemokine receptor [5], suggesting a general ligand entrance mechanism for nonpolar ligands to G protein-coupled receptors (GPCRs). The identification of a novel allosteric binding cavity in the TM domain of CXCR2, in addition to the previously identified intracellular binding site, shows the diversity in ligand recognition mechanisms by this receptor and offers new opportunities for the structure-based design of small allosteric modulators of CXCR2 in the future.

Acknowledgements

This study was performed within the framework of the Dutch Top Institute Pharma project T101-3

Introduction

The chemokine receptor CXCR2 belongs to the rhodopsin-like family of G-protein coupled receptors (GPCRs) [6]. It is expressed on endothelial cells and on different inflammatory cells such as eosinophils, natural killer cells, neutrophils, macrophages, mast cells and monocytes [6, 7]. CXCR2 interacts with the chemokines CXCL1, CXCL2, CXCL3, CXCL5, CXCL6, CXCL7 and CXCL8. Upon production of these chemokines, CXCR2 is responsible for the transmigration of inflammatory cells towards sites of inflammation. Several *in vivo* studies have shown an important role for CXCR2 in inflammatory diseases like atherosclerosis [8], chronic obstructive pulmonary disease [9], rheumatoid arthritis [10] and multiple sclerosis [11]. Furthermore, the expression of CXCR2 is increased in psoriatic epidermis [12] and in bronchial biopsies of chronic obstructive pulmonary disease patients [13]. These studies indicate that CXCR2 is an interesting drug target. In view of this therapeutic potential, different CXCR2 antagonists are being developed (see e.g. [14-17]). Amongst them, SCH527123 and repertaxin are currently in phase II clinical trial (ThomsonPharma database; <http://partnering.thomson-pharma.com>).

Previously, we investigated in detail the mechanism of action of CXCR2 antagonists that belong to the diarylurea, imidazolylpyrimidine and thiazolopyrimidine classes [1]. Using the tritium labeled diarylurea [^3H]-SB265610, we discovered that small molecule CXCR2 antagonists of different classes bind to distinct binding sites. The imidazolylpyrimidine compounds (like compound 1, see Fig. 4.1) were not able to displace [^3H]-SB265610, while the diarylurea (like SB255610, see Fig. 4.1) and thiazolopyrimidine compounds could compete for [^3H]-SB265610 binding. Recently, two groups have provided evidence that compounds belonging to the diarylurea and thiazolopyrimidine class most likely bind intracellularly to CXCR2 [2, 3]. The binding site of imidazolylpyrimidine CXCR2 antagonists remained to be investigated. Recently, the first chemokine receptor crystal structures have been solved [5]. These structures show overlapping but distinct binding pockets in the TM binding domain of CXCR4 for the small molecule antagonist IT1t and the cyclic peptide CVX15. Furthermore, site-directed mutagenesis studies with various chemokine receptors demonstrated that compounds can bind either in the minor subpocket (between transmembrane (TM) helices 1, 2, 3, and 7) or in the major subpocket (between TM3, 4, 5, 6, and 7) [18]. The primary aim of the current study was to probe the binding site of compound 1 in the TM binding domain.

Animal models are still crucial to investigate the therapeutic potential of compounds. Translating the results of animal studies to humans can however be hampered by differences between receptor orthologs. Species-related differences in the sequences of protein targets ('natural mutants') have previously been used to identify the molecular determinants of ligand binding to GPCRs [19-21]. Species differences have also been observed for CXCR2. While imidazolylpyrimidine compounds like compound 1 (Fig. 4.1) are potent antagonists of human CXCR2, these compounds have no affinity for rodent CXCR2 receptors (J.C.H.M.W., M.L.W., D.S.A., unpublished data). Human CXCR2 has a significantly higher

DNA Constructs and Site-Directed Mutagenesis

The wild-type human CXCR2 cloned in pcDNA3.1+ (Genbank ACC # P25025) was purchased from the Missouri S&T cDNA Resource Center (Rollo, MO). The CXCR2 receptors from baboon (Genbank ACC # Q8HZN3), chimpanzee (Genbank ACC # Q28807), gorilla (Genbank ACC # Q8HZN7), orangutan (Genbank ACC # Q8HZN6), rhesus (Genbank ACC# Q8HZN5) and vervet (Genbank ACC # Q8HZN4) were cloned and characterized as described by Horlick and co-workers [24]. Briefly, baboon, chimpanzee, gorilla and orangutan genomic DNA were isolated from lymphoblast cells, whereas vervet genomic DNA was isolated from a liver biopsy specimen obtained from Dr. Frank Ervin (Caribbean Primates Ltd., Caribbean Primates Ltd., Madison). Next, polymerase chain reaction (PCR) was used to amplify the coding sequences of these orthologs. Rhesus genomic DNA was purchased from Clontech (Palo Alto, Calif). The cDNA of cynomolgus CXCR2 [25] was made by PCR mutagenesis of rhesus CXCR2 residues, including E2Q/L9F/K11E/G12N in the N-terminus and L228F at the bottom of transmembrane V.

Chimeric receptor constructs were created by exchanging the domains between residue Lys120^{3,26} (EcoN1 restriction site in the cDNA) and residue Arg212^{3,39} (BamHI restriction site in the cDNA) of the human CXCR2 (see Fig. 4.3B) with that of the baboon CXCR2 or vice versa, resulting in the chimeric receptors HHB (human-human-baboon), BBH (baboon-baboon-human), HBB (human-baboon-baboon), BHH (baboon-human-human), HBH (human-baboon-human) and BHB (baboon-human-baboon). Site-directed mutagenesis was performed by PCR with the use of DNA primers with single-, double- or triple-base mismatches, resulting in a codon change for the desired amino acid substitution. The correct sequence of all DNA constructs was confirmed by sequencing analysis (Macrogen, Amsterdam, The Netherlands).

Cell Culturing and Transfection

COS-7 cells were grown at 5% CO₂ and 37°C in Dulbecco's modified Eagle's medium supplemented with 5% (v/v) fetal bovine serum, 50 IU/ml penicillin and 50 µg/ml streptomycin. Cells were transiently transfected (per 10 cm dish) with 2.5 µg of cDNA encoding the receptor supplemented with 2.5 µg of pcDNA by using linear polyethylenimine (PEI) with a molecular weight of 25 kDa. In brief, 5 µg of total DNA was diluted in 250 µl 150 mM NaCl. Next, 30 µg of PEI in 250 µl of 150 mM NaCl was added to the DNA solution. This mixture was incubated for 5 to 10 min at room temperature before it was added onto subconfluent COS-7 monolayer.

Membrane preparation

Two days after transfection, cells were detached from the plastic surface using ice-cold phosphate-buffered saline (PBS) and centrifuged at 1500g for 10 min at 4°C. Next, the pellet was resuspended in the ice-cold PBS and centrifuged again at 1500g for 10 min at 4°C. Later, cells were resuspended in ice-cold membrane buffer (15 mM Tris, 1 mM EGTA, 0.3 mM EDTA, and 2 mM MgCl₂, pH 7.5), followed by homogenization by 10 strokes at 1100 to 1200 rpm using a Teflon-glass homogenizer and rotor. The membranes were subjected to two freeze-thaw cycles using liquid nitrogen, followed by centrifugation at 40,000g for 25 min at 4°C. The pellet was rinsed once with ice-cold Tris-sucrose buffer (20 mM Tris and 250 mM sucrose, pH 7.4) and subsequently resuspended in the same buffer and frozen at -80°C until use. Protein concentration was determined using a BCA-protein assay (Thermo Scientific, Rockford, USA).

Radioligand binding assays

Membranes were incubated in 96-well plates in binding buffer (50 mM Na₂HPO₄ and 50 mM KH₂PO₄, pH 7.4) supplemented with 0.5% BSA, approximately 100 pM [¹²⁵I]-CXCL8 and indicated concentrations of CXCL8 or CXCR2 antagonist in a final volume of 100 µl. The reaction mixtures were incubated for 1 hour at room temperature, harvested with rapid filtration through Unifilter GF/C 96-well filterplates (PerkinElmer, USA) pretreated with 0.3% polyethylenimine and washed three times with ice-cold wash buffer (50 mM Na₂HPO₄ and 50 mM KH₂PO₄, pH 7.4). Bound radioactivity was determined using a MicroBeta (PerkinElmer, USA). Binding data were evaluated by a non-linear curve fitting procedure using GraphPad Prism 4.0 (GraphPad Software, inc., San Diego, CA). Ligand affinities (pK_i) from competition binding experiments were calculated from binding IC₅₀ using the Cheng-Prusoff equation [26].

[³⁵S]-GTPγS binding assay

Membranes were incubated in 96-well plates in assay buffer (50 mM Hepes, 10 mM MgCl₂, 100 mM NaCl, pH 7.2) supplemented with 5 µg saponin/well, 3 µM GDP and approximately 400 pM of [³⁵S]-GTPγS and indicated concentrations of CXCL8 in a final volume of 100 µl. When CXCR2 antagonists were applied to EC₈₀ concentration of CXCL8, membranes were pre-incubated for 30 min at room temperature. The reaction mixtures were incubated for 1 hour at room temperature, harvested with rapid filtration through Unifilter GF/B 96-well filterplates (PerkinElmer, USA) and washed three times with ice-cold wash buffer (50 mM Tris-HCl and 5 mM MgCl₂, pH 7.4). [³⁵S]-GTPγS incorporation was determined using a Microbeta scintillation counter (Perkin Elmer, USA). Functional data were evaluated by a nonlinear curve fitting procedure using GraphPad Prism 4.0 (GraphPad Software Inc.).

Residue numbering and Nomenclature

The Ballesteros-Weinstein residue number [27] is given as superscript throughout the article for the enumeration of GPCR transmembrane helix residues in addition to the UniProt number [28]. The residues inside the extracellular loops are enumerated based on the Ballesteros and Weinstein numbering of the preceding transmembrane helix.

Construction CXCR2 in silico model

A three dimensional model of the CXCR2 receptor was built with MOE version 2009.10 (Chemical Computing Group Inc, Montreal, Canada) based on the recently elucidated crystal structure of its family member, the chemokine receptor CXCR4 solved with a small molecule (pdb code: 3ODU, [5]). To this end, the primary sequence of CXCR2 (Genbank ACC # P25025) was aligned to that of the crystal structure of CXCR4, disregarding the fused T4 lysozyme (Supp Fig. 4.1). The N-terminal residues 1-37 were omitted from model construction due to a lack of crystal data. Furthermore, due to the disordered region in the CXCR4 structure, the C-terminal residues 315-330 corresponding to half of TM7 and intracellular helix 8 of CXCR2 were modeled based on the crystal structure of human adrenergic beta 2 (ADRB2, pdb code 2RH1, [29]).

Protein-ligand interactions

Compound 1 was docked into the CXCR2 model using the program GOLD v4 [30]. The docking was specifically aimed at the pocket between TMs 3, 4, 5, 6 and 7, delineating the major pocket within the TM domain, since this region was identified to determine the binding of compound 1 to CXCR2 in the chimera study of this. Protein-ligand interactions were optimized in MOE by energy minimization during which the heavy atoms of the pocket residues were tethered with a 10.0 kcal/mol restraint and the remainder of the receptor was fixed in space. Compound 1 was docked and optimized in a similar manner for the binding pose on the outside of the transmembrane region.

Results

Cloning and pharmacological characterization of CXCR2 Orthologs

To elucidate the binding mode of compound 1 at human CXCR2, we started the study with different CXCR2 orthologs. The CXCR2 receptor cDNA's of rhesus, vervet, baboon, chimpanzee, gorilla and orangutan were cloned and amplified by using polymerase chain reaction (PCR) [24], while the cynomolgus ortholog was derived from rhesus CXCR2 by site-directed mutagenesis. Sequence analysis confirmed that the sequences indeed correspond to the CXCR2 ortholog sequences (Fig. 4.2). Comparison of the protein sequences of the seven CXCR2 orthologs and human CXCR2 revealed that all have a high homology with each other ranging from 89% to 100% (Fig. 4.3A). Due to the high homology of the CXCR2 orthologs, we have used them as 'natural mutants' to identify which amino acids are involved in the binding of compound 1. To determine the binding affinity of compound 1 to all CXCR2 orthologs, membranes of COS-7 cells transiently transfected with human CXCR2 or a CXCR2 ortholog were incubated with [¹²⁵I]-CXCL8 and indicated concentrations of CXCL8, SB265610 or compound 1 (Fig. 4.4A, Table 4.1). Figure 4.4 clearly shows that the binding affinity of compound 1 is significantly abolished at baboon CXCR2 compared to human CXCR2, whereas the binding affinity for both CXCL8 and SB265610 are not different. Analysis of homologous displacement with CXCL8 to all CXCR2 orthologs revealed binding of [¹²⁵I]-CXCL8, with a pK_d ranging from 9.1 to 9.6. SB265610 dose-dependently displaces [¹²⁵I]-CXCL8 from all CXCR2 orthologs with pK_i values from 7.3 to 7.7, whereas compound 1 only displaces [¹²⁵I]-CXCL8 from human, chimpanzee, gorilla and orangutan with pK_i values from 6.4 to 7.2 (Table 4.1).

Tabel 4.1: Affinity (pK_d or pK_i) of CXCR2 ligands at various CXCR2 orthologs. Displacement of [¹²⁵I]-CXCL8 binding to COS-7 cell membranes expressing indicated CXCR2 orthologs. The data are presented as mean \pm S.E.M. of at least three independent experiments.

	pK_d	pK_i	pK_i
CXCR2	CXCL8	SB265610	compound 1
Rhesus	9.55 \pm 0.19	7.71 \pm 0.16	<4
Cynomolgus	9.21 \pm 0.05	7.44 \pm 0.05	<4
Vervet	9.31 \pm 0.18	7.71 \pm 0.11	<4
Baboon	9.33 \pm 0.08	7.28 \pm 0.10	<4
Human	9.40 \pm 0.14	7.68 \pm 0.11	7.18 \pm 0.13
Chimpanzee	9.29 \pm 0.18	7.72 \pm 0.17	6.81 \pm 0.18
Gorilla	9.33 \pm 0.03	7.70 \pm 0.12	6.90 \pm 0.10
Orangutan	9.12 \pm 0.15	7.42 \pm 0.07	6.38 \pm 0.16

Differences of amino acids between the CXCR2 orthologs that cannot bind compound 1 (rhesus, cynomolgus, vervet and baboon) and the orthologs that bind compound 1 (human, chimpanzee, gorilla and orangutan) are indicated in Figure 4.2. Four residues are located

within the TM domain (L92^{2.48}, S107^{2.63}, S217^{5.44} and N268^{6.52}), two intracellular (Y75^{1.59} and I331^{7.80}), five extracellular (V192^{4.73}, N206^{5.32}, L210^{5.36}, V281^{6.65} and E287^{6.71}) and four in the N-terminus (S10, L34, A36 and E40) (Fig. 4.2, 4.3B). In the remainder of the study, we will denote the non-binders as class A orthologs and the binders as class B orthologs, respectively.

```

rhesus      -----MESFNFEDLWKGEDFSNYSYSSDLPSPFDVAPCRPESLEINKYFVVIIYALVFL 55
cynomolgus -----MQSFNFEDFWENEDLSNYSYSSDLPSPFDVAPCRPESLEINKYFVVIIYALVFL 55
vervet      -----MEISNFEDLWKSEDFSNYSYSSDLPSPFDVTPCRPESLEINKYFVVIIYALVFL 55
baboon      -----MESFNFEDFWTGEDFSNYSYSSDLPSPFDVAPCRPESLEINKYFVVIIYALVFL 55
human       MEDFNMESDSFEDFWKGEDLSNYSYSSDLPSPFDVAPCRPESLEINKYFVVIIYALVFL 60
chimpanzee -----MESDSFEDFWKGEDLSNYSYSSDLPSPFDVAPCRPESLEINKYFVVIIYALVFL 55
gorilla     -----MESDSFEDFWKGEDLSNYSYSSDLPSPFDVAPCRPESLEINKYFVVIIYALVFL 55
orangutan   -----MESDSFEDFLKGEDFSNYSYSSDLPSPFDVAPCRPESLEINKYFVVIIYALVFL 55
              *:  .*:  .*:*****  *  *:  .*:*****.*****

rhesus      LSLLGNSLVMVLVIIHSRVGRSITDVYLLNLAMADLLFALTLPWAASAKVNGWIFGTFLCK 115
cynomolgus  LSLLGNSLVMVLVIIHSRVGRSITDVYLLNLAMADLLFALTLPWAASAKVNGWIFGTFLCK 115
vervet      LSLLGNSLVMVLVIIHSRVGRSITDVYLLNLAMADLLFALTLPWAASAKVNGWIFGTFLCK 115
baboon      LSLLGNSLVMVLVIIHSRVGRSITDVYLLNLAMADLLFALTLPWAASAKVNGWIFGTFLCK 115
human       LSLLGNSLVMVLVIIHSRVGRSITDVYLLNLAMADLLFALTLPWAASAKVNGWIFGTFLCK 120
chimpanzee  LSLLGNSLVMVLVIIHSRVGRSITDVYLLNLAMADLLFALTLPWAASAKVNGWIFGTFLCK 115
gorilla     LSLLGNSLVMVLVIIHSRVGRSITDVYLLNLAMADLLFALTLPWAASAKVNGWIFGTFLCK 115
orangutan   LSLLGNSLVMVLVIIHSRVGRSITDVYLLNLAMADLLFALTLPWAASAKVNGWIFGTFLCK 115
              *****:*****:*****:*****:*****:*****:*****

rhesus      VVSLKKEVNFYSYGILLACISVDRYLAIVHATRTLTKQRYLVKVFCLSIWLSLALLALPV 175
cynomolgus  VVSLKKEVNFYSYGILLACISVDRYLAIVHATRTLTKQRYLVKVFCLSIWLSLALLALPV 175
vervet      VVSLKKEVNFYSYGILLACISVDRYLAIVHATRTLTKQRYLVKVFCLSIWLSLALLALPV 175
baboon      VVSLKKEVNFYSYGILLACISVDRYLAIVHATRTLTKQRYLVKVFCLSIWLSLALLALPV 175
human       VVSLKKEVNFYSYGILLACISVDRYLAIVHATRTLTKQRYLVKVFCLSIWLSLALLALPV 180
chimpanzee  VVSLKKEVNFYSYGILLACISVDRYLAIVHATRTLTKQRYLVKVFCLSIWLSLALLALPV 175
gorilla     VVSLKKEVNFYSYGILLACISVDRYLAIVHATRTLTKQRYLVKVFCLSIWLSLALLALPV 175
orangutan   VVSLKKEVNFYSYGILLACISVDRYLAIVHATRTLTKQRYLVKVFCLSIWLSLALLALPV 175
              *****:*****:*****:*****:*****:*****

rhesus      LLFRRTVYLTYSIPVCYEDMGNNNTAKWRMVLRLILPQTGFILPLLIMLCYGLTLRTLFK 235
cynomolgus  LLFRRTVYLTYSIPVCYEDMGNNNTAKWRMVLRLILPQTGFILPLLIMLCYGLTLRTLFK 235
vervet      LLFRRTVYPTYSIPVCYEDMGNNNTAKWRMVLRLILPQTGFILPLLIMLCYGLTLRTLFK 235
baboon      LLFRRAVYPPYISIPVCYEDMGNNNTAKWRMVLRLILPQTGFIVPLLMLCYGYFTLRTLFK 235
human       LLFRRTVYSSNVSPACYEDMGNNNTAKWRMVLRLILPQSGFIVPLLMLCYGYFTLRTLFK 240
chimpanzee  LLFRRTVYSSNVSPACYEDMGNNNTAKWRMVLRLILPQSGFIVPLLMLCYGYFTLRTLFK 235
gorilla     LLFRRTIYPSNVSPVCYEDMGNNNTAKWRMVLRLILPQSGFIVPLLMLCYGYFTLRTLFK 235
orangutan   LIFRKTIYPPYISIPVCYEDMGNNNTAKWRMVLRLILPQSGFIVPLLMLCYGYFTLRTLFK 235
              *:  .*:  .*:*****:*****:*****:*****:*****

rhesus      AHMGQKHRAMRVIFAVVLIFLLCWLPHYHLVLLADTLMRTRLINETQRRNNIDQALDATE 295
cynomolgus  AHMGQKHRAMRVIFAVVLIFLLCWLPHYHLVLLADTLMRTRLINETQRRNNIDQALDATE 295
vervet      AHMGQKHRAMRVIFAVVLIFLLCWLPHYHLVLLADTLMRTRLIKETQRRNNIDRALDATE 295
baboon      AHMGQKHRAMRVIFAVVLIFLLCWLPHYHLVLLADTLMRTRLINETQRRHSDINQALDATE 295
human       AHMGQKHRAMRVIFAVVLIFLLCWLPHYHLVLLADTLMRTQVIQETCERRNHIDRALDATE 300
chimpanzee  AHMGQKHRAMRVIFAVVLIFLLCWLPHYHLVLLADTLMRTQVIQETCERRNHIDRALDATE 295
gorilla     AHMGQKHRAMRVIFAVVLIFLLCWLPHYHLVLLADTLMRTQVIQETCERRNHIDRALDATE 295
orangutan   AHMGQKHRAMRVIFAVVLIFLLCWLPHYHLVLLADTLMRTQVIQETCERRNHIDRALDATE 295
              *****:*****:*****:*****:*****:*****

rhesus      ILGILHSCLNPLIYAFIGQKFRHGLLKILATHGLISKDSLPKDSRPSFVGSSSGHTSTTL 355
cynomolgus  ILGILHSCLNPLIYAFIGQKFRHGLLKILATHGLISKDSLPKDSRPSFVGSSSGHTSTTL 355
vervet      ILGILHSCLNPLIYAFIGQKFRHGLLKILATHGLISKDSLPKDSRPSFVGSSSGHTSTTL 355
baboon      ILGIFHSCLNPLIYAFIGQKFRHGLLKILATHGLISKDSLPKDSRPSFVGSSSGHTSTTL 355
human       ILGILHSCLNPLIYAFIGQKFRHGLLKILATHGLISKDSLPKDSRPSFVGSSSGHTSTTL 360
chimpanzee  ILGILHSCLNPLIYAFIGQKFRHGLLKILATHGLISKDSLPKDSRPSFVGSSSGHTSTTL 355
gorilla     ILGILHSCLNPLIYAFIGQKFRHGLLKILATHGLISKDSLPKDSRPSFVGSSSGHTSTTL 355
orangutan   ILGILHSCLNPLIYAFIGQKFRHGLLKILATHGLISKDSLPKDSRPSFVGSSSGHTSTTL 355
              *****:*****:*****:*****:*****:*****

```

Figure 4.2: Alignment of the sequences of various CXCR2 orthologs. The boxed residues differ all between the orthologs that are not able to bind compound 1 (rhesus, cynomolgus, vervet and baboon; 'class A') and the orthologs that are able to bind compound 1 (human, chimpanzee, gorilla and orangutan; 'class B'). Residues indicated in bold differ between the human and baboon CXCR2.

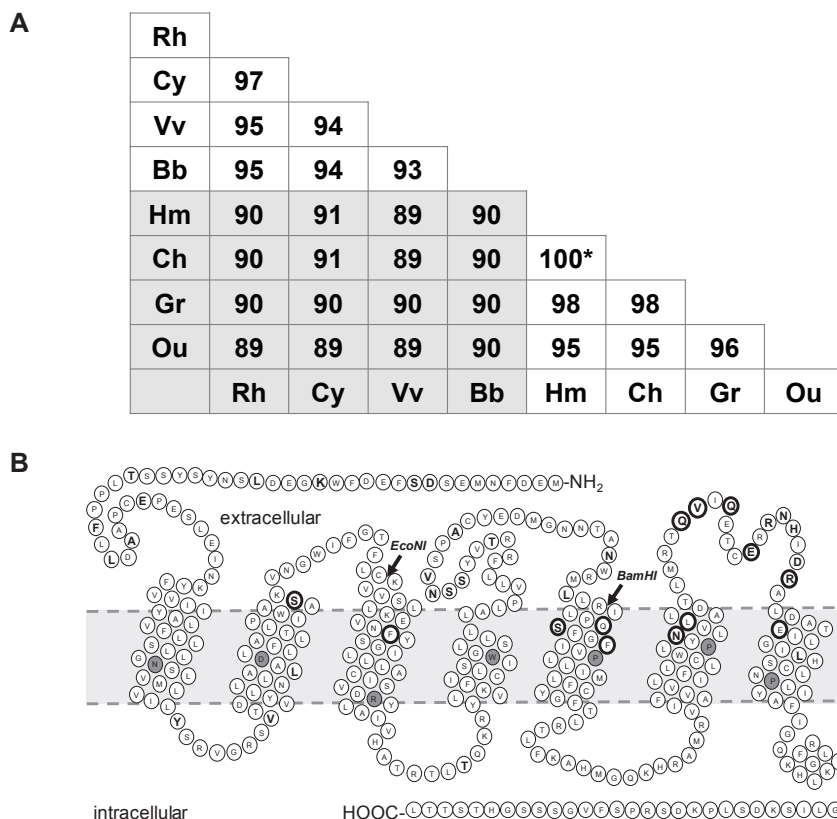


Figure 4.3: Homology (%) of protein sequences of the CXCR2 receptor of human (Hm), baboon (Bb), chimpanzee (Ch), cynomolgus (Cy), gorilla (Gr), orangutan (Ou), rhesus (Rh) and vervet (Vv) calculated by ClusterW. *: Chimpanzee CXCR2 lacks first five amino acids of human CXCR2 receptor. Besides that, all amino acid residues are identical (A). Snake plot of the human CXCR2 receptor. The residues indicated in bold and with a bigger font differ between human and baboon receptor. Residues indicated in a thick circle have been mutated whereas residues indicated in grey are the conserved residues for the Ballesteros-Weinstein numbering scheme (B).

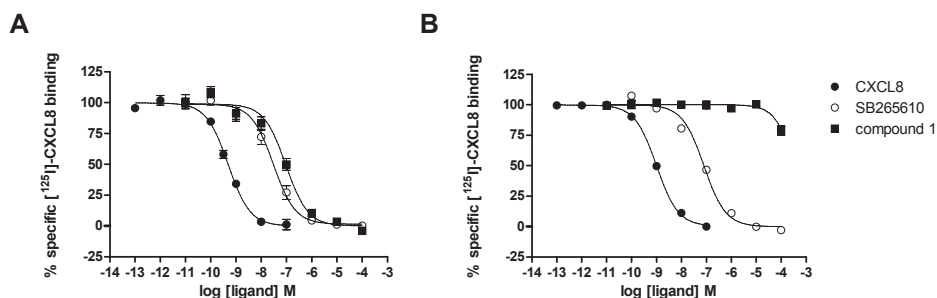

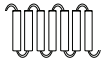








Figure 4.4: Displacement of [125 I]-CXCL8 binding to COS-7 cell membranes expressing human CXCR2 (A) or baboon CXCR2 (B). Membranes were incubated with indicated concentrations of CXCL8 (●), SB265610 (○) or compound 1 (■) and approximately 100 pM [125 I]-CXCL8 for 1 hour at room temperature. The error bars indicate the S.E.M. of results of at least three independent experiments.

Chimeric Human-Baboon CXCR2 Approach

To investigate which part of the human CXCR2 receptor is involved in the binding of compound 1, we choose baboon CXCR2 as a representative of the class A orthologs. Next, using the restriction sites EcoNI and BamHI (Fig. 4.3B) we created the chimeric constructs HHB (human-human-baboon), BBH (baboon-baboon-human), HBB (human-baboon-baboon), BHH (baboon-human-human), HBH (human-baboon-human) and BHB (baboon-human-baboon). The binding affinity of [¹²⁵I]-CXCL8 is equal to human and baboon CXCR2 at the chimeras BBH, BHH, HBH and BHB, whereas the chimeras HHB and HBB are unable to bind the chemokine (Table 4.2). HHB and HBB are expressed on the cell surface as indicated by ELISA (data not shown). SB265610 displaces [¹²⁵I]-CXCL8 from the chimeras with almost equipotent affinity. Compared to the wild type baboon CXCR2 receptor, the chimera BBH gains affinity for compound 1, whereas compound 1 has no affinity for the chimera BHB. Other chimeric receptors show results in line with this observation. Thus, we hypothesized that the region from TM5 to the C-terminus is important for the binding of compound 1 to human CXCR2.

Table 4.2: Affinity (pK_d or pK_i) of CXCR2 ligands at human-baboon chimeras. Displacement of [¹²⁵I]-CXCL8 binding to COS-7 cell membranes expressing indicated chimeric receptors HHB (human-human-baboon), BBH (baboon-baboon-human), HBB (human-baboon-baboon), BHH (baboon-human-human), HBH (human-baboon-human) and BHB (baboon-human-baboon). The data are presented as mean ± S.E.M. of at least three independent experiments.

CXCR2		pK _d CXCL8	pK _i SB265610	pK _i compound 1
	human	9.40 ± 0.14	7.68 ± 0.11	7.18 ± 0.13
	baboon	9.33 ± 0.08	7.28 ± 0.10	<4
	HHB chimera	-	-	-
	BBH chimera	9.41 ± 0.21	7.17 ± 0.19	6.70 ± 0.10
	HBB chimera	-	-	-
	BHH chimera	9.52 ± 0.09	6.93 ± 0.20	6.66 ± 0.11
	HBH chimera	9.49 ± 0.11	7.33 ± 0.16	6.90 ± 0.10
	BHB chimera	9.43 ± 0.07	7.20 ± 0.04	<4

-: [¹²⁵I]-CXCL8 does not bind to this construct.

Site-Directed Mutagenesis of the CXCR2 Receptor to probe Baboon-Human Species Differences

Following the results of the chimeric approach, we decided to continue with a site-directed mutagenesis approach to further pinpoint the amino acids involved in the binding of compound 1 at the human CXCR2 receptor. The amino acids from the human and baboon CXCR2 receptor differ at 35 positions; 13 of them are located in the region from TM5 to the C-terminus (Fig. 4.2, 4.3B). Only the residues that differ between the class A and B orthologs were subsequently mutated from the human to the respective baboon counterparts. Thus, we generated the mutants S217^{5.44}T, N268^{6.52}H, V281^{6.65}L, and E287^{6.71}Q (Fig. 4.3B). To extensively investigate differences between the human and baboon receptor in the extracellular loop 3, we also created the mutants Q280^{6.64}R, Q283^{6.67}N and R294^{7.33}Q. Since the binding site for SB265610 was previously identified to be intracellularly [2, 3], and [³H]-SB265610 was not displaced by compound 1 [1], we suggested that the intracellular isoleucine 331^{7.80} is not involved in the binding of compound 1 and thus did not mutate this residue.

All human to baboon single point mutant cDNAs were transiently transfected in COS-7 cells. Competition binding analysis showed that all mutants were expressed and bind [¹²⁵I]-CXCL8 with nanomolar affinity, i.e., comparable to wild-type human CXCR2 (Table 4.3). SB265610 displaces [¹²⁵I]-CXCL8 from the mutants with almost equal binding affinity. Interestingly, compound 1 shows a significantly decreased affinity for the mutants S217^{5.44}T and N268^{6.52}H (Table 4.3, Fig. 4.5A-B) whereas the affinity for the other mutants is unaltered. The N268^{6.52}H mutant causes a greater decrease in affinity for compound 1 than S217^{5.44}T, indicating that asparagine 268^{6.52} has a more important role in the binding of compound 1 to human CXCR2 than serine 217^{5.44}.

To confirm the important role of the serine and asparagine residues, we constructed the reciprocal baboon to human mutants T212^{5.44}S and H263^{6.52}N. As clearly shown in Figure 4.5A-B, mutation of the baboon residues into the human residues results in a gain of affinity of compound 1 (Table 4.3). In line with the results with the human to baboon mutant receptors, the baboon CXCR2 mutant H263^{6.52}N causes a greater increase in binding affinity for compound 1 than T212^{5.44}S. To investigate the role of these two residues in more detail, we created the double mutants S217^{5.44}T/N268^{6.52}H and T212^{5.44}S/H263^{6.52}N. The human CXCR2 double mutant S217^{5.44}T/N268^{6.52}H showed, like the wild-type baboon receptor, no [¹²⁵I]-CXCL8 displacement by compound 1, whereas the baboon CXCR2 double mutant T212^{5.44}S/H263^{6.52}N showed equal affinity for compound 1 as the wild-type human receptor (Fig. 4.5C, Table 4.3). Taken together, compound 1 shows only a markedly decreased affinity at the human CXCR2 mutants S217^{5.44}T, N268^{6.52}H and S217^{5.44}T/N268^{6.52}H. Given these results, we conclude that compound 1 binds to the trans-membrane (TM) regions, 5 and 6, of the CXCR2 receptor.

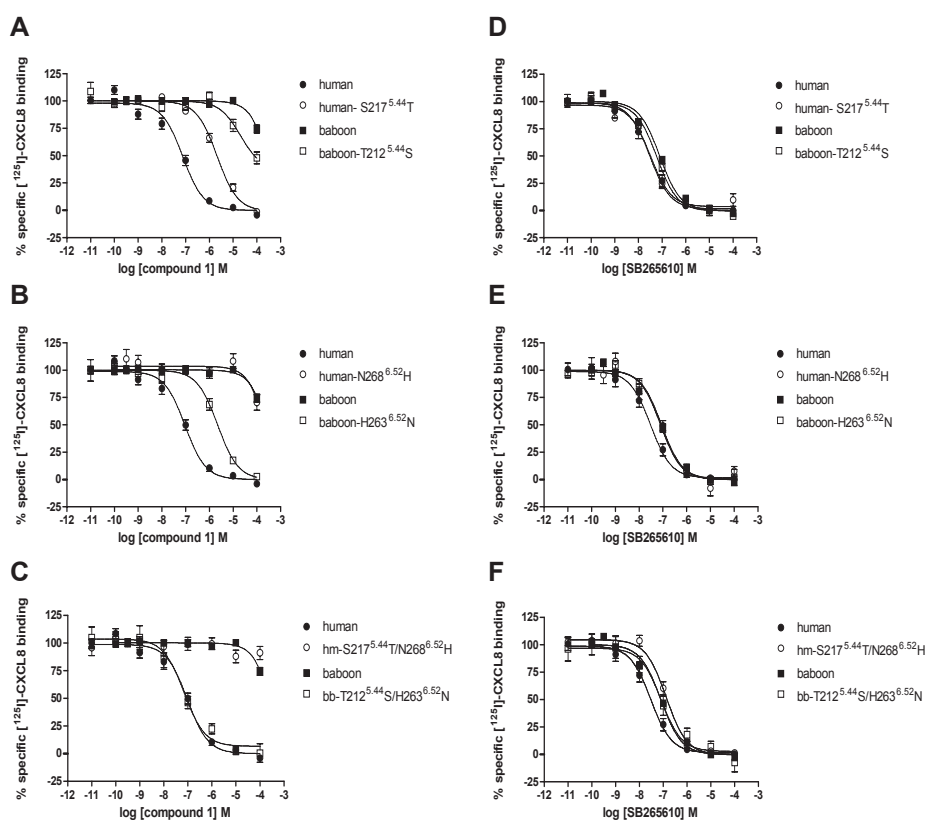


Figure 4.5: Displacement of $[^{125}\text{I}]\text{-CXCL8}$ binding to COS-7 cell membranes expressing human CXCR2 (●), baboon CXCR2 (■) or indicated mutants by compound 1 (A-C) or SB265610 (D-F). Membranes were incubated with indicated concentrations of compound 1 or SB265610 and approximately 100 pM $[^{125}\text{I}]\text{-CXCL8}$ for 1 hour at room temperature. The error bars indicate the S.E.M. of results of at least three independent experiments.

To investigate whether the (double mutant) receptors display the same properties in functional studies as observed in $[^{125}\text{I}]\text{-CXCL8}$ displacement assays, we performed $[^{35}\text{S}]\text{-GTP}\gamma\text{S}$ binding assays on membranes of COS7 cells transiently transfected with CXCR2. As shown in Figure 4.6A, CXCL8 shows a higher potency at baboon CXCR2 compared to human CXCR2 (Table 4.4). Mutations in either the human or baboon receptor do not alter the potency of CXCL8 compared to WT receptors. This is in agreement with the $[^{125}\text{I}]\text{-CXCL8}$ displacement studies. To test the dose-dependent antagonism of CXCL8-induced signal by compound 1 and SB265610, indicated concentrations of antagonists were used in combination with approximate EC_{80} concentration of CXCL8 (Fig. 4.6B-C). SB265610 is able to inhibit the CXCL8 induced $[^{35}\text{S}]\text{-GTP}\gamma\text{S}$ binding dose-dependently at all receptors tested with pK_b values around 8.5 (Fig. 4.6B, Table 6.4). At the highest tested concentrations, SB265610 displays inverse agonism at the baboon constructs. In agreement with our $[^{125}\text{I}]\text{-CXCL8}$ displacement studies, compound 1 inhibits the CXCL8-induced $[^{35}\text{S}]\text{-GTP}\gamma\text{S}$ binding at human WT and baboon double mutant T212^{5.44}S/H263^{6.52}N with pK_b values of

7.5 and 6.9, respectively. Furthermore, compound 1 hardly inhibits CXCL8 induced [35 S]-GTP γ S binding at baboon WT and human double mutant S217^{5.44}T/N268^{6.52}H (Fig. 4.6C, Table 4.4).

Table 4.3: Affinity (pK_d or pK_i) of CXCR2 ligands at site-directed mutagenesis CXCR2 human or baboon mutants to probe human-baboon species differences. Displacement of [125 I]-CXCL8 binding to COS-7 cell membranes expressing indicated human to baboon or baboon to human CXCR2 mutants. The data are presented as mean \pm S.E.M. of at least three independent experiments.

CXCR2	pK_d CXCL8	pK_i SB265610	pK_i compound 1
human WT	9.40 \pm 0.14	7.68 \pm 0.11	7.18 \pm 0.13
human S217 ^{5.44} T	9.20 \pm 0.11	7.92 \pm 0.06	5.77 \pm 0.12
human N268 ^{6.52} H	9.18 \pm 0.11	7.14 \pm 0.08	<5
human S217 ^{5.44} T/N268 ^{6.52} H	9.43 \pm 0.20	7.27 \pm 0.16	<4
human Q280 ^{6.64} R	9.13 \pm 0.04	7.29 \pm 0.14	7.10 \pm 0.11
human V281 ^{6.65} L	9.17 \pm 0.16	7.33 \pm 0.14	7.22 \pm 0.09
human Q283 ^{6.67} N	9.41 \pm 0.09	7.24 \pm 0.16	7.07 \pm 0.17
human E287 ^{6.71} Q	9.11 \pm 0.11	7.39 \pm 0.25	6.99 \pm 0.12
human R294 ^{7.33} Q	9.15 \pm 0.12	7.24 \pm 0.16	7.04 \pm 0.12
baboon	9.33 \pm 0.08	7.28 \pm 0.10	<4
baboon T212 ^{5.44} S	9.89 \pm 0.29	7.10 \pm 0.13	<5
baboon H263 ^{6.52} N	9.69 \pm 0.19	6.85 \pm 0.21	5.72 \pm 0.13
baboon T212 ^{5.44} S/H263 ^{6.52} N	9.61 \pm 0.08	7.13 \pm 0.17	7.40 \pm 0.14

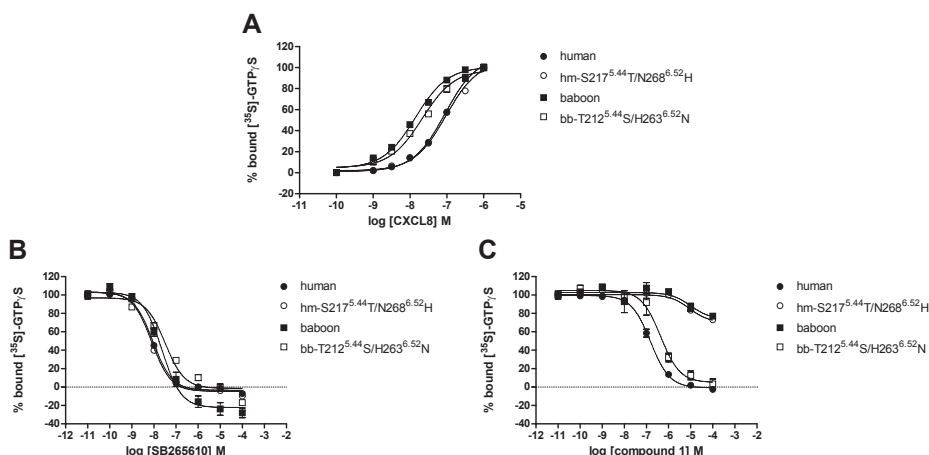


Figure 4.6: Stimulation of [35 S]-GTP γ S by CXCL8 from COS7 membranes expressing indicated receptors. Membranes were incubated with 3 μ M GDP and approximately 400 pM [35 S]-GTP γ S for 1 hour at room temperature (A). Inhibition of the CXCL8-induced [35 S]-GTP γ S binding by SB265610 (B) or compound 1 (C). Membranes were pre-incubated with indicated concentrations of CXCR2 antagonists for 30 min at room temperature, followed by stimulation of approximately EC₈₀ concentration of CXCL8 for 1 hour at room temperature. Data are expressed in percentage in which 0% represents basal signal and 100% CXCL8 signal without presence of antagonist (B-C). The error bars indicate the S.E.M. of results of at least three independent experiments.

Table 4.4: Affinity (pK_d or pK_i) and inhibition of CXCL8-induced [35 S]-GTP γ S binding (pK_b) of CXCR2 ligands at key constructs. Displacement of [35 S]-CXCL8 binding to COS-7 cell membranes expressing indicated key receptors. The data are presented as mean \pm S.E.M. of at least three independent experiments. CXCL8 stimulated [35 S]-GTP γ S binding to COS-7 membranes expressing indicated receptors and inhibition of CXCL8-induced [35 S]-GTP γ S after 30 min pre-incubation with SB265610 and compound 1. The data are presented as mean \pm S.E.M. of at least three independent experiments.

CXCR2	pK_d CXCL8	pK_i SB265610	pK_i compound 1	pEC_{50} CXCL8	pK_b SB265610	pK_b compound 1
Human WT	9.40 \pm 0.14	7.68 \pm 0.11	7.18 \pm 0.13	7.06 \pm 0.07	8.71 \pm 0.06	7.48 \pm 0.13
Baboon WT	9.33 \pm 0.08	7.28 \pm 0.10	<4	7.86 \pm 0.06	8.51 \pm 0.13	<4
Human S217 ^{5.44} T/N268 ^{6.52} H	9.43 \pm 0.20	7.27 \pm 0.16	<4	7.03 \pm 0.07	8.73 \pm 0.07	<4
Baboon T212 ^{5.44} S/H263 ^{6.52} N	9.61 \pm 0.08	7.13 \pm 0.17	7.40 \pm 0.14	7.68 \pm 0.06	8.11 \pm 0.23	6.86 \pm 0.20

In Silico Based Site-Directed Mutagenesis of the CXCR2 Receptor.

Since the chimeric and site-directed mutagenesis data only provided a rough indication that compound 1 is a TM-binder, we characterized the binding mode of compound 1 in more detail by constructing additional mutations guided by *in silico* modeling. A CXCR2 model was constructed based on the recently resolved structure of the chemokine receptor CXCR4 [5]. Wu *et al* co-crystallized the CXCR4 receptor with the ligand IT1t in the minor subpocket of the TM bundle encompassing TM1, TM2, TM3 and TM7, where it interacts

with residues D97^{2.63} and E288^{7.39} (Fig. 4.7A). Furthermore, the crystal structure shows two lipids in the major subpocket of the TM bundle encompassed by TM3, TM4, TM5, TM6 and TM7 (Fig. 4.7B). The same major subpocket is occupied by the peptide ligand CVX15 in another CXCR4 crystal structure [5].

Based on our chimera and point mutant data, we hypothesized its binding site to be part of the major subpocket (Fig. 4.7C-D). To confirm this, we created the mutants S107^{2.63}A, E300^{7.39}Q and E300^{7.39}S as these residues interact with ligand IT1t in the CXCR4 structure in the minor subpocket between TM2, TM3, and TM7 (Fig. 4.7A, [5]). S107^{2.63} was mutated to an alanine residue present in baboon CXCR2 (S107^{2.63}A). E300^{7.39} was mutated to a glutamine to prevent ionic interactions, and to a serine (E300^{7.39}S) as the inverse S^{7.39}E mutation in CXCR3 enables binding of CXCR4 antagonists [31]. The affinity of compound 1 at the mutants S107^{2.63}A, E300^{7.39}Q and E300^{7.39}S is unchanged compared to the human wild-type receptor. Also [¹²⁵I]-CXCL8 and SB265610 bind with the same affinity as that of the wildtype (Fig. 4.7, Table 4.5). These results indicate that indeed compound 1 does not bind to the minor subpocket.

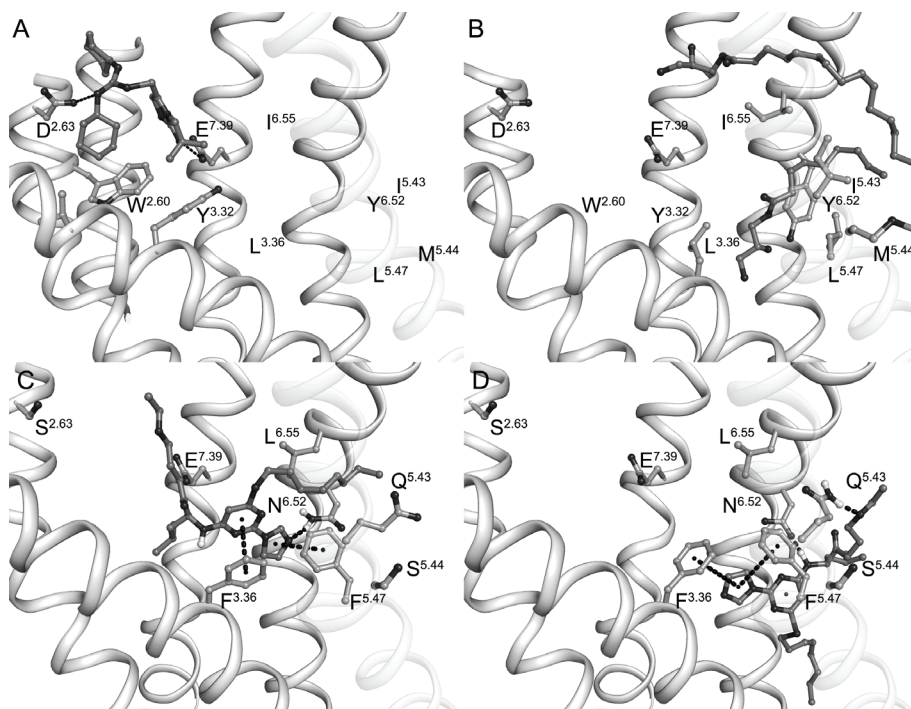


Figure 4.7: Positioning of the small ligand IT1t in the minor subpocket of the CXCR4 receptor (pdb code 3ODU) (A), and the lipids in the major subpocket of the CXCR4 receptor (pdb code 3ODU) (B). Suggested binding modes of compound 1 in the major subpocket of the human CXCR2 receptor with the octane moiety pointing into the lipid membrane between TM5 and TM6 (C), and in the lipid membrane before entering the trans-membrane major subpocket (D). The interactions between compound 1 and F3.36, Q5.43, F5.47, N6.52 and L6.55 are in line with experimental data; they are annotated with dotted lines.

Subsequently, molecular docking results of compound 1 in the CXCR2 model suggested the residues F130^{3.36}, Q216^{5.43}, F220^{5.47}, N268^{6.52} and L271^{6.55} to interact with compound 1 (Fig. 4.7C and Fig. 4.7D). Surprisingly, S217^{5.44} showed no direct interaction with compound 1. Due to the high conservation of the TM structure, none of the currently known crystal structures possess residue 5.44 pointing into the major pocket. As such, this is also true in our CXCR2 model. Therefore, we believe that our model is justified and we propose that the influence of this residue is of indirect nature. Our model suggests two binding modes representing different states along the same ligand binding pathway. In the binding mode presented in Figure 4.7C, the pyrimidine and imidazole moieties of compound 1 interact with F130^{3.36} and F220^{5.47} through π - π stacking, while the imidazole moiety forms a hydrogen bond with N268^{6.52}. In Figure 4.7D the imidazole moiety of compound 1 interacts with F130^{3.36} and F220^{5.47} through π - π interactions, the aminopyrimidine forms hydrogen bonds with N268^{6.52}, and the ether moiety interacts with Q216^{5.43}. In both binding modes, the octane moiety protrudes through TM5 and TM6 between residues Q216^{5.43} and L271^{6.55} similar to the CXCR4 lipids (Fig. 4.7B). The interactions of compound 1 in both models are in line with the structure-activity relationship investigation described by Ho *et al* [15] which emphasizes the importance of the long hydrophobic octane moiety as well as the geometry and directionality of the imidazole acceptor group. To assess the involvement of these five residues, we constructed the mutants F130^{3.36}A, Q216^{5.43}E, F220^{5.47}A and L271^{6.55}A (N268^{6.52} has already been mutated, see above). However, since F220^{5.47}A did not bind [¹²⁵I]-CXCL8, we created the additional mutant F220^{5.47}L. Compared to wild type CXCR2 ($pK_i = 7.2$, Table 4.5) the affinity of compound 1 is slightly decreased at Q216^{5.43}E ($pK_i = 6.5$) and significantly decreased for F220^{5.47}L ($pK_i = 6.1$) and L271^{6.55}A ($pK_i = 6.2$). Figure 4.8 clearly shows that compound 1 binding is completely abolished in the mutant F130^{3.36}A (Table 4.5). None of the mutants affected the binding affinity of [¹²⁵I]-CXCL8. In line with the binding studies, compound 1 hardly inhibits the CXCL8 induced [³⁵S]-GTP γ S binding at F130^{3.36}A (pK_b is <4; see supplementary Fig. 4.2).

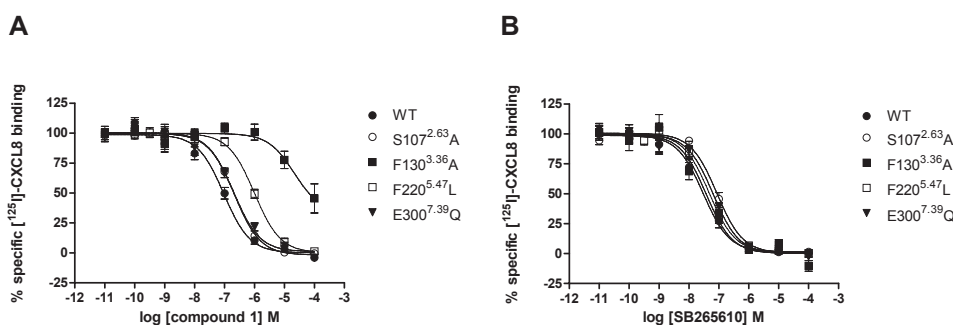


Figure 4.8: Displacement of [¹²⁵I]-CXCL8 binding to COS-7 cell membranes expressing indicated human CXCR2 mutants by compound 1 (A) or SB265610 (B). Membranes were incubated with indicated concentrations of SB265610 or compound 1 and approximately 100 pM [¹²⁵I]-CXCL8 for 1 hour at room temperature. The error bars indicate the S.E.M. of results of at least three independent experiments.

Table 4.5: Affinity (pK_d or pK_i) of CXCR2 ligands at in silico based site-directed mutagenesis human CXCR2 mutants. Displacement of [125 I]-CXCL8 binding to COS-7 cell membranes expressing indicated human single point mutants. The data are presented as mean \pm S.E.M. of at least three independent experiments.

CXCR2	pK_d CXCL8	pK_i SB265610	pK_i compound 1
WT	9.40 ± 0.14	7.68 ± 0.11	7.18 ± 0.13
S107 ^{2.63} A	9.09 ± 0.07	7.10 ± 0.13	6.73 ± 0.09
F130 ^{3.36} A	9.65 ± 0.29	7.55 ± 0.17	<4
Q216 ^{5.43} E	9.01 ± 0.12	7.56 ± 0.09	6.47 ± 0.11
F220 ^{5.47} L	9.06 ± 0.05	7.34 ± 0.12	6.07 ± 0.08
L271 ^{6.55} A	9.18 ± 0.12	6.76 ± 0.31	6.22 ± 0.04
E300 ^{7.39} S	9.04 ± 0.13	7.21 ± 0.12	6.79 ± 0.05
E300 ^{7.39} Q	9.00 ± 0.14	7.26 ± 0.09	6.69 ± 0.09

Discussion

CXCR2 is a potential drug target because of its involvement in several inflammatory diseases like atherosclerosis, chronic obstructive pulmonary disease, psoriasis, rheumatoid arthritis, inflammatory bowel disease and multiple sclerosis [8-11, 32, 33]. In view of its therapeutic potential, the search for CXCR2 antagonists have been extensively and has led to the identification of different classes of CXCR2 antagonist [14-17]. In our previous publication [1], we discovered that CXCR2 antagonists of the diarylurea (like SB265610, see Fig. 4.1) and the thiazolopyrimidine class bind to a distinct site compared to compounds of the imidazolylopyrimidine class (like compound 1, see Fig. 4.1). Recent studies show that diarylurea and thiazolopyrimidine compounds most likely bind intracellularly to CXCR2 [2, 3]. In this study we indentified a binding site for the imidazolylopyrimidine compound 1 within the trans-membrane (TM) region.

Identification of a novel allosteric binding site in CXCR2 by ‘natural mutants’

Different monkey CXCR2 orthologs (Fig. 4.2, 4.3) were used as ‘natural mutants’ to identify key residues involved in the binding of compound 1 to human CXCR2. In all experiments we defined the binding affinity of SB25610 as a control. As this compound showed to bind intracellularly [3], we expected no significantly change in binding affinity at the different CXCR2 receptors. Our results show that the rhesus, cynomolgus, vervet and baboon orthologs are devoid of affinity for compound 1, whereas the human, chimpanzee, gorilla and orangutan orthologs bind this compound with high affinity (Fig. 4.4, Table 4.1). We have labeled these species as class A and B, respectively. Using human-baboon chimeric proteins and subsequently human to baboon reciprocal single point mutants, we identified S217^{5.44} and N268^{6.52} as key residues distinguishing class A and B orthologs. Imidazolylopyrimidine compounds have also no affinity for the mouse, rat and rabbit CXCR2 orthologs (J.C.H.M.W., M.L.W., D.S.A., unpublished data). Since the rodent orthologs all possess N^{6.52}, but do contain T^{5.44} instead of S^{5.44} (supplementary Fig 4.3.), we hypothesize that in

these rodent receptors T^{5.44} and possibly other residues are responsible for the lack of affinity for compound 1.

Investigation of the CXCR2 minor subpocket

In the recently resolved crystal structure of the CXCR4 receptor, the small ligand IT1t interacts with the residues D97^{2.63} and E288^{7.39} in the minor subpocket [5]. Furthermore, studies with CXCR1, that has 77% sequence homology to CXCR2, revealed that both (R)ketoprofen and repertaxin interact also with residues located in the minor subpocket, like I43^{1.36}, Y46^{1.39}, K99^{2.64}, V113^{3.28} and E291^{7.39} [34-36]. Moreover, E^{7.39} plays a role in binding of antagonists at various other chemokine receptor as reviewed by Scholten and co-workers [18]. Since the binding affinity of compound 1 was not changed at the mutants S107^{2.63}A, E300^{7.39}S and E300^{7.39}Q (Fig. 4.8, Table 4.5), we conclude that compound 1 does not bind to the minor subpocket at CXCR2. From the chimeric studies we already expected that S107^{2.63} was not a key residue in the binding of compound 1 to human CXCR2, because TM2 was not essential for the difference between the class A and class B orthologs.

In silico guided mutagenesis of the CXCR2 major subpocket to elucidate antagonist binding mode

A CXCR2 model was constructed based on the recently resolved CXCR4 crystal structure [5]. Molecular docking results of compound 1 in this model suggested that the residues F130^{3.36}, Q216^{5.43}, F220^{5.47}, N268^{6.52} and L271^{6.55} could interact with compound 1 (Fig. 4.7C and Fig. 4.7D). Although we showed that the S217^{5.44}, like the N268^{6.52}, was essential for compound 1 binding, it showed no direct interaction with compound 1 in our model. Threonine (class A orthologs) and serine (class B orthologs) residues in combination with proline residues are known to cause kinks in TM helices [37], as for example demonstrated by the T^{2.56}XP^{2.58} induced kink in TM2 in chemokine receptors [5, 38]. The presence of an extra proline residue at position 5.42 might even emphasize the induction of TM5 kinks. The involvement of serine 217^{5.44} in compound 1 binding might be explained by a different rotation state of the TM5 helix compared to a threonine, thereby affecting the binding of compound 1 by changing the shape of the ligand binding pocket and entrance channel between TM5 and TM6 (Fig. 4.7C-D). To investigate how compound 1 binds to the major subpocket, we constructed additional mutants based on *in silico* modeling.

Our binding studies with the mutants F130^{3.36}A, Q216^{5.43}E, F220^{5.47}L and L271^{6.55}A revealed that these residues, like N268^{6.52}, interact with compound 1 (Fig. 4.8, Table 4.5). To the best of our knowledge, this is the first investigation in which the imidazolylpyrimidine CXCR2 antagonists have been characterized to bind inside the TM domain of the CXCR2 receptor (major pocket). As shown in Figure 4.7C, the proposed binding location is similar to the location of the fatty acids co-crystallized with the CXCR4 receptor (pdb code: 3ODU) pointing partially into the lipid bilayer. The binding mode is also in line with the structure-activity relationship investigation described by Ho *et al* [15] which emphasizes the importance of the long hydrophobic octane moiety (which lies between TM5 and TM6) as well as the geometry and directionality of the imidazole acceptor group. The data from the

F130^{3,36}A and F220^{5,47}L mutants can be explained by a loss of aromatic interactions with the pyrimidine and imidazole moieties, the N268^{6,52}H mutant by the loss of a hydrogen bonding interaction with the imidazole moiety, and the L271^{6,55}A mutant by a loss of hydrophobic matching with the octane moiety of compound 1. No direct indication for the small loss of activity by Q216^{5,43}E mutation could be derived.

CXCR2 Ligand Entry Mechanism

We propose additionally a binding mode on the interface of the major pocket and the lipid bilayer (Fig. 4.7D) which is in line with the structure-activity data. This binding mode involves similar interactions for F130^{3,36}, F220^{5,47} and N268^{6,52} as the binding mode in the major pocket (Fig. 4.7C), but in which Q216^{5,43} forms a hydrogen bonding interaction with the ether group, and the L271^{6,55} shows no direct interaction. We postulate that compound 1 first binds to the interface coming from the lipid bilayer (Fig. 4.7D), followed by a rotation to get into the major pocket (Fig. 4.7C), in analogy with *sn*-2-arachidonoylglycerol (2-AG) in the cannabinoid 2 receptor [39]. During ligand entry, S217^{5,44} might play a crucial role by adapting the conformation of TM5 to open the entry channel for compound 1, whereby N268^{6,52} supports ligand entry to the major subpocket. An entry channel between these TMs has been earlier described for the opsin receptor [4]. In this receptor the residues I205^{5,40}, F208^{5,43}, F273^{6,56} and F276^{6,59} accommodate an entry channel for 11-*cis*-retinal between TM5 and TM6.

Although it may seem counter-intuitive that a ligand fits partially in the entrance channel of the TM domain, recent advances in CXCR2-ligand binding pocket elucidations have shown that also an intracellular binding site for CXCR2 antagonists exists [2, 3], a result only seen for two other GPCRs, the chemokine receptors CCR4 and CCR5 [40]. As such, this does not only imply that CXCR2 behaves different from other GPCRs, but it could also mean that we should be thinking out of the metaphoric box that is the TM domain.

Conclusions

Taken together, using different CXCR2 orthologs, chimeras, site-directed mutagenesis and *in silico* modeling, we have identified binding modes in the trans-membrane domain for the imidazolylpyrimidine compound 1 at the human CXCR2 receptor. Our *in silico* guided mutagenesis studies indicate a new ligand binding cavity in CXCR2 located between trans-membrane (TM) helices 3, 5, and 6 and suggest the imidazolylpyrimidine antagonist to enter CXCR2 via the TM5-TM6 interface. A ligand entry channel at the same interface was already described for the opsin receptor [4]. Furthermore, lipid molecules in the recently solved crystal structure of the CXCR4 receptor [5] are encompassed by the same interface. This suggest a general ligand entrance mechanism for nonpolar ligands to G protein-coupled receptors (GPCRs). Our identification of a novel allosteric binding cavity in the TM domain of CXCR2, in addition to the previously identified intracellular binding site, shows the

diversity in ligand recognition mechanisms by this receptor and offers new opportunities for the structure-based design of small allosteric modulators of CXCR2 in the future.

References

1. de Kruijf, P., et al., Nonpeptidergic allosteric antagonists differentially bind to the CXCR2 chemokine receptor. *J Pharmacol Exp Ther*, 2009. 329(2): p. 783-90.
2. Nicholls, D.J., et al., Identification of a Putative Intracellular Allosteric Antagonist Binding-Site in the CXC Chemokine Receptors 1 and 2. *Mol Pharmacol*, 2008. 74(5): p. 1193-202.
3. Salchow, K., et al., A common intracellular allosteric binding site for antagonists of the CXCR2 receptor. *Br J Pharmacol*, 2010. 159(7): p. 1429-39.
4. Park, J.H., et al., Crystal structure of the ligand-free G-protein-coupled receptor opsin. *Nature*, 2008. 454(7201): p. 183-7.
5. Wu, B., et al., Structures of the CXCR4 chemokine GPCR with small-molecule and cyclic peptide antagonists. *Science*, 2010. 330(6007): p. 1066-71.
6. Murphy, P.M., et al., International union of pharmacology. XXII. Nomenclature for chemokine receptors. *Pharmacol Rev*, 2000. 52(1): p. 145-76.
7. Kraneveld, A.D., et al., Chemokine receptors in inflammatory diseases, in *Chemokine Receptors as Drug Targets*, M.J. Smit, S.A. Lira, and R. Leurs, Editors. 2011.
8. Boisvert, W.A., et al., A leukocyte homologue of the IL-8 receptor CXCR-2 mediates the accumulation of macrophages in atherosclerotic lesions of LDL receptor-deficient mice. *J Clin Invest*, 1998. 101(2): p. 353-63.
9. Chapman, R.W., et al., A novel, orally active CXCR1/2 receptor antagonist, Sch527123, inhibits neutrophil recruitment, mucus production, and goblet cell hyperplasia in animal models of pulmonary inflammation. *J Pharmacol Exp Ther*, 2007. 322(2): p. 486-93.
10. Podolin, P.L., et al., A potent and selective nonpeptide antagonist of CXCR2 inhibits acute and chronic models of arthritis in the rabbit. *J Immunol*, 2002. 169(11): p. 6435-44.
11. Liu, L., et al., Myelin repair is accelerated by inactivating CXCR2 on nonhematopoietic cells. *J Neurosci*, 2010. 30(27): p. 9074-83.
12. Kulke, R., et al., The CXC receptor 2 is overexpressed in psoriatic epidermis. *J Invest Dermatol*, 1998. 110(1): p. 90-4.
13. Qiu, Y., et al., Biopsy neutrophilia, neutrophil chemokine and receptor gene expression in severe exacerbations of chronic obstructive pulmonary disease. *Am J Respir Crit Care Med*, 2003. 168(8): p. 968-75.
14. Baxter, A., et al., Hit-to-Lead studies: the discovery of potent, orally bioavailable thiazolopyrimidine CXCR2 receptor antagonists. *Bioorg Med Chem Lett*, 2006. 16(4): p. 960-3.
15. Ho, K.K., et al., Imidazolylpyrimidine based CXCR2 chemokine receptor antagonists. *Bioorg Med Chem Lett*, 2006. 16(10): p. 2724-8.
16. Li, J.J., et al., Synthesis and structure-activity relationship of 2-amino-3-heteroaryl-quinoxalines as non-peptide, small-molecule antagonists for interleukin-8 receptor. *Bioorg Med Chem*, 2003. 11(17): p. 3777-90.
17. Widdowson, K.L., et al., Evaluation of potent and selective small-molecule antagonists for the CXCR2 chemokine receptor. *J Med Chem*, 2004. 47(6): p. 1319-21.
18. Scholten, D.J., et al., Pharmacological Modulation of Chemokine Receptor Function. *British Journal of Pharmacology*, 2011. In press.
19. Lim, H.D., et al., Molecular determinants of ligand binding to H4R species variants. *Mol Pharmacol*, 2010. 77(5): p. 734-43.
20. Milligan, G., Orthologue selectivity and ligand bias: translating the pharmacology of GPR35. *Trends Pharmacol Sci*, 2011. 32(5): p317-325.
21. Reinhart, G.J., et al., Species selectivity of nonpeptide antagonists of the gonadotropin-releasing hormone receptor is determined by residues in extracellular loops II and III and the amino terminus. *J Biol Chem*, 2004. 279(33): p. 34115-22.
22. Bizzarri, C., et al., ELR+ CXC chemokines and their receptors (CXC chemokine receptor 1 and CXC chemokine receptor 2) as new therapeutic targets. *Pharmacol Ther*, 2006. 112(1): p. 139-49.
23. Erickson, S., et al., Preparation of pyrimidine amino acid derivatives as interleukin-8 (IL-8) receptor antagonists., in *International patent application*. 2004. WO2004062609.
24. Horlick, R., et al., Orthologues of human receptors and methods of use. 2006. United states patent US7,041,463 B2.
25. Hipkin, R.W., et al., Cloning and pharmacological characterization of CXCR1 and CXCR2 from *Macaca fascicularis*. *J Pharmacol Exp Ther*, 2004. 310(1): p. 291-300.
26. Cheng, Y. and W.H. Prusoff, Relationship between the inhibition constant (K_i) and the concentration of inhibitor which causes 50 per cent inhibition (I₅₀) of an enzymatic reaction. *Biochem Pharmacol*, 1973. 22(23): p. 3099-108.
27. Ballesteros, J.A. and H. Weinstein, Integrated methods for the construction of three-dimensional models and computational probing of structure-function relations in G protein-coupled receptors. *Methods Neurosci* 1995. 25: p366-428
28. UniProt, Ongoing and future developments at the Universal Protein Resource. *Nucleic Acids Res*, 2011. 39(Database issue): p. D214-9.

-
29. Cherezov, V., et al., High-resolution crystal structure of an engineered human beta2-adrenergic G protein-coupled receptor. *Science*, 2007. 318(5854): p. 1258-65.
 30. Verdonk, M.L., et al., Improved protein-ligand docking using GOLD. *Proteins*, 2003. 52(4): p. 609-23.
 31. Rosenkilde, M.M., et al., Molecular mechanism of AMD3100 antagonism in the CXCR4 receptor: transfer of binding site to the CXCR3 receptor. *J Biol Chem*, 2004. 279(4): p. 3033-41.
 32. Ajuebor, M.N., et al., Contrasting roles for CXCR2 during experimental colitis. *Exp Mol Pathol*, 2004. 76(1): p. 1-8.
 33. Buane, P., et al., Crucial pathophysiological role of CXCR2 in experimental ulcerative colitis in mice. *J Leukoc Biol*, 2007. 82(5): p. 1239-46.
 34. Allegretti, M., et al., 2-Arylpropionic CXC chemokine receptor 1 (CXCR1) ligands as novel noncompetitive CXCL8 inhibitors. *J Med Chem*, 2005. 48(13): p. 4312-31.
 35. Bertini, R., et al., Noncompetitive allosteric inhibitors of the inflammatory chemokine receptors CXCR1 and CXCR2: prevention of reperfusion injury. *Proc Natl Acad Sci U S A*, 2004. 101(32): p. 11791-6.
 36. Moriconi, A., et al., Design of noncompetitive interleukin-8 inhibitors acting on CXCR1 and CXCR2. *J Med Chem*, 2007. 50(17): p. 3984-4002.
 37. Deupi, X., et al., Influence of the g- conformation of Ser and Thr on the structure of transmembrane helices. *J Struct Biol*, 2010. 169(1): p. 116-23.
 38. Govaerts, C., et al., The TXP motif in the second transmembrane helix of CCR5. A structural determinant of chemokine-induced activation. *J Biol Chem*, 2001. 276(16): p. 13217-25.
 39. Hurst, D.P., et al., A lipid pathway for ligand binding is necessary for a cannabinoid G protein-coupled receptor. *J Biol Chem*, 2010. 285(23): p. 17954-64.
 40. Andrews, G., C. Jones, and K.A. Wreggett, An intracellular allosteric site for a specific class of antagonists of the CC chemokine G protein-coupled receptors CCR4 and CCR5. *Mol Pharmacol*, 2008. 73(3): p. 855-67.
-


```

CXCR2_HUMAN MEDFNMESDSFEDFWKGEDLSNYSYSTLPPFLDAAAPCEPESLEINKYFVVIIYALVFL 60
CXCR2_BABOON ----MESNFEDFWTGEDFSNYSYSSDLPPSLPDVAPCRPESLEINKYFVVIIYALVFL 55
CXCR2_RABIT MQEFTWENYSYEDFFG--DFSNNYSYSTDLPPTLDSAPCRSESLETNSVYVLIYILVFL 58
CXCR2_MOUSE MGEFKVDKFNIEDFFSG-DLDFNYSSGMP SILPDVAPCHSENLEINSYAVVVYVVLVFL 59
CXCR2_RAT MGEIRVDNFSLEDFFSG-DIDSNNYSDDPPFTLSDAAPCPSANLDINRYAVVVYVVLVFL 59
      :. . ***: *. :.***: * * * .** . .*: * * *: * * *
CXCR2_HUMAN LSLLGNSLVMLVILYSRVGRSVTDVYLLNLALADLLFALTLPWAASKVNGWIFGTFLCK 120
CXCR2_BABOON LSLLGNSLVMLVILHSRVGRSITDVYLLNLAMADLLFALTLPWAASKVNGWIFGTFLCK 115
CXCR2_RABIT LSLLGNSLVMLVILYSRSTCSVTDVYLLNLAIADLLFALTLPWAASKVNGWIFGTFLCK 118
CXCR2_MOUSE LSLVGNSLVMLVILYNRSTCSVTDVYLLNLAIADLFFALTLPVWAASKVNGWIFGTFLCK 119
CXCR2_RAT LSLVGNSLVMLVILYNRSTCSVTDVYLLNLAIADLFFALTLPVWAASKVNGWIFGTFLCK 119
      ***:*****:.* *:*****:***:* * **:****:***: * * *
CXCR2_HUMAN VVSLLEKVNIFYSGILLACISVDRYLAIVHATRTLQKRYLVKFICLSIWGLSLLLALPV 180
CXCR2_BABOON VVSLLEKVNIFYSGILLACISVDRYLAIVHATRTLQKRYLVKFICLSIWGLSLLLALPV 175
CXCR2_RABIT VVSLVKEVNIFYSGILLACISVDRYLAIVHATRTMIQKRHLVKFICLSMWGVSILSLPI 178
CXCR2_MOUSE IFSYVKEVTIFYSSVLLACISMDRYLAIVHATSTLIQKRHLVKFVICIAMWLLSVILALPI 179
CXCR2_RAT VFSFLQETIFYSSVLLACISMDRYLAIVHATSTLIQKRHLVKFVICITMWFLSLVLSLPI 179
      :.* :*:.*.***:*****:***** * : * **:****:***: * :*:.*:***:
CXCR2_HUMAN LLFRRTVYSSNVSPACYEDMGNNNTANWRMLLRILPQTFGFIIVPLLIIMFCYGTFLRTLKF 240
CXCR2_BABOON LLFRRAVYPPYISPVCYEDMGNNNTAKWRMVLRIPLQTFGFIIVPLLIIMFCYGTFLRTLKF 235
CXCR2_RABIT LLFRNAIFPPNSSPVCYEDMGNSTAKWRMVLRIPLQTFGFIIVPLLIIMFCYGTFLRTLKF 238
CXCR2_MOUSE LILRNPVKVNLSTLVCYEDVGNNTSRLRVVLRILPQTFGFIIVPLLIIMFCYGTFLRTLKF 239
CXCR2_RAT FILRTPVKANPSTVVCYENIGNNTSKWRVVLRIPLQTFGFIIVPLLIIMFCYGTFLRTLKF 239
      :*: * : : .***:***.*. :*:*****:***:***:***** *****
CXCR2_HUMAN AHMGQKHRAMRVIFAVVLIFLLCWLPYNLVLLADTLMRTQVIQETCERRNHIDRALDATE 300
CXCR2_BABOON AHMGQKHRAMRVIFAVVLIFLLCWLPYNLVLLADTLMRTLINETCQRHSDINQALDATE 295
CXCR2_RABIT AHMGQKHRAMRVIFAVVLIFLLCWLPYNLVLLDTLMRTHVIQETCERRNDIDRALDATE 298
CXCR2_MOUSE AHMGQKHRAMRVIFAVVLIFLLCWLPYNLVLFDTLMRTKLIKETCERRDDIKALNATE 299
CXCR2_RAT AHMGQKHRAMRVIFAVVLIFLLCWLPYNLVLFDTLMRTKLIKETCERQNEINKALEATE 299
      *****:*****:***:*****:***:***:***:***:***
CXCR2_HUMAN ILGILHSLNPLIYAFIGQKFRHGLLKILAIHGLISKDSLPKDSRPSFVGSSSGHTSTTL 360
CXCR2_BABOON ILGIFHSLNPLIYAFIGQKFRHGLLKILATHGLISKDSLPKDSRPSFVGSSSGHTSTTL 355
CXCR2_RABIT ILGFLHSLNPIIYAFIGQKFRYGLLKILAAHGLISKEFLAKESRPSFVASSSGNTSTTL 358
CXCR2_MOUSE ILGFLHSLNPIIYAFIGQKFRHGLLKIMATYGLVSKFLAKEGRPSFVSSSSANTSTTL 359
CXCR2_RAT ILGFLHSLNPIIYAFIGQKFRHGLLKIMANYGLVSKFLAKEGRPSFVGSSSANTSTTL 359
      ***:*****:*****:*****: * :*:***: *.*.*****.*.*:*****

```

Supp. Fig 4.3: Alignment of the sequences of the human, baboon, mouse, rat and rabbit CXCR2 orthologs. Boxed residues are S5.44 and N6.52.

The collagen-breakdown product N-acetyl-Proline-Glycine-Proline (N- α -PGP) does not interact directly with human CXCR1 and CXCR2

Chapter 5

Petra de Kruijf ^A, Herman D. Lim ^A, Saskia A. Overbeek ^B, Guido J.R. Zaman ^C,
Aletta D. Kraneveld ^B, Gert Folkerts ^B, Rob Leurs ^A and Martine J. Smit ^A

^A Leiden/Amsterdam Center for Drug Research, Division of Medicinal Chemistry,
Vrije Universiteit Amsterdam, The Netherlands

^B Division of Pharmacology and Pathophysiology, Utrecht Institute for Pharmaceutical Sciences,
Faculty of Science, Utrecht University, The Netherlands

^C Merck Research Laboratories, Oss, The Netherlands

Published as:

De Kruijf *et al*, Eur J Pharmacol. 2010 Sep 15;643(1):29-33.

Abstract

Neutrophils transmigrate from the blood into inflamed tissue via the interaction of chemokines produced in this tissue with chemokine receptors, such as CXCR1 and CXCR2, which are expressed on the membranes of neutrophils. Subsequently, activation of neutrophils will in turn lead to increased tissue damage and thereby enhanced clinical symptoms of inflammatory diseases like chronic obstructive pulmonary disease, inflammatory bowel disease and psoriasis. Besides chemokines, also the collagen-breakdown product N-acetyl-Proline-Glycine-Proline (N- α -PGP) attracts neutrophils. In a recent article [1] it was suggested that N- α -PGP exerts its effect via CXCR1 and CXCR2. In this study, we show that N- α -PGP, in contrast to CXCL8, does not directly activate or interact with CXCR1 or CXCR2. N- α -PGP was not able to displace the radioligand [125 I]-CXCL8 from CXCR1 and CXCR2 expressing HEK293T cells or neutrophils. In addition, N- α -PGP did not displace the radioligand [3 H]-SB265610, a CXCR2 antagonist, from CXCR2 expressing cells. Furthermore, N- α -PGP was not able to activate G protein signalling in cells expressing CXCR1 and CXCR2. N- α -PGP was also not able to recruit β -arrestin2, an intracellular scaffolding protein involved in G protein-independent signalling, in cells expressing CXCR2. These studies indicate that N- α -PGP is not a ligand of CXCR1 or CXCR2.

Acknowledgements

This study was performed within the framework of the Dutch Top Institute Pharma project T101-3

Introduction

Neutrophils are polymorph nuclear cells that are key mediators in a variety of inflammatory diseases like chronic obstructive pulmonary disease [2], inflammatory bowel disease [3] and psoriasis [4]. Upon inflammation, different inflammatory stimuli induce the production of various chemokines, leading to the infiltration of leukocytes, such as neutrophils and monocytes, into inflamed tissue via the interaction with chemokine receptors that are expressed on the cell membrane of those leukocytes [5]. Chemokine receptors belong to the rhodopsin-like family of G protein-coupled receptors [6]. Neutrophils and monocytes express amongst others the chemokine receptors CXCR1 and CXCR2 [5]. Both CXCR1 and CXCR2 bind with high affinity the chemokines CXCL6 (granulocyte chemotactic peptide-2), CXCL7 (neutrophil activating peptide-2) and CXCL8 (interleukin-8 (IL-8)), whereas CXCR2 also binds with high affinity to CXCL1, CXCL2, CXCL3 (growth-related protein α , β or γ , respectively) and CXCL5 (epithelial cell-derived neutrophil attractant-78) [7]. *In vivo* studies have shown that the influx of neutrophils into inflamed tissue can be inhibited by a neutralizing CXCR2 antibody [8] or small molecular weight antagonists, like the CXCR1/2 antagonist Sch527123 [9, 10]. Subsequently, the neutrophil associated tissue damage is reduced resulting in attenuated symptoms of ulcerative colitis or chronic obstructive pulmonary disease.

In addition to the above mentioned chemokines, it was shown that both in *in vitro* and *in vivo*, also the collagen-breakdown product N-acetyl-Proline-Glycine-Proline (N- α -PGP) is able to attract neutrophils [1, 11]. N- α -PGP was first identified in a rabbit model in which alkaline degradation of whole cornea generates this tripeptide [12]. In addition, mice challenged with lipopolysaccharide showed also the production of N- α -PGP. Furthermore, in BAL-fluid or sputum of chronic obstructive pulmonary disease patients N- α -PGP was detected, suggesting that N- α -PGP can be a biomarker for this disease [1, 13]. The N- α -PGP-induced neutrophil chemotaxis was inhibited by CXCR1 and/or CXCR2 antibodies *in vitro* [1]. Furthermore, the accumulation of neutrophils seen in BALB/C mice, upon intratracheally administration of N- α -PGP, was not detected in Cxcr2^{-/-} mice [1]. Those results indicate a role for both CXCR1 and CXCR2 in the N- α -PGP-induced neutrophil infiltration into tissue.

In this study, we investigated in detail the interaction of N- α -PGP with human CXCR1 and CXCR2 *in vitro*. Our data indicate that N- α -PGP is not a ligand of these chemokine receptors.

Materials and Methods

Dulbecco's modified Eagle's medium (DMEM), RPMI-1640 medium, penicillin and streptomycin were all obtained from PAA Laboratories (Pasching, Austria). Fetal bovine serum was purchased from Integro B.V. (Dieren, The Netherlands). DMEM containing 25 mM HEPES and L-glutamine, Earle's inositol-free minimal essential medium, OPTI-MEM, RPMI-1640 medium with glutamax-I with 25 mM HEPES, certified FBS, Hygromycin-

B and Geneticin were obtained from Invitrogen (Paisley, United Kingdom) and fetal calf serum was purchased from Cambrex Bio Sciences (Verviers, Belgium). Nonessential amino acids, sodium pyruvate, 2-mercaptoethanol and sodium butyrate were purchased from Sigma-Aldrich. Bovine Serum Albumin Fraction V (BSA) was obtained from Roche (Mannheim, Germany). ^{125}I and myo-[2- ^3H]inositol were purchased from PerkinElmer Life Sciences (Boston, MA, USA). Chemokines were obtained from PeproTech (Rock Hill, NJ, USA) or from R&D systems (Minneapolis, USA). N- α -PGP was purchased from AnaSpec (San Jose, CA, USA) and checked for purity by high-performance liquid chromatography and mass spectrometry. Polyethylenimine (PEI) was obtained from Polysciences (Warrington, PA, USA). Poly-L-lysine was purchased from Sigma-Aldrich (St. Louis, MO, USA) and Ficoll-Paque™ PLUS was obtained from GE Healthcare (Uppsala, Sweden). [^3H]-1-(2-bromophenyl)-3-(4-cyano-1H-benzo[d][1,2,3]triazol-7-yl)urea, ([^3H]-SB265610) (26.07 Ci/mmol) and ((R)-5-(benzylthio)-7-(1-hydroxybutan-2-ylamino)thiazolo[4,5-d]pyrimidin-2-ol), (VUF10948) [14, 15] were synthesized at Merck Research Laboratories (MSD, Oss, The Netherlands).

Cell culturing and transfection

HEK293T cells were grown at 5% CO_2 and 37°C in Dulbecco's modified Eagle's medium supplemented with 10% (v/v) fetal bovine serum, 50 IU/ml penicillin and 50 $\mu\text{g}/\text{ml}$ streptomycin. Cells were transiently transfected (per 10 cm dish) with 2.5 μg of cDNA encoding the receptor (human CXCR1 or human CXCR2) supplemented with either 2.5 μg of pcDEF3 or 2.5 μg pcDNA1-HA-mG α_{q15} (for phospholipase C activation experiments) by using linear polyethylenimine (PEI) with a molecular weight of 25 kDa as previously described [16].

The murine pre-B L1.2 cells (kindly provided by Dr. Pease, Imperial College London, London, UK) were grown in RPMI 1640 medium with GlutaMax-I and 25 mM HEPES, supplemented with 10% heat-inactivated certified FBS, 50 IU/ml penicillin, 50 $\mu\text{g}/\text{ml}$ streptomycin, glutamine, nonessential amino acids, 2-mercaptoethanol and sodium pyruvate. L1.2 cells were transfected with 10 μg receptor/ 1×10^7 cells using a Bio-Rad Gene Pulser Xcell (330 V and 975 μF), and subsequently grown overnight in culture medium supplemented with 10 mM sodium butyrate.

PathHunter™ HEK293-CXCR2 cells (DiscoverX, Fremont, USA), were grown at 5% CO_2 and 37°C in DMEM with 25 mM HEPES and L-glutamine supplemented with 10% (v/v) heat-inactivated fetal calf serum, 50 IU/ml penicillin, 50 $\mu\text{g}/\text{ml}$ streptomycin, 800 $\mu\text{g}/\text{ml}$ Geneticin and 200 $\mu\text{g}/\text{ml}$ Hygromycin-B.

COS-7 cells were grown at 5% CO_2 and 37°C in Dulbecco's modified Eagle's medium supplemented with 5% (v/v) fetal bovine serum, 50 IU/ml penicillin and 50 $\mu\text{g}/\text{ml}$ streptomycin. COS-7 cells were transiently transfected using the DEAE-dextran method [17] as previously described [14]. After 48 h, the cells were washed once in PBS, scraped and collected as pellets for preparation of membranes.

Isolation of human neutrophils

Neutrophils were isolated from fresh whole blood, for which donors signed written consent forms. The neutrophils were obtained by centrifugation on Ficoll-Paque™ PLUS (density: 1.077 g/ml), followed by hypotonic lysis of erythrocytes with sterile lysis buffer (0.15 M NH_4Cl , 0.01 M KHCO_3 and 0.1 mM EDTA; pH 7.4 at 4°C). After lysis, the neutrophils were washed with PBS and finally resuspended in either RPMI 1640 medium (without L-glutamine and phenol red) supplemented with 1% heat-inactivated FBS (chemotaxis assay) or in binding buffer (radioligand binding assay).

Chemotaxis assay neutrophils

Chemotaxis assay was performed as previously described [1]. Briefly, indicated concentrations of CXCL8 or N- α -PGP were placed in the bottom wells of a 3- μ m 96-well polycarbonate filter plate (Millipore) in RPMI 1640 medium (without L-glutamine and phenol red). 2×10^5 neutrophils, isolated from fresh whole blood, were added to the top portion. The plate was incubated for one hour at 37°C in 5% CO₂. After removing the upper portion, the cells in each bottom well were counted for 30 seconds using a BD FACSCalibur Flow Cytometer with CellQuest Pro Software (version 5.2.1.). Data were standardized to a chemotactic index (the number of cells per well migrating to chemo-attractant divided by the number of cells per well migrating to medium).

Chemotactic assay L1.2 cells

Twenty-four hours after transfection, migration of L1.2 cells towards CXCL8 or N- α -PGP was determined using 5- μ m pore ChemoTx 96-well plates (Neuro Probe). First the lower wells of the ChemoTx plates were blocked for 30 min using RPMI 1640 medium with GlutaMAX-I and 25 mM HEPES supplemented with 1% (w/v) BSA. CXCL8 or N- α -PGP was diluted in the same medium supplemented with 0.1% (w/v) BSA, and dispensed in the bottom wells of the chemotaxis plate after removing the blocking buffer. The membrane was placed on top of these wells and 2.5×10^5 cells in the same buffer were applied to the upper surface (total 31 μ l) and incubated for 4 h in a humidified chamber at 37°C in the presence of 5% CO₂. The number of cells that traversed the 5- μ m pore membrane and migrated into the bottom wells was quantified on the Victor2 1420 multilabel plate reader upon the incorporation of the Calcein AM dye (Invitrogen). Data are shown as the percentage migrated cells.

Radioligand binding assays

Twenty-four h after transfection HEK293T cells were plated out at 100.000 cells/well (48-wells format; poly-L-lysine coated). Forty-eight h after transfection, binding was performed on whole cells for 3–4 h at 4°C using [¹²⁵I]-CXCL8 (approximately 200 pM) in binding buffer (50 mM HEPES, 1 mM CaCl₂, 5 mM MgCl₂, 0.5% BSA; pH 7.4 at 4°C) containing indicated concentrations of either unlabeled chemokine or N- α -PGP. After incubation, cells were washed three times in ice-cold binding buffer supplemented with 0.5 M NaCl. Subsequently, cells were lysed and counted in a Wallac Compu-Gamma counter.

To perform binding studies on neutrophils, neutrophils were resuspended in binding buffer immediately after isolation. Binding was performed for 3–4 h at 4°C with 2×10^5 neutrophils per datapoint in a final volume of 100 μ l using [¹²⁵I]-CXCL8 (approximately 100 pM) and indicated concentrations of either unlabeled chemokine or N- α -PGP. After incubation, cells were harvested with rapid filtration through Unifilter GF/C 96-well filter plates (PerkinElmer Life and Analytical Sciences) pretreated with 0.3% polyethylenimine and washed three times with ice-cold binding buffer supplemented with 0.5M NaCl. Bound radioactivity was determined using a MicroBeta (PerkinElmer Life and Analytical Sciences).

Pellets of COS-7 membranes expressing human CXCR2 were resuspended in ice cold binding buffer (50 mM Na₂HPO₄ and 50 mM KH₂PO₄, pH 7.4) and homogenized 15 times with a Dounce homogenizer. Protein concentration in membrane preparations was determined using the BioRad Protein Determination assay 18 from BioRad Laboratories (München, Germany). Binding was performed with COS-7 membranes expressing human CXCR2 (8 μ g) in binding buffer (50 mM Na₂HPO₄ and 50 mM KH₂PO₄, pH 7.4) at room temperature for 1 hour in a final volume of 100 μ l with indicated concentrations of N- α -PGP or the CXCR2 antagonist VUF10948 and [³H]-SB265610 (approximately 1 nM). After incubation, membranes were harvested and residual radioactivity was counted similar as described above for the human neutrophils.

Inositol phosphates production

Twenty-four h after transfection of HEK293T cells with human CXCR1 or CXCR2 and $G_{\alpha_{q/11}}$, cells were plated out at 100,000 cells/well (48-wells format, poly-L-lysine coated). Four h after plating out, cells were labeled overnight in Earle's inositol-free minimal essential medium supplemented with myo-[2- 3 H]inositol (1 μ Ci/ml). Cells were washed with assay buffer (20 mM HEPES, 140 mM NaCl, 5 mM KCl, 1 mM $MgSO_4$, 1 mM $CaCl_2$ and 10 mM glucose; pH 7.4 at 37°C) and incubated for 2 h at 37°C and 5% CO_2 in the same buffer supplemented with 0.05% BSA, 10 mM LiCl and indicated concentrations of CXCL8 or N- α -PGP. The incubation was stopped by aspiration of the medium and addition of ice-cold 10 mM formic acid. After 90 min of incubation on ice, [3 H]-inositol phosphates were isolated by anion exchange chromatography (Dowex AG1-X8 columns, Bio-Rad, CA, USA) and counted by liquid scintillation.

β -arrestin recruitment assay

PathHunter™ HEK293-CXCR2 cells were plated out overnight at 10,000 cells/well (384-wells format) in 20 μ l OPTI-MEM. A pre-incubation with vehicle (PBS + 0.1 % BSA) of 30 min at 37°C and 5% CO_2 , was followed by 60 min CXCL8 and/or N- α -PGP stimulation at 37°C and 5% CO_2 . Next, the plate was placed at room temperature for 30 min, whereafter 12 μ l PathHunter Detection Reagents (DiscoverX, Fremont, USA) was added. After an incubation of 60 min at room temperature, β -galactosidase fragment complementation, as an indicator of β -arrestin-CXCR2 interaction, was measured for 0.3 sec in an Envision 2102 Multilabel Reader (PerkinElmer). Functional data were evaluated by a non-linear curve fitting procedure using GraphPad Prism 4.0 (GraphPad Software, inc., San Diego, CA).

Statistical analyses

For all statistical analyses, GraphPad Prism version 4.0 was used. For comparing three or more groups with a control group, the data were analyzed using a one-way ANOVA followed by Dunnett post hoc analysis. Data were considered significant at $P < 0.05$.

Results

N- α -PGP does not displace [125 I]-CXCL8 and [3 H]-SB265610 binding

We used a transwell chemotaxis system to evaluate the chemotactic effect of N- α -PGP on freshly isolated human neutrophils. As shown in Figure 5.1, N- α -PGP dose-dependently attracted neutrophils at a concentration of 0.1 to 3 mM. As neutrophils express the chemokine receptors CXCR1 and CXCR2, and as N- α -PGP was inactive *in vivo* in *Cxcr2*^{-/-} mice [1], we studied the interaction of N- α -PGP *in vitro*.

HEK293T cells transiently transfected with either CXCR1 or CXCR2 were incubated with [125 I]-CXCL8 and CXCL1, CXCL8 or N- α -PGP (Fig. 5.2A-B). In accordance with the reported affinities of CXCL1 and CXCL8 for CXCR1 (IC_{50} >100 nM and 2-7 nM, respectively) and CXCR2 (IC_{50} 1-4 nM and 1-5 nM, respectively) [7, 18, 19], CXCL8 (100 nM) fully displaced [125 I]-CXCL8 binding to both receptors (Fig. 5.2A-B) whereas CXCL1 (100 nM) could only fully displace [125 I]-CXCL8 binding to CXCR2 (Fig. 5.2B).

Yet, N- α -PGP (0.3-3 mM) did not displace [125 I]-CXCL8 binding to either CXCR1 or CXCR2 (Fig. 5.2A-B).

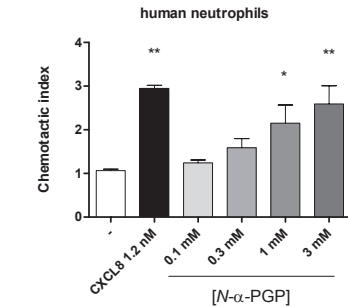


Figure 5.1: Chemotaxis of freshly isolated human neutrophils to CXCL8 or N- α -PGP. Cells were placed on top wells and chemo-attractants in the bottom wells. After 1 h incubation at 37°C and 5% CO₂, cells in the bottom well were counted. Data of triplicate determinations are expressed as chemotactic index \pm S.E.M (cells migrated per well to chemo-attractant / cells migrated per well to medium) (n=6). P value < 0.05 (*) or < 0.01 (**) vs. control group (RPMI 1640 medium).

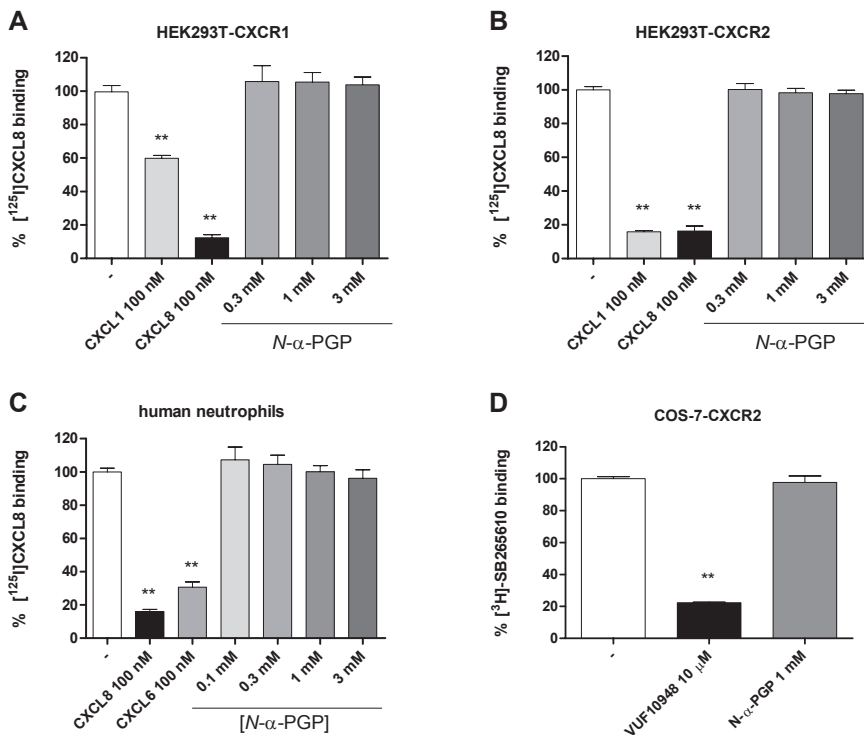


Figure 5.2: Displacement of [125 I]-CXCL8 binding to HEK293T cells expressing either human CXCR1 (A) or human CXCR2 (B), or to freshly isolated human neutrophils (C). Cells were incubated with indicated concentrations of chemokines or N- α -PGP and 100-200 pM [125 I]-CXCL8 for 3-4 h at 4°C. Displacement of [3 H]-SB265610 binding to COS-7 membranes expressing human CXCR2 (D). Membranes were incubated with indicated concentrations of VUF10948 or N- α -PGP and approximately 1 nM [3 H]-SB265610 for 1 h at room temperature. Data of triplicate determinations are expressed as the percentage of [125 I]-CXCL8 binding or [3 H]-SB265610 binding \pm S.E.M (n=2-4). P value < 0.01 (**) vs. control group (binding buffer).

To determine the ability of N- α -PGP to bind to CXCR1 and/or CXCR2 on human neutrophils, freshly isolated neutrophils were incubated with [125 I]-CXCL8 and CXCL6, CXCL8 or N- α -PGP (Fig. 5.2C). Similar to transfected HEK293T cells, the unlabeled chemokines (100 nM) displaced [125 I]-CXCL8 binding, but N- α -PGP (0.1-3 mM) did not displace [125 I]-CXCL8 binding. Furthermore, when we incubated membranes of COS-7 cells expressing CXCR2 with the recently described CXCR2 antagonist [3 H]-SB265610 [14, 20] and VUF10948 or N- α -PGP (Fig. 5.2D), N- α -PGP (1 mM) did not displace [3 H]-SB265610 binding. In contrast, the CXCR2 antagonist VUF10948 (10 μ M) was able to displace the binding of [3 H]-SB265610.

N- α -PGP has no effect on G-protein signalling

As other compounds, such as the CXCR1/2 antagonist Repertaxin [21], do not displace [125 I]-CXCL8 binding from CXCR1 and CXCR2, but are nevertheless able to inhibit the chemokine-induced signalling of those receptors, we examined the effect of N- α -PGP on the activation of G-proteins, using a phospholipase C activation assay. HEK293T cells transiently transfected with either CXCR1 or CXCR2 and G α_{q15} were stimulated with either CXCL8 or N- α -PGP (Fig. 5.3A-B). CXCL8 (1-100 nM) was able to activate phospholipase C via CXCR1 and CXCR2 in a dose-dependent manner, while N- α -PGP (0.3-3 mM) showed no effect at all (Fig. 5.3A-B).

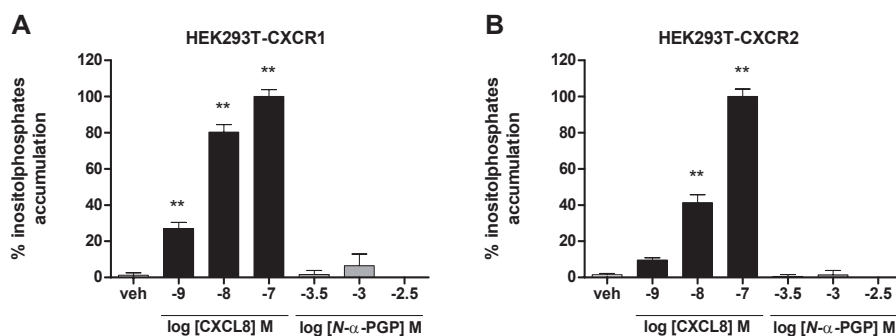


Figure 5.3: Activation of phospholipase C by human CXCR1 (A) or human CXCR2 (B). HEK293T cells were transfected with cDNAs encoding human CXCR1 or human CXCR2 and G α_{q15} . After 48 h, [3 H]-inositol phosphates accumulation was determined. Data of triplicate determinations are expressed as percentage of the maximal response \pm S.E.M. obtained with 100 nM CXCL8 (n=2-3). P value < 0.01 (**) vs. control group (assay buffer).

N- α -PGP does not recruit transfected L1.2 cells

Since N- α -PGP is chemotactic for neutrophils, we examined the ability of N- α -PGP to induce chemotaxis of CXCR1 and CXCR2 expressing pre-B lymphocyte L1.2 cells. Whereas CXCL8 showed the classical bell-shaped curve for CXCR1 and CXCR2, N- α -PGP did not show any chemotactic response at both receptors (Fig. 5.4).

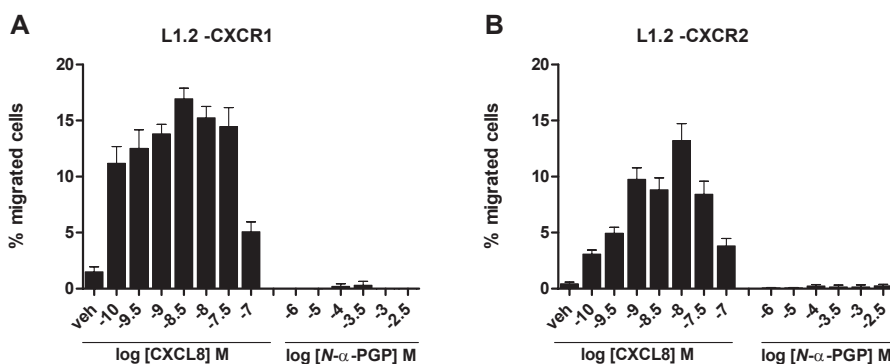


Figure 5.4: Chemotactic response of L1.2 cells transiently expressing either CXCR1 (A) or CXCR2 (B) towards CXCL8 or N- α -PGP. After 4 h incubation at 37°C and 5% CO₂, cells in the bottom well were counted. Data of triplicate determinations are expressed as % migrated cells \pm S.E.M (n=3).

N- α -PGP does not recruit β -arrestin2

Previously, we have shown that CXCR2 activation by CXCL8 leads to recruitment of β -arrestin2 using a novel chemiluminescent assay (PathHunter™) based on enzyme fragment complementation [14]. Pre-treatment with pertussis toxin, a well known G α_i -inhibitor, did not influence the CXCL8-induced β -arrestin2 recruitment (data not shown), indicating that the recruitment of β -arrestin2 by CXCR2 is independent of G α_i -protein in this assay. A similar observation has been made for other receptors studied in this assay format [22, 23]. Next, we determined whether N- α -PGP was able to induce recruitment of β -arrestin2 to CXCR2. Whereas stimulation of the PathHunter-hCXCR2 cells with CXCL8 induced recruitment of β -arrestin2 ($pEC_{50} = 8.49 \pm 0.04$, n=16), stimulation of cells with N- α -PGP had no effect (Fig. 5.5A). Furthermore, N- α -PGP (1 mM) had no effect on the recruitment of β -arrestin2 by CXCL8 ($pEC_{50} = 8.45 \pm 0.06$, n=3) (Fig. 5.5B).

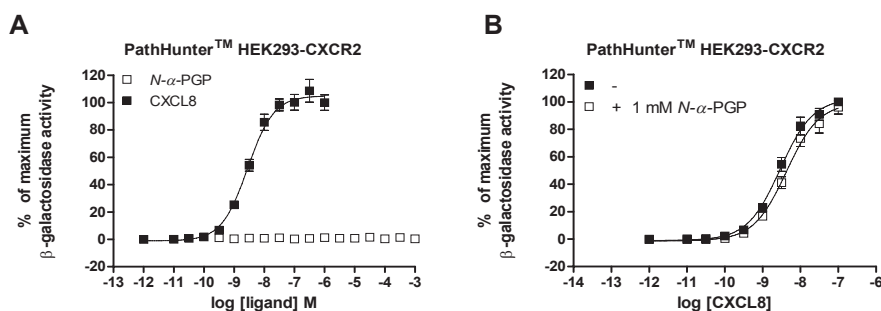


Figure 5.5: (A) β -arrestin2 recruitment in PathHunter™ HEK293-hCXCR2 cells by CXCL8 (■) or N- α -PGP (□). CXCL8 induced β -arrestin2 recruitment is dose-dependent ($pEC_{50} = 8.49 \pm 0.04$, n=16) and N- α -PGP does not show β -arrestin2 recruitment. (B) β -arrestin2 recruitment in PathHunter™ HEK293-hCXCR2 cells by CXCL8 in absence (■) or presence of 1 mM N- α -PGP (□). Data of triplicate determinations are expressed as percentage of β -galactosidase activity \pm S.E.M (n=3-16).

Discussion

The data presented in this study show that N- α -PGP does not directly activate or interact with human CXCR1 or human CXCR2. N- α -PGP did neither displace the radioligand [125 I]-CXCL8 from either CXCR1 or CXCR2 nor the low molecular weight CXCR2 antagonist [3 H]-SB265610 [14, 20] from CXCR2. SB265610 and CXCL8 were previously shown to bind to distinct sites at CXCR2 (de Kruijf *et al.*, 2009). Thus, N- α -PGP does not bind to the chemokine or CXCR2 antagonist binding site of CXCR2, to the chemokine binding sites of CXCR1 or other sites at the receptors leading to a conformational change resulting in loss of binding of [125 I]-CXCL8 or [3 H]-SB265610. Also in neutrophils N- α -PGP did not displace [125 I]-CXCL8 from CXCR1 or CXCR2. Furthermore, N- α -PGP was not able to directly activate CXCR1 or CXCR2, as shown by a lack of chemotactic response in transfected L1.2 cells, and a lack of activity in both the G-protein dependent phospholipase C activation assay and G-protein independent β -arrestin2 recruitment assay. In addition, N- α -PGP did not change the CXCL8-induced phospholipase C activation (data not shown) and CXCL8-induced β -arrestin2 recruitment, indicating that N- α -PGP is not acting as an allosteric modulator at CXCR2.

Since N- α -PGP is able to attract neutrophils, as shown in our study as well as in earlier publications [1, 11], but does not interact directly with either CXCR1 or CXCR2, N- α -PGP is likely to mediate its effect by a different mode of action. We propose that N- α -PGP interacts indirectly with CXCR1 or CXCR2 possibly via the release of chemokines, known to bind to these receptors, or through activation of other receptors expressed on neutrophils to induce chemotaxis. Additional studies are required to further delineate the mode of action of N- α -PGP and determine the characteristics of the other putative receptors. In case N- α -PGP is able to release chemokines, known to interact with CXCR1 and CXCR2, from neutrophils, this will result in enhanced recruitment of neutrophils into sites of inflammation *in vivo* via the interaction with CXCR1 and CXCR2 expressed on neutrophils [5]. Subsequently, this will lead to increased tissue damage and thereby enhanced clinical symptoms of inflammatory diseases like chronic obstructive pulmonary disease, inflammatory bowel disease and psoriasis [2-5].

Taken together, these studies indicate that N- α -PGP exerts its effect via an indirect interaction with CXCR1 and CXCR2. Future research should delineate the mechanism(s) by which N- α -PGP induced neutrophil chemotaxis and the indirect roles of CXCR1 and CXCR2 in this process.

References

1. Weathington, N.M., et al., A novel peptide CXCR ligand derived from extracellular matrix degradation during airway inflammation. *Nat Med*, 2006. 12(3): p. 317-23.
2. Barnes, P.J., New molecular targets for the treatment of neutrophilic diseases. *J Allergy Clin Immunol*, 2007. 119(5): p. 1055-62.
3. Chin, A.C. and C.A. Parkos, Neutrophil transepithelial migration and epithelial barrier function in IBD: potential targets for inhibiting neutrophil trafficking. *Ann N Y Acad Sci*, 2006. 1072: p. 276-87.
4. Nickoloff, B.J. and F.O. Nestle, Recent insights into the immunopathogenesis of psoriasis provide new therapeutic opportunities. *J Clin Invest*, 2004. 113(12): p. 1664-75.
5. Viola, A. and A.D. Luster, Chemokines and Their Receptors: Drug Targets in Immunity and Inflammation. *Annu Rev Pharmacol Toxicol*, 2008. 48: p. 171-197.
6. Murphy, P.M., et al., International union of pharmacology. XXII. Nomenclature for chemokine receptors. *Pharmacol Rev*, 2000. 52(1): p. 145-76.
7. Lutichau, H.R., The cytomegalovirus UL146 gene product vCXCL1 targets both CXCR1 and CXCR2 as an agonist. *J Biol Chem*, 2010. 285(12): p. 9137-46.
8. Ajuebor, M.N., et al., Contrasting roles for CXCR2 during experimental colitis. *Exp Mol Pathol*, 2004. 76(1): p. 1-8.
9. Chapman, R.W., et al., A novel, orally active CXCR1/2 receptor antagonist, Sch527123, inhibits neutrophil recruitment, mucus production, and goblet cell hyperplasia in animal models of pulmonary inflammation. *J Pharmacol Exp Ther*, 2007. 322(2): p. 486-93.
10. Thatcher, T.H., et al., Role of CXCR2 in cigarette smoke-induced lung inflammation. *Am J Physiol Lung Cell Mol Physiol*, 2005. 289(2): p. L322-8.
11. Pfister, R.R., J.L. Haddox, and C.I. Sommers, Injection of chemoattractants into normal cornea: a model of inflammation after alkali injury. *Invest Ophthalmol Vis Sci*, 1998. 39(9): p. 1744-50.
12. Pfister, R.R., et al., Identification and synthesis of chemotactic tripeptides from alkali-degraded whole cornea. A study of N-acetyl-proline-glycine-proline and N-methyl-proline-glycine-proline. *Invest Ophthalmol Vis Sci*, 1995. 36(7): p. 1306-16.
13. O'Reilly, P., et al., N-alpha-PGP and PGP, potential biomarkers and therapeutic targets for COPD. *Respir Res*, 2009. 10: p. 38.
14. de Kruijf, P., et al., Nonpeptidergic allosteric antagonists differentially bind to the CXCR2 chemokine receptor. *J Pharmacol Exp Ther*, 2009. 329(2): p. 783-90.
15. Willis, P.A., et al., Preparation of novel thiazolo[4,5-d]pyrimidines as modulators of chemokine receptors, in International patent application, W.I.P. Organization, WO2001025242.
16. Verzijl, D., et al., Noncompetitive antagonism and inverse agonism as mechanism of action of nonpeptidergic antagonists at primate and rodent CXCR3 chemokine receptors. *J Pharmacol Exp Ther*, 2008. 325(2): p. 544-55.
17. Brakenhoff, R.H., E.M. Knippels, and G.A. van Dongen, Optimization and simplification of expression cloning in eukaryotic vector/host systems. *Anal Biochem*, 1994. 218(2): p. 460-3.
18. Ahuja, S.K. and P.M. Murphy, The CXC chemokines growth-regulated oncogene (GRO) alpha, GRObeta, GROgamma, neutrophil-activating peptide-2, and epithelial cell-derived neutrophil-activating peptide-78 are potent agonists for the type B, but not the type A, human interleukin-8 receptor. *J Biol Chem*, 1996. 271(34): p. 20545-50.
19. Lutichau, H.R., The CMV UL146 gene product vCXVL1 targets both CXCR1 and CXCR2 as an agonist. *J Biol Chem*, 2009. 285: p. 9173-9146.
20. Bradley, M.E., et al., SB265610 is an allosteric, inverse agonist at the human CXCR2 receptor. *Br J Pharmacol*, 2009. 158(1): p. 328-38.
21. Bertini, R., et al., Noncompetitive allosteric inhibitors of the inflammatory chemokine receptors CXCR1 and CXCR2: prevention of reperfusion injury. *Proc Natl Acad Sci U S A*, 2004. 101(32): p. 11791-6.
22. van der Lee, M.M., et al., Pharmacological characterization of receptor redistribution and beta-arrestin recruitment assays for the cannabinoid receptor 1. *J Biomol Screen*, 2009. 14(7): p. 811-23.
23. van Der Lee, M.M., et al., beta-Arrestin recruitment assay for the identification of agonists of the sphingosine 1-phosphate receptor EDG1. *J Biomol Screen*, 2008. 13(10): p. 986-98.

*Polymorphisms in HCMV-encoded viral chemokine
vCXCL1 and CXCR1/CXCR2 interaction*

Chapter 6

Jinho Heo ^B, Petra de Kruijf ^A, Tom Masi ^B, Martine J. Smit ^A and Tim E. Sparer ^B

^A Leiden/Amsterdam Center for Drug Research, Division of Medicinal Chemistry,
Vrije Universiteit Amsterdam, The Netherlands

^B Department of Microbiology, The University of Tennessee, Knoxville, USA

Manuscript in preparation

Partly modified from:
Dissertation Jinho Heo, 2010, Chapter 4

Abstract

The human cytomegalovirus (HCMV) viral chemokine vCXCL1, encoded by *UL146* ORF, is hypervariable. Eleven distinct vCXCL1 genotypic groups were previously found in clinical isolates from congenitally infected infants [1]. In these groups, the N-loop region of vCXCL1, which is important for receptor binding, was variable. One isolate also contained a modified ELR motif, which is known to be crucial for binding to CXCR1 and CXCR2 receptors. In this study, representative vCXCL1 proteins from each of 11 genotypic groups were produced and purified using a baculovirus protein expression system. All vCXCL1s were able to induce calcium flux and integrin expression on human neutrophils at a similar level. Interestingly, potency differences were observed in chemotaxis assay with human neutrophils. Competition binding assays revealed that vCXCL1s bind with different binding affinities to CXCR2. Only vCXCL1s that bind with high affinity to CXCR2, also bind CXCR1. Furthermore, vCXCL1s display different potencies in [³⁵S]-GTPγS and β-arrestin2 recruitment assays. Our data suggest that the vCXCL1 polymorphisms elicit different binding affinities, receptor usage, and differential cellular activation, which might cause a variable role of vCXCL1 in HCMV dissemination.

Acknowledgements

We acknowledge the students Priscilla van Beek and Esther Holdinga for their help with performing the β-arrestin recruitment experiments. This study was partly performed within the framework of the Dutch Top Institute Pharma project T101-3 (to P.d.K., M.J.S.).

Introduction

Human cytomegalovirus (HCMV) is a ubiquitous pathogen that is well adapted to modulate host immune responses [2, 3]. HCMV contains genes for immune evasion that could function to increase viral survival, dissemination, or may contribute to pathogenesis [4-6]. There are a large number of open reading frames (~62), referred to as the UL/b' region in HCMV, that are not essential for virus replication *in vitro* but may have a role in immune evasion *in vivo* [7, 8]. Among the UL/b' open reading frames (ORFs), *UL146* and *UL147* encode CXC chemokines. The *UL146* ORF from the Toledo strain of HCMV has been shown to produce a functional chemokine [4]. vCXCL1_{Toledo} binds to CXCR1 and CXCR2, induces neutrophil chemotaxis and calcium mobilization [9]. These data suggest that vCXCL1 produced from CMV-infected endothelial cells recruits neutrophils and contributes to viral dissemination [4, 9, 10]. Sequencing of different HCMV strains [7, 11-15] showed that *UL146* is one of the most variable genes in the entire HCMV genome [11].

Chemokines are categorized into C, CC, CXC and CX3C chemokines based on the number and spacing between conserved cysteine residues in their N-terminus. The CXC chemokines are further divided into ELR⁺ and ELR⁻ chemokines, depending on the presence of the glutamate-leucine-arginine motif in their N-terminus. The ELR motif is known to be critical for recognition and activation of CXCR1/CXCR2, receptors present on e.g. neutrophils [16, 17]. Following the second conserved cysteine, chemokines possess a flexible N-loop of approximately ten residues. This N-loop is considered to be essential in the first step in receptor binding [18, 19].

Eleven distinct vCXCL1 genotypic groups were previously found in clinical isolates from congenitally infected infants [1]. Interestingly, in these groups, the N-loop region of vCXCL1 was variable. Furthermore, one of them, vCXCL1_{TX15}, lacks the ELR motif (see Fig. 6.1). Although the genetic variability of vCXCL1 did not show a definite correlation with clinical symptoms [1], the hypervariability within the N-loop region suggest that vCXCL1s may have different interactions with the chemokine receptors CXCR1 and CXCR2. In order to address functional variability of the vCXCL1s, recombinant vCXCL1s from each genotypic group were generated and competition binding assays and functional assays were performed to assess how vCXCL1 variability affects function.

Materials and methods

Dulbecco's modified Eagle's medium (DMEM), penicillin and streptomycin were all obtained from PAA Laboratories (Pasching, Austria). Fetal bovine serum was purchased from Integro B.V. (Dieren, The Netherlands). DMEM containing 25 mM HEPES and L-glutamine, OPTI-MEM, Hygromycin-B and Geneticin were obtained from Invitrogen (Paisley, United Kingdom). RPMI-1640 (Biowhittaker) was purchased from Lonza Walkersville (Walkersville, USA). Bovine Serum Albumin Fraction V (BSA) was obtained from Roche (Mannheim, Germany). Poly-

ethylenimine (PEI) was purchased from Polysciences (Warrington, PA, USA). [125 I]-CXCL8 and [35 S]-GTP γ S were obtained from PerkinElmer Life Sciences (Boston, MA, USA).

Cell culturing and transfection

HEK293T cells were grown at 5% CO $_2$ and 37°C in Dulbecco's modified Eagle's medium supplemented with 10% (v/v) fetal bovine serum, 50 IU/ml penicillin and 50 μ g/ml streptomycin. For [35 S]-GTP γ S experiments, cells were transiently transfected (per 10 cm dish) with 2.5 μ g of cDNA encoding human CXCR2 supplemented with 2.5 μ g of pcDEF3 by using linear polyethyleneimine (PEI) with a molecular weight of 25 kDa as previously described [20]. PathHunterTM HEK293-CXCR2 cells (DiscoverX, Fremont, USA), were grown at 5% CO $_2$ and 37°C in DMEM with 25 mM HEPES and L-glutamine supplemented with 10% (v/v) heat-inactivated fetal bovine serum, 50 IU/ml penicillin, 50 μ g/ml streptomycin, 800 μ g/ml Geneticin and 200 μ g/ml Hygromycin-B.

Neutrophil isolation

Peripheral blood neutrophils (PBN) were isolated from EDTA-treated blood from healthy human volunteers using dextran sedimentation and density gradient centrifugation as previously described [21]. Erythrocytes were removed with hypotonic lysis in 0.2% NaCl. After removal neutrophils were resuspended in the buffers for the individual assays. Viable neutrophils were quantified with trypan blue exclusion using a hemacytometer. The use of human subjects has been approved by the University of Tennessee Institutional Review Board (IRB# 6476B).

Production of recombinant vCXCL1s

The vCXCL1 gene, *UL146*, was PCR amplified from HCMV DNA of each of the 11 groups from a representative clinical isolate and cloned into the baculovirus transfer plasmid 1392 (Invitrogen, Paisley, United Kingdom) which contains homologous regions for recombination into the baculovirus genome. PCR primers were designed to include the open reading frame (ORF) and included an additional 2-4 glycines and six histidines on the carboxyl terminus of the proteins for purification. For generation of baculoviruses, SF9 cells were transfected with the 1392/*UL146* ORF plasmid construct and Sapphire linearized baculovirus DNA (Orbigen, San Diego, USA) according to the manufacturer's instructions. Recombinant baculovirus containing the *UL146* gene was titrated and used to infect Hi5 cells for optimum protein expression. 48 hrs after infection, cells and supernatants were harvested. Recombinant protein was isolated from the supernatants using Ni-NTA agarose beads (Qiagen, Hamburg, Germany) and resuspended in PBS. Matrix assisted laser desorption/ionisation (MALDI) was used to determine the size of the proteins.

Intracellular calcium mobilization assays

Release of calcium from intracellular stores was determined on freshly isolated PBN resuspended in PBS. Cells were loaded with 3 μ g/ml Indo-1-AM (Molecular Probes, Invitrogen, Paisley, United Kingdom) for 60 min at 37°C. Cells were washed with PBS and diluted to 1×10^6 cells/ml in Hanks' balanced salt solution (HBSS) containing Ca $^{2+}$ and Mg $^{2+}$ and 1% FBS. Chemokines were added to 2 ml of cells at a final concentration of 100 nM. All host chemokines were purchased from Peprtech (Rocky Hill, NJ) and endotoxin levels were less than 0.1 ng per μ g (1 EU/ μ g). Calcium flux was measured using a Photon Technology International Spectrophotometer (Birmingham, NJ, USA) at an excitation of 350 nm and FeliX32 software for analysis. Relative intracellular calcium levels were expressed as the ratio of emissions at 490 nm / 400 nm.

β 2 integrins staining

1×10^6 cells PBN were resuspended in RPMI-1640 with 1% FBS and exposed to 100 nM of chemokines for 2 h at 37°C. Cells were washed with PBS and blocked with 1% goat serum. PBN were incubated with fluorescently conjugated CD11a, CD11b, and CD11c antibodies (Caltag, Los Angeles, USA) on ice for 30 min. and fixed with 4% paraformaldehyde. Cells were analyzed with flow cytometry (FacsCalibur, BD Bioscience).

Human PBN chemotaxis assays

Chemotaxis assays were performed on freshly isolated human PBN resuspended in HBSS with 0.1% BSA and 10 mM HEPES. Assays were performed in triplicate in 96-well chemotaxis plates. 20 μ l of chemokines (500 nM) were loaded into the lower well of the modified Boyden chamber (Neuroprobe) and fitted with a 5 μ m filter. 1×10^6 PBN in 30 μ l were added to the upper well. The cells were incubated for 3h at 37°C. Migration of PBN was measured by staining migrated cells with the CalceinAM dye (Invitrogen).

Receptor binding analysis

The ability of vCXCL1s to compete for binding to either CXCR1 or CXCR2 was evaluated as previously described [22]. Briefly, $1-3 \times 10^5$ HEK293 cells over-expressing CXCR1 or CXCR2 were incubated with approximately 100 pM 125 I-labeled CXCL8 and increasing concentrations of unlabeled chemokines. Cells were collected on glass filters, washed twice, and bound radioactivity was measured with liquid scintillation counting. The graph was plotted and competition constants (K_i) were analyzed using GraphPad Prism 4.00 for Windows.

[35 S]-GTP γ S binding assay

Two days after transfection, HEK293T cells were detached from the plastic surface using ice-cold phosphate-buffered saline (PBS) and centrifuged at 1500g for 10 min at 4°C. Next, the pellet was resuspended in the ice-cold PBS and centrifuged again at 1500g for 10 min at 4°C. Later, cells were resuspended in ice-cold membrane buffer (15 mM Tris, 1 mM EGTA, 0.3 mM EDTA, and 2 mM MgCl_2 , pH 7.5), followed by homogenization by 10 strokes at 1100 to 1200 rpm using a Teflon-glass homogenizer and rotor. The membranes were subjected to two freeze-thaw cycles using liquid nitrogen, followed by centrifugation at 40,000g for 25 min at 4°C. The pellet was rinsed once with ice-cold Tris-sucrose buffer (20 mM Tris and 250 mM sucrose, pH 7.4) and subsequently resuspended in the same buffer and frozen at -80°C until use. Protein concentration was determined using a BCA-protein assay (Thermo Scientific, Rockford, USA).

Membranes (2.5 μ g/well) were incubated in 96-well plates in assay buffer (50 mM Hepes, 10 mM MgCl_2 , 100 mM NaCl, pH 7.2) supplemented with 5 μ g saponin/well, 3 μ M GDP and approximately 500 pM of [35 S]-GTP γ S and indicated concentrations of CXCL8 or (viral) CXCL1 in a final volume of 100 μ l. The reaction mixtures were incubated for 1 hour at room temperature, harvested with rapid filtration through Unifilter GF/B 96-well filterplates (PerkinElmer, USA) and washed three times with ice-cold wash buffer (50 mM Tris-HCl and 5 mM MgCl_2 , pH 7.4). [35 S]-GTP γ S incorporation was determined using a Microbeta scintillation counter (PerkinElmer, USA). Functional data were evaluated by a non-linear curve fitting procedure using GraphPad Prism 4.0 (GraphPad Software, inc., San Diego, CA).

β -arrestin recruitment assay

PathHunter™ HEK293-CXCR2 cells were plated out overnight at 10,000 cells/well (384-wells format) in 20 μ l OPTI-MEM. A pre-incubation with vehicle (PBS + 0.1 % BSA) of 30 min at 37°C and 5% CO₂, was followed

by 90 min CXCL8 or (viral) CXCL1 stimulation at 37°C and 5% CO₂. Next, 12 µl PathHunter Detection Reagents (DiscoverX, Fremont, USA) was added. After an incubation of 60 min at room temperature, β-galactosidase fragment complementation, as an indicator of β-arrestin-CXCR2 interaction, was measured for 0.3 sec in an Victor² 1420 Multilabel Reader. Functional data were evaluated by a non-linear curve fitting procedure using GraphPad Prism 4.0 (GraphPad Software, inc., San Diego, CA).

Results

Amino acid sequences alignment

Previously, the UL146 gene from 51 clinical isolates were sequenced and showed that it comprised 11 genotypic groups [1]. From the 11 groups, representative isolates were selected and aligned with vCXCL1 from the Toledo strain. As shown in Figure 6.1, the percent amino acid identities of the mature forms of the (v)CXCL1s, varies between 16.8 – 61.2% compared to vCXCL1_{Toledo}. The vCXCL1s contain around 20 additional residues at their C-terminus compared to endogenous CXCL1 and CXCL8. The function of these extra residues is unknown. The alignment of the vCXCL1s and the endogenous chemokines show seven conserved residues, including the arginine in the ELR motif, two cysteines in the N-terminus (CXC), a proline at position 32, cysteines at position 35 and 55, and a leucine at position 56. Furthermore, all vCXCL1s, but not CXCL1 or CXCL8, contain a glycine, valine, histidine, tryptophan and a proline at position 21, 54, 60, 65 and 87, respectively. The ELR motif is conserved, except in vCXCL1_{TX15}. Since the vCXCL1s display variability in the N-loop region, in the C-terminus and even in the ELR motif, we hypothesized that the viral chemokines show differences in chemokine receptor binding and functional response.

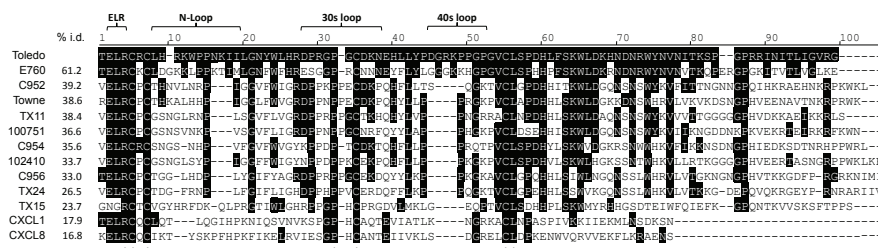


Figure 6.1: Amino-acid alignment of the mature form of recombinant vCXCL1s and the endogenous chemokines CXCL1 and CXCL8 with vCXCL1_{Toledo}. Seven amino acid residues are conserved, as indicated with a *.

vCXCL1 production using the baculovirus expression system

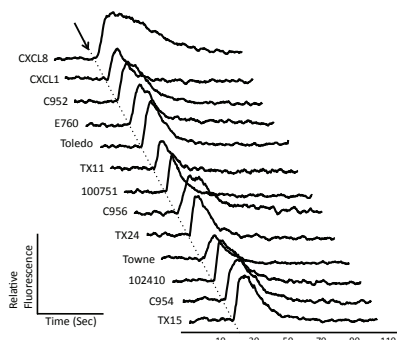
To compare the functional responses of the different vCXCL1s, recombinant vCXCL1 were generated by use of the baculovirus protein expression system. Baculovirus expression provides mammalian signal-sequence cleavage and generates eukaryotic glycosylation patterns and protein folding. vCXCL1s were 6 His-tagged and purified using Ni-NTA agarose beads.

The actual molecular weights were measured by Matrix-assisted laser desorption/ionization (MALDI) and resulted in molecular weight ranging from 11077 to 14137 (see Table 6.1).

vCXCL1s stimulate calcium release in human peripheral blood neutrophils

Release of intracellular calcium is a common indicator of chemokine receptor activation of peripheral blood neutrophils (PBNs) [4, 23]. To investigate the activation of human PBNs by vCXCL1s, vCXCL1s of different strains were added to 2 ml of freshly isolated human PBNs at a final concentration of 100 nM and 3 µg/ml Indo-1-AM. All vCXCL1s show a similar activation potential (Fig. 6.2), demonstrating that vCXCL1 polymorphisms do not affect calcium mobilization in human PBNs at this concentration.

Figure 6.2: Intracellular calcium mobilization ability of CXCL8, CXCL1 or the different vCXCL1s on human PBNs. Changes in fluorescence were measured over time after exposure to 100 nM chemokines (as indicated with an arrow). Data shown are representative figures of three independent experiments.



vCXCL1s upregulate CD11b and CD11c on surface of human PBN

β2 integrins are receptors that form heterodimers composed of an α component, such as CD11a, CD11b, and CD11c, and a β component, CD18. They are present on circulating leukocytes and, once in an activated state, they initiate leukocyte adhesion to endothelial cells and subsequently transmigration across the endothelium [24]. Previous studies demonstrated the ability of CXCL8 to upregulate CD11b and CD11c expression [25, 26]. Moreover, vCXCL1_{Toledo} and viral chemokine from chimpanzee CMV (vCXCL1_{CCMV}) also increased CD11b and CD11c expression on the cell surface on PBNs [23]. In this study, we tested the ability of vCXCL1s to alter the surface expression of these receptors on human PBNs. As shown in Figure 6.3, exposure of human PBNs to 100 nM vCXCL1s or the endogenous chemokines CXCL1 and CXCL8 do not change the levels of CD11a expression on the cell surface. As seen for CXCL8, CD11b and CD11c levels are increased upon exposure to all vCXCL1s (Fig. 6.3, Table 6.1). The percent changes in the mean fluorescent intensity of CD11b were 57-91%, which were similar to CXCL1 (82%) but less than CXCL8 (143%). Likewise, the percent changes of CD11c were 35-55%, which were similar to CXCL1 (43%), but less than CXCL8 (80%). These results imply that the (viral) chemokines selectively induce β2 integrin upregulation, with no significant differences observed between the different viral chemokines tested at 100 nM.

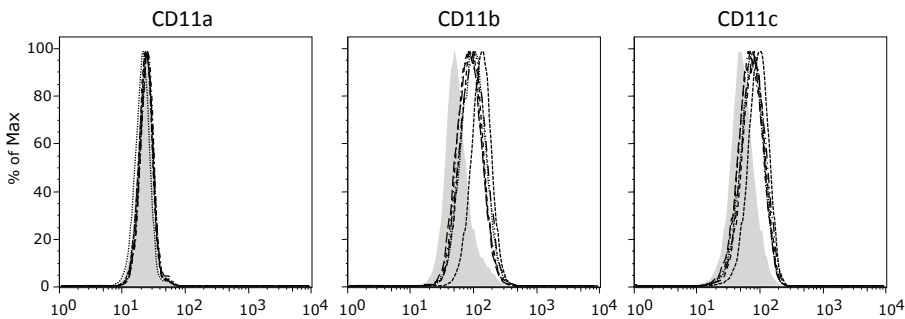


Figure 6.3: Change in surface expression of $\beta 2$ integrins on human PBNs upon 100 nM (viral) chemokine incubation for 2 hours. The shaded curve represents expression levels of unstimulated human PBNs. Graphs are shown of a representative experiments of three independent experiments.

vCXCL1s induce differential migration of human PBN

Previously, it has been shown that both CXCL8 and vCXCL1_{Toledo} are potent chemoattractants for human PBNs [4, 17]. Since the vCXCL1s are able to induce $\beta 2$ integrin expression after chemokine stimulation, we wondered whether the vCXCL1s are able to cause migration of human PBNs as well. Figure 6.4 clearly shows that all chemokines are able to induce chemotaxis at 500 nM. Interestingly, different effects are observed. For example, vCXCL1_{Toledo}, vCXCL1_{C952} and vCXCL1_{E760} cause a high chemotactic signal, whereas vCXCL1_{TX15} and vCXCL1_{TX24} only elicit a low chemotactic signal.

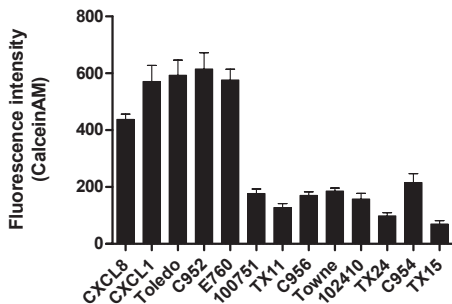


Figure 6.4: Chemotactic response of human PBNs to 500 nM of CXCL8, CXCL1 or indicated vCXCL1s. The chemotactic response is given in fluorescence intensity (basal chemotaxis subtracted), as cells were stained with the CalceinAM dye. Data shown are representative data of three independent experiments performed in triplo.

Different binding affinities for vCXCL1s

Since the N-loop of the vCXCL1s from different viral strains is hypervariable, and this might result in different binding affinity for CXCR2 or CXCR1, we wondered if differences observed in chemotactic assays might be correlated to differences in CXCR1 or CXCR2 binding affinity. To this end, competition binding experiments were performed in HEK293

cells expressing CXCR2 or CXCR1. Cells were incubated with [125 I]-CXCL8 and indicated concentrations of either vCXCL1s or CXCL8 (Fig. 6.5). As shown in Figure 6.5, vCXCL1 from the Toledo, C952 and E760 strain are able to fully displace [125 I]-CXCL8 from CXCR2 with high affinity, whereas at CXCR1 they have a markedly lower affinity. Also vCXCL1s from the 100751 and TX11 strain are able to fully displace the radioligand at CXCR2 (data not shown). In contrast, vCXCL1s from the Towne (and C956 or TX24 (data not shown)) strain and vCXCL1s from the TX15 (and 102410 or C954 (data not shown)) strains are only able to reduce [125 I]-CXCL8 binding to 20% or 30% at CXCR2, respectively. Interestingly, the non-ELR CXC chemokine, vCXCL1_{TX15}, still binds to CXCR2 albeit with very reduced affinity. Only the vCXCL1s that bind with high affinity to CXCR2 show binding to CXCR1 (Fig. 6.5). Thus, differences in binding affinity for CXCR2 and CXCR1 correlate well with differences in PBN migration in response to the vCXCL1s.

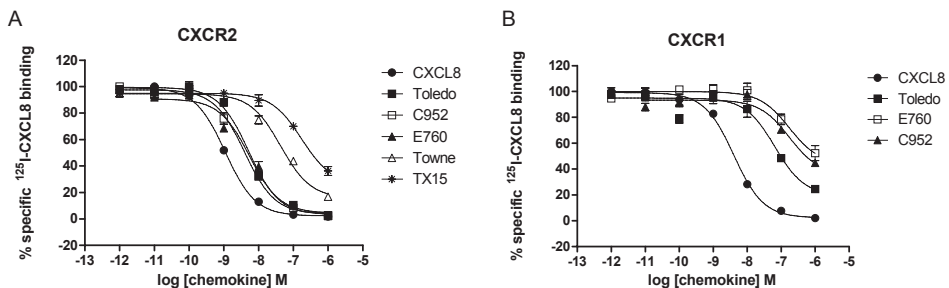


Figure 6.5: Displacement of [125 I]-CXCL8 binding to HEK293 cells expressing human CXCR2 (A) or CXCR1 (B). Cells were incubated with indicated concentration of (viral) chemokines and approximately 100 pM [125 I]-CXCL8.

vCXCL1s differentially induce [35 S] GTP γ S binding and β -arrestin2 recruitment

Chemotactic responses can be mediated via G-protein dependent and/or G-protein independent signaling mechanisms [26-29]. Our interest was to investigate whether the vCXCL1s display differences in G-protein and G-protein independent signaling. [35 S]-GTP γ S binding experiments were performed with HEK293T membranes expressing human CXCR2. The pEC₅₀ values of CXCL8 in this assay is 6.9 (Table 6.1). As shown in Figure 6.6A-B, only CXCL8, CXCL1 and vCXCL1_{Toledo} are able to reach a maximal response similar to 1 μ M CXCL8. Therefore, only for these three chemokines an pEC₅₀ value is presented in Table 6.1. Based on the obtained dose-response curves, we made a potency order of the chemokines of: CXCL8 ~ CXCL1 ~ Toledo \geq 100751 ~ C952 ~ C954 ~ C956 ~ E760 ~ 102410 \geq TX24 ~ TX11 ~ TX15 ~ Towne. To measure chemokine-induced β -arrestin2 recruitment, we used the PathHunterTM-HEK293-CXCR2 cell line. The pEC₅₀ values of CXCL8 in this assay is 9.1. Figure 6.6C-D shows that CXCL8, CXCL1, vCXCL1_{Toledo}, vCXCL1_{C952} and vCXCL1_{E760} reach maximal response equal to CXCL8, whereas the other viral chemokines do not reach a plateau up to 1 μ M or no β -arrestin2 recruitment at all. Again, only for the chemokines that do reach a plateau, an pEC₅₀ value is given in Table 6.1. The potency order

of the vCXCL1s in the β -arrestin2 recruitment is: CXCL8 \geq CXCL1 \sim Toledo \geq E760 \geq C952 \geq 102410 \sim 100751 \sim C954 \sim Towne \sim TX24 \geq TX11 \sim TX15 \sim C956. In both assays, the chemokines with high affinity for CXCR2, show the highest potency. Vice versa, low affinity chemokines demonstrate low responses. Thus, like in the chemotactic assay in human PBNs, differences in functional responses are correlated with differences in binding affinity.

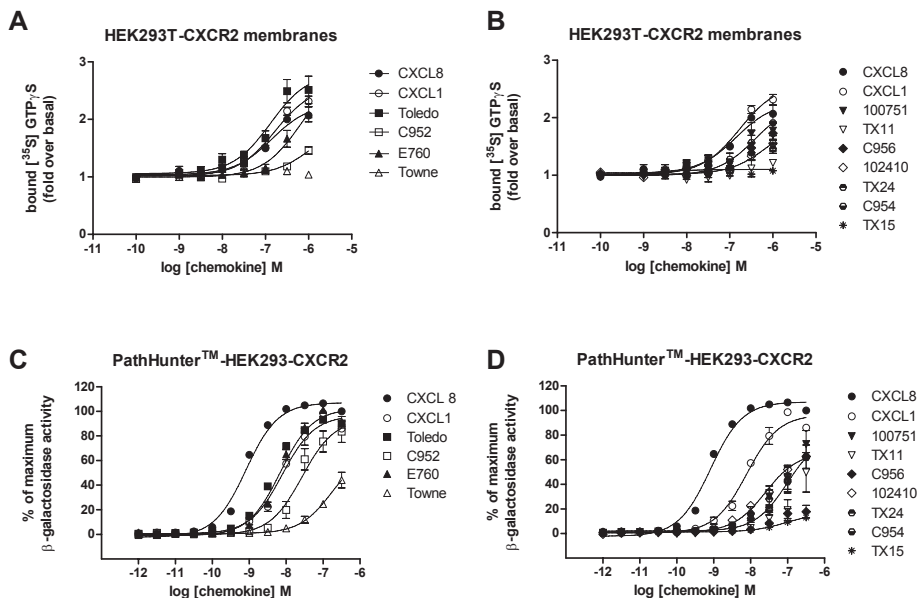


Figure 6.6: $[^{35}\text{S}]\text{-GTP}\gamma\text{S}$ binding to HEK293T membranes expressing CXCR2 induced by indicated (viral) chemokines (A-B). Data of triplicate determinations are corrected to basal $[^{35}\text{S}]\text{-GTP}\gamma\text{S}$ binding ($n=3-4$). β -arrestin2 recruitment in PathHunterTM cells by indicated (viral) chemokines (C-D). Data of triplicate determinations are expressed as percentage of β -galactosidase activity, in which the response to 1 μM CXCL8 is set to 100% ($n=3-4$).

Discussion

The *UL146* ORF, encoding for a viral chemokine vCXCL1, is one of the most variable genes in the HCMV genomes [1]. The alignment of the mature vCXCL1 (Fig. 6.1), cloned from congenitally CMV infected children, showed a highly conserved ELR motif, whereas the N-loop region followed by the second conserved cysteine residue is hypervariable. Since the N-loop region is known to be important for binding of chemokines to their receptor [18, 19], the hypervariability within the N-loop region of the different vCXCL1s may be associated with altered binding and function, possibly influencing clinical symptoms. This is the first study examining in detail potential functional differences between the 11 different vCXCL1s. We analyzed the cell Ca^{2+} mobilization and the induction of adhesion molecules upon vCXCL1

Table 6.1: Properties of CXCL8, CXCL1 and viral CXCL1s of different strains. Size determined with Matrix-assisted laser desorption/ionization (MALDI) is given. [¹²⁵I]-CXCL8 competition binding was performed on HEK293 cells expressing CXCR2. Change in surface expression of β2 integrins upon 100 nM (viral) chemokine incubation has been measured at human PBNs. Data shown are % change in fluorescence intensity for CD11a, CD11b and CD11c compared to non-stimulated human PBNs. Chemotactic response to 500 nM (viral) chemokines is determined with human PBNs. We distinguished the chemokines to 'high', intermediate' and 'low' responders (n=3). [³⁵S]-GTPγS binding to HEK293T membranes expressing CXCR2 induced by different (viral) chemokines. Data shown are mean values of triplicate determinations (n=3-4) ± S.E.M. PathHunter™ HEK293-CXCR2 cells were incubated with different (viral) chemokines. Data shown are mean values of triplicate determinations (n=3-4) ± S.E.M.

chemokine	size (MW)	CXCR2 binding K _i	% change in mean fluorescence intensity			human PBN chemotaxis signal	[³⁵ S]-GTPγS HEK293T-CXCR2		β-arrestin recruitment PathHunter™-CXCR2	
			CD11a	CD11b	CD11c		pEC ₅₀	intrinsic activity	pEC ₅₀	intrinsic activity
CXCL8		0.7	6.8	142.6	80.3	high	6.85 ± 0.13	1	9.10 ± 0.02	1.00
CXCL1		not tested	-5.0	82.4	42.8	high	6.84 ± 0.08	1.28 ± 0.11	8.30 ± 0.09	0.87 ± 0.03
Toledo	14317	0.52	12.3	80.7	50.5	high	6.98 ± 0.08	1.39 ± 0.33	8.35 ± 0.05	0.91 ± 0.03
C952	11959	1.63	10.5	91.2	55.3	high	-	-	7.51 ± 0.25	0.81 ± 0.11
E760	11077	2.36	8.2	71.1	39.1	high	-	-	8.16 ± 0.04	0.91 ± 0.05
100751	11853	7.48	6.8	71.9	50.3	intermediate/low	-	-	-	-
TX11	11157	8.10	11.4	57.7	43.7	intermediate/low	-	-	-	-
C956	12912	10.7	11.8	91.2	54.9	intermediate/low	-	-	-	-
Towne	11960	19.8	10.5	57.0	34.9	intermediate/low	-	-	-	-
102410	11880	27.3	6.4	64.5	47.8	intermediate/low	-	-	-	-
TX24	13036	35.2	8.6	81.4	55.3	low	-	-	-	-
C954	11961	35.8	7.3	73.7	37.0	intermediate/low	-	-	-	-
TX15	12032	119	13.2	62.5	36.2	low	-	-	-	-

- : not able to calculate pEC₅₀ values, sicne curves do not reach a plateau.

treatment, which can affect neutrophil chemotaxis and subsequent cell-mediated viral dissemination. The neutrophil shuttle model puts the neutrophil forward as the main vehicle for HCMV dissemination [30]. It has been reported that neutrophils are infected by HCMV during neutrophil transendothelial migration across infected endothelium and subsequently transmit infectious virus to fibroblasts [10, 31]. This would allow more opportunities for the virus to infect surrounding tissues or different cells. This has for example been shown for the guinea pig CMV (GPCMV), which encode a MIP homolog that interact with the CCR1 receptors, and that appears to play a role in viral dissemination *in vivo* [32, 33].

In this study we showed that all vCXCL1s induce intracellular calcium mobilization in PBN (Fig. 6.2) and upregulate $\beta 2$ integrin expression on the surface of PBNs (Fig. 6.3) to a similar extent as human CXCL1 (Table 6.1). As chemotaxis of circulating neutrophils is thought to be dependent on adhesion to and extravasation across the endothelium, all vCXCL1s are capable to affect PBN to increase contact with the endothelium and might employ them as the vehicle for the dissemination. Interestingly, albeit all vCXCL1s showed similar activation patterns in both calcium flux and $\beta 2$ integrin induction (Fig. 6.2-6.3), they display different potencies in chemotaxis. The different potencies in chemotaxis correlate with differences in binding affinities of the vCXCL1s to CXCR2 (Table 6.1). As expected, vCXCL1_{TX15} which lacks the ELR motif, shows the lowest binding affinity and shows a low chemotactic signal as well. The vCXCL1s with high affinity for CXCR2 (vCXCL1_{Toledo}, vCXCL1_{C952} and vCXCL1_{E760}) most effectively induce chemotaxis. Moreover, this subset of vCXCL1s also binds CXCR1 although with lower affinity (Fig. 6.5, Table 6.1). The finding that vCXCL1_{Toledo} also binds CXCR1 is in line with recent studies [9]. The unrestricted binding to both CXCR1 and CXCR2 is advantageous as it can promote stronger cellular responses, like chemotaxis in PBNs.

Our data also indicate that calcium mobilization and induction of integrin $\beta 2$, induced by all vCXCL1s, do not play a major role in vCXCL1 induced chemotaxis. Besides involvement of G_i proteins, others demonstrated a role for β -arrestin2 in the chemotaxis of CXCR2 expressing cells [34-36]. Traditionally, it was thought that β -arrestin proteins were only present to desensitized activated receptors. However, in the last decade several publications have provided evidence that β -arrestins can induce intracellular signaling as well [37]. The involvement of β -arrestins in chemokine-induced chemotaxis has been first described for the CXCR4/CXCL12 axis in 2002 [28]. The vCXCL1s with a high affinity for the CXC chemokine receptors show the highest potency in [³⁵S]-GTP γ S binding and β -arrestin recruitment, while the chemokines with low affinity for CXCR2 or CXCR1, like e.g. vCXCL1_{TX15}, show the lowest potency in cellular responses. Thus, in general, binding affinities are well correlated with potencies in G protein coupling and β -arrestin recruitment and appear important in chemotaxis. Markedly, previous studies show that the Toledo strain is more virulent than Towne [38]. Since we show in the present study that vCXCL1_{Toledo} has a higher affinity for CXCR2 and CXCR1, and induces functional responses to a higher extent than vCXCL1_{Towne}, difference in clinical outcome might be caused by differential activity of the vCXCL1s.

In conclusion, our data show that the polymorphism in vCXCL1 elicit different binding affinity to CXCR1 and CXCR2, generating various degrees of cellular responses. The interaction of vCXCL1s with their receptor(s) can contribute to HCMV pathogenesis by accelerating viral dissemination and/or providing diverse cellular activities to manipulate host immune responses. We hypothesize that differences in binding affinity of vCXCL1s can lead to a variable role of vCXCL1 in HCMV pathogenesis.

References

1. Heo, J., et al., Polymorphisms within human cytomegalovirus chemokine (UL146/UL147) and cytokine receptor genes (UL144) are not predictive of sequelae in congenitally infected children. *Virology*, 2008. 378(1): p. 86-96.
2. Mocarski, E.S., Jr., Immunomodulation by cytomegaloviruses: manipulative strategies beyond evasion. *Trends Microbiol*, 2002. 10(7): p. 332-9.
3. Miller-Kittrell, M. and T.E. Sparer, Feeling manipulated: cytomegalovirus immune manipulation. *Virol J*, 2009. 6: p. 4.
4. Penfold, M.E., et al., Cytomegalovirus encodes a potent alpha chemokine. *Proc Natl Acad Sci U S A*, 1999. 96(17): p. 9839-44.
5. Hansen, S.G., et al., Evasion of CD8+ T cells is critical for superinfection by cytomegalovirus. *Science*, 2010. 328(5974): p. 102-6.
6. Saederup, N. and E.S. Mocarski, Jr., Fatal attraction: cytomegalovirus-encoded chemokine homologs. *Curr Top Microbiol Immunol*, 2002. 269: p. 235-56.
7. Prichard, M.N., et al., A review of genetic differences between limited and extensively passaged human cytomegalovirus strains. *Rev Med Virol*, 2001. 11(3): p. 191-200.
8. Cha, T.A., et al., Human cytomegalovirus clinical isolates carry at least 19 genes not found in laboratory strains. *J Virol*, 1996. 70(1): p. 78-83.
9. Lutichau, H.R., The cytomegalovirus UL146 gene product vCXCL1 targets both CXCR1 and CXCR2 as an agonist. *J Biol Chem*, 2010. 285(12): p. 9137-46.
10. Grundy, J.E., et al., Cytomegalovirus-infected endothelial cells recruit neutrophils by the secretion of C-X-C chemokines and transmit virus by direct neutrophil-endothelial cell contact and during neutrophil transendothelial migration. *J Infect Dis*, 1998. 177(6): p. 1465-74.
11. Dolan, A., et al., Genetic content of wild-type human cytomegalovirus. *J Gen Virol*, 2004. 85(Pt 5): p. 1301-12.
12. Stanton, R., et al., Stability of human cytomegalovirus genotypes in persistently infected renal transplant recipients. *J Med Virol*, 2005. 75(1): p. 42-6.
13. Lurain, N.S., et al., Analysis of the human cytomegalovirus genomic region from UL146 through UL147A reveals sequence hypervariability, genotypic stability, and overlapping transcripts. *Virol J*, 2006. 3: p. 4.
14. Hassan-Walker, A.F., et al., Sequence variability of the alpha-chemokine UL146 from clinical strains of human cytomegalovirus. *J Med Virol*, 2004. 74(4): p. 573-9.
15. Arav-Boger, R., et al., Human cytomegalovirus-encoded alpha -chemokines exhibit high sequence variability in congenitally infected newborns. *J Infect Dis*, 2006. 193(6): p. 788-91.
16. Schraufstatter, I.U., et al., Multiple sites on IL-8 responsible for binding to alpha and beta IL-8 receptors. *J Immunol*, 1993. 151(11): p. 6418-28.
17. Clark-Lewis, I., et al., Structure-activity relationships of interleukin-8 determined using chemically synthesized analogs. Critical role of NH2-terminal residues and evidence for uncoupling of neutrophil chemotaxis, exocytosis, and receptor binding activities. *J Biol Chem*, 1991. 266(34): p. 23128-34.
18. Rajagopalan, L. and K. Rajarathnam, Structural basis of chemokine receptor function--a model for binding affinity and ligand selectivity. *Biosci Rep*, 2006. 26(5): p. 325-39.
19. Allen, S.J., S.E. Crown, and T.M. Handel, Chemokine: receptor structure, interactions, and antagonism. *Annu Rev Immunol*, 2007. 25: p. 787-820.
20. Verzijl, D., et al., Noncompetitive antagonism and inverse agonism as mechanism of action of nonpeptidergic antagonists at primate and rodent CXCR3 chemokine receptors. *J Pharmacol Exp Ther*, 2008. 325(2): p. 544-55.
21. Markert, M., P.C. Andrews, and B.M. Babior, Measurement of O2- production by human neutrophils. The preparation and assay of NADPH oxidase-containing particles from human neutrophils, in *Meth Enzymol*. 1984. p. 358-65.
22. Penfold, M.E., et al., Cytomegalovirus encodes a potent alpha chemokine, in *Proc Natl Acad Sci USA*. 1999. p. 9839-44.
23. Miller-Kittrell, M., et al., Functional characterization of chimpanzee cytomegalovirus chemokine, vCXCL-1(CCMV). *Virology*, 2007. 364(2): p. 454-65.
24. Mayadas, T.N. and X. Cullere, Neutrophil beta2 integrins: moderators of life or death decisions. *Trends Immunol*, 2005. 26(7): p. 388-95.

25. Detmers, P.A., et al., Neutrophil-activating protein 1/interleukin 8 stimulates the binding activity of the leukocyte adhesion receptor CD11b/CD18 on human neutrophils. *J Exp Med*, 1990. 171(4): p. 1155-62.
26. Berger, M., et al., Different G(i)-coupled chemoattractant receptors signal qualitatively different functions in human neutrophils. *J Leukoc Biol*, 2002. 71(5): p. 798-806.
27. Smit, M.J., et al., CXCR3-mediated chemotaxis of human T cells is regulated by a Gi- and phospholipase C-dependent pathway and not via activation of MEK/p44/p42 MAPK nor Akt/PI-3 kinase. *Blood*, 2003. 102(6): p. 1959-65.
28. Fong, A.M., et al., Defective lymphocyte chemotaxis in beta-arrestin2- and GRK6-deficient mice. *Proc Natl Acad Sci U S A*, 2002. 99(11): p. 7478-83.
29. Sun, Y., et al., Beta-arrestin2 is critically involved in CXCR4-mediated chemotaxis, and this is mediated by its enhancement of p38 MAPK activation. *J Biol Chem*, 2002. 277(51): p. 49212-9.
30. van der Strate, B.W., et al., Dissemination of rat cytomegalovirus through infected granulocytes and monocytes in vitro and in vivo. *J Virol*, 2003. 77(20): p. 11274-8.
31. Sinzger, C., et al., Fibroblasts, epithelial cells, endothelial cells and smooth muscle cells are major targets of human cytomegalovirus infection in lung and gastrointestinal tissues. *J Gen Virol*, 1995. 76 (Pt 4): p. 741-50.
32. Penfold, M., et al., A macrophage inflammatory protein homolog encoded by guinea pig cytomegalovirus signals via CC chemokine receptor 1. *Virology*, 2003. 316(2): p. 202-12.
33. Haggerty, S.M. and M.R. Schleiss, A novel CC-chemokine homolog encoded by guinea pig cytomegalovirus. *Virus Genes*, 2002. 25(3): p. 271-9.
34. Su, Y., et al., Altered CXCR2 signaling in beta-arrestin-2-deficient mouse models. *J Immunol*, 2005. 175(8): p. 5396-402.
35. Richardson, R.M., et al., Role of the cytoplasmic tails of CXCR1 and CXCR2 in mediating leukocyte migration, activation, and regulation. *J Immunol*, 2003. 170(6): p. 2904-11.
36. Fan, G.H., et al., Identification of a motif in the carboxyl terminus of CXCR2 that is involved in adaptin 2 binding and receptor internalization. *Biochemistry*, 2001. 40(3): p. 791-800.
37. Shukla, A.K., K. Xiao, and R.J. Lefkowitz, Emerging paradigms of beta-arrestin-dependent seven transmembrane receptor signaling. *Trends Biochem Sci*, 2011.
38. Plotkin, S.A., et al., Protective effects of Towne cytomegalovirus vaccine against low-passage cytomegalovirus administered as a challenge. *J Infect Dis*, 1989. 159(5): p. 860-5.

*Expression of chemotactic receptors in bowel tissue
from patients with Inflammatory Bowel Disease*

Chapter 7

Petra de Kruijf ^{A,1}, Yongjun Qin ^B, Pim Koelink ^C, Saskia Overbeek ^C,
Hein W. Verspaget ^D, Simone C. Wolfkamp ^E, Anje A. te Velde ^E,
Aletta D. Kraneveld ^C, Cees Tensen ^B, Rob Leurs ^A and Martine J. Smit ^A

^A Leiden/Amsterdam Center for Drug Research, Division of Medicinal Chemistry,
Vrije Universiteit Amsterdam, The Netherlands

^B Department of Dermatology, Leiden University Medical Center, Leiden, The Netherlands

^C Division of Pharmacology and Pathophysiology, Utrecht Institute for Pharmaceutical Sciences,
Faculty of Science, Utrecht University, Utrecht, The Netherlands

^D Department of Gastroenterology-Hepatology, Leiden University Medical Centre,
Leiden, The Netherlands

^E Department of Gastroenterology and Hepatology, Academic Medical Center,
Amsterdam, The Netherlands

Abstract

Real-Time quantitative Polymerase Chain Reaction (RT-qPCR) has become a widely used technique to easily detect and quantify specific mRNA levels of genes of interest. We have established a RT-qPCR primer set of different chemotactic receptors, including chemokine receptors. Chemotactic receptors and their ligands are important regulators of leukocyte trafficking towards sites of inflammation, leading to clinical symptoms of inflammatory diseases. To identify potential therapeutic targets in inflammatory bowel disease (IBD), we profiled different chemotactic receptor mRNA expression levels in both non-inflamed and inflamed bowel tissue of IBD patients, suffering from Crohn's Disease (CD) or Ulcerative Colitis (UC). Of all tested receptors, only S1P₂ mRNA expression levels showed to be significantly increased in inflamed tissue of CD patients, whereas in UC patients the increase was not significant. Other chemotactic receptors were either not expressed or no significant difference between inflamed and non-inflamed tissue was apparent. Our results show that RT-qPCR is an elegant technique to easily investigate mRNA expression levels of chemotactic receptors from different patient materials. As such, this technique can be used as a fast first step to identify receptors that might play a role in IBD pathogenesis.

Acknowledgements

We like to thank the department of Gastroenterology and Hepatology of the Leiden University Medical Center for providing us several bowel tissue samples from either inflammatory bowel disease patients or non-inflamed material from colon cancer patients. The study was performed within the framework of the Dutch Top Institute Pharma project T101-3.

Introduction

A change in expression profile of receptors and/or their corresponding ligands are often correlated with the development of clinical symptoms of diseases. As we already discussed in **chapter 2** [1], the chemokine/chemokine receptors axis plays an important role in chronic inflammatory diseases. Chemokines expressed at sites of inflammation cause the transmigration of leukocytes expressing chemokine receptors, subsequently causing increased clinical symptoms. Patients with Chronic Obstructive Pulmonary Disease (COPD) show e.g. increased expression of the chemokines CCL2, CCL5, CXCL8, CXCL9, CXCL10 and CXCL11 in the sputum or bronchoalveolar lavage fluid. Also the expression of the chemokine receptor CXCR2 is increased in bronchial biopsies from COPD patients [2-7]. Furthermore, in the synovium of rheumatoid arthritis patients abundant expression of CCL5, CCL15 and the receptors CCR1, CCR5 and CXCR4 was measured [8]. In atherosclerotic lesions CCL5, CXCL9, CXCL10, CXCL11 and CX3CL1 were highly expressed [9-12], and CD4⁺ lymphocytes of multiple sclerosis patients show an increased expression of the chemokine receptor CXCR3 [13]. Moreover, CCL20 and its receptor CCR6 were up-regulated in psoriatic skin lesions [14]. In addition, inflammatory bowel disease (IBD) patients show increased levels of CXCL2, CXCL5, CXCL8 [15-20], CCL2, CCL3, CCL4, CCL7, CCL8 and CCL20 [16, 21-25] in their bowel tissue. Besides chemokines, also other chemotactic ligands like e.g. LTB₄, C5a, histamine, formyl-methionyl-leucyl-phenylalanine and spingolipids can cause infiltration of leukocytes via interaction with their cognate receptors. Differential expression of (chemotactic) receptors and their ligands in tissue from patients compared to healthy controls might lead to the identification of new potential drug targets. One of the well-accepted techniques used to investigate quantitative changes in mRNA expression levels is by means of Real-Time quantitative Polymerase Chain Reaction (RT-qPCR).

RT-qPCR was originally developed by Higuchi *et al* [26], who reported for the first time the quantitative analysis of mRNA through simultaneous amplification of specific DNA sequences and detection of the product formation using ethidium bromide. Since the fluorescence of ethidium bromide increases in the presence of double stranded DNA, the product formation can be followed in time. Nowadays, ethidium bromide is replaced for example by SYBR Green [27, 28]. SYBR Green does not show fluorescence when it is in free solution. However, when bound to DNA it becomes brightly fluorescent [28]. The fluorescence signal increases proportionally to the amount of double stranded DNA formed [29]. These dyes are sequence non-specific, showing an increase in fluorescence signal with every type of double stranded DNA including undesired primer-dimer products. One should therefore analyze the melting curve after the RT-qPCR experiment [30]. During this analysis, temperature increases gradually and the fluorescence signal is monitored. Once the temperature is high enough to denature the double stranded DNA product, dyes are released thereby causing a sharp drop in fluorescence. As primer-dimers are small products, they will denature at a lower temperature than the desired product. Thus, undesired products are easily detected with melting curve analysis [28].

During the detection of product formed in the RT-qPCR reaction, four different phases are distinguished [31, 32]. At the initial phase (normally 10-15 PCR cycles), fluorescence signal is at the background level showing a linear line in the amplification plot (Fig. 7.1A). In the early exponential phase, the fluorescence signal reaches a threshold that is above background level. The cycle at which this occurs is called the threshold cycle (Ct) [27, 31]. The fewer cycles are needed to reach this threshold, the higher amount of mRNA template molecules were initially present in the sample. In general, a reference gene should have a Ct value between 17 and 22, whereas genes of interest can have a Ct value of maximal 35. During the next phase, the fluorescence signal increases exponentially. Thereafter the signal levels off in the plateau phase and the fluorescence signal is no longer related to the amount of starting template. The signal saturates due to depletion of e.g. primers and/or dNTPs [28, 31, 32].

In this study, we generated a RT-qPCR primer set for different chemotactic receptors, including the family of chemokine receptors. Subsequently, these primers were used to profile cell lines. Furthermore, we determined the mRNA expression levels of the chemotactic receptors in bowel tissue from inflammatory bowel disease patients, both Crohn's Disease and Ulcerative Colitis, and in neutrophils isolated from either inflammatory bowel disease (IBD) patients or healthy controls. Hence, we used RT-qPCR as a fast first step to search for potential drug targets in IBD.

Material and Methods

Dulbecco's modified Eagle's medium (DMEM), penicillin and streptomycin were obtained from PAA Laboratories (Pasching, Austria). Fetal bovine serum was purchased from Integro B.V. (Dieren, The Netherlands). Ficoll-Paque™ PLUS was obtained from GE Healthcare (Uppsala, Sweden). TRIzol was purchased from Invitrogen (Carlsbad, USA). RNeasy kit was obtained from Qiagen (Frederick, USA). DNase and EDTA were purchased from Fermentas (St. Leon-Rot, Germany). The Iscript reverse transcriptase kit and iQ™ SYBR® Green were obtained from BioRad (Hercules, USA). Primers were designed with Beacon Designer (Palo Alto, USA) and ordered at Biolegio (Nijmegen, The Netherlands) or validated primers from SA BioSciences were obtained from Qiagen (Frederick, USA). Nuclease-free water was purchased from Ambion (Austin, USA). Human reference total RNA was obtained from Stratagene (Agilent Technologies, Santa Clara, USA).

Cell culturing

HEK293 cells and COS-7 cells were grown at 5% CO₂ and 37°C in Dulbecco's modified Eagle's medium supplemented with either 10% (v/v) fetal bovine serum (HEK293) or 5% (v/v) fetal bovine serum (COS-7), 50 IU/ml penicillin and 50 µg/ml streptomycin. Cells were trypsinized and subsequently counted. Next, 5x10⁶ HEK293 or 2x10⁶ COS-7 cells were collected as pellets and immediately frozen in liquid nitrogen and stored at -80°C until use.

Isolation of human polymorphonuclear leukocytes

Inflammatory bowel disease patients and healthy controls were recruited through the outpatient clinic at the department of Gastroenterology in the Academic Medical Center (AMC) Amsterdam, Netherlands as part of the Elephant Study. All patients and controls gave informed consent and the Elephant Study was approved by the

ethics review committee of the AMC. Human polymorphonuclear leukocytes (PMNs) were isolated from fresh whole blood. The PMNs were obtained by centrifugation on Ficoll-Paque™ PLUS (density: 1.077 g/ml), followed by hypotonic lysis of erythrocytes with sterile lysis buffer (0.15 M NH_4Cl , 0.01 M KHCO_3 and 0.1 mM EDTA; pH 7.4 at 4°C). After lysis, the PMNs were washed with PBS and finally 10×10^6 PMNs were resuspended in 1 ml of TRIzol and frozen at -80°C until use.

Human bowel tissue

Tissue samples used in this study were obtained from surgical resection specimens and include pairs of macroscopically inflamed and normal-appearing (non-inflamed) mucosa from patients with Crohn's disease (CD) and ulcerative colitis (UC), both clinically and histologically confirmed, as earlier described in Gao et al [33]. As control we used normal tissue from patients with a colorectal carcinoma, at least 10 cm from the tumour.

RNA isolation

Total RNA was isolated from cell lines using the RNeasy kit from Qiagen. Following the manufactures protocol, total RNA was taken up in 30-50 µl nuclease-free water. Total RNA from isolated tissue samples were either isolated by the method of Chomczynski and Sacchi [34] or with the RNeasy kit from Qiagen. As the RNeasy kit is not suitable for human polymorphonuclear leukocytes (PMNs), we used TRIzol to extract total RNA from PMNs. After defrosting, the homogenized samples were incubated for 3 min at room temperature. Next, 200 µl chloroform was added to 1 ml TRIzol reagent. After vigorously shaking for 15 sec, the samples were again incubated for 3 min at room temperature and then centrifuged at 12,000 g for 15 min at 4°C. The aqueous phase was transferred to a new tube and ice-cold 500 µl isopropyl alcohol was added to this tube. After vigorously shaking for 15 sec, the samples were incubated for 30 min at -20°C. Next, the samples were centrifuged at 18,000 g for 10 min at 4°C. Subsequently, the supernatant was removed and washed with 1 ml 70% ice-cold ethanol and centrifuged at 18,000 g for 5 min at 4°C. After removing the supernatant, the RNA pellet was dried by using air-dry for 5-10 min. Finally, the pellet was resuspended in 30 µl nuclease-free water.

cDNA synthesis

A NanoDrop 2000 spectrophotometer (Thermo Scientific, Wilmington, USA) was used to both determine the concentration of RNA (absorbance at 260 nm) and the purity of RNA (ratio of absorbance at 260 and 280 nm (best between 1.8-2.0) and ratio of absorbance at 260 and 230 nm (best around 2.0)). Furthermore, the quality of the RNA was checked by running a 1% agarose gel (detection of 28S and 18S rRNA bands). cDNA synthesis was either performed in 20 µl (small scale) or at 100 µl (big scale) with an input of 200 ng or 500 ng total RNA, respectively. First, in a total volume of 10 µl, the RNA was treated for 30 min at 37°C with DNase. To inactivate the DNase, 1 µl EDTA was added and the reaction was set for 10 min at 65°C. Subsequently, the treated RNA was directly subjected to cDNA synthesis (IscripT, Bio-Rad) for 60 min at 42°C, followed by 5 min at 85°C. The synthesized cDNA was diluted 10 times in nuclease-free water and stored at -20°C until use.

Quantitative RT-PCR

Quantitative RT-PCR was performed in duplicate using a MyiQ detection system (Biorad, Hercules, USA), and consisted of 9 min initial denaturation at 95°C, followed by 40 thermal cycles of 10 sec at 95°C and 30 sec at 60°C. To confirm the specificity of the PCR amplification, a dissociation curve (65°C-95°C, each 10 sec temperature increases with 0.5°C) was taken as well. The RT-qPCR reactions were carried out in 96-well Clear-Hard-Shells (HSS-9601) from Biorad. Each well contained 10 µl 2x iQTM SYBR® Green, 5 µl cDNA and 5 µl primers. Primers

were designed either with the Beacon Designer software (Palo Alto, USA) and ordered at Biolegio or purchased from SA Biosciences. For the self-designed primers, primer mixes per gene of interest of forward and reverse primers were made at a concentration of 5 pmol/μl. Adding 5 μl of this mixture per well, results in 25 pmol per primer per reaction. Primer mixes from SA Biosciences have a concentration of 10 μM. Adding 1 μl of this mixture (+ 4 μl water to have a total of 5 μl) leads to 10 pmol per primer in the reaction. Determination of B-actin expression was included to normalize the results of the different samples. The relative expression per gene of interest was analyzed by setting B-actin arbitrary on 10,000 and by use of the formula: $10,000 \cdot 2^{(Ct\text{-value B-actin} - Ct\text{ value gene of interest})}$.

Statistical Analysis

For all statistical analyses, GraphPad Prism version 4.0 was used. For comparing mRNA expression levels between non-inflamed and inflamed bowel tissue material, the data were analyzed with a two-tailed paired-t-test. Comparing mRNA expression levels between neutrophils from inflammatory bowel disease patients and healthy control, the data were analyzed with a two-tailed non-paired t-test. Data were considered significant at $P < 0.05$.

Results

Validation RT-qPCR primers for chemotactic receptors

To establish a RT-qPCR primer set for various chemotactic receptors, we designed primers using the software of Beacon Designer. Primer lengths were kept between 20-25 base pairs and amplicon size between 100-200 base pairs. Subsequently, primers were validated using cDNA synthesized from human reference total RNA. Criteria to validate a primer pair include: specific amplification on reference cDNA (as determined on a 2% agarose gel), one peak in melting curve analysis (Fig. 7.1B) and a reliable standard curve. The amplification plot (Fig. 7.1A) should have equal spacing (1 cycle) between the different 2-fold dilutions points, ideally resulting in a standard curve (Fig. 7.1C) with an amplification efficiency (E) of 100%, r^2 close to 1 and slope of -3.3 [35]. We accepted primers with amplification efficiencies of 60 till 150%, r^2 of 0.8 till 1 and a slope of -2.5 till -4.8. For 19 chemotactic receptors and the housekeeping gene β-actin, we designed and validated primer pairs (sequences given in Table 7.1). For those chemotactic receptors for which no proper primer-pairs were obtained, using above mentioned criteria, we ordered validated primers at SA Biosciences (Table 7.1).

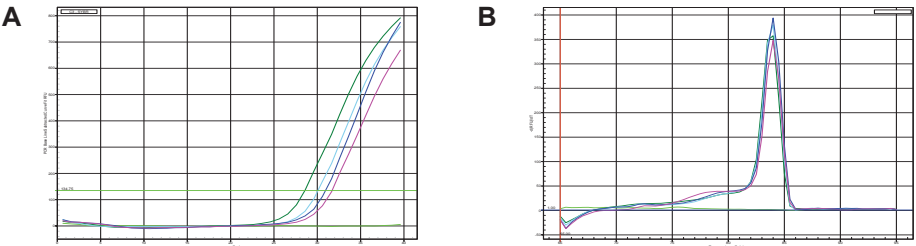


Figure 7.1, Continued on next page

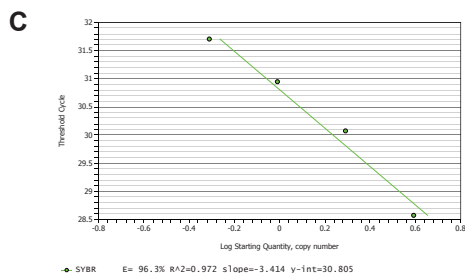


Figure 7.1: Analysis of a validated primer pair. Amplification plot (A), melting curve analysis (B) and the standard curve (C) are shown.

Profiling cell lines

As a proof of concept, we profiled the cell lines HEK293, COS-7, U2OS and MDA-MB-231 (Fig. 7.2). The HEK293 cell line shows high mRNA levels of BLT_1 , BLT_2 and $S1P_2$, moderate expression levels of CXCR3 and CXCR4 and relative low mRNA expression levels of CXCR6, CCR2, CCR6, CX₃CR1, and C5AR1. The COS-7 cell line demonstrates high mRNA expression levels of both CXCR3 and CXCR4, whereas CCR1 and CCR8 mRNA expression levels are low. For the U2OS and MDA-MB231 we primarily focused on profiling chemokine receptors. The U2OS cell line shows high expression levels of CXCR7 mRNA and low expression levels for CXCR5, CXCR6, CCR1, CCR4, CCR6, CCR10 and CX₃CR1. The MDA-MB-231 cell line demonstrates relative high mRNA expression levels of BLT_1 , moderate expression of CXCR4 and BLT_2 mRNA and relative low mRNA expression levels of CXCR3, CXCR5, CXCR6, CXCR7, CCR1, CCR2, CCR4, CCR5, CCR7, CCR10 and C5AR1.

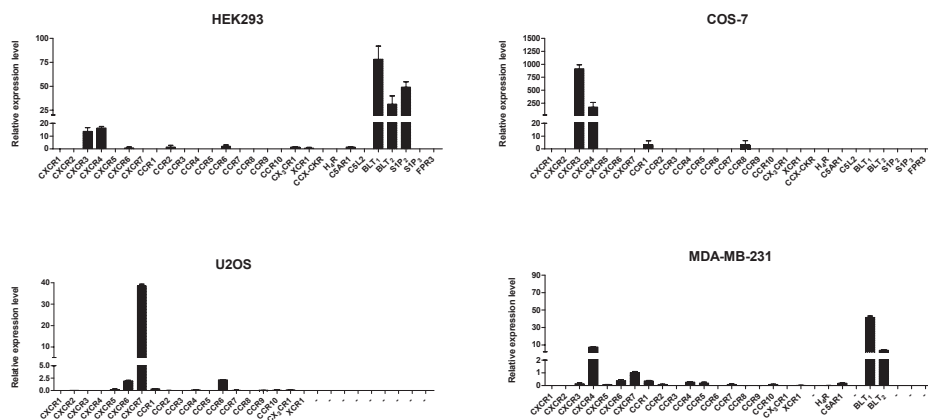


Figure 7.2: The mRNA expression levels of indicated chemotactic receptors in HEK293, COS-7, U2OS and MDA-MB-231 cells. The mRNA levels were normalized to B-actin.

Table 7.1: Validated primers of chemotactic receptors.

Gene	NM_Number	NM_Number	Forward Primer	Reverse Primer	NTC	Product
CXCR1	NM_000634	-	SA Biosciences: product code PPH01040E		N/A	84.5C
CXCR2	NM_001557	-	SA Biosciences: product code PPH00608E		N/A	81.5C
CXCR3	NM_001504	-	SA Biosciences: product code PPH01041A		N/A	89C
CXCR4	NM_001008540	NM_003467	TCTTTGCCAAGCTCAGTGAG	CCATGATGTGCTGAAACTGG	N/A	81.5-82C
CXCR5	NM_001716	NM_032966	SA Biosciences: product code PPH01034A		N/A- 78.5	89-89.5
CXCR6	NM_006564	-	SA Biosciences: product code PPH01343A		N/A	83.5-84
CXCR7	NM_020311	-	CGGAGTACTCTGCCTTGGAG	AGCATCAAGACCCGGAAGCTA	N/A - 82C	84C
CCR1	NM_001295	-	ACCCAGTGATCTACGCCTTC	TGAGTCAGAAACCCAGCAGAG	N/A	87C
CCR2	NM_000647	NM_000648	CAGTGTGAATCTTGGTGCTACG	AGTCTGAACTCTATGCCCTGTATTCT	N/A -74C	82C
CCR3	NM_001837	NM_178329	AGGCTCCGAATTATGACCAACATC	GGCAACACACAGCATGGACAATG	73C	84.5-85C
CCR4	NM_005508	-	GAGAAAGAAGAACAAAGGCGGTGAAG	GATGGGATTAAAGGCAGCAGTGAAC	N/A	84-84.5C
CCR5	NM_000579	NM_001100168	SA Biosciences: product code PPH00615E		77C	83C
CCR6	NM_004367	NM_031409	AAATCATCTGCCCTTGTGTGG	ACCTGATGGGCTCCGAGAC	N/A -78C	83-83.5C
CCR7	NM_001838	-	SA Biosciences: product code PPH00617A		N/A	84.5C
CCR8	NM_005201	-	CCTGGTCAATCCTGGTCTCTGTG	CCTGATCGTCCCTCACCTTTAGGG	N/A	84.5-85C
CCR9	NM_006641	NM_031200	GCGATGAGAGCAACCAACTGAAG	ACCACGAAGGGAAGGAAGAAC	N/A	81.5C
CCR10	NM_016602	-	GACAACTAGGGCTGCGAATC	GCAAGGCACAGAGGTAGTCC	N/A -78C	85-85.5C

Table continued at next page

Continued Tabel 7.1

Gene	NM_Number	NM_Number	Forward Primer	Reverse Primer	NTC	Product
CX ₃ CR1	NM_001337	-	GTGACTGAGACGGTTGCATTTAGC	GCAATTTCCCATACAGGTGGTAAAGG	76C - N/A	80.5C
XCR1	NM_005283	-	GCTTTCTTCGGGGCTGTGATTATCC	TTGGAGCGTGAGCGGAACAG	80.5C	84.5C
CCX-CKR	NM_016557	-	SA Biosciences; product code PPH01336A		N/A	81C
BLT ₁	NM_181657	-	GCCCTCCAGCCCTCTCAAGTTAAAC	GCCCTCCACGCCCCCTCCAC	N/A	82.5-83C
BLT ₂	NM_019839	-	CCTCCTATTTCCTTCCACCACCAG	CTCCCTCACGCTGCTCCTTCC	N/A - 78C	89C
C5AR1	NM-001736	-	ACTCCCTGTGTGCTCTCCTTTGC	GTGAATGACTTGTCTCTCCTTAACC	N/A	86.5-87C
C5L2	NM_018485	-	SA Biosciences; product code PPH59963A		N/A	89C
H ₄	NM_021624	-	AGCCTGTGGAAGCGTGATC	CTCCTCTGTCTCTCTGAATGAAAG	N/A	82.5-83C
S1P ₂	NM_004230	-	TCAAGACGGTCACCATCG	ACAGGCATAGTCCAGAAAG	N/A	84-84.5C
S1P ₃	NM_005226	-	CATCCTGCCCCCTCTACTC	AACACGCTCACCAACAATC	N/A	87C
FPR3	NM_002030	-	CCAGTTGAGACACAAGTCACAAATCC	ACACACGGAGGT'TCCCAGAGG	N/A	84C
B-actin	NM_001101	-	CGGGACCTGACTGACTACCTC	CTCCTTAATGTCACGCACGATTTC	N/A-84C	86C
CXCL8	NM_00584	-	SA Biosciences; product code PPH00568A		N/A	81C

Note: we were not successful in finding good primer pairs for S1P₁, S1P₄, S1P₅, FPR1 and FPR3.

Expression chemotactic receptors in bowel tissue

Next, we used RT-qPCR to identify differences between the mRNA expression levels of various chemotactic receptors in bowel tissue from inflammatory bowel disease (IBD) patients. For each patient, bowel material from inflamed and non-inflamed tissue was obtained after surgery. Non-inflamed colon tissue from patients suffering from colon cancer were used as a control. As shown in Figure 7.3-7.5, we analyzed the mRNA expression profiles separately for Crohn's Disease (CD) and Ulcerative Colitis (UC) patients. In addition we pooled the CD and UC results together, to investigate difference between non-inflamed and inflamed material of the complete set of IBD patients material.

As shown in Figure 7.3, bowel tissues from inflamed and non-inflamed IBD patients show relative high mRNA expression levels of CXCR4. In addition, also mRNA levels of CXCR6 and CXCR7 are well detected. Moderate mRNA expression levels are shown for CXCR1 and CXCR2, whereas CXCR3 and CXCR5 mRNA levels are relatively low (Table 7.2). None of the CXC chemokine receptors are significantly different expressed comparing non-inflamed and inflamed tissue. The expression of both CXCR1 and CXCR2 mRNA are slightly increased in inflamed tissue of most patients, however this is not significant. We observe a trend that most CD patients show a decreased CXCR7 mRNA expression in inflamed tissue, whereas UC patients show equal or higher expression in inflamed tissue.

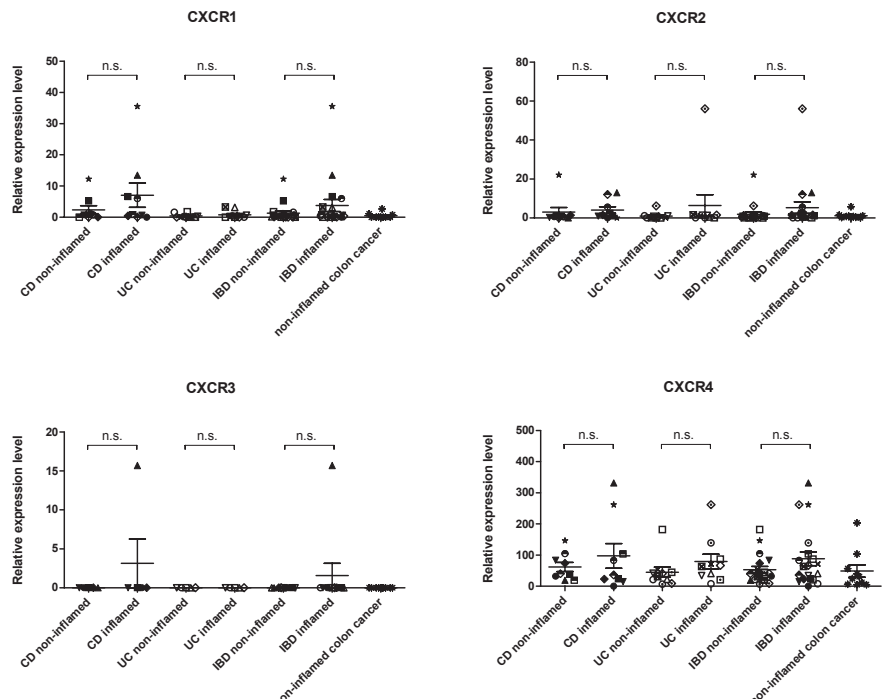


Fig 7.3, continued on next page.

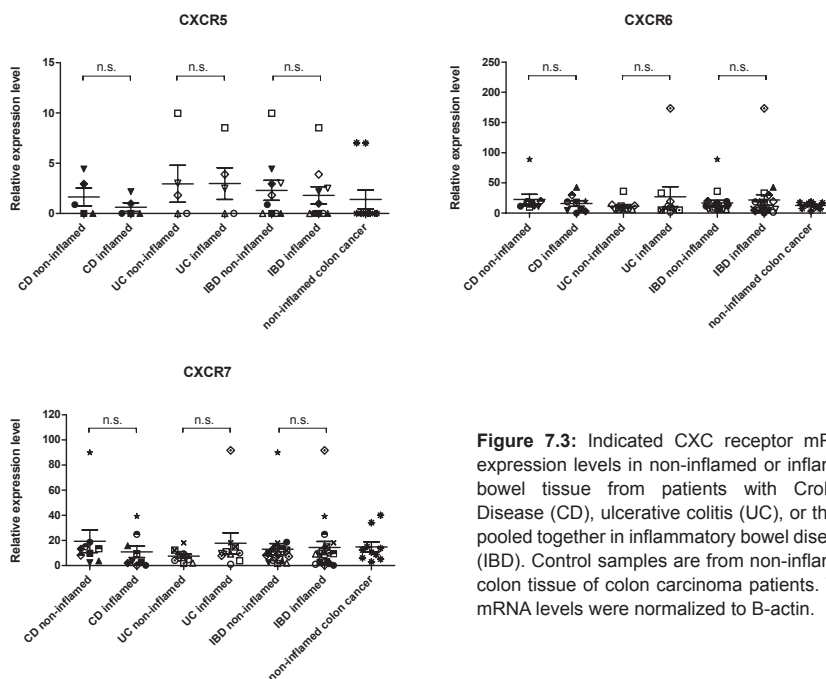


Figure 7.3: Indicated CXC receptor mRNA expression levels in non-inflamed or inflamed bowel tissue from patients with Crohn's Disease (CD), ulcerative colitis (UC), or those pooled together in inflammatory bowel disease (IBD). Control samples are from non-inflamed colon tissue of colon carcinoma patients. The mRNA levels were normalized to B-actin.

Figure 7.4 shows that CCR9, CCR7 and CCR6 mRNAs are relatively high expressed in a subset of patient bowel material. The other CC chemokine receptor mRNA levels are relatively low or not present in both CD and UC patients (Table 7.2). Significant differences between non-inflamed and inflamed bowel tissue are not observed. CCR7 mRNA levels of five CD patients decrease in inflamed tissue, whereas two patients show an increase and two patients equal expression levels. Similar to CCR7, also CCR9 mRNA levels decrease in most CD patients in inflamed tissue, but two patients show an increase in mRNA levels. Thus, variation between different patients results in non-conclusive patterns.

As shown in Figure 7.5, the mRNA levels of $S1P_2$, BLT_1 , BLT_2 , CCX-CKR and $C5AR1$ are relatively high in bowel tissue. In addition, also mRNA levels of the histamine H_4R and CX_3CR1 are in some patients well detected, whereas $XCR1$, $S1P_3$, $FPR3$ and $C5L2$ mRNA levels are relatively low (Table 7.2). The mRNA levels of the chemokine receptors CX_3CR1 , $XCR1$ and the decoy CCX-CKR are not significantly changed (Fig. 7.5). In both the CX_3CR1 and CCX-CKR graph, two outliers with high expression levels are observed, although most patients show only a relative expression level around 2 and 15, respectively. We observe a trend that the mRNA expression level of CX_3CR1 is decreased in inflamed tissue of most CD patients as well as in most UC patients. In addition, also CCX-CKR levels are in most CD patients decreased in inflamed tissue. The $XCR1$ mRNA levels were not changed. Most patients do not express the histamine H_4R mRNA, except three patients that show a relatively high expression. $C5AR1$ mRNA levels were detected in all IBD patients, but there

was no difference between non-inflamed and inflamed tissue. The mRNA expression levels from the other C5a receptor, C5L2, were not found. Interestingly, S1P₂ receptor mRNA is significantly increased in inflamed tissue of CD patients. Also, in most UC patients the expression level of mRNA of S1PR₂ is increased in inflamed tissue, but this was not significant.

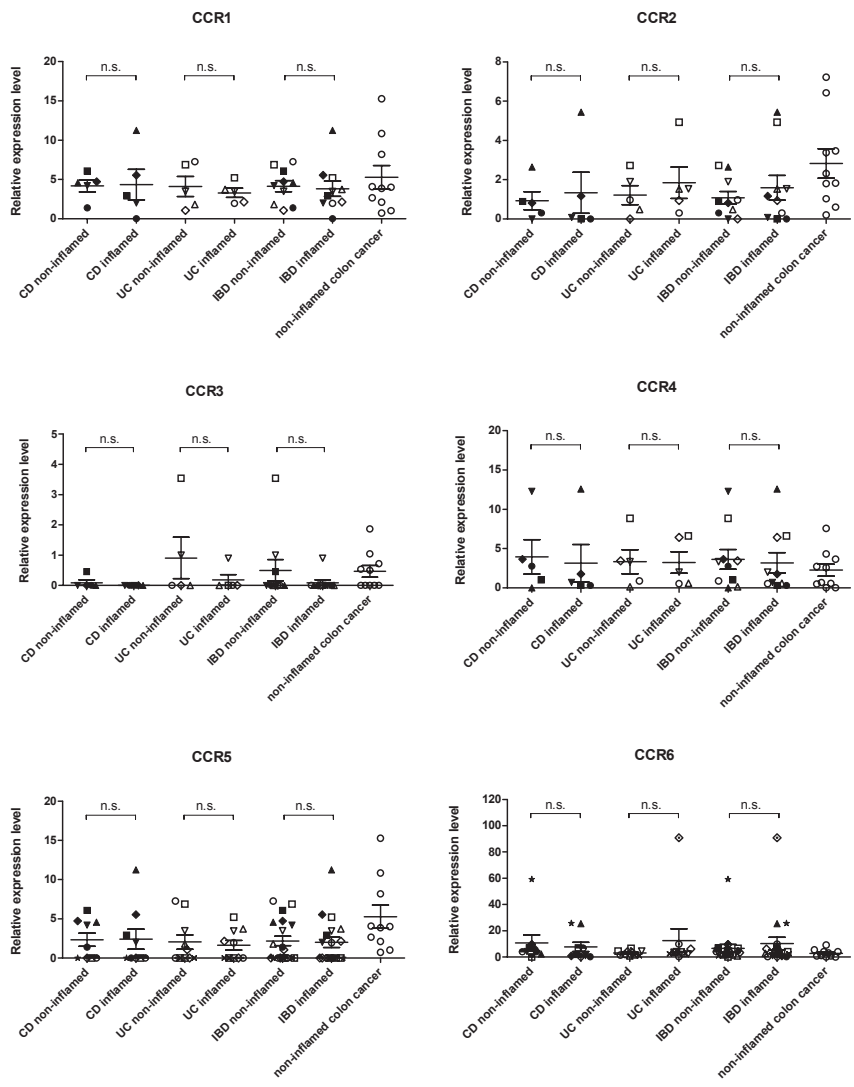


Figure 7.4, continued on next page.

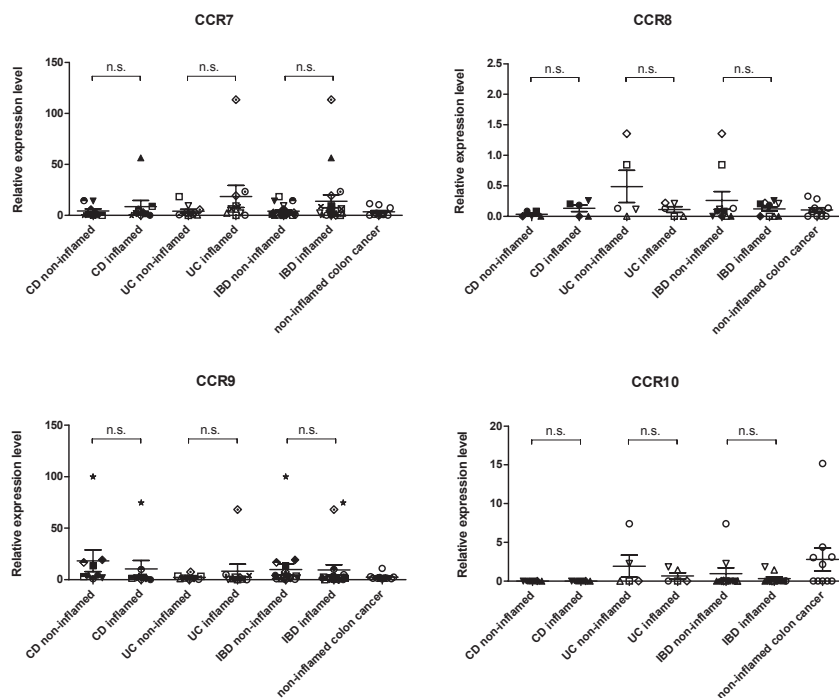


Figure 7.4: Indicated CC receptor mRNA levels in non-inflamed or inflamed bowel tissue from patients with Crohn's Disease (CD), ulcerative colitis (UC), or those pooled together in inflammatory bowel disease (IBD). Control samples are from non-inflamed colon tissue of colon carcinoma patients. The mRNA levels were normalized to B-actin.

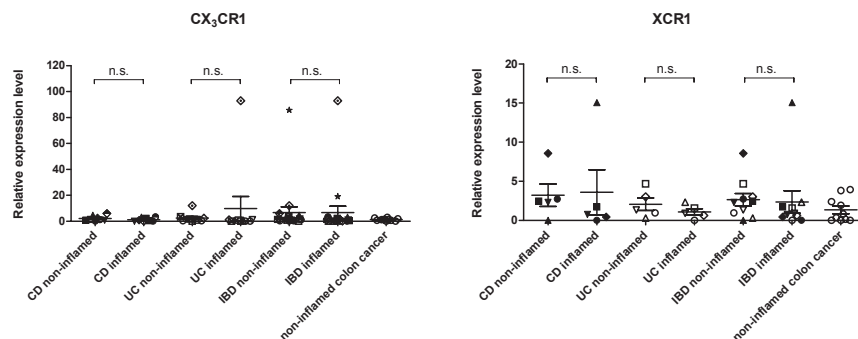


Figure 7.5, continued on next page.

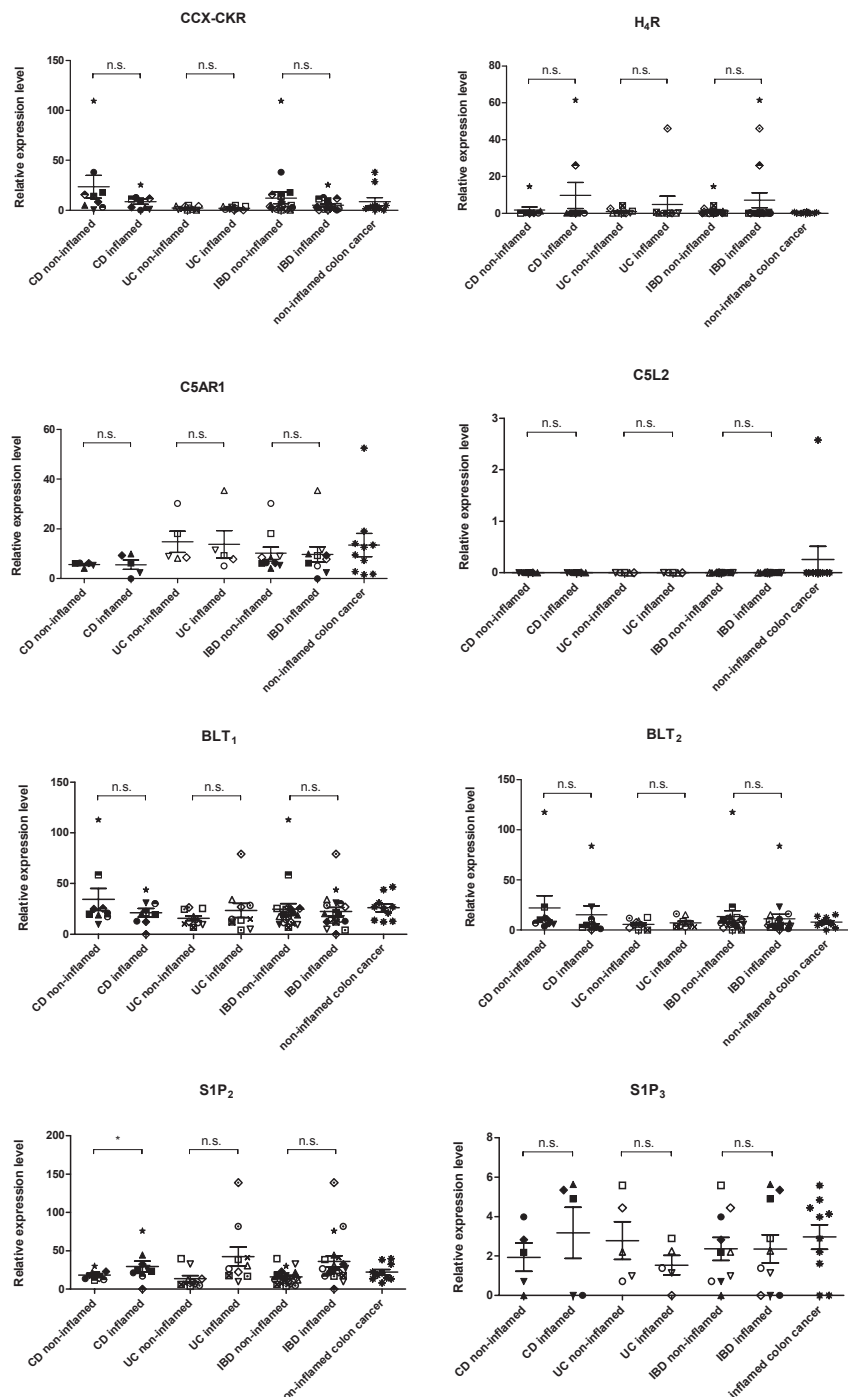


Figure 7.5, continued on next page.

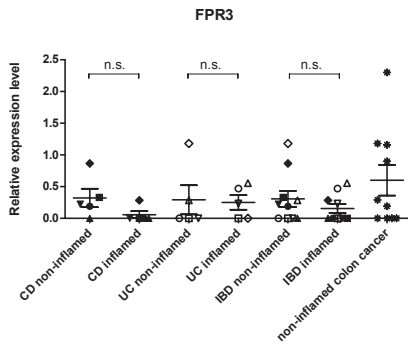


Figure 7.5: Indicated chemotactic receptor mRNA expression levels in non-inflamed or inflamed bowel tissue from patients with Crohn's Disease (CD), ulcerative colitis (UC), or those pooled together in inflammatory bowel disease (IBD). Control samples are from non-inflamed colon tissue of colon carcinoma patients. The mRNA levels were normalized to B-actin.

Expression levels of CXCL8

Since this thesis focuses primarily on CXCR2 (and CXCR1), and CXCL8 has been reported to show differential expression in various disease states [2, 4, 5, 16, 17, 19], we determined the expression level of this chemokine as well. The expression level of CXCL8 mRNA was determined in the same IBD tissues used in the chemotactic receptor profiling study. In most IBD patients, CXCL8 mRNA levels are increased in inflamed tissue (Fig. 7.6). The increase in CXCL8 mRNA expression is significant in UC patients, but not for CD patients. Furthermore, we investigated the CXCL8 mRNA levels in neutrophils isolated from seven healthy volunteers and twenty-five IBD patients (Fig. 7.6). Interestingly, the decrease of CXCL8 mRNA in neutrophils of IBD patients is significant. It should be noted that three healthy people show a relatively very high expression level and four people show a high mRNA expression level. In addition, only one IBD patient shows a very high expression level, seven a high expression level and seventeen patients a relatively lower expression level (see insert Fig. 7.6).

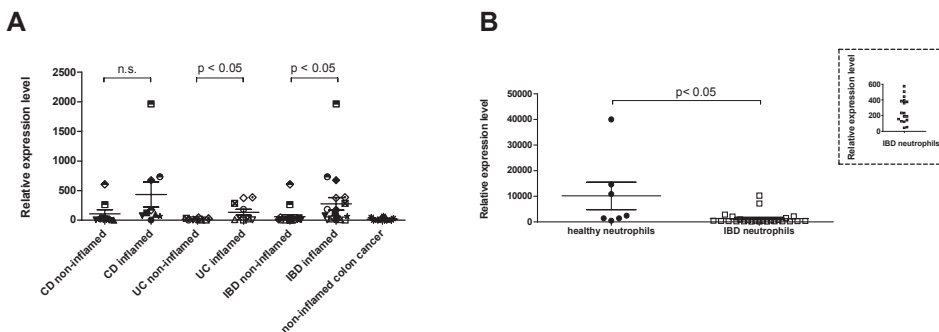


Figure 7.6: CXCL8 mRNA expression levels in non-inflamed or inflamed bowel tissue from patients with Crohn's Disease (CD), ulcerative colitis (UC), or those pooled together in inflammatory bowel disease (IBD). Control samples are from non-inflamed colon tissue of colon carcinoma patients (A). CXCL8 mRNA expression levels in neutrophils from inflammatory bowel disease patients or healthy control (B). The mRNA levels were normalized to B-actin.

Expression level CXCR1 and CXCR2 in neutrophils

Both CXCR1 and CXCR2 are expressed on neutrophils [36]. As stated above, CXCL8 mRNA is significantly higher expressed in inflamed IBD tissue (Fig. 7.6), and also CXCR1 and CXCR2 levels are slightly increased in most patients (Fig. 7.3). Since the bowel tissue material consist of different kind of cells, including infiltrating immune system cells, we also investigated the expression levels of CXCR1 and CXCR2 of isolated neutrophils from healthy persons and IBD patients (Fig. 7.7). We observe a trend that mRNA levels of both receptors are increased in neutrophils from IBD patients, however the increases are not significant. This is probably caused by the fact that also in healthy persons the mRNA levels of these receptors is somewhat variable.

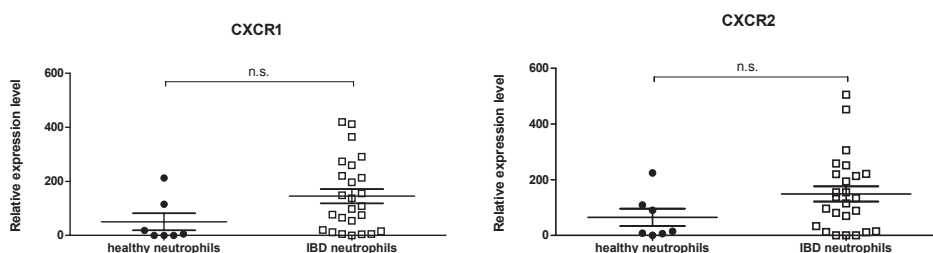


Figure 7.7: CXCR1 or CXCR2 mRNA expression levels in neutrophils from inflammatory bowel disease patients or healthy control. The mRNA levels were normalized to B-actin.

Discussion

Since RT-qPCR has become a widely used technique to quantitatively detect specific mRNA levels of genes of interest [31], we established a RT-qPCR primer set of different chemotactic receptors to determine mRNA expression levels in cell lines and inflammatory bowel disease patient material. Hence, we used this technique to screen for the presence of chemotactic receptors in certain cell lines. In addition, RT-qPCR was used as a first step in screening for potential drug targets in inflammatory bowel disease.

As initial test for our primer set, we profiled the cell lines HEK293, COS-7, U20S and MDA-MB-231. Recently, another research group investigated the mRNA levels of a large set of GPCRs in HEK293, AtT20, BV2 and N18 cell lines using microarrays [37]. To our knowledge, so far the mRNA expression levels of chemotactic receptors have not been extensively investigated at COS-7, US02 and MDA-MB-231 cells. In agreement with the data of Atwood et al [37], we found relatively high levels of CXCR4 and BLT₁ mRNA in HEK293 cells, and also CCR6, CX₃CR1 and BLT₂ mRNA levels were detected. However in HEK293 cells, we also detected expression of CXCR3, CXCR6, CCR2, XCR1, S1P₂ mRNA levels, while they detected CXCR2, CCR4, CCR7, CCR10 and S1P₃ mRNA levels.

Tabel 7.2: Average relative mRNA expression levels of chemotactic receptors in non-inflamed (non-infl.) or inflamed bowel tissue from patients with Crohn's Disease (CD), ulcerative colitis (UC), or those pooled together in inflammatory bowel disease (IBD). Control samples are from non-inflamed colon tissue of colon carcinoma patients.

	Crohn's Disease		Ulcerative Colitis		IBD		colon cancer
	non-infl.	inflamed	non-infl.	inflamed	non-infl.	inflamed	non-infl.
CXCR4	60-65	95-100	45-50	75-80	50-55	85-90	45-50
S1P ₂	15-20	25-30	10-15	40-45	15-20	35-40	20-25
BLT ₁	30-35	20-25	15-20	20-25	20-25	20-25	25-30
CCX-CKR	20-25	5-10	0-5	0-5	10-15	0-5	5-10
CXCR7	15-20	10-15	5-10	15-20	10-15	10-15	10-15
CCR9	15-20	10-15	0-5	5-10	5-10	5-10	0-5
C5AR1	5-10	5-10	10-15	10-15	10-15	10-15	10-15
CCR7	0-5	5-10	0-5	15-20	0-5	10-15	0-5
CCR6	10-15	5-10	0-5	10-15	5-10	5-10	0-5
H ₄	0-5	5-10	0-5	0-5	0-5	5-10	0-5
CX ₃ CR1	0-5	0-5	0-5	5-10	5-10	5-10	0-5
CXCR2	0-5	0-5	0-5	5-10	0-5	5-10	0-5
CXCR1	0-5	5-10	0-5	0-5	0-5	0-5	0-5
CCR1	0-5	0-5	0-5	0-5	0-5	0-5	0-5
CCR4	0-5	0-5	0-5	0-5	0-5	0-5	0-5
CXCR5	0-5	0-5	0-5	0-5	0-5	0-5	0-5
XCR1	0-5	0-5	0-5	0-5	0-5	0-5	0-5
CCR5	0-5	0-5	0-5	0-5	0-5	0-5	0-5
S1P ₃	0-5	0-5	0-5	0-5	0-5	0-5	0-5
CCR10	0-5	0-5	0-5	0-5	0-5	0-5	0-5
CCR2	0-5	0-5	0-5	0-5	0-5	0-5	0-5
CCR3	0-5	0-5	0-5	0-5	0-5	0-5	0-5
CCR8	0-5	0-5	0-5	0-5	0-5	0-5	0-5
FPR3	0-5	0-5	0-5	0-5	0-5	0-5	0-5
CXCR3	0-5	0-5	0-5	0-5	0-5	0-5	0-5
C5L2	0-5	0-5	0-5	0-5	0-5	0-5	0-5

This can be explained by assuming that we have been profiling a specific HEK293 subclone. Furthermore, the passage number or culture conditions may affect the mRNA expression levels of the chemotactic receptors. These results underline the importance to determine the expression levels (mRNA and protein) in cell lines used in your own research group, instead of using published data for a certain cell line. Studies with antibodies or radioligands have to be performed in order to determine the expression levels of the chemotactic receptors at protein level.

To our knowledge, we investigated for the first time the whole chemokine receptor superfamily mRNA expression levels in IBD mucosa tissue with RT-qPCR. In the present study, we show that CXCR4, CXCR6, CXCR7, CCR6, CCR7, CCR9, CCX-CKR, C5AR1, BLT₁, BLT₂ and S1P₂ mRNA levels are relatively high in bowel material from IBD patients (Table 7.2). Also in the non-inflamed tissue of colon cancer patients CXCR4, BLT₁ and S1P₂ mRNA levels are abundantly expressed. Noteworthy, colon cancer has been associated with an inflammatory state [38]. Jordan *et al* [39] investigated the mRNA expression levels of CCR1-10 and CXCR1-5 on the human colonic carcinoma epithelial cell line HT29 with RT-qPCR. Of these chemokine receptors, only CXCR4 mRNA was detected. Furthermore, also the BLT₁ receptor was shown to be expressed at protein level in the HT29 cell line [40]. In Caco2, another human epithelial colorectal cancer cell line, CXCR4 and BLT₁ receptors were as well detected at protein level [40, 41]. Thus, the elevated mRNA levels in non-inflamed colon cancer tissue are in agreement with mRNA/protein expression levels in the cell lines HT29 and Caco2. No publications are available yet about S1P₂ expression levels in these cell lines. Furthermore, to our best knowledge, normal colon cell lines (like the colon epithelial cell line CCD841 CoN or colon fibroblasts CCD-18Co, CCD-33Co and CCD-112CoN) have not been subjected to expression profiling of chemotactic receptors yet.

As shown in our RT-qPCR studies, no significant differences in mRNA expression levels of chemokine receptors between non-inflamed and inflamed IBD tissue (UC and/or CD) were apparent. Using RT-qPCR analysis for only CXCR1, CXCR2 and CCR6, Puleston *et al* [42] identified a significant increase of CXCR1 and CXCR2 mRNA levels in CD and UC colon biopsies compared to control. Furthermore, they found significantly elevated mRNA levels of CCR6 in UC colon biopsy material. Discrepancy between these studies might be explained due to different samples used and different kind of control samples. They used material from 21 patients and analyzed for each patient six colon biopsies, whereas we analyzed biopsies of non-inflamed and inflamed region of the tissue from 19 patients. Furthermore, Puleston *et al* [42] used control samples of people who underwent diagnostic colonoscopy, but were not diagnosed with IBD. We compared non-inflamed and inflamed bowel tissue of each IBD patient and control samples were non-inflamed bowel tissue of colon cancer patients. As such, actually all our control samples might also be in a certain inflammation state and therefore identifying significant differences in mRNA expression levels is challenging. Ideally, non-inflamed tissue of healthy persons should be used to compare with inflamed tissue of IBD patients. However, this is not available due to ethic reasons.

Although chemokine receptor expression levels are not extensively studied in IBD bowel tissue, several studies investigated the expression levels of (a subset) of chemokines in IBD biopsies [15-25, 42]. Since the chemokine/chemokine receptor axis is the most important regulator of leukocyte trafficking towards sites of inflammation [51], those studies provided important insights of a potential role of different chemokine receptors. So far, we only investigated the expression levels of CXCL8. Our results show a significant increase of CXCL8 mRNA levels in IBD mucosa material. Using microarray analysis and RT-qPCR, Puleston *et al* [42] investigated the entire chemokine superfamily mRNA expression levels

in colonic biopsies of either CD and UC patients or non-IBD control. They found that CXCL1, CXCL2, CXCL3, CXCL8 and CCL20 mRNAs are significantly higher expressed in active colonic CD and UC tissue. This increase was strongly correlated with chronic inflammation. Furthermore, also other studies show an increase of CXCR1 and CXCR2 interacting chemokines, like CXCL2, CXCL5 and CXCL8 in IBD mucosa tissue [15-20] and the increase of the CCR6 chemokine CCL20 [22, 23]. In addition, also increased levels of CCL2, CCL3, CCL4, CCL7 and CCL8 were detected in different colonic biopsies of IBD patients [16, 21, 24, 25]. Thus, all above mentioned chemokines might increase the influx of leukocytes expressing CXCR1, CXCR2, CCR1, CCR2, CCR3, CCR5 and/or CCR6 causing an increase of the disease symptoms. Consequently, those chemokine receptors have therapeutic potential. Our data showed indeed a trend towards a slight increase in expression of CXCR1 and CXCR2 mRNA in agreement with Puleston *et al* [42], but no difference in the CCR receptors was apparent. It would be interesting to include immunohistochemistry studies to determine which leukocytes are mostly present in inflamed IBD tissue. The expression of different chemokine receptors on these cells might be potential drug targets by inhibiting the influx of specific leukocytes.

As mentioned above, we measured significant increases in mRNA levels of CXCL8 in IBD inflamed tissue material. Since other studies showed that the expression of CXCL8 is increased in neutrophils, macrophages and intestinal epithelial cells located in inflamed IBD mucosa [21, 52], we investigated the CXCL8 mRNA levels in freshly isolated neutrophils. Surprisingly, the CXCL8 mRNA levels were significantly decreased in neutrophils from IBD patients compared to control. Thus, the increased CXCL8 mRNA levels in IBD mucosa might not be caused by neutrophils. However, we should be careful with this statement, since we measured the CXCL8 mRNA levels of neutrophils from circulation and not from neutrophils migrated into the inflamed tissue. Therefore, to make a stronger statement, immunohistochemistry studies have to be included to determine the expression of CXCL8 in the different cell types in inflamed tissue compared to non-inflamed tissue.

Like chemokines, also leukotriene B₄ can stimulate the infiltration of neutrophils into inflamed IBD tissue by interacting with its receptors BLT₁ and BLT₂ expressed on these leukocytes. Elevated levels of leukotriene B₄, synthesized by epithelial cells, are detected in colonic mucosa of both UC and CD patients [53-55]. In our study, we found high mRNA expression levels of both LTB₄ receptors. However, no differences were apparent between either inflamed, non-inflamed or tissue obtained from colon cancer.

Although several studies showed complement activation in human IBD patients [56-58], the anaphylatoxin C5a was not especially mentioned. So far, only animal studies show a positive correlation between C5a and its receptor C5AR1 in inflammatory bowel disease associated mucosal damage [59, 60]. Also, mice suffering from chronic colitis showed only enhanced mRNA expression of C5L2 in the presence of C5AR1 [59]. We showed in all human tissue samples C5AR1 mRNA expression levels, however C5L2 was not detected. Thus, so far, the

C5AR1 seems to be more interesting to investigate than the C5L2 receptor in the case of IBD.

Elevated histamine levels are observed in the mucosa of both CD and UC patients [61, 62]. Histamine can interact with four different receptors (histamine H_1R , H_2R , H_3R and H_4R). Of these receptors, the histamine H_4R is the most recently cloned receptor [63, 64]. Since this receptor is present on different leukocytes [65-67], the histamine/ H_4R axis might also play a role in the pathogenesis of IBD. Interestingly, rats suffering from colitis treated with an H_4R antagonist showed a decrease in disease symptoms [68]. In our RT-qPCR studies, we detected mRNA expression levels of the histamine H_4R in three patients. Increasing the number of patients should give us a better insight in the role of the histamine H_4R in IBD. Furthermore, determining the protein expression levels of the histamine H_4R in IBD patient material is also essential to establish the receptor as a potential therapeutic target in IBD.

The chemoattractant peptide formyl-methionyl-leucyl-phenylalanine (fMLP) is produced by intestinal bacteria, thereby causing the recruitment of neutrophils expressing FPR1 and FPR2 [69]. Subsequently, clinical symptoms of IBD can occur. Neutrophils from CD patients show a markedly increased expression of FPR1 and FPR2, whereas neutrophils from UC patients show no increased expression of these receptors [69]. So far, we were not able to validate primers for FPR1 and FPR2. Therefore, we only investigated the mRNA expression levels of FPR3. This receptor is not expressed on neutrophils, however it is expressed on dendritic cells, eosinophils and colonic macrophages [70]. Both F2L and N-formyl humanin are known to interact with this receptor, whereas fMLP shows no interaction [71, 72]. In our study, FPR3 mRNA expression levels were very low in IBD tissue. Furthermore, no publications are known that show a role for F2L and N-formyl humanin in inflammatory bowel disease. Thus FPR3 seems so far not a promising therapeutic target in IBD.

Sphingolipids, like sphingosine-1-phosphate (S1P) are present throughout the whole intestinal tract [73]. S1P is secreted by activated mast cells [74] and interacts with the receptors $S1P_1$, $S1P_2$, $S1P_3$, $S1P_4$ and $S1P_5$ [75]. Both $S1P_1$ and $S1P_2$ are expressed on mast cells [76]. S1P is chemoattractive for neutrophils and macrophages [73]. Furthermore, by activating $S1P_2$, degranulation and cytokine/chemokine release of human mast cells occurs [74, 76]. Administration of S1P agonists, like FTY720 and KRP-203, in mice suffering from colitis caused less clinical symptoms due to sequestration of lymphocytes to the lymph nodes [77-79]. Furthermore, mice lacking the sphingosine kinase SK1, that produces S1P, show less intestinal damage in colitis animal models [80]. Thus, a correlation between sphingolipids and inflammatory bowel disease is shown. In our study, we found a significant higher mRNA level of $S1P_2$ in inflamed tissue of CD patients, whereas no difference of expression level was apparent for $S1P_3$. It would be interesting to investigate whether the increase $S1P_2$ mRNA expression level is due to the influx of mast cells expressing this receptor.

Conclusion

In our opinion, RT-qPCR is an elegant method to use as a first step to identify differences of mRNA expression levels of chemotactic receptors, that may serve as potential drug target in diseases. The next step involves the validation of these targets at protein levels by means of antibody detection or radioligand displacement studies. In addition, immunohistochemistry data will provide us more information which cell types are present in the bowel tissue. This will provide insight on the presence of chemotactic receptors expressed on these cells. Based on our data and published data, CXCR1, CXCR2, CCR6, CCR9, FPR1, FPR2 and S1P₂ might be of interest as potential drug targets in IBD. In addition, CCR1, CCR2, CCR3, CCR5, BLT₁, BLT₂ and C5AR1 might also interesting as ligands of these receptors are shown to be upregulated [16, 21, 24, 25, 53-55, 61, 62] or a correlation between receptor and IBD has been shown in animal models [59, 60, 68].

References

1. Kraneveld, A.D., et al., Chemokine receptors in inflammatory diseases, in *Chemokine Receptors as Drug Targets* M.J. Smit, Lira, S.A., Leurs, R, Editor. 2011, Wiley-VCH verlag GmbH&Co. KGaA, Weinheim. p. 105-150.
2. Barnes, P.J., Mediators of chronic obstructive pulmonary disease. *Pharmacol Rev*, 2004. 56(4): p. 515-48.
3. Costa, C., et al., CXCR3 and CCR5 chemokines in induced sputum from patients with COPD. *Chest*, 2008. 133(1): p. 26-33.
4. Fujimoto, K., et al., Airway inflammation during stable and acutely exacerbated chronic obstructive pulmonary disease. *Eur Respir J*, 2005. 25(4): p. 640-6.
5. Qiu, Y., et al., Biopsy neutrophilia, neutrophil chemokine and receptor gene expression in severe exacerbations of chronic obstructive pulmonary disease. *Am J Respir Crit Care Med*, 2003. 168(8): p. 968-75.
6. Saetta, M., et al., Increased expression of the chemokine receptor CXCR3 and its ligand CXCL10 in peripheral airways of smokers with chronic obstructive pulmonary disease. *Am J Respir Crit Care Med*, 2002. 165(10): p. 1404-9.
7. Traves, S.L., et al., Increased levels of the chemokines GROalpha and MCP-1 in sputum samples from patients with COPD. *Thorax*, 2002. 57(7): p. 590-5.
8. Haringman, J.J., et al., Chemokine and chemokine receptor expression in paired peripheral blood mononuclear cells and synovial tissue of patients with rheumatoid arthritis, osteoarthritis, and reactive arthritis. *Ann Rheum Dis*, 2006. 65(3): p. 294-300.
9. Mach, F., et al., Differential expression of three T lymphocyte-activating CXC chemokines by human atheroma-associated cells. *J Clin Invest*, 1999. 104(8): p. 1041-50.
10. von Hundelshausen, P., et al., RANTES deposition by platelets triggers monocyte arrest on inflamed and atherosclerotic endothelium. *Circulation*, 2001. 103(13): p. 1772-7.
11. Greaves, D.R., et al., Linked chromosome 16q13 chemokines, macrophage-derived chemokine, fractalkine, and thymus- and activation-regulated chemokine, are expressed in human atherosclerotic lesions. *Arterioscler Thromb Vasc Biol*, 2001. 21(6): p. 923-9.
12. Wong, B.W., D. Wong, and B.M. McManus, Characterization of fractalkine (CX3CL1) and CX3CR1 in human coronary arteries with native atherosclerosis, diabetes mellitus, and transplant vascular disease. *Cardiovasc Pathol*, 2002. 11(6): p. 332-8.
13. Sorensen, T.L., et al., Expression of specific chemokines and chemokine receptors in the central nervous system of multiple sclerosis patients. *J Clin Invest*, 1999. 103(6): p. 807-15.
14. Homey, B., et al., Up-regulation of macrophage inflammatory protein-3 alpha/CCL20 and CC chemokine receptor 6 in psoriasis. *J Immunol*, 2000. 164(12): p. 6621-32.
15. Autschbach, F., et al., Cytokine/chemokine messenger-RNA expression profiles in ulcerative colitis and Crohn's disease. *Virchows Arch*, 2002. 441(5): p. 500-13.
16. Banks, C., et al., Chemokine expression in IBD. Mucosal chemokine expression is unselectively increased in both ulcerative colitis and Crohn's disease. *J Pathol*, 2003. 199(1): p. 28-35.
17. Izzo, R.S., et al., Interleukin-8 and neutrophil markers in colonic mucosa from patients with ulcerative colitis. *Am J Gastroenterol*, 1992. 87(10): p. 1447-52.
18. Yamamoto, T., et al., Systemic and local cytokine production in quiescent ulcerative colitis and its relationship to future relapse: a prospective pilot study. *Inflamm Bowel Dis*, 2005. 11(6): p. 589-96.
19. Zahn, A., et al., Transcript levels of different cytokines and chemokines correlate with clinical and endoscopic activity in ulcerative colitis. *BMC Gastroenterol*, 2009. 9: p. 13.

20. Z'Graggen, K., et al., The C-X-C chemokine ENA-78 is preferentially expressed in intestinal epithelium in inflammatory bowel disease. *Gastroenterology*, 1997. 113(3): p. 808-16.
21. Grimm, M.C., et al., Enhanced expression and production of monocyte chemoattractant protein-1 in inflammatory bowel disease mucosa. *J Leukoc Biol*, 1996. 59(6): p. 804-12.
22. Kaser, A., et al., Increased expression of CCL20 in human inflammatory bowel disease. *J Clin Immunol*, 2004. 24(1): p. 74-85.
23. Kwon, J.H., et al., Colonic epithelial cells are a major site of macrophage inflammatory protein 3 α (MIP-3 α) production in normal colon and inflammatory bowel disease. *Gut*, 2002. 51(6): p. 818-26.
24. Mazzucchelli, L., et al., Differential in situ expression of the genes encoding the chemokines MCP-1 and RANTES in human inflammatory bowel disease. *J Pathol*, 1996. 178(2): p. 201-6.
25. Wedemeyer, J., et al., Enhanced production of monocyte chemotactic protein 3 in inflammatory bowel disease mucosa. *Gut*, 1999. 44(5): p. 629-35.
26. Higuchi, R., et al., Simultaneous amplification and detection of specific DNA sequences. *Biotechnology (N Y)*, 1992. 10(4): p. 413-7.
27. Bustin, S.A., Absolute quantification of mRNA using real-time reverse transcription polymerase chain reaction assays. *J Mol Endocrinol*, 2000. 25(2): p. 169-93.
28. Kubista, M., et al., The real-time polymerase chain reaction. *Mol Aspects Med*, 2006. 27(2-3): p. 95-125.
29. Wittwer, C.T., et al., Continuous fluorescence monitoring of rapid cycle DNA amplification. *Biotechniques*, 1997. 22(1): p. 130-1, 134-8.
30. Ririe, K.M., R.P. Rasmussen, and C.T. Wittwer, Product differentiation by analysis of DNA melting curves during the polymerase chain reaction. *Anal Biochem*, 1997. 245(2): p. 154-60.
31. Wong, M.L. and J.F. Medrano, Real-time PCR for mRNA quantitation. *Biotechniques*, 2005. 39(1): p. 75-85.
32. VanGuilder, H.D., K.E. Vrana, and W.M. Freeman, Twenty-five years of quantitative PCR for gene expression analysis. *Biotechniques*, 2008. 44(5): p. 619-26.
33. Gao, Q., et al., Expression of matrix metalloproteinases-2 and -9 in intestinal tissue of patients with inflammatory bowel diseases. *Dig Liver Dis*, 2005. 37(8): p. 584-92.
34. Chomczynski, P. and N. Sacchi, Single-Step Method of Rna Isolation by Acid Guanidinium Thiocyanate Phenol Chloroform Extraction. *Analytical Biochemistry*, 1987. 162(1): p. 156-159.
35. D'Haene, B., J. Vandesompele, and J. Hellemans, Accurate and objective copy number profiling using real-time quantitative PCR. *Methods*, 2010. 50(4): p. 262-70.
36. Viola, A. and A.D. Luster, Chemokines and Their Receptors: Drug Targets in Immunity and Inflammation. *Annu Rev Pharmacol Toxicol*, 2008. 48: p. 171-197.
37. Atwood, B.K., et al., Expression of G protein-coupled receptors and related proteins in HEK293, AtT20, BV2, and N18 cell lines as revealed by microarray analysis. *BMC Genomics*, 2011. 12: p. 14.
38. Klampfer, L., Cytokines, inflammation and colon cancer. *Curr Cancer Drug Targets*. 11(4): p. 451-64.
39. Jordan, N.J., et al., Expression of functional CXCR4 chemokine receptors on human colonic epithelial cells. *J Clin Invest*, 1999. 104(8): p. 1061-9.
40. Ihara, A., et al., Blockade of leukotriene B4 signaling pathway induces apoptosis and suppresses cell proliferation in colon cancer. *J Pharmacol Sci*, 2007. 103(1): p. 24-32.
41. Ottaiano, A., et al., Inhibitory effects of anti-CXCR4 antibodies on human colon cancer cells. *Cancer Immunol Immunother*, 2005. 54(8): p. 781-91.
42. Puleston, J., et al., A distinct subset of chemokines dominates the mucosal chemokine response in inflammatory bowel disease. *Aliment Pharmacol Ther*, 2005. 21(2): p. 109-20.
43. Comerford, I., et al., Regulation of chemotactic networks by 'atypical' receptors. *Bioessays*, 2007. 29(3): p. 237-47.
44. Comerford, I., et al., The atypical chemokine receptor CCX-CKR scavenges homeostatic chemokines in circulation and tissues and suppresses Th17 responses. *Blood*, 2010. 116(20): p. 4130-40.
45. Kaser, A. and H. Tilg, Novel therapeutic targets in the treatment of IBD. *Expert Opin Ther Targets*, 2008. 12(5): p. 553-63.
46. Koenecke, C. and R. Forster, CCR9 and inflammatory bowel disease. *Expert Opin Ther Targets*, 2009. 13(3): p. 297-306.
47. Papadakis, K.A., et al., CCR9-positive lymphocytes and thymus-expressed chemokine distinguish small bowel from colonic Crohn's disease. *Gastroenterology*, 2001. 121(2): p. 246-54.
48. Svensson, M., et al., CCL25 mediates the localization of recently activated CD8 α lymphocytes to the small-intestinal mucosa. *J Clin Invest*, 2002. 110(8): p. 1113-21.
49. Wurbel, M.A., et al., Impaired accumulation of antigen-specific CD8 lymphocytes in chemokine CCL25-deficient intestinal epithelium and lamina propria. *J Immunol*, 2007. 178(12): p. 7598-606.
50. Eksteen, B. and D.H. Adams, GSK-1605786, a selective small-molecule antagonist of the CCR9 chemokine receptor for the treatment of Crohn's disease. *IDrugs*, 2010. 13(7): p. 472-781.
51. Moser, B., et al., Chemokines: multiple levels of leukocyte migration control. *Trends Immunol*, 2004. 25(2): p. 75-84.
52. Mazzucchelli, L., et al., Expression of interleukin-8 gene in inflammatory bowel disease is related to the histological grade of active inflammation. *Am J Pathol*, 1994. 144(5): p. 997-1007.
53. Cole, A.T., et al., Mucosal factors inducing neutrophil movement in ulcerative colitis: the role of interleukin 8 and leukotriene B4. *Gut*, 1996. 39(2): p. 248-54.
54. Peskar, B.M., et al., Enhanced formation of sulfidopeptide-leukotrienes in ulcerative colitis and Crohn's disease: inhibition by sulfasalazine and 5-aminosalicylic acid. *Agents Actions*, 1986. 18(3-4): p. 381-3.
55. Sharon, P. and W.F. Stenson, Enhanced synthesis of leukotriene B4 by colonic mucosa in inflammatory bowel disease. *Gastroenterology*, 1984. 86(3): p. 453-60.

56. Halstensen, T.S. and P. Brandtzaeg, Local complement activation in inflammatory bowel disease. *Immunol Res*, 1991. 10(3-4): p. 485-92.
57. Halstensen, T.S., et al., Surface epithelium related activation of complement differs in Crohn's disease and ulcerative colitis. *Gut*, 1992. 33(7): p. 902-8.
58. Ueki, T., et al., Distribution of activated complement, C3b, and its degraded fragments, iC3b/C3dg, in the colonic mucosa of ulcerative colitis (UC). *Clin Exp Immunol*, 1996. 104(2): p. 286-92.
59. Johsrich, K., et al., Role of the C5a receptor (C5aR) in acute and chronic dextran sulfate-induced models of inflammatory bowel disease. *Inflamm Bowel Dis*, 2009. 15(12): p. 1812-23.
60. Xu, D.Z., et al., Elimination of C5aR prevents intestinal mucosal damage and attenuates neutrophil infiltration in local and remote organs. *Shock*, 2009. 31(5): p. 493-9.
61. Knutson, L., et al., The jejunal secretion of histamine is increased in active Crohn's disease. *Gastroenterology*, 1990. 98(4): p. 849-54.
62. Raithel, M., et al., Mucosal histamine content and histamine secretion in Crohn's disease, ulcerative colitis and allergic enteropathy. *Int Arch Allergy Immunol*, 1995. 108(2): p. 127-33.
63. Nakamura, T., et al., Molecular cloning and characterization of a new human histamine receptor, HH4R. *Biochem Biophys Res Commun*, 2000. 279(2): p. 615-20.
64. Oda, T., et al., Molecular cloning and characterization of a novel type of histamine receptor preferentially expressed in leukocytes. *J Biol Chem*, 2000. 275(47): p. 36781-6.
65. Damaj, B.B., et al., Functional expression of H4 histamine receptor in human natural killer cells, monocytes, and dendritic cells. *J Immunol*, 2007. 179(11): p. 7907-15.
66. Gutzmer, R., et al., The histamine H4 receptor is functionally expressed on T(H)2 cells. *J Allergy Clin Immunol*, 2009. 123(3): p. 619-25.
67. Hofstra, C.L., et al., Histamine H4 receptor mediates chemotaxis and calcium mobilization of mast cells. *J Pharmacol Exp Ther*, 2003. 305(3): p. 1212-21.
68. Varga, C., et al., Inhibitory effects of histamine H4 receptor antagonists on experimental colitis in the rat. *Eur J Pharmacol*, 2005. 522(1-3): p. 130-8.
69. Anton, P.A., S.R. Targan, and F. Shanahan, Increased neutrophil receptors for and response to the proinflammatory bacterial peptide formyl-methionyl-leucyl-phenylalanine in Crohn's disease. *Gastroenterology*, 1989. 97(1): p. 20-8.
70. Devosse, T., et al., Formyl peptide receptor-like 2 is expressed and functional in plasmacytoid dendritic cells, tissue-specific macrophage subpopulations, and eosinophils. *J Immunol*, 2009. 182(8): p. 4974-84.
71. Harada, M., et al., N-Formylated humanin activates both formyl peptide receptor-like 1 and 2. *Biochem Biophys Res Commun*, 2004. 324(1): p. 255-61.
72. Migeotte, I., et al., Identification and characterization of an endogenous chemotactic ligand specific for FPRL2. *J Exp Med*, 2005. 201(1): p. 83-93.
73. Duan, R.D. and A. Nilsson, Metabolism of sphingolipids in the gut and its relation to inflammation and cancer development. *Prog Lipid Res*, 2009. 48(1): p. 62-72.
74. Oskeritzian, C.A., et al., Essential roles of sphingosine-1-phosphate receptor 2 in human mast cell activation, anaphylaxis, and pulmonary edema. *J Exp Med*, 2010. 207(3): p. 465-74.
75. El Alwani, M., et al., Bioactive sphingolipids in the modulation of the inflammatory response. *Pharmacol Ther*, 2006. 112(1): p. 171-83.
76. Jolly, P.S., et al., Transactivation of sphingosine-1-phosphate receptors by FcepsilonRI triggering is required for normal mast cell degranulation and chemotaxis. *J Exp Med*, 2004. 199(7): p. 959-70.
77. Daniel, C., et al., FTY720 ameliorates Th1-mediated colitis in mice by directly affecting the functional activity of CD4+CD25+ regulatory T cells. *J Immunol*, 2007. 178(4): p. 2458-68.
78. Nixon, G.F., Sphingolipids in inflammation: pathological implications and potential therapeutic targets. *Br J Pharmacol*, 2009. 158(4): p. 982-93.
79. Song, J., et al., A novel sphingosine 1-phosphate receptor agonist, 2-amino-2-propanediol hydrochloride (KRP-203), regulates chronic colitis in interleukin-10 gene-deficient mice. *J Pharmacol Exp Ther*, 2008. 324(1): p. 276-83.
80. Snider, A.J., et al., A role for sphingosine kinase 1 in dextran sulfate sodium-induced colitis. *FASEB J*, 2009. 23(1): p. 143-52.

Discussion and Future Perspectives

Chapter 8

Acknowledgements

We acknowledge Herman Lim for constructing the CXCR2-CXCR3 chimeric proteins, Luc Roumen en Chris de Graaf for building the *in silico* CXCR2 models, Pim Koelink and the department of Gastroenterology and Hepatology of the Leiden University Medicinal Center for providing bowel tissue samples, Paul Chazot for being so kind to have me as a guest researcher in his lab, and the students Priscilla van Beek, Erik Bom, Esther Holdinga and Ilse Oosterom for their help with performing several experiments for this chapter.

This thesis describes the interaction of small molecular weight antagonists and (viral) chemokines with the chemokine receptor CXCR2. Furthermore, we used RT-qPCR as a fast first step to identify chemotactic receptors that might play a crucial role in inflammatory bowel disease.

Binding pocket of small molecular weight antagonists

In **Chapter 3** [1] we extensively investigated the mechanism of action of antagonists belonging to the diarylurea, thiazolopyrimidine and imidazolylpyrimidine chemical classes. All antagonists antagonize CXCL8 most probably via a non-competitive, allosteric mechanism. Interestingly, using the diarylurea [³H]-SB265610 compound, we discovered that CXCR2 antagonists of different chemical classes bind to distinct binding sites at the CXCR2 receptor. Recently, two research groups provided evidence that compounds belonging to the diarylurea and thiazolopyrimidine class most likely bind to the intracellular region of CXCR2 [2, 3]. This is an interesting finding, since small molecular weight antagonists are mostly considered to bind to the 7 trans-membrane (TM) domain of chemokine receptors [4], including repertaxin to CXCR1 [5, 6], AMD3100 to CXCR4 [7, 8], BX-471 to CCR1 [9], TAK-779 to CCR2 / CCR5 [10-14] and Maraviroc to CCR5 [14].

The first evidence of an intracellular binding site at a chemokine receptor was given by Andrews *et al* [15]. By reciprocal swapping the C-terminal domains between CCR4 and CCR5, they identified that compounds belonging to the pyrazinyl-sulfonamides interact with the C-terminal domain of CCR4. Furthermore, using a [³H]-pyrazinyl-sulfonamide compound, they demonstrated that CCR4-interacting chemokines are not able to displace the radioligand. Also a structural unrelated BMS-397 compound was not able to displace this radioligand, indicating that (like for CXCR2 (**Chapter 3**) distinct binding sites for small molecular weight antagonists exist at CCR4. To localize binding sites for CXCR2, Nicholls *et al* [2] have performed domain swapping studies with CXCR1 and CXCR2. Whereas chimeric proteins with the reciprocal second extracellular loop and sections of the TM regions show no difference in antagonism profile of CXCR2 antagonists belonging to the diarylurea and thiazolopyrimidine class, chimeric proteins with the reciprocal C-tail do. Next, they identified lysine 320^{7,59} (located in the intracellular helix 8) as an important residue that interacts with both the diarylurea and thiazolopyrimidine compound. Mutagenesis studies of intracellular residues of CXCR2 by Salchow *et al* [3] indicate that besides lysine 320^{7,59}, also aspartate 84^{2,40} located in intracellular loop 1 and tyrosine 314^{7,53} located in the C-terminal domain (in NPxxY motif) are involved in the binding of the CXCR2 antagonists SB265610, Pteridone-1 and Sch527123 (see snakeplot in Fig. 8.1). We constructed chimeric proteins by swapping the intracellular loops and the C-terminal domain of CXCR3 with CXCR2 (sequence intracellular loops given in Fig. 8.2). All chimeric proteins have around 1 log unit lower affinity for [¹²⁵I]-CXCL8 than WT CXCR2 (Fig. 8.3, Table 8.1). In agreement with the above mentioned studies, we also obtained evidence that intracellular parts of CXCR2 are involved in the binding of SB265610. As shown in Figure 8.3, SB265610 has a lower affinity for CXCR2 at the chimeric proteins CXCR2-IL1, CXCR2-IL3 and CXCR2-CT. The dramatic drop in affinity (Table 8.1) for the CXCR2-IL1 protein is in agreement with Salchow *et al*

[3], who demonstrated complete loss of [³H]-SB265610 binding at D84^{2.40}N and markedly reduced binding at T83^{2.39}A. Whereas Salchow *et al* [3] show a markedly reduced affinity for D143^{3.49}R, we do not observe a drop in affinity for SB265610 at CXCR2-IL2. This can be explained by the presence of the well conserved DRY motif in both intracellular loops (see Fig. 8.2). We observe a reduced affinity for SB265610 for CXCR2-IL3, while the A249^{6.33}L mutation located in intracellular loop 3 showed no effect on the binding affinity for [³H]-SB265610 [3]. These data indicate that probably other residues in intracellular loop 3 of CXCR2 interact with SB265610. Finally, the drop in affinity of SB265610 at the CXCR2-CT protein is in agreement with Salchow *et al* [3], who show lower affinity for [³H]-SB265610 at the mutant Y314^{7.53}A and K320^{7.59}A.

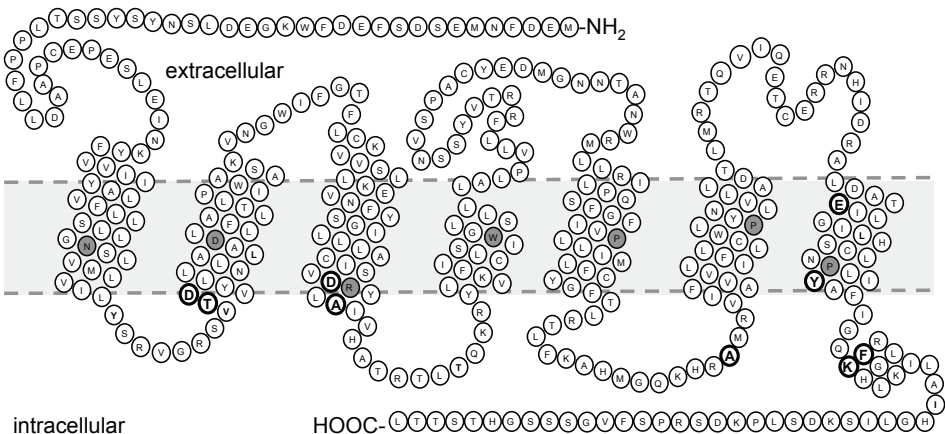


Figure 8.1: Snakeplot of the human CXCR2 receptor. The residues indicated with a solid circle and a larger font have been mutated by Salchow *et al* [3]. Residues indicated in grey are the conserved residues of the Ballousteros-Weinstein numbering scheme.

Tabel 8.1: Displacement of [¹²⁵I]-CXCL8 binding to COS-7 cells membranes expressing indicated CXCR2 constructs. The data are presented as mean ± S.E.M. of at least two independent experiments (n indicated in table).

	CXCL8		SB265610	
construct	pK _d ± S.E.M	n	pK _i ± S.E.M	n
CXCR2-WT	8.99 ± 0.36	5	7.30 ± 0.15	6
CXCR2-IL1	7.86 ± 0.19		4.36 ± 0.26	2
CXCR2-IL2	8.00 ± 0.12	2	6.91 ± 0.07	2
CXCR2-IL3	7.76 ± 0.04	2	5.63 ± 0.28	2
CXCR2-Ct	8.19 ± 0.04	2	5.81 ± 0.02	3

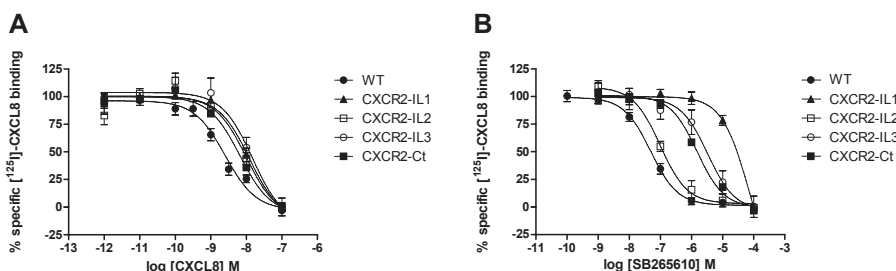


Figure 8.3: Displacement of $[^{125}\text{I}]$ -CXCL8 binding to COS-7 cell membranes expressing human CXCR2 WT or indicated CXCR2-CXCR3 chimeric proteins for at least two independent experiments performed in triplicate. Membranes were incubated with indicated concentration of CXCL8 (A) or SB265610 (B) and approximately 100 pM $[^{125}\text{I}]$ -CXCL8. Assay details are described in Material and Methods of Chapter 3 and 4.

Interestingly, Maeda *et al* [16] recently published that also nicotinamide glycolates interact with CXCR2 through an intracellular mechanism. Comparing $[^{125}\text{I}]$ -CXCL8 displacement studies in whole cells versus membrane studies, they describe that the acid form is able to displace $[^{125}\text{I}]$ -CXCL8 in membrane binding, but not at whole cells. Yet, the ester form displaces $[^{125}\text{I}]$ -CXCL8 at whole cells, but not in membrane binding. They describe a mechanism in which the uncharged (inactive) ester form accesses the intracellular space by passive diffusion through the cell membrane. Next, the ester is hydrolyzed to the acid form and will subsequently interact with CXCR2 at an intracellular site. The precise binding pocket of the acid form of nicotinamide glycolates remains to be investigated. Since the molecule contains two ring structures, like SB265610, it might bind in the same binding pocket as SB265610, although the essential linker (NH-CO-NH) is not present. Noteworthy, also Andrews *et al* [15] show that the ester form of pyrazinyl-sulfonamides cross the cell-membrane and is intracellularly converted to the active acid, which subsequently interacts with the C-terminal domain of CCR4. Whereas the above mentioned antagonists require intracellular conversion [15, 16], CXCR2 antagonists belonging to the diaryurea and thiazolopyrimidine class do not. Important for those compounds is the lipophilicity. Compounds with lower lipophilicity, and therefore poorer penetration of the biological membrane, have shown reduced antagonistic properties [2].

In silico model of CXCR2

In 2000 the first crystal structure of a GPCR, bovine rhodopsin, was solved [17]. The bovine rhodopsin structures served a long time as the only templates for *in silico* modeling of GPCRs, as it appeared to be challenging to crystallize other GPCRs, mainly due to stability issues. Using either a T4-lysosome fusion strategy or the use of a modified antibody (Fab), there was a break-through in 2007: two crystal structures of the β_2 -adrenergic receptor were solved [18-20]. Also other crystal structure of in-active forms of GPCRs followed, including recently the chemokine receptor CXCR4 [21] (see for more details **Chapter 1**). Active conformations of GPCRs are less stable and therefore more difficult to obtain in crystal form. However, a series of break-throughs came this year. Rasmussen *et al* [22] crystallized the β_2 -adrenergic receptor in an active conformation using besides the T4 lysozyme fusion

also a nanobody that acts as a surrogate Gs protein. Xu *et al* [23] crystallized the adenosine A_{2A} receptor in its active conformation with the agonist UK432097 in the binding site. All the above mentioned crystal structures provide insight to created better *in silico* models of GPCRs of interest, such as CXCR2.

To model the interaction of SB265610 and VUF10948 (compound originally created by AstraZeneca) with the intracellular site of CXCR2, we constructed a CXCR2 model based on the CXCR4 crystal structure [21] and the β_2 -adrenergic receptor [18-20]. This merged template was deemed necessary to overcome a disarrangement of the intracellular part of transmembrane helix 7 and the intracellular helix 8 in the CXCR4 crystal structure. As shown in Figure 8.4, the model of CXCR2 portrays SB265610 to possess a hydrogen bonding interaction with the residues threonine 83^{2,39}, aspartic acid 84^{2,40}, lysine 320^{7,39} and glutamine 319^{7,58}, as well as a ring-ring interaction with tyrosine 314^{7,53}. VUF10948 demonstrates to interact in the same fashion with these residues except that it lacks the interaction with glutamine 319^{7,58}. Subsequently, this model can be used to screen for novel hits at this receptor. To our knowledge, so far only two publications exist which model the intracellular site of GPCRs. Espinoza-Fonseca and Trujillo-Ferrara [24] demonstrated in a homology model of the M₁ muscarinic receptor an allosteric intracellular binding place for KT5720 close to intracellular loop 3. Furthermore, Taylor et al [25] described a combined study design, of *in silico* modeling and experimental data, to discover inhibitors that target the interface of activated bovine rhodopsin (intracellular loops) and its G protein.

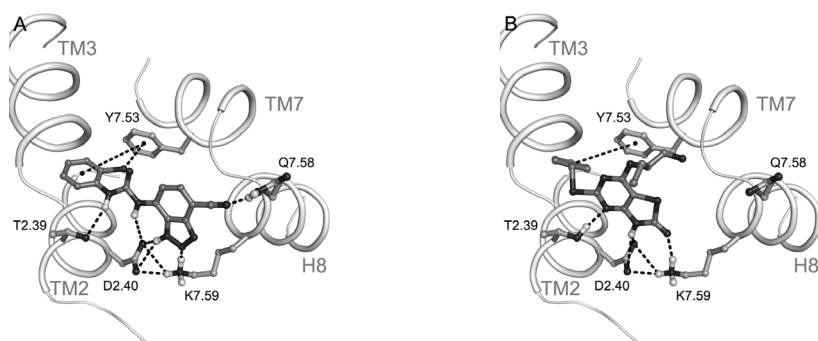


Figure 8.4: Positioning of SB265610 (A) and VUF10948 (B) in the intracellular binding pocket of human CXCR2. Interactions are annotated with dotted lines.

In **Chapter 4**, we describe a novel allosteric binding mode of an imidazolylpyrimidine CXCR2 antagonist at the chemokine receptor CXCR2. To unravel the binding mode, we used a combined approach of site-directed and *in silico* modeling. We demonstrate that the imidazolylpyrimidine compound binds to the trans-membrane (TM) domain of the receptor. In more detail, the compound shows interactions with residues located in the major subpocket (between TM3, 4, 5, 6 and 7). Interestingly, we suggest that the imidazolylpy-

rimidine antagonist enters CXCR2 via the TM5-TM6 interface, as described previously for the opsin receptor [26].

To summarize, at the moment three different binding pockets of CXCR2 small-molecular weight antagonists have been published (see Fig. 8.5). First, repertaxin is reported to bind to the minor subpocket (between TM 1, 2, 3 and 7) of the CXCR1 receptor [5, 6, 27]. Since CXCR1 and CXCR2 show a high homology to each other (77%), it is suggested that repertaxin will also bind to the minor subpocket in the trans-membrane (TM) domain of CXCR2. Noteworthy, repertaxin is 100-fold more potent to inhibit CXCL8 induced chemotaxis at CXCR1 than CXCR2 [5]. Second, imidazolyipyrimidine CXCR2 antagonists have a binding pocket located in the major subpocket of the TM domain. Third, compounds belonging to the diarylurea and thiazolopyrimidine class bind to the intracellular region of CXCR2 [2, 3]. Interestingly, both repertaxin (TM domain) and Sch527123 (intracellular) are currently in Phase II clinical trial (ThomsonPharma database; www.thomson-pharma.com). In conclusion, all these allosteric binding pockets give new opportunities to discover new CXCR2 antagonists.

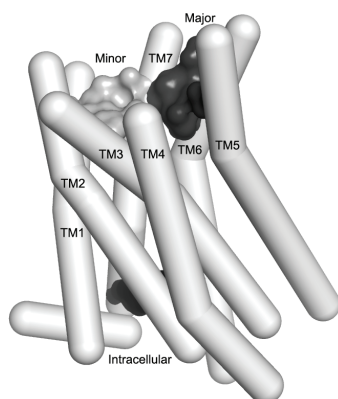


Figure 8.5: Three different binding pockets for small molecular weight antagonists at CXCR2; the minor subpocket (TM 1, 2, 3 and 7), the major subpocket (TM 3, 4, 5, 6 and 7) and the intracellular located subpocket.

Interaction of N-acetyl-PGP with CXCR1 and CXCR2?

Neutrophil recruitment to sites of inflammation can potentiate tissue damage due to release of proteases, subsequently leading to clinical symptoms of inflammatory diseases. Weathington *et al* [28] reported that also the collagen breakdown product N-acetyl-PGP is able to attract neutrophils, thereby contributing to the continuous influx of neutrophils. A role for CXCR1 and CXCR2 is implicated, since CXCR1 and/or CXCR2 antibodies inhibit the N-acetyl-PGP induced chemotaxis of neutrophils. In addition, also an imidazolyipyrimidine CXCR2 antagonist is able to inhibit the N-acetyl-PGP induced chemotaxis [29]. Yet, in **chapter 5** [30], we provide evidence that N-acetyl-PGP does not directly interact with either CXCR1 or CXCR2. N-acetyl-PGP does not displace [125 I]-CXCL8 or [3 H]-SB265610 and is not

able to activate G-protein dependent and G-protein independent signaling in transfected HEK293T cells and L1.2 cells, while CXCL8 does. Recently, Jackson *et al* [31] describe the four cis/trans isomers of N-acetyl-PGP. The LL-isomer shows the highest chemotactic activity for HL60 cells, followed by the DL- and LD- isomers. Interestingly, the DD-isomer is not chemotactic, suggesting that this isomer can be used as an antagonist for CXCL8-induced chemotaxis. Furthermore, Jackson *et al* [31] demonstrated that displacement of [¹²⁵I]-CXCL8 from neutrophils by DD-N-acetyl-PGP can only be detected when cells were pre-incubated with DD-N-acetyl-PGP. They conclude that N-acetyl-PGP directly interacts with CXCR2 and discrepancies between their recent study and ours [30] is caused by the fact that we did not pre-incubate HEK293T cells or neutrophils with N-acetyl-PGP for 30 min. However, experiments performed with 30 min pre-incubation in our lab, also do not show [¹²⁵I]-CXCL8 displacement by N-acetyl-PGP in transfected HEK293T cells or human neutrophils. Intriguingly, Kim *et al* [32] published that FITC labeled N-acetyl-PGP binds to mouse CXCR2 expressed in RBL-2H3 cells. It will be interesting to test this labeled N-acetyl-PGP as well in our assays in cells expressing human CXCR2.

Viral CXCLs interact with CXCR2

Recently, Lutichau *et al* [33] demonstrated that vCXCL1, encoded by the human cytomegalovirus (HCMV), is a potent agonist for CXCR2. Furthermore, vCXCL1 also interacts with CXCR1 but with a lower potency. vCXCL1 has shown to induce neutrophil chemotaxis and calcium mobilization [33, 34]. Published data suggest that vCXCL1 produced by CMV-infected endothelial cells recruits neutrophils and contributes to viral dissemination [33-35]. Sequencing of different HCMV strains showed that the gene for vCXCL1, *UL146*, is one of the most variable gene in the HCMV genome [36]. The N-loop of the chemokine, important for binding to the N-terminus of the receptor [37, 38], displays hypervariability, suggesting that the different vCXCL1s can interact differentially at CXCR2 and CXCR1. The lab of Tim Sparer produced vCXCL1s from 11 different CMV strains in a baculovirus protein expression system. In collaboration with our lab, we characterized the different forms of vCXCL1 in G protein dependent and G protein independent signaling. As described in **Chapter 6**, the 11 vCXCL1s display different affinities for CXCR2 and only three vCXCL1s show weak affinity for CXCR1. Furthermore, looking at various signaling pathways in either transfected cells or neutrophils, we found that in general the vCXCL1s with a high affinity for the receptors shows the highest potency in chemotaxis, [³⁵S]-GTPγS binding and β-arrestin recruitment experiments. As such, differences in binding affinity of the different vCXCL1s may display as well variability in the role of vCXCL1 in HCMV dissemination.

CXCR2 interacting chemokines: redundancy or not?

CXCR2 binds seven endogenous ligands: CXCL1, CXCL2, CXCL3, CXCL5, CXCL6, CXCL7 and CXCL8. All these chemokines bind to CXCR2 with high affinity [33, 39, 40]. As discussed in **Chapter 2** [41], upregulation of these chemokines is associated with an increased influx of neutrophils into sites of inflammation. Subsequently, this leads to clinical symptoms of several inflammatory diseases. The question arises why the human body produces seven different chemokines that interact with the same receptor. Recently, in the GPCR field lots of

attention is given to ‘ligand-biased signaling’ [42–46]. This phenomenon entails that a given ligand can activate one pathway (e.g. G-protein dependent versus G-protein independent) with higher potency compared to another pathway.

We investigated the potencies of all seven CXCR2-interacting chemokines in both a [35 S]-GTP γ S and a β -arrestin recruitment assay. As shown in Figure 8.6, all chemokines enhance dose-dependently the levels of [35 S]-GTP γ S in membranes expressing CXCR2 and induce dose-dependently β -arrestin recruitment in PathHunter™ HEK293-CXCR2 cells. In both assays, CXCL8 shows the highest potency of all chemokines (Table 8.2). The potency order in the [35 S]-GTP γ S assay is: CXCL8 > CXCL1 ~CXCL2 ~CXCL7 > CXCL3 ~ CXCL5 ~CXCL6. Noteworthy, the curves of CXCL3, CXCL5 and CXCL6 do not reach maximal effects at concentration of 1000 nM chemokine. In the β -arrestin recruitment assay all chemokines show higher potency compared to the [35 S]-GTP γ S assay. The potency order in this assay is: CXCL8 > CXCL1-3 and CXCL5-7 (Table 8.2). Whereas in the [35 S]-GTP γ S assay the intrinsic activity is comparable between the chemokines, in the β -arrestin recruitment assay clear differences can be demonstrated. In particular, the chemokines CXCL2 and CXCL7 appear to be partial agonists compared to CXCL8.

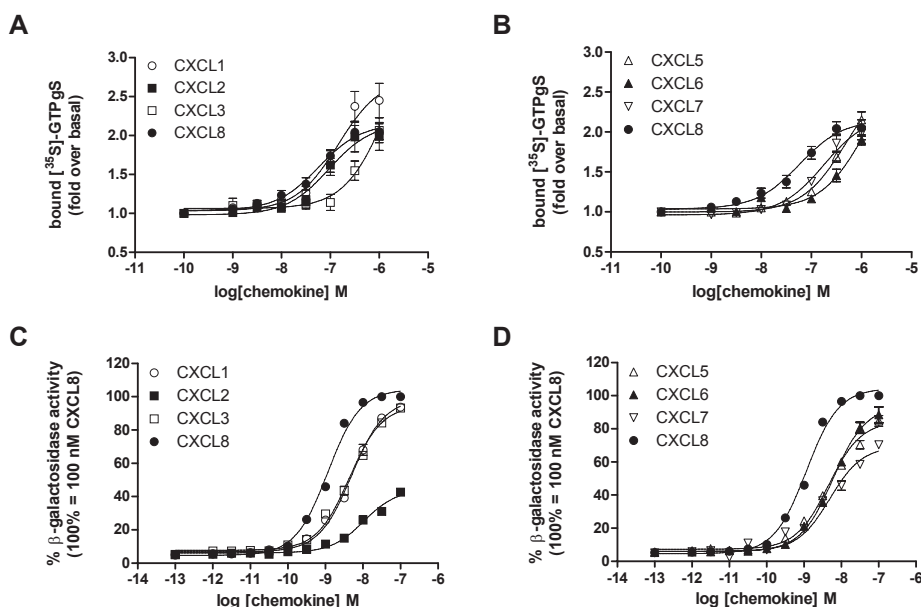


Figure 8.6: [35 S]-GTP γ S binding in HEK293T-CXCR2 membranes induced by CXCL1, CXCL2, CXCL3 and CXCL8 (A) and CXCL5, CXCL6, CXCL7 and CXCL8 (B). Data are expressed as fold over basal of at least three independent experiments performed in triplicate \pm S.E.M. Chemokine-induced β -arrestin2 recruitment in PathHunter™ HEK293-CXCR2 cells by CXCL1, CXCL2, CXCL3 and CXCL8 (C) and CXCL5, CXCL6, CXCL7 and CXCL8 (D). Data are expressed as percentage of maximum β -galactosidase activity \pm S.E.M. of a representative experiment performed in triplicate (at least $n=3$). Assay details are described in Material and Methods of Chapter 6.

Table 8.2: β -arrestin2 recruitment in PathHunter™ HEK293-CXCR2 cells induced by indicated chemokines. Data are expressed as percentage of maximum β -galactosidase activity \pm S.E.M. performed in triplicate (at least $n=3$). [35 S]-GTP γ S binding to HEK293T-CXCR2 membranes induced by indicated chemokines. Data are expressed as fold over basal of at least three independent experiments performed in triplicate \pm S.E.M. Assay details are described in Material and Methods of Chapter 5.

chemokine	[35 S]-GTP γ S assay			β -arrestin recruitment assay		
	(stimulation 60 min)			(stimulation 90 min)		
	pEC $_{50} \pm$ S.E.M	rank	intrinsic activity	pEC $_{50} \pm$ S.E.M	rank	intrinsic activity
CXCL1	6.91 \pm 0.09	2	1.22 \pm 0.05	8.30 \pm 0.08	2	0.85 \pm 0.05
CXCL2	7.06 \pm 0.02	2	1.06 \pm 0.07	7.94 \pm 0.02	2	0.50 \pm 0.07
CXCL3	(6.63 \pm 0.01)	(3)	(1.01 \pm 0.01)	8.40 \pm 0.18	2	0.80 \pm 0.04
CXCL5	(6.54 \pm 0.24)	(3)	(1.16 \pm 0.20)	8.19 \pm 0.09	2	0.73 \pm 0.02
CXCL6	(6.14 \pm 0.37)	(3)	(1.01 \pm 0.14)	8.27 \pm 0.06	2	0.89 \pm 0.02
CXCL7	6.89 \pm 0.02	2	0.92 \pm 0.04	8.38 \pm 0.30	2	0.64 \pm 0.02
CXCL8	7.43 \pm 0.19	1	1.00	9.16 \pm 0.04	1	1.00

Next, we investigated in more detail the β -arrestin recruitment assay for the chemokines CXCL8, CXCL6 and CXCL7. As shown in Figure 8.7, maximal responses are dependent on the stimulation time. CXCL8 reaches its maximal response after 90 min (the standard condition), CXCL6 after 120 min and CXCL7 after 180 min. Interestingly, after a longer stimulation time, the partial agonism profile (Fig. 8.6D) of CXCL7 is no longer present (Fig. 8.7D). Therefore, we conclude that with a longer stimulation time, also CXCL7 is able to recruit β -arrestin to almost the same extent as CXCL8 after 90 min. In general, we should be careful with the recognition of partial agonism profiles in enzyme-complementation assays, since we show that stimulation time can strongly affect this profile.

We wondered if the potency differences of the chemokines are due to differences in binding affinity. Membranes were made of PathHunter™ HEK293-CXCR2 cells and subjected to a [125 I]-CXCL8 equilibrium binding assay. The B_{\max} of CXCR2 on these membranes is 54.9 \pm 15.3 fmol/mg protein ($n=3$). CXCL8 shows high affinity (pK $_d$ of 10.23 \pm 0.06), whereas pK $_i$ values are 8.56 \pm 0.09 and 8.29 \pm 0.03 for CXCL6 and CXCL7, respectively (Table 8.3). Noteworthy, at a concentration of 100 nM, CXCL7 was not able to fully displace [125 I]-CXCL8 (Fig. 8.8A). Next, we performed equilibrium binding experiments with [125 I]-CXCL7 and [125 I]-CXCL8 at HEK293T cells expressing CXCR2 (Fig. 8.8B-C, Table 8.3). The observed pK $_d$ values are 9.01 \pm 0.32 and 9.65 \pm 0.09 for [125 I]-CXCL7 and [125 I]-CXCL8, respectively. Therefore, lower potencies of CXCL6 and CXCL7 compared to CXCL8 in the β -arrestin recruitment assay might be caused due to lower affinities of these chemokines for CXCR2 in this specific cellular background. Another explanation can be differences in binding kinetics of the chemokines, but so far, we have no experimental evidence for this option.

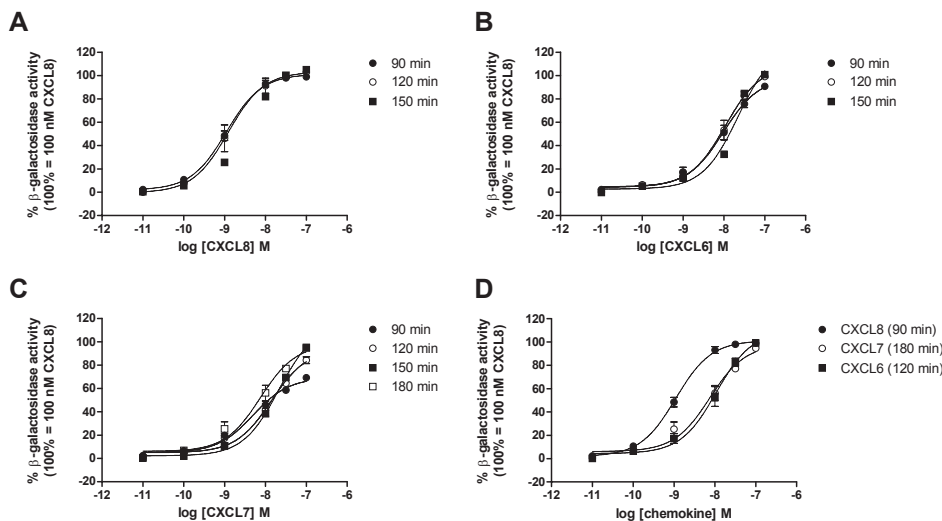


Figure 8.7: Time-dependent chemokine-induced β -arrestin2 recruitment in PathHunter™ HEK293-CXCR2 cells by CXCL8 (A), CXCL6 (B), CXCL7 (C) and combined maximal response graphs (D). Data are expressed as percentage of maximum β -galactosidase activity \pm S.E.M. (at least $n=2$). Assay details are described in Material and Methods of Chapter 3 and 6.

Table 8.3: Displacement of [125 I]-CXCL8 binding to PathHunter™ HEK293-CXCR2 membranes. And displacement of [125 I]-CXCL7 or [125 I]-CXCL8 binding to HEK293T cells expressing CXCR2. The data are presented as mean \pm S.E.M. of at least three independent experiments performed in triplicate.

	PathHunter HEK293-CXCR2	HEK293T-CXCR2	
	membranes	whole cells	
	[125 I]-CXCL8	[125 I]-CXCL7	[125 I]-CXCL8
chemokine	$pK_d/pK_i \pm$ S.E.M	$pK_d/pK_i \pm$ S.E.M	$pK_d/pK_i \pm$ S.E.M
CXCL6	8.56 ± 0.09	8.48 ± 0.14	8.39 ± 0.13
CXCL7	8.29 ± 0.03	9.01 ± 0.32	8.18 ± 0.15
CXCL8	10.23 ± 0.06	9.19 ± 0.10	9.65 ± 0.09

In our [35 S]-GTP γ S assay, CXCL7 gave a slightly higher potency than CXCL6 whereas in the β -arrestin recruitment assay these chemokines show equal potency. This may indicate that these chemokines show ligand bias towards G-protein dependent compared to G-protein independent signalling. Lutichau *et al* [33] show that CXCL6 has a higher potency (pEC_{50} is 10.1 ± 0.07) than CXCL7 (pEC_{50} is 8.85 ± 0.63) in a Ca^{2+} mobilization assay in HEK293T cells expressing CXCR2. Furthermore, in an inositol phosphate accumulation assay with COS7 cells expressing CXCR2 and G_{q15myr} , CXCL6 shows higher activity than CXCL7, although no pEC_{50} can be calculated since the curves are not reaching maximal response yet [33]. Last, Lutichau *et al* [33] show that CXCL6 causes a higher chemotactic signal than CXCL7 in L1.2 cells expressing CXCR2. All these experiments are performed in different

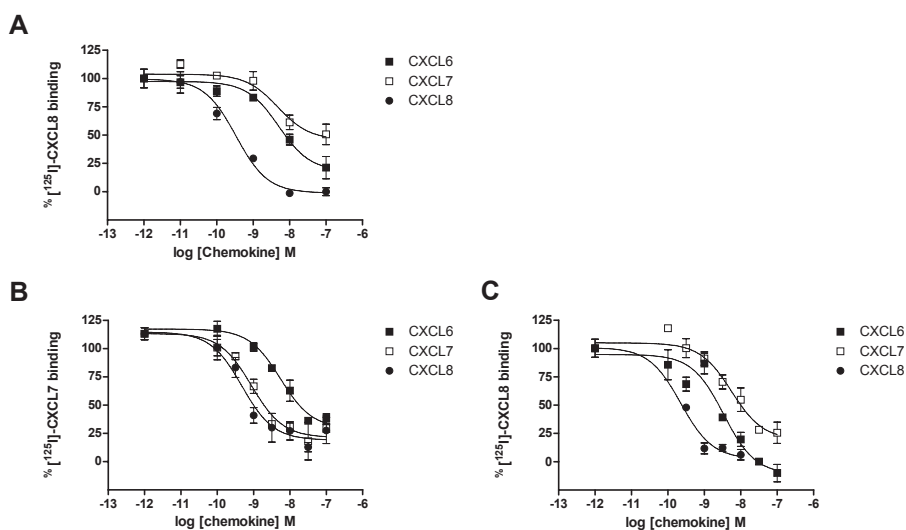


Figure 8.8: Displacement of [¹²⁵I]-CXCL8 binding to PathHunter™ HEK293-CXCR2 proteins for a representative experiment performed in triplicate (A, n=3). Membranes were incubated with indicated concentrations of CXCL6, CXCL7 or CXCL8 and approximately 100 pM [¹²⁵I]-CXCL8. Assay details are described in Material and Methods of Chapter 3 and 4. However, binding buffer used is HBB binding buffer with 0.5% BSA (similar to HEK293T whole cells and neutrophil binding as described in Chapter 5). Displacement of [¹²⁵I]-CXCL7 (B) or [¹²⁵I]-CXCL8 (C) binding to HEK293T cells expressing human CXCR2 of a representative experiment performed in triplicate (n=3-5). Cells were incubated with indicated concentration of CXCL6, CXCL7 or CXCL8 and approximately 100 pM [¹²⁵I]-CXCL7 or [¹²⁵I]-CXCL8, respectively. Assay details are described in Material & Methods of Chapter 5.

cell lines. Since the cellular background as well as the system used can influence the functional outcome, it remains to be investigated if chemokines interacting with CXCR2 show real biased signaling. An elegant experiment will be to determine ERK phosphorylation for all chemokines in time. Rapid ERK phosphorylation correspond to G-protein dependent induced signaling, whereas a later onset of ERK phosphorylation is associated with β -arrestin induced signaling [47]. Based on our [³⁵S]-GTP γ S and β -arrestin recruitment data, we would expect differences in early onset of ERK phosphorylation for CXCL6 and CXCL7, whereas for the late onset it will be the same signal. However, Feniger-Barish *et al* [48] showed a functional hierarchy for (G-protein independent) CXCR2 internalization in HEK293 cells following CXCL8 > CXCL6 > CXCL7, indicating that late onset differences of ERK phosphorylation might occur as well.

Binding pocket of chemokines at CXCR2

In this thesis we focus on the binding pocket of several small molecular weight CXCR2 antagonists. So far, knowledge about the precise binding pocket of chemokines at CXCR2 is however also lacking. In general, a two-step binding model for chemokines have been described [50, 51]. First, the core region of the chemokines (N-terminal and N-loop) is thought to interact with the N-terminus and extracellular loops of the receptor protein. Next, the N-terminus of the chemokine interacts with the extracellular loops and the trans-

membrane domains of the receptor, leading to receptor activation. As observed for several chemokine receptors, Jensen *et al* [52] e.g. demonstrated that the N-terminus of CCR1 binds to CCL3 and CCL5. Furthermore, using different mutants they describe that CCL5 and small molecular weight agonists interact with the right part (TM3, TM7) of the major binding pocket of CCR1. Yet, CCL3 probably interacts only with the extracellular regions of CCR1. CCL5 was not able to displace [125 I]-CCL3, whereas CCL3 can displace [125 I]-CCL5. Interestingly, they show that the small molecular weight agonists act as competitive blockers of CCL5 (overlapping binding sites) and as allosteric enhancers for CCL3 (non-overlapping binding sites). Thus, depending on the endogenous ligand tested, the small molecular weight agonists displays different effects. Therefore, it is recommended to investigate agonist/antagonists behavior with all endogenous ligands of a receptor of interest. So far, we only investigated the mode of action of different CXCR2 antagonists on CXCL8-induced signalling (**Chapter 3-4**). The inhibition of CXCL1-, CXCL2-, CXCL3-, CXCL5-, CXCL6- and CXCL7-induced signalling by different classes of CXCR2 antagonists remains to be investigated.

Table 8.4: Displacement of [125 I]-CXCL1, [125 I]-CXCL5, [125 I]-CXCL7 and [125 I]-CXCL8 from HEK293 cells, performed by Ahuja *et al* [40].

chemokine	IC ₅₀ (nM) [125 I]-CXCL1	IC ₅₀ (nM) [125 I]-CXCL5	IC ₅₀ (nM) [125 I]-CXCL7	IC ₅₀ (nM) [125 I]-CXCL8
CXCL1	3 ± 1.5	0.5 ± 0.4	5 ± 1	8 ± 2
CXCL2	10 ± 0.5	0.8 ± 0.5	8 ± 1.3	100 ± 20
CXCL3	5 ± 1	9 ± 7	4 ± 1.4	14 ± 3
CXCL5	10 ± 0.4	1 ± 0.5	9 ± 0.7	125 ± 25
CXCL6	-	-	-	-
CXCL7	100 ± 10	0.5 ± 0.5	15 ± 3	500 ± 50
CXCL8	4 ± 0.8	0.4 ± 0.5	7 ± 2	5 ± 2

In our binding studies (Table 8.3), we show that CXCL6 has the same affinity for CXCR2 using either [125 I]-CXCL7 or [125 I]-CXCL8, whereas CXCL7 shows around 1 log unit higher affinity for CXCR2 displacing [125 I]-CXCL7 compared to displacing [125 I]-CXCL8. Furthermore, CXCL8 demonstrates around 0.5 log unit higher affinity for CXCR2 using [125 I]-CXCL8 compared to [125 I]-CXCL7. These results are in line with Ahuja *et al* [40], who investigated the binding affinities of CXCL1, CXCL2, CXCL3, CXCL5, CXCL7 and CXCL8 using [125 I]-CXCL1, [125 I]-CXCL5, [125 I]-CXCL7 and [125 I]-CXCL8 (Table 8.4). As shown in Table 8.4, chemokines display different binding affinities depending on the radiolabeled chemokine used. This might indicate that different binding places for the endogenous chemokines exist at CXCR2 or that the chemokines recognize different receptor conformations. Noteworthy, the N-loop of the different CXCR2 interacting chemokines display variability (see Fig. 8.9). Thus, differential interaction with the N-terminus of CXCR2 is possible. A NMR structure of CXCL8 with CXCR1 shows that K11, K15 and R47 have an ionic interaction with the N-terminus of the receptor [53]. We do not know if

these residues are also important for binding to CXCR2, since so far no NMR data exist of a chemokine with CXCR2.

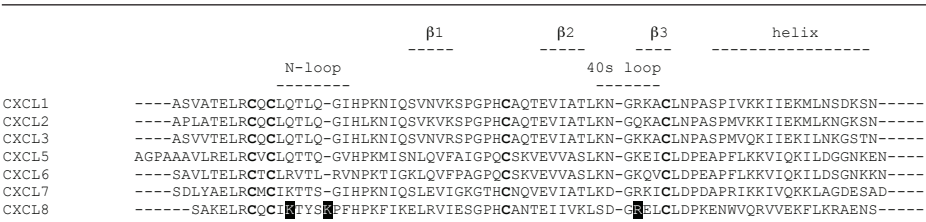


Figure 8.9: Amino acid alignment of the CXCR2-interacting chemokines. The amino acids indicated with a black box and a white font are residues shown to have ionic interactions with CXCR1 [53].

To our best knowledge, only Katancik *et al* [54] investigated amino residues involved in chemokine binding at CXCR2. They describe that mutating glutamic acid 7, aspartic acid 9 and glutamic acid 12 (snakeplot, see Fig. 8.10) to an alanine gives a significant drop of [¹²⁵I]-CXCL1 binding affinity. In addition, [¹²⁵I]-CXCL8 binding affinity is reduced at the alanine mutants of aspartic acid 9, glutamic acid 12, lysine 108 and lysine 120. Yet, [¹²⁵I]-CXCL7 binding is not affected by the alanine mutants in both the N-terminus and extracellular loop 1 of CXCR2. Noteworthy, amino acids involved in binding are not necessarily involved in activation, as indicated with Ca²⁺ mobilization experiments [54]. Thus, in depth analysis which amino acids of the receptor are involved in the binding and functional response of chemokines, will provide insight how chemokines interact with their

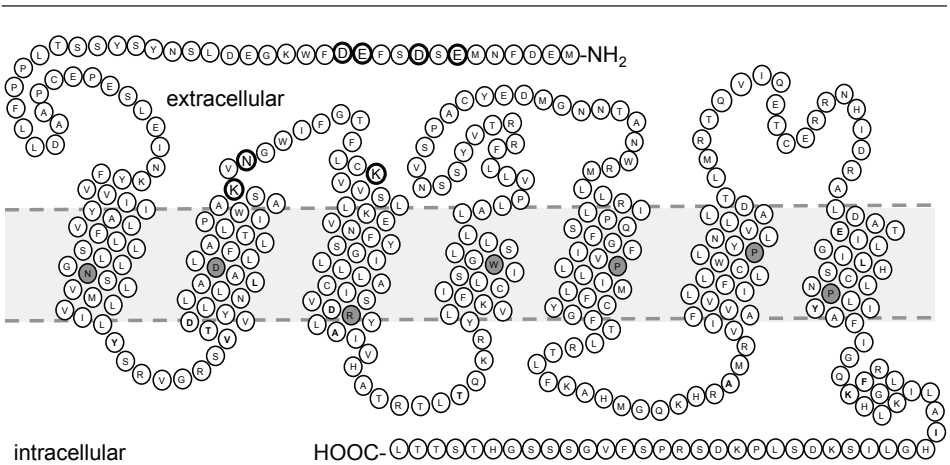


Figure 8.10: Snakeplot of the human CXCR2 receptor. The residues indicated with a solid circle and a larger font have been mutated by Katancik *et al* [54]. Residues indicated in grey are the conserved residues of the Ballousteros-Weinstein numbering scheme.

receptor. Reciprocal, mutating the chemokines will give information which amino acids of the chemokine are important to interact with the receptor. In the end, detailed insight on the binding and action of the endogenous chemokines will ultimately help to better understand the action of CXCR2-directed therapeutics.

The quest for other therapeutically relevant chemotactic GPCRs

While we focused for the major part of this thesis on the interaction of small molecules with CXCR2, in another part we searched for potential new drug targets. In **Chapter 7** we identified mRNA expression levels of chemotactic receptors in macroscopically identified inflamed and non-inflamed tissue of Crohn's Disease (CD) and Ulcerative Colitis (UC) patients (collaboration with group of Aletta Kraneveld, Utrecht University). Change in expression profile of receptors (and their ligands) are often correlated with the development of clinical symptoms of diseases. As such, RT-qPCR can be used to easily investigate differences in mRNA expression levels, that might indicate receptors that play a role in disease pathogenesis.

In inflamed and non-inflamed bowel tissue from IBD patients as well as non-inflamed bowel tissue from colon cancer patients, mRNA expression levels are relatively high of CXCR4, CXCR6, CXCR7, CCR6, CCR7, CCR9, CCX-CKR, BLT₁, BLT₂, C5AR1 and S1P₂. Interestingly, S1P₂ mRNA expression levels are significantly higher expressed in inflamed tissue compared to non-inflamed tissue of CD patients. Other chemotactic receptors do not show significant differences. Protein levels of S1P₂ in non-inflamed and inflamed tissue of CD patients remains to be investigated. Especially, double staining with immunohistochemistry will also provide insight which cell types do express S1P₂ and to establish whether S1P₂ can be a potential drug target in CD.

Besides chemokine receptors, also other receptors play a role in chemotaxis of immune system cells, including the H₄R. Of all the chemotactic receptors mentioned in **Chapter 7**, we only investigated protein levels of the H₄R in inflamed and non-inflamed bowel tissue of inflammatory bowel disease (IBD) patients. As shown in Figure 8.11, the H₄R protein is mainly detected on epithelial cells. Differences between non-inflamed and inflamed tissue are not apparent. Double staining should provide information which inflammatory cell types are present in these tissue sections and on which inflammatory cell types H₄R is present.

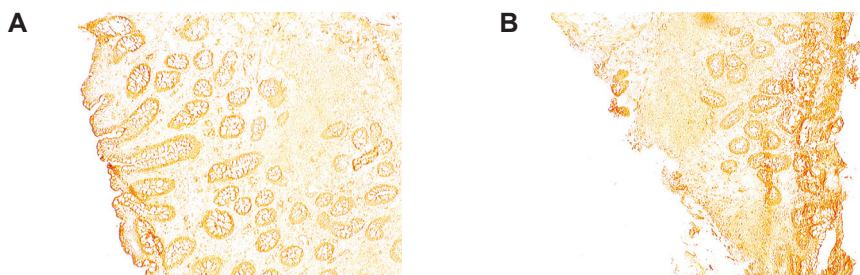


Figure 8.11, continued on next page

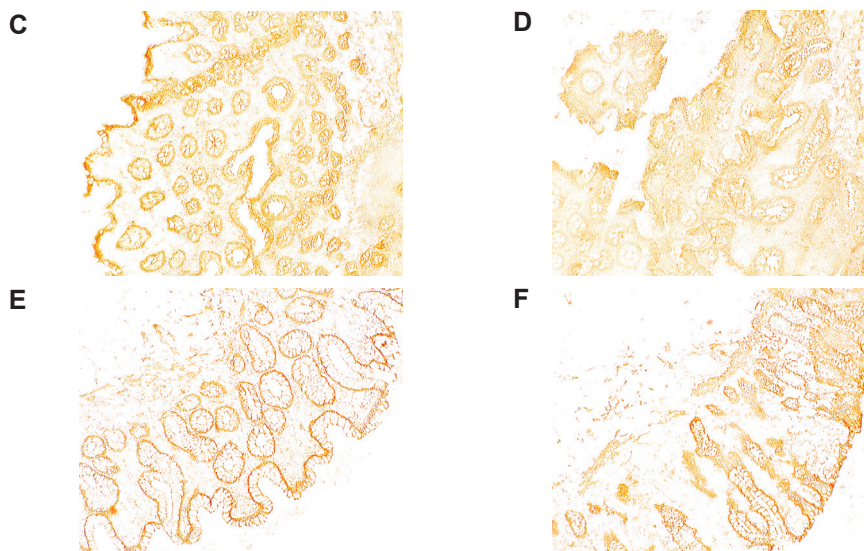


Figure 8.11: Detection of the H₄R protein on macroscopically non-inflamed (A, C, E) and inflamed (B, D, F) human bowel tissue of IBD patients (10x magnified). A-B, C-D and E-F are corresponding tissues of three patients. Tissue details are described in Material & Methods of Chapter 7. Methods: Frozen tissues sections (5 μ m) were defrosted and fixed for 30 min with 4% formaldehyde. Next, slides were washed three times with TBS and incubated with 10% v/v methanol and 3% H₂O₂ for 30 min. After three washes with 0.2% w/v Triton X100 in TBS, slides were incubated for 30 min with 0.2% w/v glycine in TBS followed by 1h blocking in blocking buffer (TBS + 0.2% w/v Triton X100 and 10% FCS) and O/N incubation with human H₄R antibody (1 μ g/ml; made in lab Paul Chazot) in TBS with 1% FCS at 4°C. The next day, slides were washed three times with 0.2% w/v Triton X100 in TBS and incubated with secondary antibody (1:200 anti-rabbit, biotinylated, Vector Laboratories) in 1% FCS in TBS. After 2 hours, slides were washed three times with 0.2% w/v Triton X100 in TBS and twice with TBS. Next, slides were stained with DAB (Vector Laboratories) using supplier conditions. Stainings were stopped by washing slides two times with water. Finally, slides were mounted and analyzed under a Nikon Eclipse E400 microscope. Pictures were made with a CoolPX, MDC Lens of Nikon.

Final conclusions

In this thesis, we identified distinct binding pockets for CXCR2 antagonists belonging to different structural classes. Furthermore, we show that the collagen break-down product N-acetyl-PGP does not interact directly with CXCR2 and that vCXCL1 isolated from different HCMV strains are ligands for CXCR2. We investigated binding affinities and the activation or inhibition of different signaling pathways by several (viral) chemokines and CXCR2 antagonists, respectively. In addition, we established a RT-qPCR primer set of chemotactic receptors to investigate different mRNA levels in patient material. As such, this technique can be used to rapidly identify potential therapeutic targets in diseases.

As stated above, CXCR2 shows diversity in ligand recognition. With the elucidation of several crystal structures of GPCRs, in particular CXCR4 [21], more accurate *in silico* models of the CXCR2 receptor can now be generated and ultimately also the CXCR2 protein structure might one day be solved. Together with the different binding pockets localized in CXCR2, this gives challenging opportunities for structure-based design of small allosteric modulators for CXCR2 in the near future.

References

1. de Kruijf, P., et al., Nonpeptidergic allosteric antagonists differentially bind to the CXCR2 chemokine receptor. *J Pharmacol Exp Ther*, 2009. 329(2): p. 783-90.
2. Nicholls, D.J., et al., Identification of a Putative Intracellular Allosteric Antagonist Binding-Site in the CXC Chemokine Receptors 1 and 2. *Mol Pharmacol*, 2008.
3. Salchow, K., et al., A common intracellular allosteric binding site for antagonists of the CXCR2 receptor. *Br J Pharmacol*, 2010. 159(7): p. 1429-39.
4. Scholten, D.J., et al., Pharmacological Modulation of Chemokine Receptor Function. *British Journal of Pharmacology*, 2011.
5. Bertini, R., et al., Noncompetitive allosteric inhibitors of the inflammatory chemokine receptors CXCR1 and CXCR2: prevention of reperfusion injury. *Proc Natl Acad Sci U S A*, 2004. 101(32): p. 11791-6.
6. Moriconi, A., et al., Design of noncompetitive interleukin-8 inhibitors acting on CXCR1 and CXCR2. *J Med Chem*, 2007. 50(17): p. 3984-4002.
7. Gerlach, L.O., et al., Molecular interactions of cyclam and bicyclam non-peptide antagonists with the CXCR4 chemokine receptor. *J Biol Chem*, 2001. 276(17): p. 14153-60.
8. Wong, R.S., et al., Comparison of the potential multiple binding modes of bicyclam, monocyclam, and noncyclam small-molecule CXC chemokine receptor 4 inhibitors. *Mol Pharmacol*, 2008. 74(6): p. 1485-95.
9. Vaidehi, N., et al., Predictions of CCR1 chemokine receptor structure and BX 471 antagonist binding followed by experimental validation. *J Biol Chem*, 2006. 281(37): p. 27613-20.
10. Berkhout, T.A., et al., CCR2: characterization of the antagonist binding site from a combined receptor modeling/mutagenesis approach. *J Med Chem*, 2003. 46(19): p. 4070-86.
11. Hall, S.E., et al., Elucidation of binding sites of dual antagonists in the human chemokine receptors CCR2 and CCR5. *Mol Pharmacol*, 2009. 75(6): p. 1325-36.
12. Maeda, K., et al., Structural and molecular interactions of CCR5 inhibitors with CCR5. *J Biol Chem*, 2006. 281(18): p. 12688-98.
13. Seibert, C., et al., Interaction of small molecule inhibitors of HIV-1 entry with CCR5. *Virology*, 2006. 349(1): p. 41-54.
14. Kondru, R., et al., Molecular interactions of CCR5 with major classes of small-molecule anti-HIV CCR5 antagonists. *Mol Pharmacol*, 2008. 73(3): p. 789-800.
15. Andrews, G., C. Jones, and K.A. Wreggett, An intracellular allosteric site for a specific class of antagonists of the CC chemokine G protein-coupled receptors CCR4 and CCR5. *Mol Pharmacol*, 2008. 73(3): p. 855-67.
16. Maeda, D.Y., et al., Nicotinamide glycolates antagonize CXCR2 activity through an intracellular mechanism. *J Pharmacol Exp Ther*, 2010. 332(1): p. 145-52.
17. Palczewski, K., et al., Crystal structure of rhodopsin: A G protein-coupled receptor. *Science*, 2000. 289(5480): p. 739-45.
18. Cherezov, V., et al., High-resolution crystal structure of an engineered human beta2-adrenergic G protein-coupled receptor. *Science*, 2007. 318(5854): p. 1258-65.
19. Rasmussen, S.G., et al., Crystal structure of the human beta2 adrenergic G-protein-coupled receptor. *Nature*, 2007. 450(7168): p. 383-7.
20. Rosenbaum, D.M., et al., GPCR engineering yields high-resolution structural insights into beta2-adrenergic receptor function. *Science*, 2007. 318(5854): p. 1266-73.
21. Wu, B., et al., Structures of the CXCR4 chemokine GPCR with small-molecule and cyclic peptide antagonists. *Science*, 2010. 330(6007): p. 1066-71.
22. Rasmussen, S.G., et al., Structure of a nanobody-stabilized active state of the beta(2) adrenoceptor. *Nature*, 2011. 469(7329): p. 175-80.
23. Xu, F., et al., Structure of an agonist-bound human A2A adenosine receptor. *Science*, 2011. 332(6027): p. 322-7.
24. Espinoza-Fonseca, L.M. and J.G. Trujillo-Ferrara, The existence of a second allosteric site on the M1 muscarinic acetylcholine receptor and its implications for drug design. *Bioorg Med Chem Lett*, 2006. 16(5): p. 1217-20.
25. Taylor, C.M., et al., Modulating G-protein coupled receptor/G-protein signal transduction by small molecules suggested by virtual screening. *J Med Chem*, 2008. 51(17): p. 5297-303.
26. Park, J.H., et al., Crystal structure of the ligand-free G-protein-coupled receptor opsin. *Nature*, 2008. 454(7201): p. 183-7.
27. Allegretti, M., et al., 2-Arylpropionic CXC chemokine receptor 1 (CXCR1) ligands as novel noncompetitive CXCL8 inhibitors. *J Med Chem*, 2005. 48(13): p. 4312-31.
28. Weathington, N.M., et al., A novel peptide CXCR ligand derived from extracellular matrix degradation during airway inflammation. *Nat Med*, 2006. 12(3): p. 317-23.
29. Overbeek, S.A., et al., N-acetylated Proline-Glycine-Proline induced G-protein dependent chemotaxis of neutrophils is independent of CXCL8 release. *Eur J Pharmacol*, 2011.
30. de Kruijf, P., et al., The collagen-breakdown product N-acetyl-Proline-Glycine-Proline (N-alpha-PGP) does not interact directly with human CXCR1 and CXCR2. *Eur J Pharmacol*, 2010. 643(1): p. 29-33.
31. Jackson, P.L., et al., A CXCL8 receptor antagonist based on the structure of N-acetyl-proline-glycine-proline. *Eur J Pharmacol*, 2011.
32. Kim, S.D., et al., Activation of CXCR2 by Extracellular Matrix Degradation Product Acetylated Pro-Gly-Pro Has Therapeutic Effects against Sepsis. *Am J Respir Crit Care Med*, 2011. 184(2): p. 243-51.
33. Lutichau, H.R., The cytomegalovirus UL146 gene product vCXCL1 targets both CXCR1 and CXCR2 as an agonist. *J Biol Chem*, 2010. 285(12): p. 9137-46.

34. Penfold, M.E., et al., Cytomegalovirus encodes a potent alpha chemokine. *Proc Natl Acad Sci U S A*, 1999. 96(17): p. 9839-44.
35. Grundy, J.E., et al., Cytomegalovirus-infected endothelial cells recruit neutrophils by the secretion of C-X-C chemokines and transmit virus by direct neutrophil-endothelial cell contact and during neutrophil transendothelial migration. *J Infect Dis*, 1998. 177(6): p. 1465-74.
36. Dolan, A., et al., Genetic content of wild-type human cytomegalovirus. *J Gen Virol*, 2004. 85(Pt 5): p. 1301-12.
37. Lowman, H.B., et al., Exchanging interleukin-8 and melanoma growth-stimulating activity receptor binding specificities. *J Biol Chem*, 1996. 271(24): p. 14344-52.
38. Fernandez, E.J. and E. Lolis, Structure, function, and inhibition of chemokines. *Annu Rev Pharmacol Toxicol*, 2002. 42: p. 469-99.
39. Ahuja, S.K., J.C. Lee, and P.M. Murphy, CXC chemokines bind to unique sets of selectivity determinants that can function independently and are broadly distributed on multiple domains of human interleukin-8 receptor B. Determinants of high affinity binding and receptor activation are distinct. *J Biol Chem*, 1996. 271(1): p. 225-32.
40. Ahuja, S.K. and P.M. Murphy, The CXC chemokines growth-regulated oncogene (GRO) alpha, GRObeta, GROgamma, neutrophil-activating peptide-2, and epithelial cell-derived neutrophil-activating peptide-78 are potent agonists for the type B, but not the type A, human interleukin-8 receptor. *J Biol Chem*, 1996. 271(34): p. 20545-50.
41. Kraneveld, A.D., et al., Chemokine receptors in inflammatory diseases, in *Chemokine Receptors as Drug Targets* M.J. Smit, Lira, S.A., Leurs, R, Editor. 2011, Wiley-VCH Verlag GmbH&Co. KGaA, Weinheim. p. 105-150.
42. Heilker, R., et al., G-protein-coupled receptor-focused drug discovery using a target class platform approach. *Drug Discov Today*, 2009. 14(5-6): p. 231-40.
43. Rajagopal, S., K. Rajagopal, and R.J. Lefkowitz, Teaching old receptors new tricks: biasing seven-transmembrane receptors. *Nat Rev Drug Discov*, 2010. 9(5): p. 373-86.
44. Violin, J.D. and R.J. Lefkowitz, Beta-arrestin-biased ligands at seven-transmembrane receptors. *Trends Pharmacol Sci*, 2007. 28(8): p. 416-22.
45. Zheng, H., H.H. Loh, and P.Y. Law, Agonist-selective signaling of G protein-coupled receptor: mechanisms and implications. *IUBMB Life*, 2010. 62(2): p. 112-9.
46. Galandrin, S., G. Oligny-Longpre, and M. Bouvier, The evasive nature of drug efficacy: implications for drug discovery. *Trends Pharmacol Sci*, 2007. 28(8): p. 423-30.
47. DeWire, S.M., et al., Beta-arrestins and cell signaling. *Annu Rev Physiol*, 2007. 69: p. 483-510.
48. Feniger-Barish, R., et al., GCP-2-induced internalization of IL-8 receptors: hierarchical relationships between GCP-2 and other ELR(+)-CXC chemokines and mechanisms regulating CXCR2 internalization and recycling. *Blood*, 2000. 95(5): p. 1551-9.
49. Mortier, A., J. Van Damme, and P. Proost, Regulation of chemokine activity by posttranslational modification. *Pharmacol Ther*, 2008. 120(2): p. 197-217.
50. Allen, S.J., S.E. Crown, and T.M. Handel, Chemokine: receptor structure, interactions, and antagonism. *Annu Rev Immunol*, 2007. 25: p. 787-820.
51. Rajagopalan, L. and K. Rajarathnam, Structural basis of chemokine receptor function--a model for binding affinity and ligand selectivity. *Biosci Rep*, 2006. 26(5): p. 325-39.
52. Jensen, P.C., et al., Positive versus negative modulation of different endogenous chemokines for CC-chemokine receptor 1 by small molecule agonists through allosteric versus orthosteric binding. *J Biol Chem*, 2008. 283(34): p. 23121-8.
53. Skelton, N.J., et al., Structure of a CXC chemokine-receptor fragment in complex with interleukin-8. *Structure*, 1999. 7(2): p. 157-68.
54. Katancik, J.A., A. Sharma, and E. de Nardin, Interleukin 8, neutrophil-activating peptide-2 and GRO-alpha bind to and elicit cell activation via specific and different amino acid residues of CXCR2. *Cytokine*, 2000. 12(10): p. 1480-8.

